Thesis for the degree of Doctor of Philosophy

Synthesis and Application of Novel Homochiral Imidazolium Salts

Nameer A. Alhashimy, B.Sc.

At Dublin City University, School of Chemical Sciences

Under The Supervision of Dr. Kieran Nolan

and (in part) Dr. Joshua Howarth

2004

Declaration

I hereby certify that this material, which I now submit for assessment on the programme of study leading to the award of Doctor of Philosophy is entirely my own work and has not been taken from the work of others save and to the extent that such work has been cited and acknowledged within the text of my work.

Signed: _____ ID No.: 98970704

Nameer Alhashimy

Date: 16/08/2004

ABBREVIATIONS

DNA	Deoxyribonucleic acid
ATP	Adenosine triphosphate
DMSO-d_6	Deuterated dimethyl sulfoxide
CD_3CN	Deuterated acetonitrile
NMR	Nuclear magnetic resonance
M	Molarity
Cp_2Co^+	Cobaltecenium cyclopentadiene
K	Association constant
bpy	Bi-pyridinyl
mV	Millivolt
$CDCl_3$	Deuterated chloroform
de	Diastereomer
ee	Enantiomeric excess
THF	Tetrahydrofuran
mol	Mole
ppm	Parts per million
t-BuOK	Potassium tertiary butoxide
cat.	Catalyst
eq.	Equivalent
C_6D_6	Deuterated benzene
D_2O	Deuterated water
n-BuLi	Normal butyl lithium
Ph	Phenyl
OAc	Acetate
Me	Methyl
EtCN	Propionitrile
MeCN	Acetonitrile
DCM	Dichloromethane
PTC	Phase transfer catalyst
DCE	Dichloroethane

Å	Molecular sieves
M-C	Metal-carbene
Min	Minutes
$Cu(OTf_2)$	Copper triflate
LAC	Ligand accelerated catalyst
DMF	*N*,*N*-Dimethylformamide
L	Ligand
IR	Infrared
h	Hour(s)
HMQC	Heteronuclear multiple quantum coherence
µg	Microgram
TLC	Thin layer chromatography
NHC	*N*-Heterocyclic carbene
b.p.	Boiling point
m.p.	Melting point
CHO	Carboxyaldehyde
$[\alpha]^{25}_D$	Specific rotation
δ	Chemical shift
ν	Frequency
w/v	Weight per volume
Calcd.	Calculated
St.	Stoichiometry
J	Coupling constant
rt.	Room temperature
CD	Circular dichrosim

Publications

The following paper was published as a part of the work contained within this thesis:

1- A homochiral tripodal receptor with selectivity for sodium (R)-amino propionate over sodium (S)-aminopropionate:
J. Howarth, N.A. Alhashimy, *Tetrahedron Lett.*, 42, 2001, 5777.

The following presentations were presented as part of the work contained within this thesis:

2- Oral presentation at Dublin City University/ Ireland:
The synthesis and application of novel homochiral tripodal azolium salts.

3- Poster presentation at Lisbon/ Portugal, International conference on the synthetic receptors, October 2003, N.A. Alhashimy, J. Howarth, D. Brougham, K. Nolan.
The synthesis and application of novel homochiral tripodal anion receptors.

ABSTRACT

Synthesis and Application of Novel Homochiral Imidazolium Salts

Nameer A. Alhashimy, B.Sc.

Imidazolium salts derived from azolium systems have diverse applications in a wide range of areas within chemistry and biology. Of particular interest is the application of imidazolium salts as potential anion and small molecule receptors. Recent work has demonstrated the potential of arranging imidazolium salts around a benzene scaffold. These new tripodal receptors demonstrated excellent selectivities and strong binding constants for halide anions. We believed that this work could be further developed to expand the range of binding capabilities for this new class of tripodal receptor. The objectives of this research was to prepare a new series of enantioselective homochiral tripodal receptors using a benzene ring scaffold.

Herein we report the synthesis of 1,3,5-tris[N-((-)-cis-myrtanylimidazolium) methyl]2,4,6,-trimethylbenzene tri(hexafluorophosphate) **(156a)**, 1,3,5-tris[((R)-3-methyl-2-butylimidazolium)methyl]2,4,5-trimethylbenzene tri(hexafluoro-osphate) **(156b)**, 1,3,5-tris[((S)-1-(2-phenyl)ethylimidazolium)methyl]2,4,6-trimethylbenzene tri(hexafluorophosphate) **(156c)**, 1,3,5-tris[((S)-1-(2-Naphthyl) ethylimidazolium)methyl]2,4,6-trimethylbenzene tri(hexafluorophosphate) **(156d)**.

All receptors were completely characterised. These new receptors were fully investigated for both anion recognition and as enantioselective anion receptors. It was found by ^{1}H NMR studies that these new chiral receptors can selectively bind chloride and bromide with high binding constants. Further ^{1}H NMR studies revealed that receptor **(156a)** is able to enantioselectively discriminate between the enantiomers of sodium 2-aminopropionate salts.

These new homochiral imidazolium receptors were also converted to their respective silver carbenes and their potential as ligands in the catalysis of 1,4 conjugate addition reactions was explored. It was found that the carbene derivatives of these tripodal receptors were inefficient as ligands, perhaps due to the small size of the receptor cavities. All of the homochiral receptors that were prepared were investigated for possible biological activity against *P. aeruginosa* and *C. albicans*.

Also reported is the preparation of a new 1,3-*N*-heterocyclic silver carbene complex which was studied as a potential ligand for 1,4 conjugate additions. This ligand was also successfully converted to its palladium complex and was explored as a potential catalyst in the Heck reaction.

ACKNOWLEDGEMENTS

First I would like to thank my supervisor Dr. Kieran Nolan for his help, encouragement and constant support, and I would also like to thank my initial supervisor Dr. Joshua Howarth for the commencement of this research, and for his help and advice.

Many thanks and appreciation to Dr. Paraic James for his continuing support in several fields.

Many thanks to Dr. Dermot Brougham for his support in the physical chemistry background to my project.

To all academic staff I would send my thanks and appreciation specially Prof. Malcolm Smith for his encouragement and care.

To Dr. Ismael and Dr. Helge I would say thanks for their excellent X-ray crystallography work.

To Michael Burke I would send him my thanks and appreciation for solving many technical problems.

Many thanks to all technical staff; Veronica, Ambrose, Anne, Damien, Maurice, and Vinny.

To Ray and Mairead for their help and effort in transfer report and also Dr. Mary Pryce.

Thanks also to all the people of (X2-49) Lab that I have worked with (Past and present); "Cathal", Keith, Jean-Luc, Colm, Ollie, Ben, Ger, Darragh, Dave, Ji-Feng, Robbie, Rachel, Yang, Ian, Frankie, Noel, Neil, Moss, Steve and Paula. The people of my research group; Steve, John, Shane, Pauline and Carol. The people in (X2-46) Lab; Karl, Wes, Jennifer, John, Kevin, Claire and Kieran.

To my friend Wadia, I would send my great thanks for his encouragement and help, and also Abu-abdalh, Firas, Safa'aldeen, Ala'aldeen, Wathic, Mostafa and Amjad Muhlhal.

Many thanks and appreciation I would send to Prof. Mansoor Mohammad and Dr. Mohammad Al'asady for their help, care and encouragement.

Finally, to Dublin Corporation I would send my thanks for their financial support.

Contents

Chapter 1

Literature Survey

1.1 Introduction

1.1.1 Imidazole

Imidazole **(1)** was first discovered in 1858 by DeBus who synthesised it from glyoxal and ammonia [1]. Initially, it was named as glyoxaline, but was later renamed imidazole by Hantzsch [2]. Imidazole is a five membered heterocyclic ring containing three carbons and two nitrogen atoms in the positions-1 and 3 (Fig.1.1). One of the annular nitrogens (N-1) is bound to a hydrogen atom which is similar to that found in pyrrole **(2)**, the second nitrogen (N-3) corresponds to the nitrogen found in pyridine **(3)**. Imidazole has aromatic character, ^{1}H NMR spectra of imidazole has proton resonances at 7.20-7.70 ppm which is in the aromatic region.

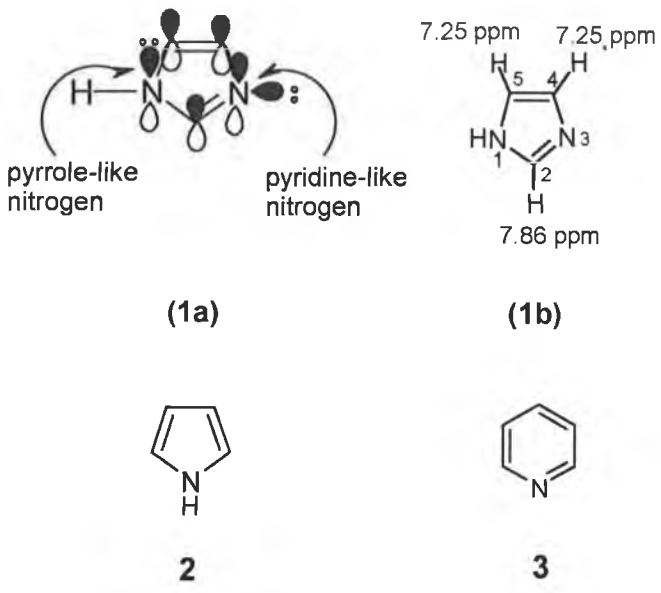

Figure 1.1. (1a) The distribution of electron density in the unsubstituted imidazole, **(1b)** ^{1}H NMR chemical shift of imidazole.

The resonance structures of the imidazole ring are shown in Scheme 1.1.

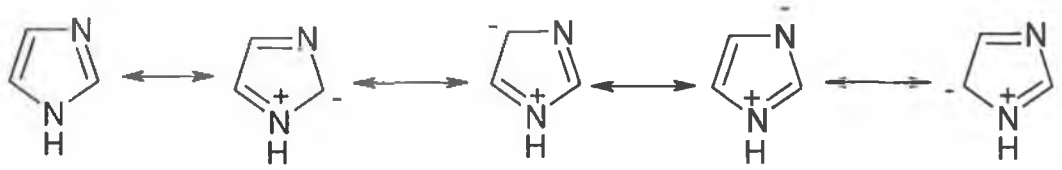

Scheme 1.1. Delocalised system of imidazole ring.

The imidazole ring system has amphoteric character which is based on a proton transfer equilibria, which allows the imidazole ring to function both as a base or as an acid. The free imidazole is a moderately strong organic base (pK_a 14.50), but it can also act as a weak acid (pK_a 7.01). Both the cationic and anionic structures are symmetrical and delocalised, Figure 1.2.

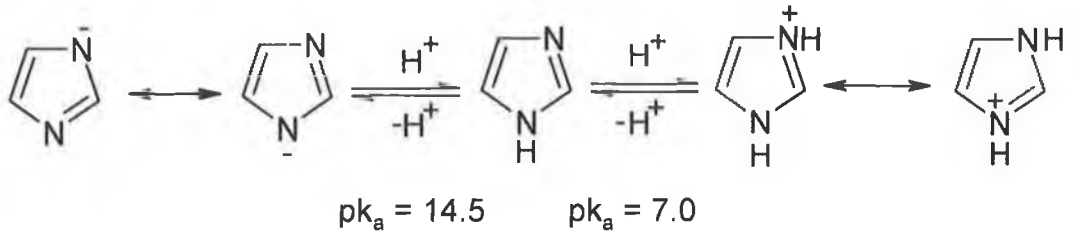

Figure 1.2. Proton transfer equilibria of imidazole.

1.1.2 Quaternization reaction

Imidazoles can undergo a quaternization reaction, quaternization of imidazole derivatives was first observed by Wyss [3] in 1877, where he generated a series of 1,3-disubstituted imidazolium salts **(4)**, as shown in Figure 1.3. The quaternization of imidazole occurs on the annular nitrogen atom since its lone pair of electrons are not conjugated with the π orbital of the imidazole rings.

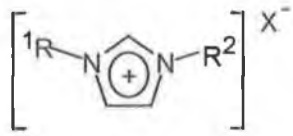

R = Alkyl/Aryl group
X = Counter anion

4

Figure 1.3. 1,3-Disubstituted imidazolium salts based on quaternization system.

These electrons are available to undergo S_N2 type reactions with a variety of alkyl halides (Scheme 1.2).

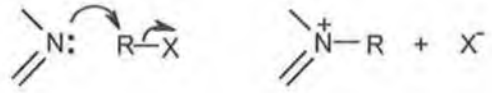

Scheme 1.2. The quarternization of imidazole.

1.1.3 Application of imidazoles

Imidazoles have diverse applications; (1) Imidazole can form stable salts with a variety of organic and inorganic acids (2) Imidazole can also form complexes with a variety of metals such as cobalt, copper and mercury, Figure 1.4.

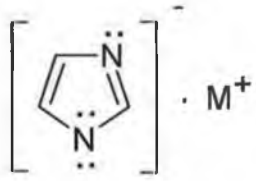

5

Figure 1.4. The possibility of imidazoles to complex with a variety of metals.

(3) The imidazole and imidazolium system are present in many active sites in enzymes. An example, histidine **(6)** is found in the active sites of ribonuclease. Its function appears to be the catalysis of proton transfer as outlined in Fig.1.2. (4) Also, imidazole is present in many drug structures such as the antibiotic 2-nitro-imidazole(azomycin) [4] **(7)**. Metronidazole **(8)** is used as a radiosensitizer in X-ray therapy, other imidazoles have found use as antifungal agents such as bifonazole **(9)** and clotrimazole**(10)**.

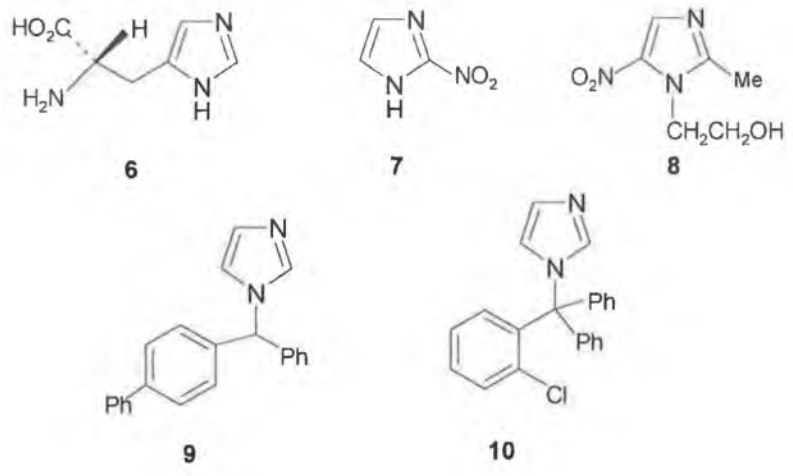

Figure 1.5. Different type of imidazoles, present in different applications.

1.2 Anion recognition

The development of artificial hosts for anion recognition has recently become a major area of interest. The first synthetic anion host receptors were developed in the 1960s [5,6]. It is perhaps surprising that the area of anion recognition has been slow to develop considering their importance in medicine and the environment. Anions play a vital role both environmentally and biologically, making their selective detection a critical research goal for modern sensor development. Various roles that anions are involved in are outlined below:

- Anions function as catalysts, bases, redox mediators.
- Anions are of great important in disease pathways. Cystic fibrosis is caused by misregulation of chloride channels [7] and Alzheimer's has been linked to anion-binding enzymes [8], so there is a real need for selective halide detection.
- Adenosine triphosphate (ATP), is an anion involved in many metabolic functions, DNA a polyphosphate anion, and the majority of enzyme substrates and cofactors are anionic.
- Anions pose a large pollution problem, particularly nitrate and phosphate, which can cause the eutrophication of rivers and lakes.

To design molecular receptors for anion detection many factors have to be considered concerning the physiochemical properties of anions which are outlined below :

- Charge: anions are larger than isoelectronic cations, and therefore have a lower charge to radius ratio. This decreases the effectiveness of electrostatic binding.
- Shape: anions species have a wide range of geometries, and therefore, a higher degree of receptor design may be required for host : guest complementarity.
- pH dependency: anions are sensitive to pH conditions, and so receptors must function within a pH window of the target anion.

- Solvation: solvent effects are a crucial consideration, since anions are often highly solvated. Potential receptors are in effect competing with solvation [9,10].

There have been common transduction modes used for molecular recognition of anions: electrochemical, optical, photo induced electron transfer and competition methods [11]. Of these the electrochemical and optical methods have been the most widely investigated.

1.2.1 Receptors based on electrostatic attraction

A number of receptors have been prepared that are able to bind anions via electrostatic attraction such as crown ethers containing Lewis acid centres [12], ammonium quaternary salts [13] and guanidines [14]. Macrocyclic molecules based on polyamines such as compound **(11)** and **(12)** were first reported by Dietrich et al. [15], Figure 1.6.

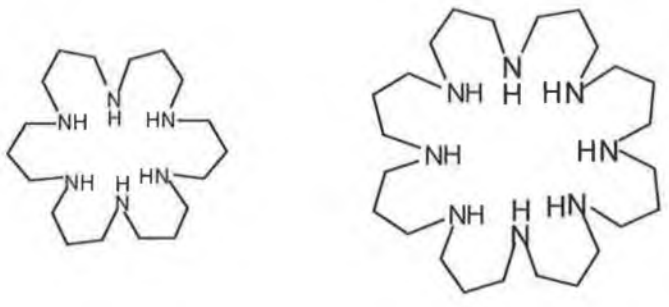

11 **12**

Figure 1.6. Macrocyclic receptors that bind anions via electrostatic attraction.

These receptors were found to exhibit strong binding properties for anions through electrostatic interactions (host-guest) by protonation of the amino groups.

Electrostatic receptors have been further developed to incorporate transition metals such as cobalt in compound **(13)** [16], Figure 1.7.

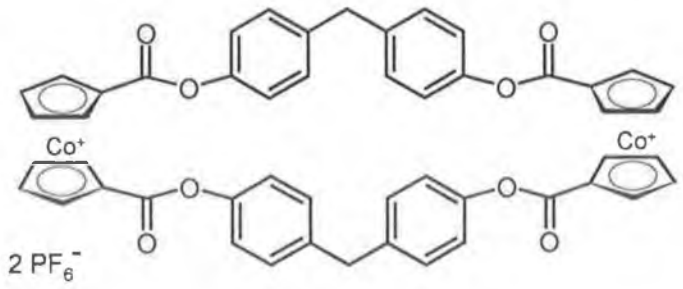

13

Figure 1.7. The development of electrostatic receptor by incorporating cobalt metals as in compound **(13)**.

This receptor was found to show that the cobaltocenium moiety was interacting electrostatically with bromide anion, producing the cathodic wave shift of the cobaltocene/cobaltocenium electro-couple.

1.2.2 Cobaltocenium based anion receptors

After the development of electrostatic attraction receptors **(13)**, work began to focus on the development of new receptors containing both H-bonding moieties and electrostatic moieties. Beer et al. developed a new class of inorganic anion receptors **(14)** and **(15)** in which hydrogen bonding was employed as a functional mode for anion-coordination [18], Figure 1.8.

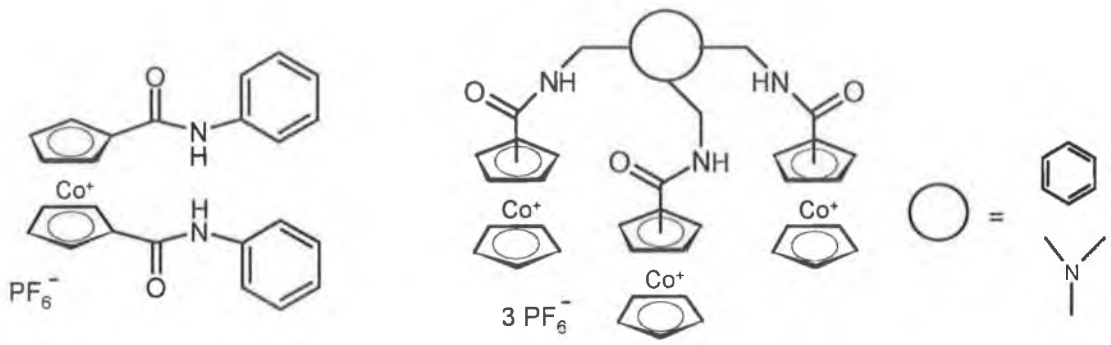

14 **15**

Figure 1.8. Inorganic anion receptors **(14)** and **(15)** containing H-bonding and electrostatic moiety as a functional site to anion binding.

^{1}H NMR anion titration studies showed considerable downfield shifts, particularly for the amide protons, indicative of a strong hydrogen bonding. A considerable degree of hydrogen bond formation was even observed in polar aprotic solvents such as acetonitrile and DMSO.

The stability constants for these receptors **(14,15)** showed differences between different anions. The stability constant of receptor **(14)** was 1200 and 100 M^{-1} for $H_2PO_4^-$ and Cl^-, respectively, whereas **(15)** was 320 and 35 M^{-1} for $H_2PO_4^-$ and Cl^- [18]. These receptors are also capable of electrochemically recognising anions. Addition of an anionic guest stabilises the positive cobalt centre, resulting in substantial cathodic shifts of the reversible Cp_2Co^+-Cp_2Co redox couple.

The importance of hydrogen bonding was further investigated by Beer et al. [19]. Receptors **(16a-c)** indicated that the strength of chloride ion binding is enhanced when additional interactions of amine-halide hydrogen bonding are sterically accessible, as it is in the case of **(16a)** and **(16b)** but not **(16c)**, Figure 1.9.

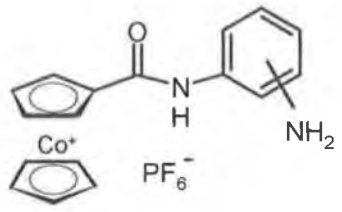

ortho **16a**
meta **16b**
para **16c**

Figure 1.9. The substituent amine in receptor **(16a-c)** would bind efficiently at an ortho position and less with meta and lesser in para position.

Aza-crown substituted cobaltocenium **(17)** has been prepared, an investigation was focused on the electrostatic effect on cobaltocenium in the presence of alkali metal guest within the crown ether rings for anion binding process [20], Figure 1.10.

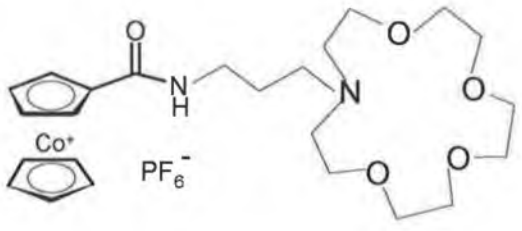

17

Figure 1.10. Crown ether moiety would enhance anion binding in receptor **(17)** in addition of electrostatic effect (cobaltocenium).

Uno et al. followed these preliminary results by preparing a chiral secondary amide possessing a cobaltocenium moiety **(18)** [21], Figure 1.11. ^{1}H NMR of this receptor revealed it could bind anions enantioselectivity, but only to a small degree (estimated at 10%) for one chiral form of the optically active camphor-10-sulfonate anion.

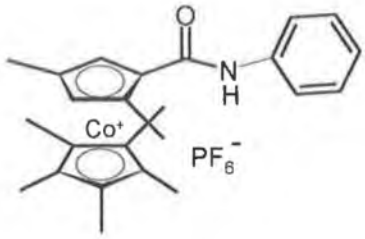

18

Figure 1.11. The ability of receptor **(18)** to bind anions enantioselectively.

A series of bis cobaltocenium systems **(19)** and **(20)** containing a cobaltocenium'arm' have been prepared [18], Figure1.12. These receptors impart further selectivity and enhance binding stability.

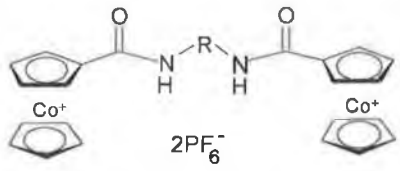

19

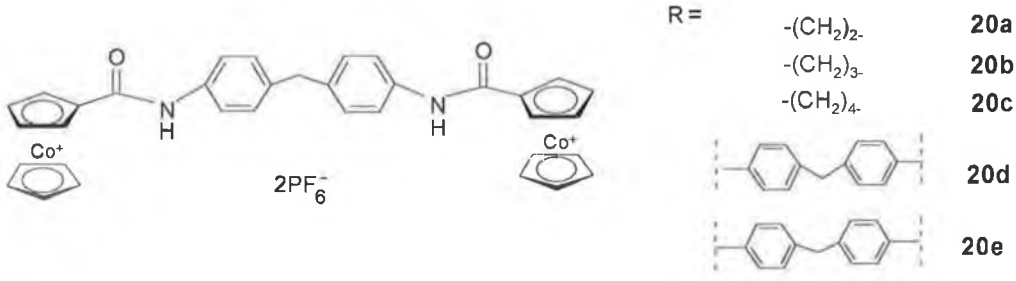

Figure1.12. Receptor **(19)** shows different result in terms of selectivity and binding by the effect of alkyl chain length and the type of amino spacer.

^{1}H NMR studies showed 1:1 complexes with halide anions for the alkyl-linked derivatives **(20a-c)**. Stability constants showed decreasing values when the length of the alkyl chain increased and the selectivity was for chloride over bromide and iodide. Larger aryl or alkyl amino spacers **20d-c** afforded 2:1 stoichiometry between halide anion and receptor.

The macrocyclic effect has been investigated with receptors **(21)** and **(22)** [22]. Stability constants determined from ^{1}H NMR titration studies with chloride anion in DMSO-d_6 gives values of 250 and 20 M^{-1} for the cyclic and acyclic analogues, respectively, thus showing its selectivity based on the "macrocyclic effect", Figure 1.13.

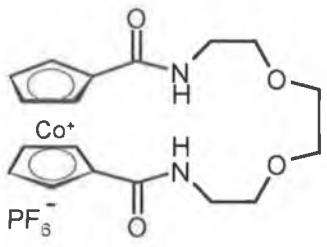

21

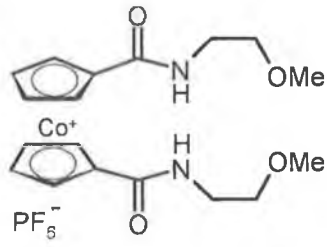

22

Figure 1.13. Different selectivity between receptor **(21)** and **(22)** and that due to macrocyclic effect.

Another macrocyclic receptor **(23)** has been prepared. This receptor acts as a switchable cobaltocenium based chloride binding host [23], Figure 1.14.

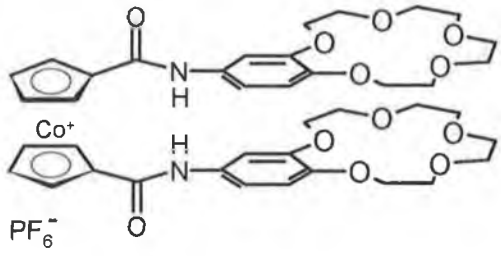

23

Figure 1.14. Switchable anion sensing present by **(23)** with inclusion of cobaltocenium into a crown-ether framework.

The free receptor was abled to bind chloride anions, but by adding potassium ions, the binding system was switched off and that presumably is due to a sandwich complex between a single potassium ion and the two crown ether

substituents which has an effect on the conformation of the amide groups, Figure1.15.

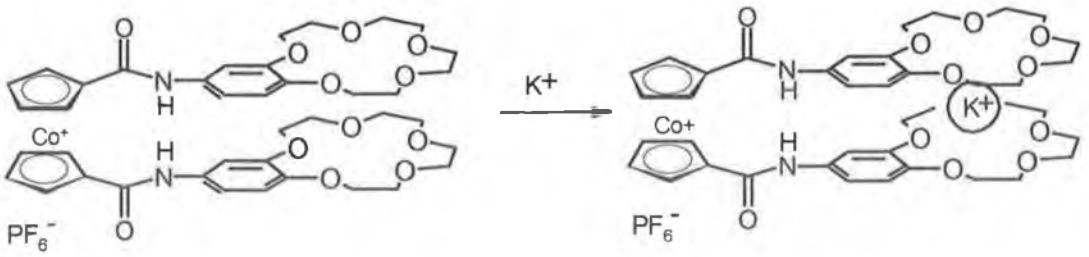

23

Figure 1.15. Addition of potassium anion into receptor **(23)** would produce sandwich complex and consequently will switch off the binding system.

A novel cobaltocenium porphyrin receptor **(24a)** has been synthesised [24], in which four metallocenes are appended to the meso carbons of porphyrin. The cis-ά,ά,ά,ά-atropisomer exhibits the following selectivity trend $Cl^- > Br^- >> NO_3^-$, Figure 1.16. The observation from ^1H NMR titrations in acetonitrile shows shifts of up to 0.70 ppm for the amide, Cp and pyrrole protons upon addition of halide anions. The stable complex was in a 1:1 stoichiometry and gave stability constants of 860 and 820 M^{-1}, respectively, whereas nitrate exhibited weaker binding with K = 90 M^{-1}. In contrast the **(24b)** and **(24c)** atropisomers show less selectivity with the following binding selectivity $NO_3^- > Br^- > Cl^-$, indicating binding is atropisomer dependent Figure 1.17.

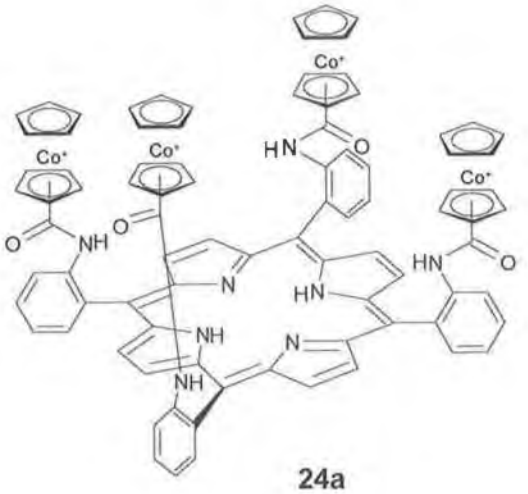

24a

Figure 1.16. Cobaltocenium porphyrin receptor **(24a)** revealed selectivity for halide over nitrate anions.

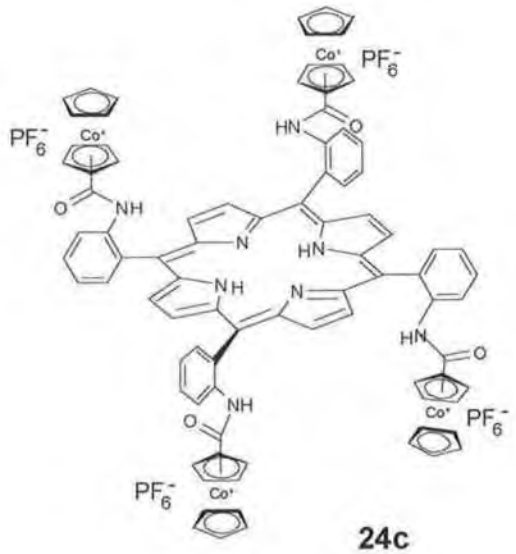

24c

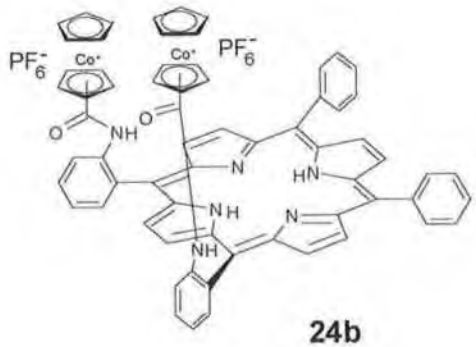

24b

Figure 1.17. Receptors **(24b,24c)** show lower selectivity for anions compared to **(24a)**.

Calixarene framework **(25)** incorporated with aditopic cobaltocenium moieties has also been prepared [18,25], Figure 1.18. ^{1}H NMR spectroscopy showed stable 1:1 anion complexes in DMSO and acetone.

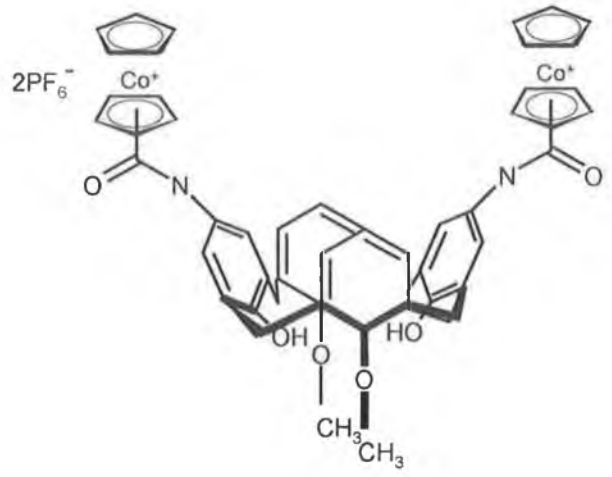

25

Figure 1.18. Aditopic cobaltocenium moieties **(25)** is including calixarene framework showing a selectivity with two anions.

This receptor displayed selectivity for chloride over dihydrogen phosphate which is uncommon. Changing the functionality on the lower rim of this receptor, altered the anion coordination properties. For example, receptor **(26)** showed a reverse trend of selectivity toward dihydrogen phosphate over chloride [26] and that presumably is due to the bulky tosyl groups which may alter the topology of the upper rim anion binding site, Figure 1.19.

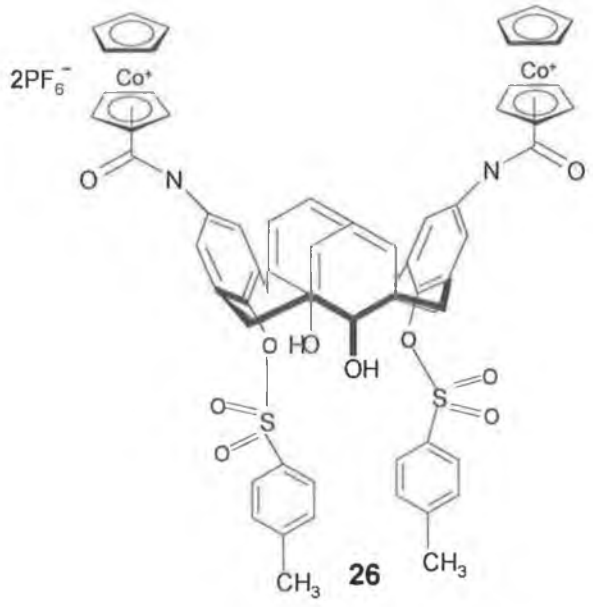

26

Figure 1.19. Receptors **(26)** bearing two tosyl groups which would effect upper rim topology, leading to a change in binding.

1.2.3 Ferrocene-based anion receptors

Ferrocene has also been incorporated into anion receptors, but the neutrality was one of the significant differences for the ferrocene analogues compared to the cobaltocenium systems, and therefore, the ferrocene derivatives possess no inherent electrostatic interaction. The ferrocene could not interact with anions until it was oxidized, thus ferrocene can be switched on for electrostatic interaction by oxidation [27]. Ferrocene units appended with secondary amides have also been employed for anion recognition and a series of simple amide-functionalised ferrocene derivatives **(27-30)** were prepared and investigated for their anion recognition properties by Beer et al. [28,29], Figure 1.20.

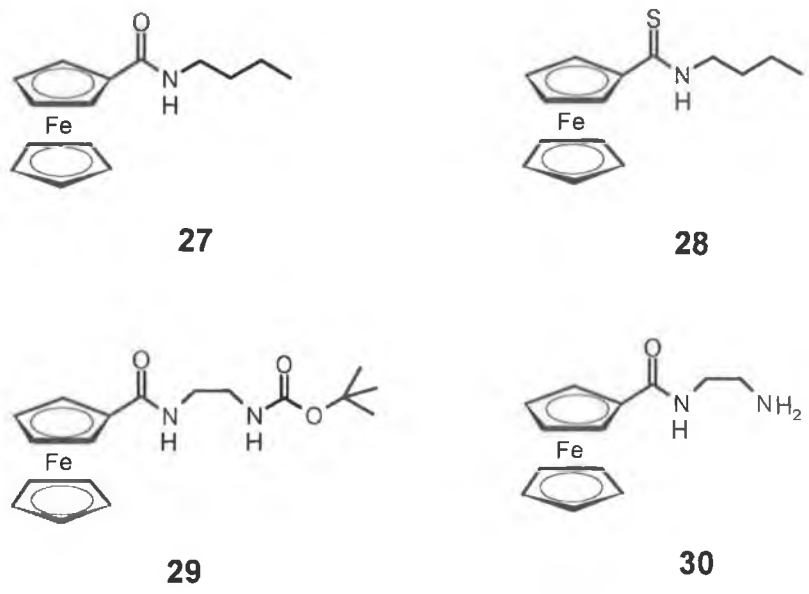

Figure 1.20. Receptors **(27-30)** based on amide-functionalised ferrocene showing different affinity for anions.

These receptors have been developed and utilized as hydrogen bond donors to introduce anion selectivity which is analogous to that of enzymes. The neutral secondary amine groups were incorporated in to this system to act as both hydrogen bond donors and acceptors (difunctional character), subsequently, enhancing the anion recognition process and selectivity. The potential for these novel receptors is for use in electrochemical anion selective redox sensors. Thioamide receptor **(28)** was found to bind halide anions more effectively than **(27)** whereas receptor **(29)** proved to be the most efficient. The example of a difunctional receptor is **(30)** which possesses improved selectivity as determined by ^{1}H NMR and electrochemical detection toward hydrogen sulphate anion. This selectivity is attributed to the presence of the basic amine which is protonated by the hydrogen sulphate anion, therefore, the protonated receptor shows a high binding affinity for sulphate anion. It is argued that two different modes of anion binding are possible. Mode **(A)** was operating for non-acidic guests and relies on the receptor donating hydrogen bonds from the amide, Figure 1.21. Mode **(B)** was operating for acidic guests where a proton is transferred from the guest anion to the receptor, followed by hydrogen bonding and electrostatic

interaction. Receptor **(30)** binds moderately to dihydrogen phosphate and it is believed that the binding mode is intermediate between the two modes of binding, therefore, the amine group would enhance the selectivity for acidic anion guests.

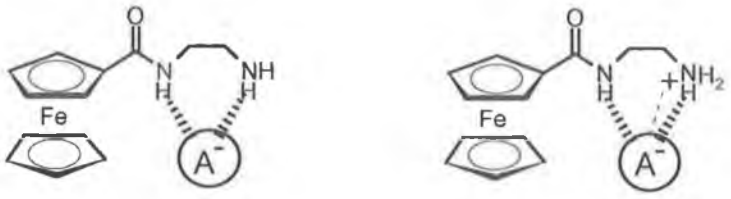

Mode A: Hydrogen bonded only.

Mode B: Electrostatic and hydrogen bonding.

Figure 1.21 The two different modes of anion binding of receptor **(30)**

In an attempt to mimic nature, anion receptors such as **(31)** and **(32)** with three dimensional arrangements of hydrogen bond donating groups were developed [30], Figure 1.22. Electrochemical experiments showed detection of $H_2PO_4^-$ anion in the presences of a ten-fold excess of HSO_4^- and Cl^- ions, where the selectivity was found to be $H_2PO_4^-$ > HSO_4^-> Cl^- in a 1:1 receptor: anion stoichoimetry for all three anions.

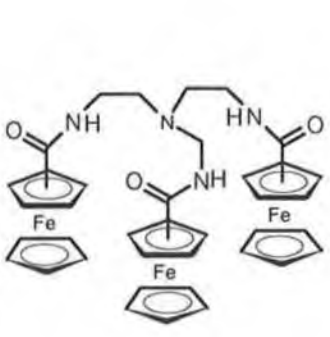

31

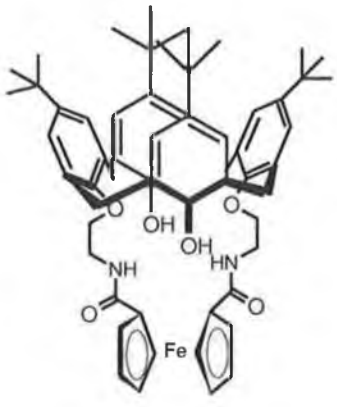

32

Figure 1.22. Anion receptors **(31,32)** showing selectivity for hydrogen phosphate even in the presence of a ten-fold of HSO_4^- and Cl^- ions.

Ferrocenyl groups were introduced onto the lower rim of the Calixarene [31,32]. Receptor **(33)** was able to bind and complex anions with a 1:1 receptor:anion stoichiometry. Cl^-, $H_2SO_4^-$ and $H_2PO_4^-$ showed the largest positive shift of the ferrocene/ferrocenium redox couple, Figure 1.23.

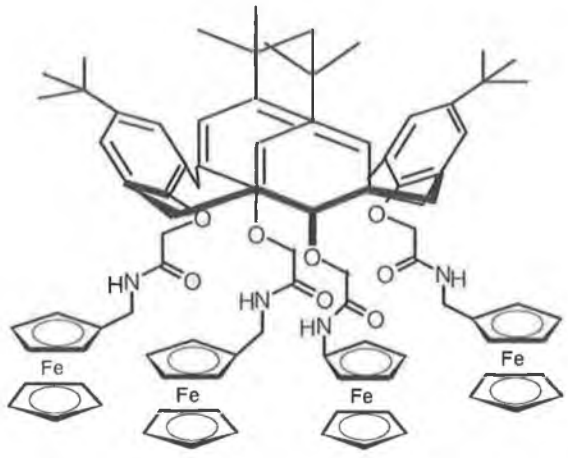

33

Figure 1.23. Calixarene receptor **(33)** with attaching ferrocenyl moiety in the lower rim enhance the complexation with anion.

Phosphine functionalities have also been introduced into ferrocene-based systems containing amide functionalities [32]. Incorporation of the phosphines to a transition metal enhances the strength of anion binding **(34-36)**, Figure 1.24. These receptors show anion recognition, in 1:1 acetonitrile/dichloromethane, via significant cathodic perturbations based on the ferrocene and transition metal oxidation wave. The greatest strength of anion binding was with Ru-(bpy)-substituted receptor **(36)**.

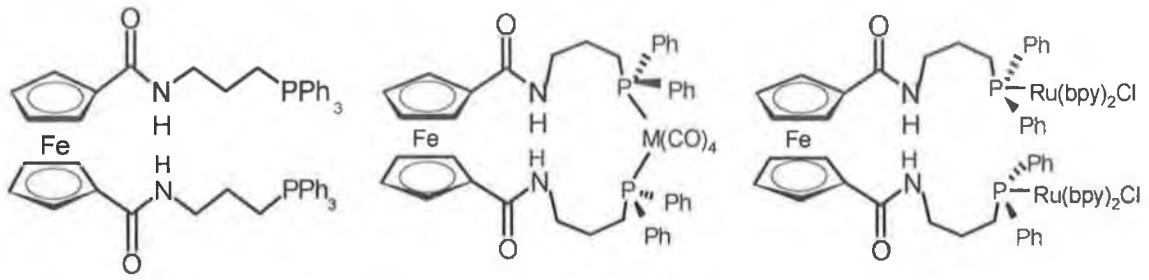

34 **35** **36**

Figure 1.24. Amide-ferrocene receptors **(34-36)** with appending phosphine moiety enhance anion binding particularly with **(36)**

Recently Beer et al. have been able to prepare a new water soluble polyaza ferrocene macrocyclic ligand that can bind and electrochemically sense phosphate and sulphate anions [33,34]. These amino ferrocenyl compounds were able to detect both transition metal cations and anions, while the selectivity depended on pH conditions. This functionality results in the so-called dual purpose sensor which are, pH dependent, showing potential as prototype amperometric sensors such as **(37)**, Scheme 1.3.

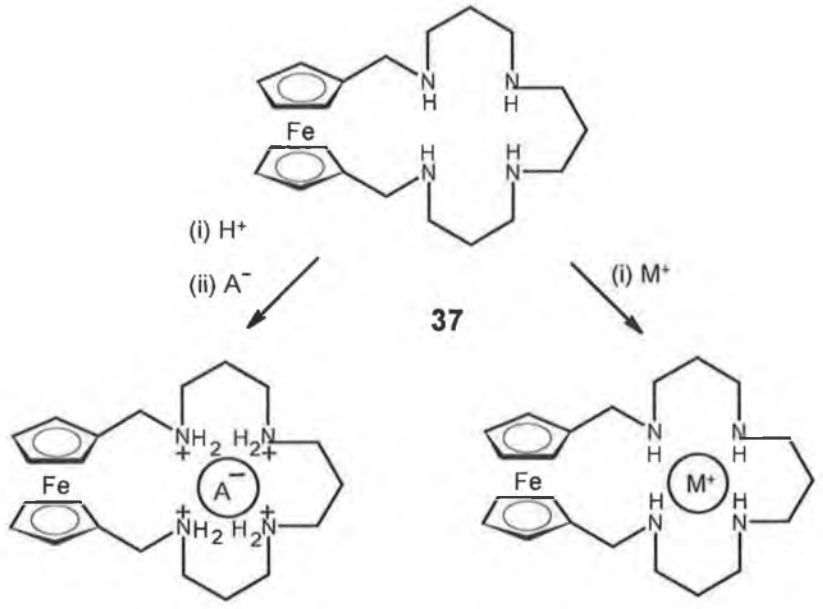

Scheme 1.3. The dual function of receptor **(37)**, presenting its potential as a prototype amperometric sensor.

Receptors **(38)**, **(39)** and **(40)** were able to complex adenosine triphosphate and hydrogen phosphate in water at pH 6.50, where at least two of the nitrogen atoms are protonated, 1:1 complexes were formed, Figure 1.25. Electrochemical studies at the same pH showed 60-80 mV cathodic shifts with phosphate anions.

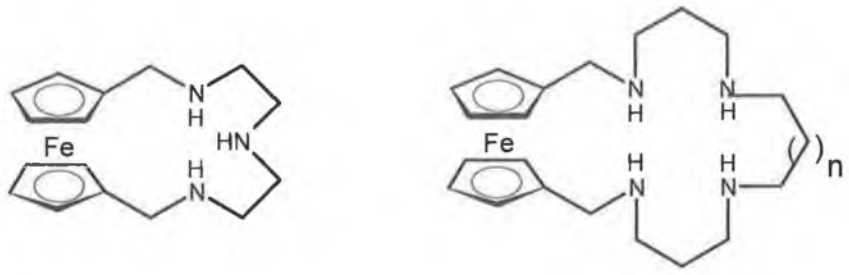

38

n=1 **39**
n=2 **40**

Figure 1.25. Receptors **(38-40)** are able to bind ATP and $H_2PO_4^-$ in water at pH 6.50.

A new class of anion receptor possessing ferrocenyl imidazolium salts have been synthesised by Howarth and co-workers [35a], Figure 1.26. They designed receptor **(45)** based on the ferrocenyl moiety as a redox site, with the added combination of a hydrogen bond on the electron deficient C-2 carbon atom of the imidazolium ring. It was found that the C-H----X^- hydrogen bonding enhanced anion recognition. This receptor was able to detect anions such as Cl^-, Br^-, I^-, NO_3^- and HSO_4^- in $CDCl_3$, whereas the H-2 proton of the imidazolium ring revealed significant shifts accompanied by signal broadening, with a 1:2 receptor:halide binding stoichiometry, and 1:1 with nitrate and sulphate. Electrochemical studies of receptors **(41-45)** showed that the oxidation potential shifted anodically with increasing substituent size. When five equivalents of a particular counter ion was added, the anodic wave was observed to shift to more negative potentials, excluding bromide salt which gave a positive shift and in each case the largest negative shift achieved when five equivalents of the HSO_4^- ion were added.

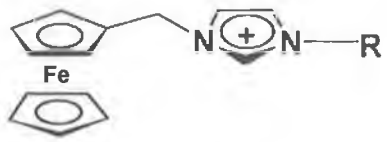

41 R = Me
42 R = Et
43 R = Pr
44 R = Bu
45 R = $FcCH_2$

Figure 1.26. Receptors **(41-45)** based on imidazolium ring and ferrocene.

Later on Howarth and co-workers (Dallas) [35b] developed series of anion receptors, based on azolium and ferrocene moieties, to be investigated for anion recognition, see Figure 1.27.

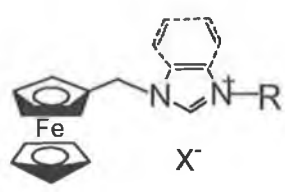

Az	R	X	
Im	$CH_2C_6H_5$	Cl	46
Bzim	CH_3	I	47
Bzim	C_2H_5	I	48
Bzim	C_3H_7	I	49
Bzim	C_4H_9	I	50
Bzim	$CH_2C_6H_5$	Cl	51

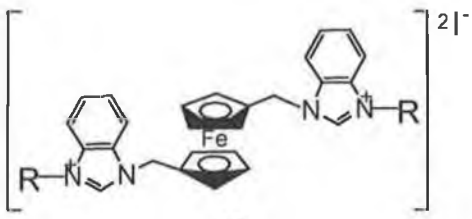

R	
CH_2	52
C_2H_9	53

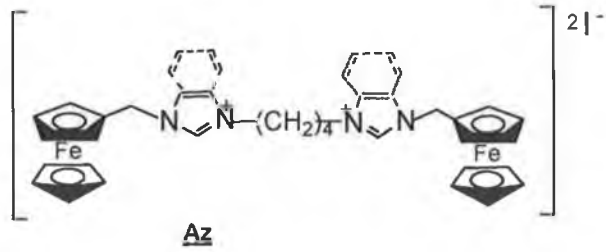

Az	
Im	54
Bzim	55

Figure 1.27. New classes of azolium ferrocene receptors **(46-55)**.

1.2.4 Imidazolium tripodal based anion receptors

More recently, the tripodal imidazolium derivative **(56)** has been described as a new anion receptor with C---H----X^- hydrogen on the electron deficient C-2 carbon atom of the imidazolium ring and guest anions such as Cl^-, Br^-, and I^- [36], Figure 1.28.

It has been demonstrated that the imidazolium based tripodal receptor **(56)** has considerable affinity for halide anions in polar solvent through electrostatic interactions and C---H---X^- hydrogen bonds. ^1H NMR studies revealed significant large downfield shifts (δ>1.30ppm) with concomitant broadening in the signal of the C-2----H of imidazolium moieties until 1 equivalent of Cl^- was added. The same was observed for Br^- and I^-.

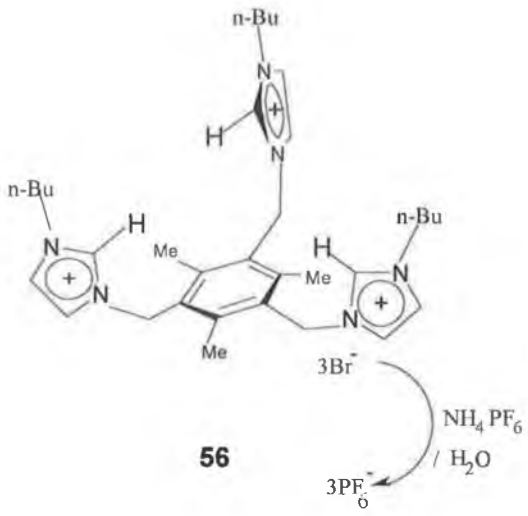

Figure 1.28. Receptor **(56)** based on tripodal imidazolium ligand, showing the ability to bind halide anions according to hydrogen bonding and electrostatic force.

Further evidence for the complexation of the halide anion via hydrogen bonding was obtained from association constants and binding free energies which were determined, from their titration curves by using a non-linear least-squares curve-fitting program [37]. The association constants are fairly large for halide anions (75000-7200 M^{-1}), and the magnitude of the chemical shift changes and association constants decrease in the order $Cl^- > Br^- > I^-$, consistent with their relative hydrogen- bonding abilities and surface charge density [38]. Sato and co-workers have also prepared two more receptors **(57)** and **(58)** for comparison purposes and have shown the same result in the case of titration, but obtained different association constants which were relatively small compared to that of **(56)**.

In receptor **(57)**, the absence of the methyl groups at the ortho position resulted in a 50-times smaller association constant compared to that of **(56)** for chloride. Presumably, this difference is a result of conformational flexibility of **(57)** compared to **(56)** [39-41], Figure 1.29.

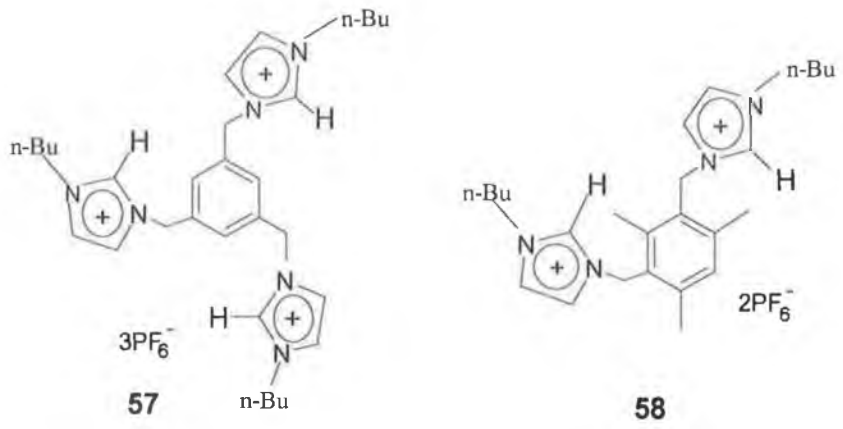

Figure 1.29. Receptors **(57,58)** show smaller association constants than **(56)**.

A similar tendency was observed in bidentate receptor **(58)**, in which one of the imidazolium methyl units was removed. Therefore, both the three imidazolium methyl groups at the positions-1,3,5 and the 2,4,6-substituents are believed to provide a favourable environment for the formation of a stable complex with halide anions. On the basis of this data they proposed a possible structure of the complex between **(56)** and halide ion in a syn conformation, Figure 1.30.

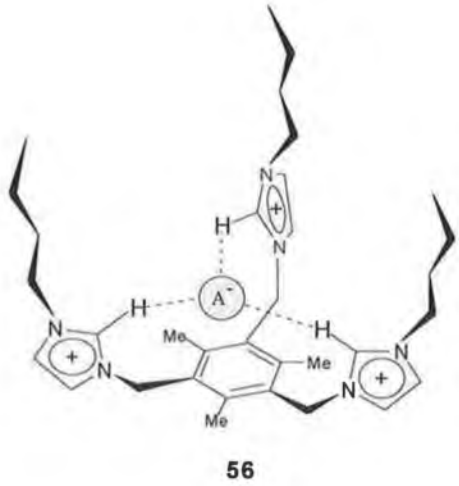

Figure 1.30. A possible structure of **(56)** with halide anions.

Other imidazolium tripodal receptors have been synthesised by Anslyn et al., [39] Figure 1.31, presenting an interesting complexation between tripodal receptors **(59-61)** and various biologically active anions: e.g. (phosphate and carboxylate) [42].

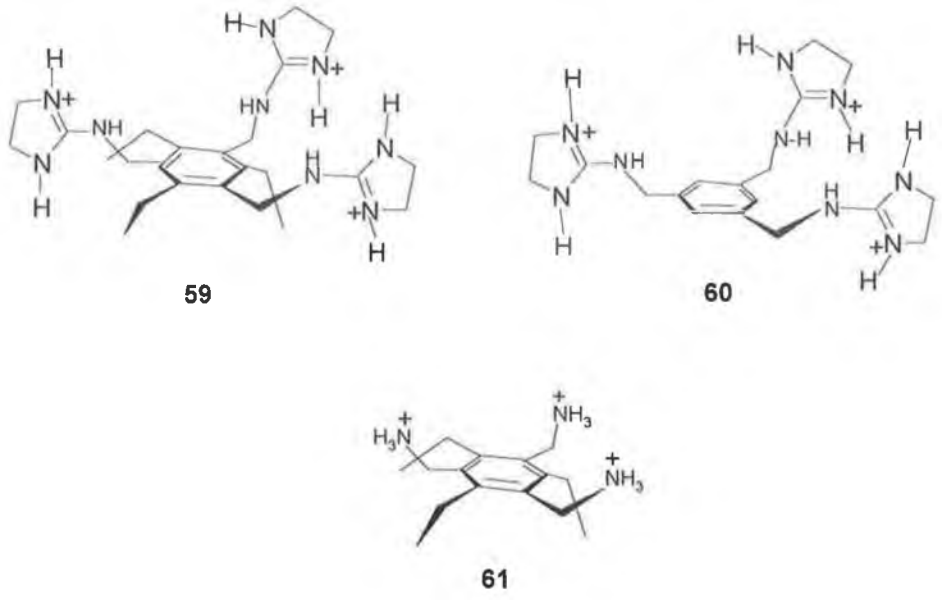

Figure 1.31. Receptors **(59-61)** target biological anions.

The complexation of several anionic guests by **(59)** was studied by ^{1}H NMR spectroscopy. Binding constants were obtained by ^{1}H NMR titration techniques [43]. Citrate and tricarballate (1,2,3-propanetricarboxylate, a citrate analogue lacking the OH) yield binding constants near 7×10^{3} M^{-1} in pure water. Although, ATP^{-4} has greater charge, it did not result in a stronger complexation, indicating the complementarity between receptor **(59)** and the anion. Smaller binding constants for succinate and glutarate were found (both near 2×10^{2} M^{-1}). Acetate showed very weak binding (estimated to be<10 M^{-1}), but the binding isotherm indicated equilibria beyond simple one to one association. Receptor **(59)** is also capable of binding citrate in a crude extract of orange juice at pH 7.40, remarkably with a binding constant of 4.60×10^{3} M^{-1}. The influence of other carboxylates in orange juice (e.g. maleate, ascorbate, and succinate) [44], ionic strength, and other compounds such as organic, inorganic phosphates as well as

sugars is small, emphasizing the selectivity of **(59)**. They were examined by verifying that guanidinium groups are important in the carboxylate recognition, the result of that shows the binding constant in pure water equals 3×10^3 M^{-1}, less than half the binding constant of **(59)**. Since ammonium cations in other hosts are typically better receptors for carboxylates in water [45], this led to the conclusion, that when extensive hydrogen bonding, and not just charge pairing is involved in the host/guest complex guanidinium groups are better receptors for carboxylate. Furthermore, they verified the advantages to binding imparted by the preorganization of **(59)**. The analogue **(60)**, which lacks steric preorganization, yielded a binding constant of only 2.4×10^3 M^{-1} with citrate. Therefore, host **(59)** is indeed quite complementary to citrate and possesses good selectivity for citrate-like structures.

Recently Steed and co-workers have synthesised a series of " venus flytrap" anion receptors. These receptors were based on podands with a hexa-substituted core and functionalised with hydrogen-bonding and cationic pyridinium groups, in which a ferrocenyl group was attached to the pyridinum **(62)** [46], Figure 1.32. The host is preorganised in a cone conformation and shows considerable binding for halides, particularly chloride. The complexation-induced chemical shifts was up to 1.54 ppm for the NH protons in CD_3CN, where the selectivity trend is Cl^-> Br^->I^-, and some selectivity is also shown for acetate. Preliminary electrochemical studies revealed a relatively poor coupling between binding and signalling moieties, but the observed selectivity sequence was in a agreement with that obtained by NMR.

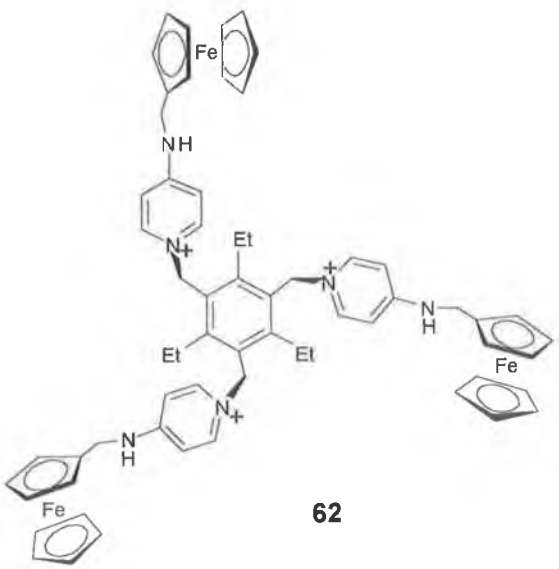

62

Figure 1.32. New tripodal anion receptor **(62)** based on ferrocenyl pyridines.

1.3 Enantiomeric discrimination

One of the great problems faced by the pharmaceutical industry involves the quantitation of undesired enantiomers in drug raw material. Quite often only one enantiomer of a chiral compound is actually a bioactive therapeutic, the other enantiomer in some cases is non-bioactive or if bioactive it may cause undesirable side effects. It is therefore essential that the final product be properly analysed for enantiomeric purity.

In order to determine enantiomeric purity, it has become desirable to create a specific host molecule which could act as a molecular sensor, with the capability to differentiate enantiomers. Such molecular sensors would afford rapid and fast effective analysis for enantiomeric materials.

To design any molecular sensor, the main issues to be addressed are; (1) recognition of the target species; (2) transduction of the binding event; (3) immobilization or controlled localization.

An excellent example of such a system is Rebeck's and co-workers receptors **(63a,b)**, which contains self-complementary [47,48] glycoluril and cyclic sulfamide functionalities [49], Figure 1.33.

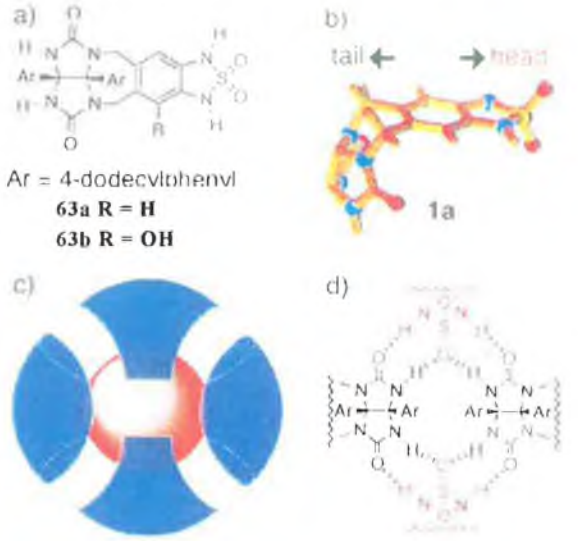

Figure 1.33. (a) The chemical structure of achiral **(63a)** and chiral **(63b)** tetramer subunits. (b) A three-dimensional representation showing the shape and curvature of **(63a)**. (c) The four identical subunits arrange in a head-to-tail manner and encapsulate a guest molecule. (d) The seam of 8 hydrogen bonds between sulfamide and glycolurils present at each end of the tetrameric capsule.

Each subunit self-assembles through hydrogen-bonding, to give a cyclic tetrameric capsule, Fig.1.33c [50], where the end of the capsule is comprised of a circular seam of 8 hydrogen bonds between the glycoluril and cyclic sulfamide functionalities Fig.1.33d. A variety of chiral guests were screened to determine if encapsulation with the cavity of (-)-**(63b)** would occur. It was revealed that racemic mixtures of various ketones were discriminated by (-)-**(63b)**, Figure 1.34. Both enantiomers of norcamphor and 3-cyclohexanone could be discriminated by (-)-**(63b)** as indicated by ^{1}H NMR Fig. 1.33. Modelling studies indicate that 3-methyl cyclohexanone binds with the ketone oxygen with one of the cavity of hydrogen bonds while the methyl group is directed at the hydroxyls of the complex.

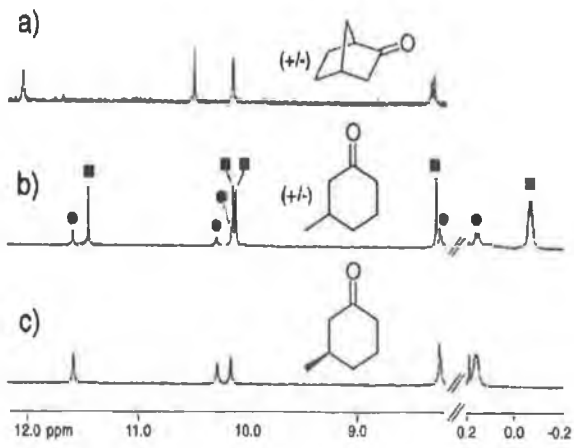

Figure 1.34. ^{1}H NMR spectrum of (-)-**63b** for enantiomeric selectivity; (a) nonselective encapsulation from a racemic mixture of norcamphor, (b) highly selective from a racemic mixture of 3-methylcyclohexanone, (c) encapsulation of (R)-(+)-3-methylcyclohexanone. (●) Resonances attributable to encapsulation of the (R)-ketone, where(■) is for the (S)-ketone.

Rebek and co-workers have investigated another system receptor **(64)** [51,52], Figure 1.35. This molecular host shows poor binding in solution [53], but forms complexes with ions in the gas phase [54] and yields host-guest complexes in the solid state [55]. They further developed **(64)** to **(65)**.

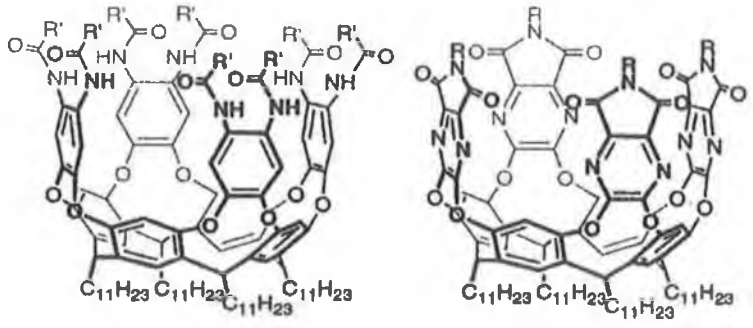

64 65

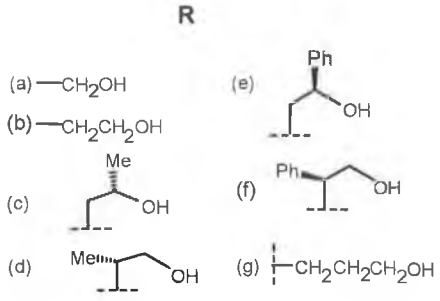

Figure 1.35. A new structural motif for synthetic receptors **(64)** and **(65)** allow for the incorporation of a variety of non-racemic groups into the structure's upper rim.

These compounds have been investigated for enantiomeric discrimination through ^{1}H NMR spectroscopy. The host-guest complexes between nonracemic or racemic trans-1,2-cyclohexanediol in **(65c)** and **(65d)** were tested, Figure 1.36, Receptor **(65c)** shows no discrimination between the enantiomers of cyclohexanediol, Fig.1.36(a,b), while the isomeric form **(65d)** shows a 33% diastereomeric discrimination for cyclohexanediol, Fig.1.36(c,d).

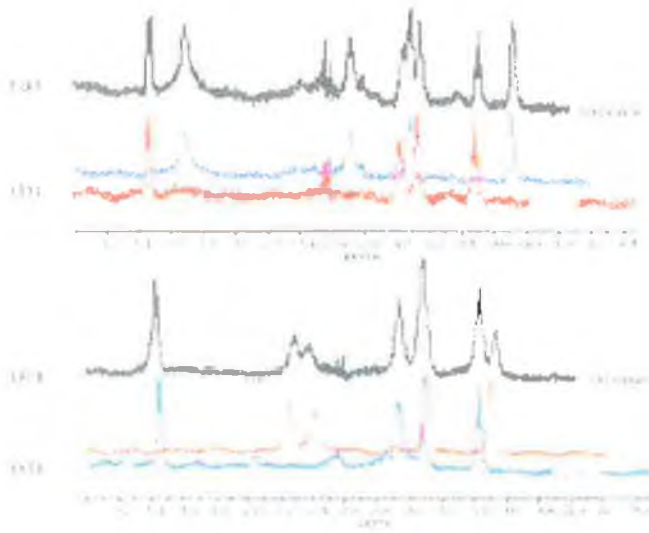

Figure 1.36. The ^{1}H NMR spectrum for host-guest complex between (a) racemic trans-1,2-cyclohexanediol and **65c**, (b) optically active trans-1,2-cyclohexanediol and **65d**, (c) racemic trans-1,2-cyclohexanediol and **65d**, and (d) optically active trans-1,2-cyclohexanediol and **65d**.

From this work it was determined that when the stereocentre is closer to the phthalimides the stereogenic environment inside the capsule becomes more pronounced (twisted). This result is in agreement with the CD experiments that show a larger induced signal for **(65d)** as compared to that of **(65c)**. It was also found that by increasing the steric bulk (by using a phenyl instead of a methyl) increases the diastereoselectivity to about 60% (de) for **(65e)** and **(65f)** [56,57].

Crown ethers **(67)** prepared from 1,1-binaphthyl skeletons **(66)** have shown an ability for enantioselective recognition [58-63], Scheme 1.4.

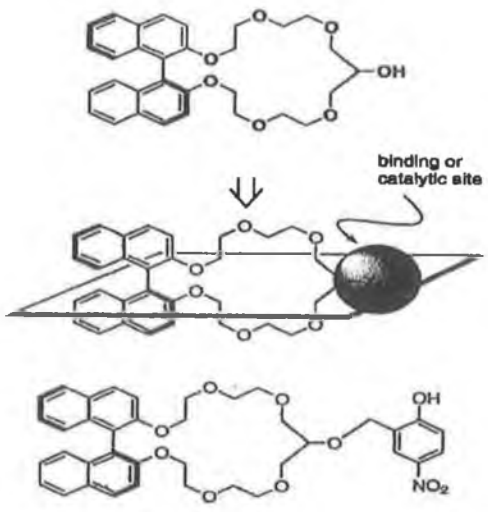

66

67

Scheme 1.4. Nitrophenol as a lartait moiety was attached to receptor **(66)**, leading to produce receptor **(67)**.

The binding properties of receptor **(67)** was evaluated by NMR titration studies with *n*-butyl amines, Figure 1.37. These experiments showed the signals of *n*-butylamine *p*-nitrophenolate shifting to lower magnetic field relative to the free *n*-butylamine. This observation could be attributed to a decrease in the electron density of the nitrogen atom Fig.1.37a, where as the signals relating to *n*-butylamine in the 1:1 complex were shifted to a higher magnetic field Fig.1.37c. This indicates that the *n*-butylamine is located within the shielding field of the naphthyl rings of host **(67)**. Furthermore this host has been examined for chiral anion recognition using UV titration, and Ka calculated. It was found that the association constants were generally moderate and enantioselectivity ratio small, with an assumed 1:1 binding. Unambiguous chiral discrimination was found for phenyl glycinol (K_R/K_s = 3.20), whereas phenyl alaninol shows some selectivity (K_s/K_R = 1.70) but the degree of selectivity was small.

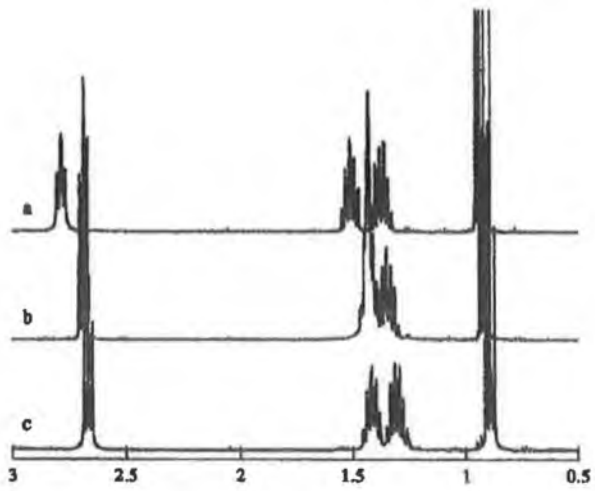

Figure 1.37. Partial ^{1}H NMR spctrum of (a) *n*-butylamine *p*-nitrophenolate, (b) *n*-butyl amine and (c) 1:1 mixture of host **(67)** and *n*-butylamine in $CDCl_3$ at 25 °C.

Dinaphthyl moieties have also being introduced into the lower rim of calixarene, an example is compound **(68)**. This compound showed enantiomeric discrimination of 1-phenylethylamine, Fig.1.38. The (R)-enantiomer causes colour change and a shift in the electronic absorption of the calixarene from 515 to 538 and 650 nm, whereas the (S)-enantiomer caused no change in colour [64]. This colour change is attributed to the deprotonation of the indophenol on one side of calixarene (long wavelength) and a hydrophobic interaction between the chiral guest amine and the binaphthyl on the other side (short wavelength). It is the hydrophobic interaction between the guest chiral amine and the binaphthyl calixarene substituent that is enantiomer-dependent. The presence of the different enantiomers can therefore be detected through colour changes.

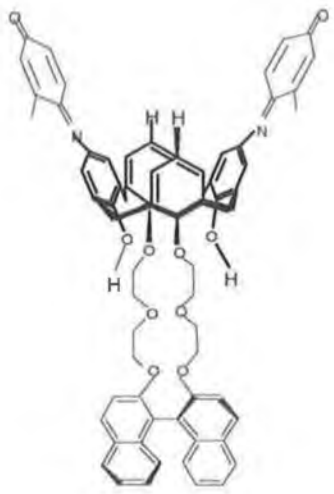

68

Figure 1.38. Compound **(68)** showed the ability to discriminate between two enantiomers of phenylethylamine by colour changes.

Recent work has been focused on hemicarcerand systems, for possible applications in bio sensing and asymmetric catalysis [65]. Warmuth and co-workers have exploited the hemicarcerands to prepare receptor **(69)** [66] with six attached glycine units [67,68], Figure 1.39. Also hemicarcerand **(69)** has two coumarin groups, which are attached via flexible ethylenedioxy linking groups. The aim of this approach was to focus on chiral recognition inside the inner phase of the achiral hemicarcerand with one extended equatorially located portal [69], [70].

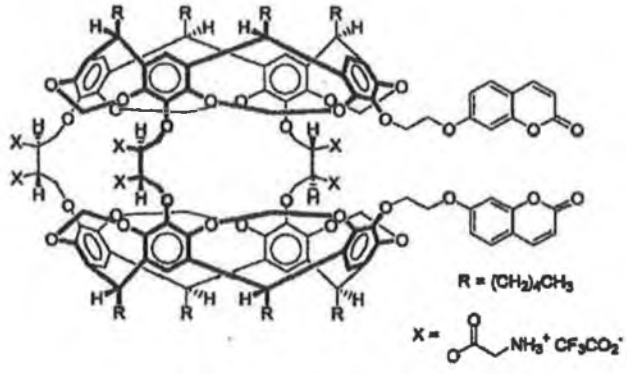

69

Figure 1.39. Hydrophilic hemicarcerand receptor **(69)** with attachment of six glycine is able to recognize chiral anions.

This receptor has been investigated for chiral recognition by applying different chiral compounds as guests **(A-F)**, Scheme 1.5, which led to the formation of diastereomeric complexes, which were characterized by NMR titration, Figure 1.40.

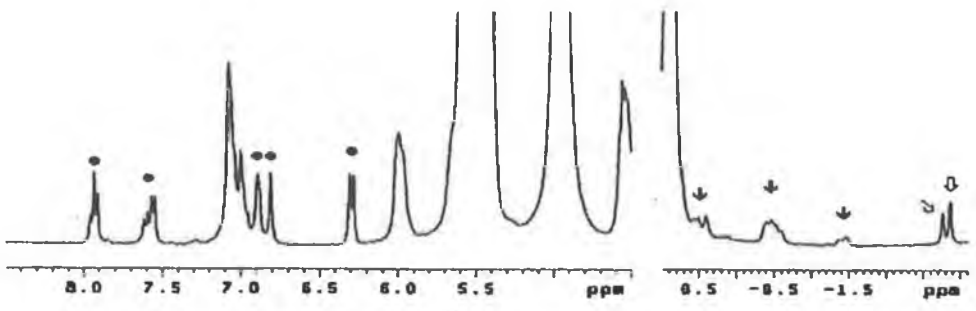

Figure 1.40. ^{1}H NMR spectrum showing diastereomeric complexes **(69)** with (+)-**E** or (-)-**E**, represented by opened white arrows. (•) indicate the protons of the coumarin moieties of **(69)**. Filled black arrows indicate methylene and methane protons of complexed **E**.

The highest diastereomeric excess de = 20% was observed for 3-methyl-cyclohex-1-ene **(E)**, Fig.1.40, when the larger enantioselectivity was observed for hemicarcerands that contain binaphthyl groups as chiral elements [71,72]. The diastereoselectivity was observed in spite of very similar size and shape of (+)-**E** and (-)-**E** compared to the enantiomers of **(B)** and **(C)**. The selectivity was attributed to the dispersion interactions between the C-H bonds of both enantiomers and the electron-rich aryl units in the asymmetrically twisted inner phase of **(69)** [73]. Both enantiomers of the more flexible **(B)** and **(C)** are able to change their conformation such as to maximize their interaction with the surrounding host, unlike **(E)** which is far more rigid. Thus the rigidity and inner phase-guest shape-complementarity are important guest properties to achieve high enantioselectivity in molecular recognition by open shell hemicarcerands [74].

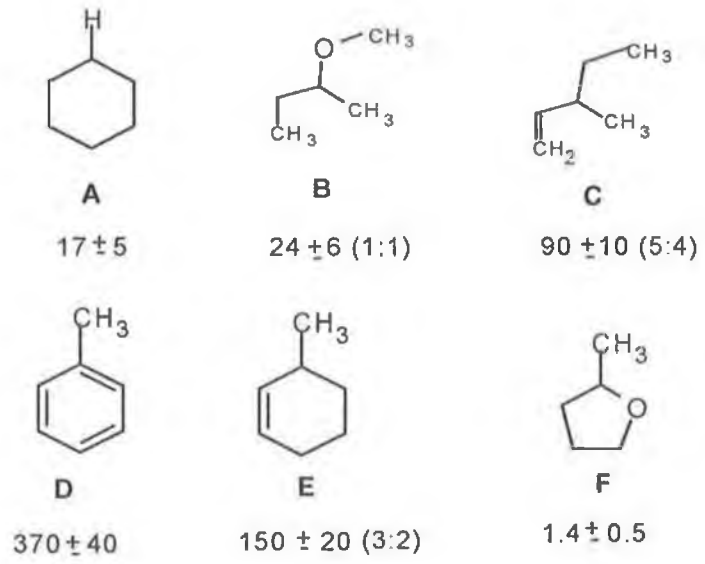

Scheme 1.5. Complexed achiral and chiral guests with receptor **(69)**. The diastereomeric ratio (in parentheses) are given underneath the compound symbol.

Recently, Diamond and co-workers prepared two new calix[4]arene derivatives **(70)** and **(71)** [75]. Calix[4]arene **(70)** has been able to discriminate between enantiomers of phenylalaninol through the quenching of the fluorescence emission in methanol, in contrast **(71)** can discriminate between the enantiomers of phenylglycinol, but not phenylalaninol, Fig. 1.41.

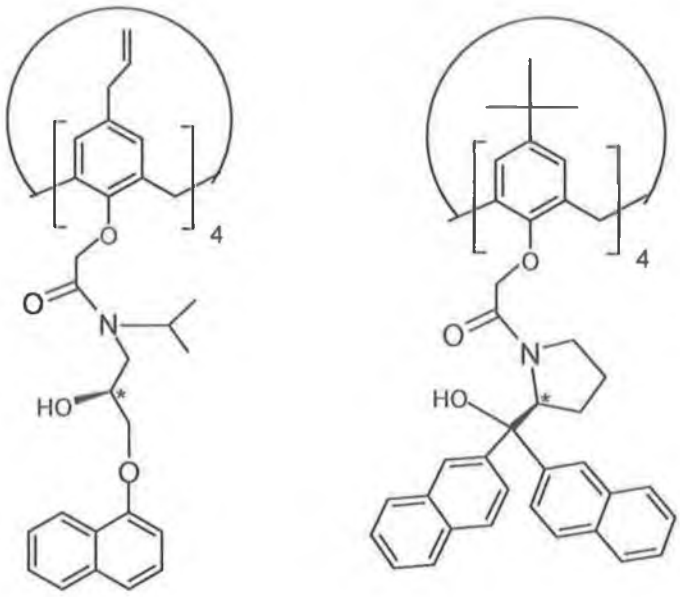

70 **71**

Figure 1.41. Two calixarene[4] derivatives of propranolol amide of *p*-allylcalix [4]- arene **(70)** and (S)-dinaphthylprolinolcalix[4]arene **(71)**.

1.4 Carbene

Carbenes have played an important role in organic chemistry. While much of the early chemistry of these laboratory curiosities was established in the 1950s by Skell [76], it was Fischer and his students who introduced carbenes into inorganic and organometallic chemistry in 1964 [77]. Suffice to say that metal carbenes have found significant applications, particularly in organic synthesis, catalysis, and macromolecular chemistry [78-81].

1.4.1 Nucleophilic carbene

The chemistry of nucleophilic carbenes dates back to the early 1960s and much of the pioneering work was done by Wanzlick [82,83]. Species such as **(72A)** and **(72B)** were examined at that time; precursors of **(72)** include the dimeric and electron-rich olefin **(73)** and imidazolidine **(74)** (by thermal elimination of chloroform), Figure 1.42. Cross coupling experiments showed that **(74)** is not in equilibrium with the two carbene units **(72)** [84], on the other hand, it is certain that the C-C double bond of **(73)** is cleaved in reactions with electrophiles with the liberation of **(72)** [85]. The influence of donor groups on the stability constant of carbene **(72)** have been clearly recognized and an even larger effect was correctly predicted for structurally related carbenes of type **(75)** which possess an" aromatic resonance structure" **(75A,B,C** and **D)** [82], Scheme 1.6. However, serious attempts to isolate carbenes of type **(72)** and **(75)** were not achieved until 1991.

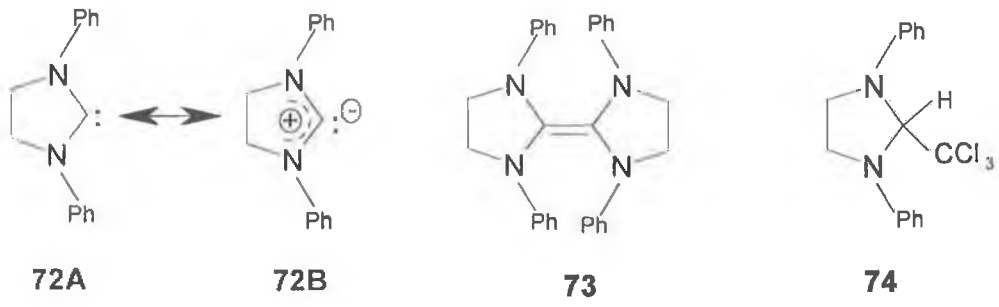

Figure 1.42. Nucleophilic carbene **(72 A,B)** and its derivatives **(73,74)**.

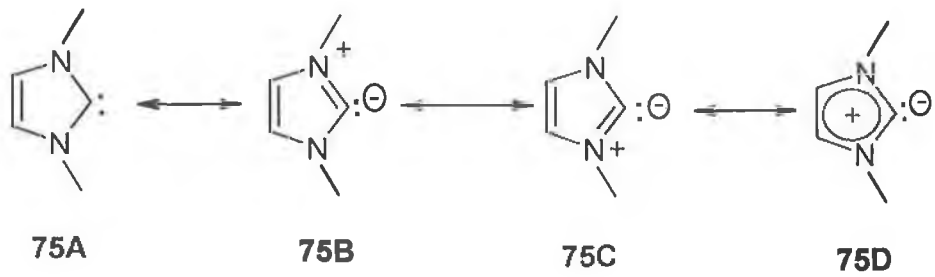

Scheme 1.6. The imidazolidine carbene **(75)**.

1.4.1.1 Imidazolium carbenes.

In 1970 Wanzlick and co-workers were able to demonstrate that imidazolium salts such as **(76)** and **(79)** can be deprotonated by potassium *tert*-butoxide to produce carbenes **(77)** and **(80)**, respectively, Scheme 1.7. By using phenyl isothiocyanate as a trapping agent, the zwitterion **(78)** [86] was isolated, and treatement with mercury acetate gave carbene-complex **(81)** [87].

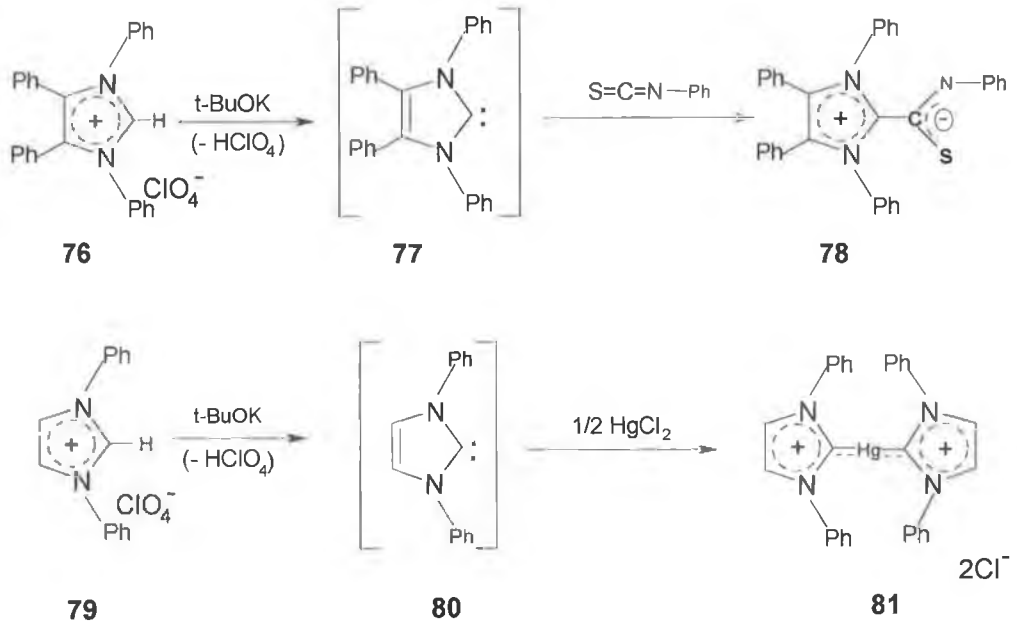

Scheme 1.7. Two imidazolium precursors **(76)** and **(79)** were successfully converted to carbenes **(77)** and **(80)**.

Two decades later Arduengo and co-workers [88] were successful in isolating electronically stabilized nucleophilic carbenes by preparing bis(1-adamantyl) imidazolium chloride **(82)**, which was deprotonated with sodium hydride in THF in the presence of dimethyl sulfoxide anion as a catalytic agent producing **(83)**, Scheme 1.8.

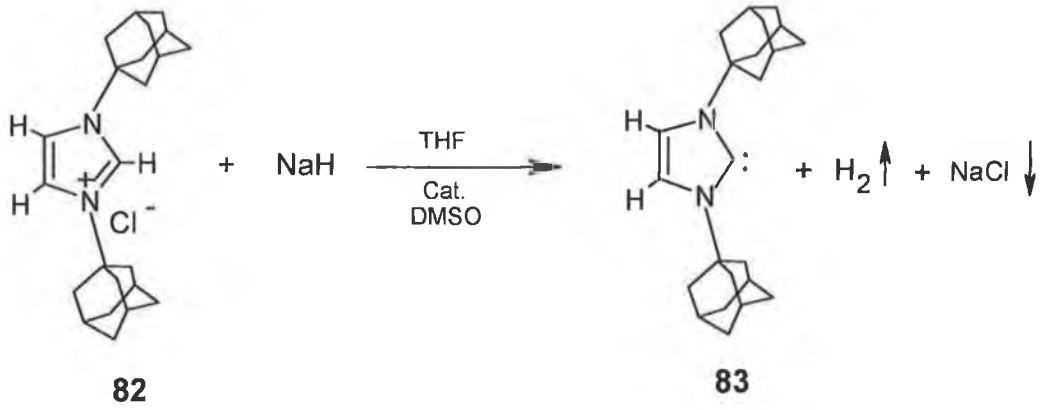

Scheme 1.8. The stability of **(83)** is attributed to a combination of steric and electronic factors [89, 90].

This compound **(83)** afforded a colourless, crystalline and thermally stable product in 96% yield. The ^{13}C NMR spectrum of **(83)** showed the position of the C-2 carbon to be at 211 ppm which is standard for carbenes.

Areduengo believed that the kinetic and thermodynamic stability of this carbene can be attributed to steric and electronic factors [91]. The electronic factors operate in both the **σ** and **π**-mode. In the **π**-mode, electron donation into the carbene out of-plane p-orbital by the electron-rich system (N-C=C-N) leads to a "moderation" of the typical electrophilic reactivity of carbenes. The **σ**-mode, would give additional stability for the carbene electron pair which may be gained from the **σ**-electron-withdrawal effects on the carbene centre by the more electronegative nitrogens, and this would serve to moderate the nucleophilic reactivity of the carbene. The overall combination of these **σ**-and **π** effects would serve to increase the singlet-triplet energy gap and stabilize the singlet carbene over the reactive triplet [92].

After the first successful attempt to isolate carbene **(83)**, Areduengo and co-workers reported a series of electronic stable carbenes **(85)**, **(87)**, **(88)** and **(91)** [90]. Carbene **(85)** was prepared when 1,3,5-tetramethyl-imidazolium chloride **(84)** was treated with 1 equivalent of sodium hydride and 5 mol % potassium *tert*-butoxide in THF, Scheme 1.9. Carbene **(85)** was obtained in 69% yield. ^{1}H NMR spectroscopy shows only two resonances of equal area at 2.01 and 3.48 ppm which is assigned to the methyl groups on the carbon and nitrogen. A peak at 213.70 ppm in the ^{13}C spectrum is also observed indicating the presence of a carbene **(83)**.

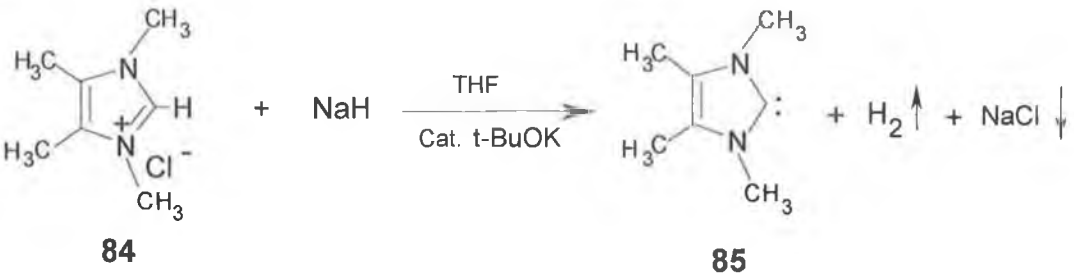

84 85

Scheme 1.9. The synthesis of carbene **(85)** by NaH and *t*-BuOK as a catalyst.

To separate the **σ** and **π** effects of the *N*-aryl substituents Arduengo et al. prepared carbenes **(87)** and **(88)**, Scheme 1.10.

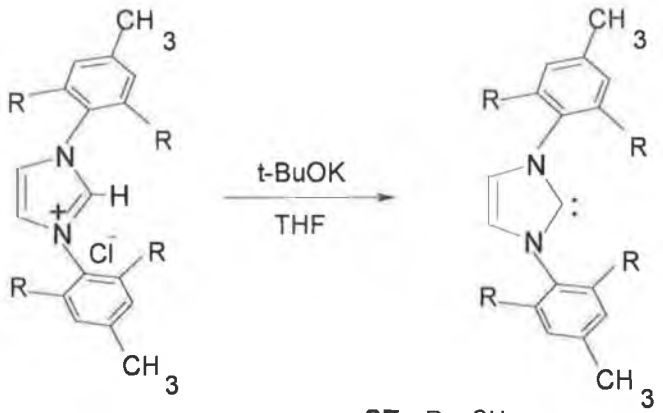

86

87 R = CH_3

88 R = H

Scheme 1.10. Carbene **(87)** and **(88)** synthesised in order to interpret the **σ** and **π** effect from substituent.

The mesityl substituents of carbene **(87)** provide an opportunity to observe the δ effect of an aryl substituent since the o-methyls will prevent conjugation between the phenyl rings and the nitrogen centres. The *p*-tolyl substituents of **(88)** will allow a **π**-effect because the rings can assume a planar (conjugating) arrangement. The ^{1}H NMR spectrum (THF-d_8) of **(87)** shows a signal for the imidazole ring protons of C4,5 at δ 7.04, which is quite similar to the values in **(88)** (δ 7.02 in THF-d_8) and **(83)** (6.92 in THF-d_8). The ^{13}C NMR spectrum

of **(87)** reveals the carbene resonance at 219.69 ppm, where as the ^{13}C NMR spectrum (THF-d_8) of **(88)** reveals the carbene centre at δ 215.79 ppm.

A similar chemical shift was observed for another aryl substituted imidazole **(90)**, obtained in 43% isolated yield, Scheme 1.11. The ^{13}C NMR spectrum (THF-d_8) of **(90)** revealed the carbene centre at δ 216.28 ppm and the remaining imidazole ring protons at δ 7.76 ppm. This downfield shift of the C4,5 protons of carbene **(90)** is due to the anisotropic effect of the unhindered aryl substituents.

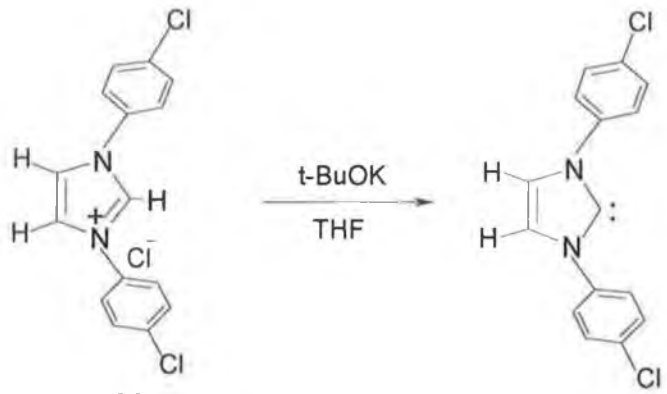

89 **90**

Scheme 1.11. The synthesis of carbene **(90)** using t-BuOK as base.

Arduengo and co-workers also investigated the synthesis of a new saturated hetrocyclic stable carbene 1,3-dimesitylimidazolin-2-ylidene **(92)** [93] which was formed through the elimination of KCl and H_2 (eq.1) and afforded pure carbene in 72% yield, Scheme 1.12.

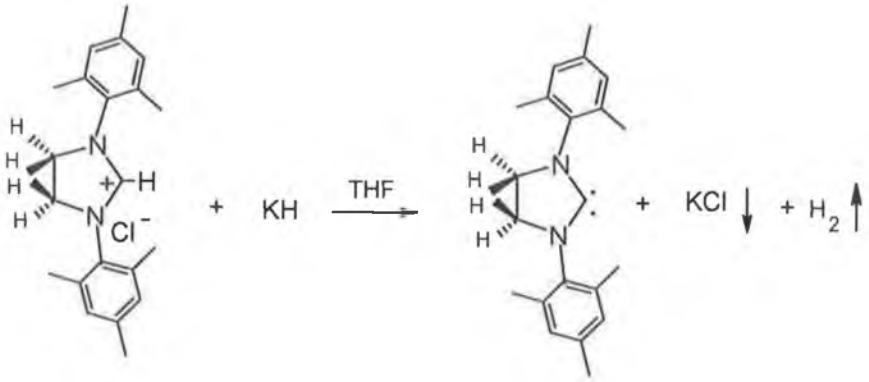

91 **92**

Scheme 1.12. The synthesis of a saturated heterocyclic carbene 1,3-dimesityl-imidazolin-2-ylidene **(92)**.

The saturated carbene **(92)** is stable in the absence of oxygen and moisture with a melting point around 107-109 °C, (see scheme 1.12). The ^{13}C NMR spectrum of **(92)** (THF-d_8) reveals a signal at δ 244.50 ppm that clearly identifies the compound as a carbene. The stability of the saturated carbene **(92)** is probably due to the bulky mesityl groups at the nitrogen which provides some measure of kinetic stability by hindering the dimerization of carbene centres along the non-least motion pathway [94]. In addition the C4-5 double bond is not critical to the construction of stable diaminocarbenes.

Herrmann and co-workers [95-97] prepared new imidazole heterocyclic carbenes by introducing a functional group such as oxygen, nitrogen and diarylalkyl phosphino donors in the side chain(s) or with chiral residues, using a liquid-ammonia route; **(93)**, **(94)**, **(95)** and **(96)**, Figure 1.43. When imidazolium salts were deprotonated in a mixture of liquid ammonia and aprotic polar solvents e.g. THF, the desired carbene was obtained in excellent yield and purity; in most cases the reaction went to completion within about 30 minutes at – 40 °C .

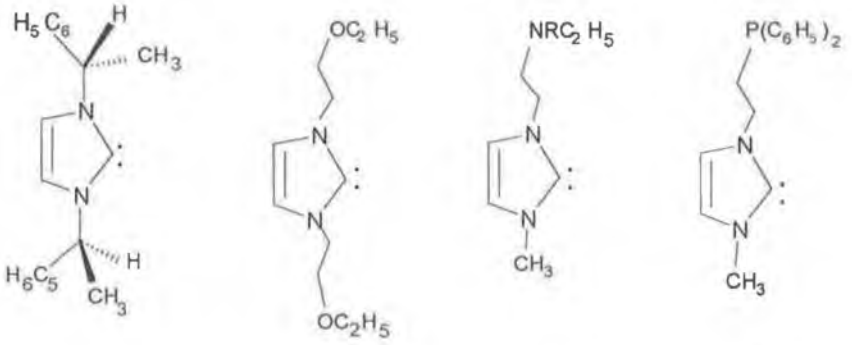

93 **94** **95** **96**

Figure 1.43. Four different N-heterocyclic carbenes **(93-96)**.

In 1998 Arduengo and co-workers [98] realized Wanzlick's dream by isolating **(98)**, Scheme 1.13.

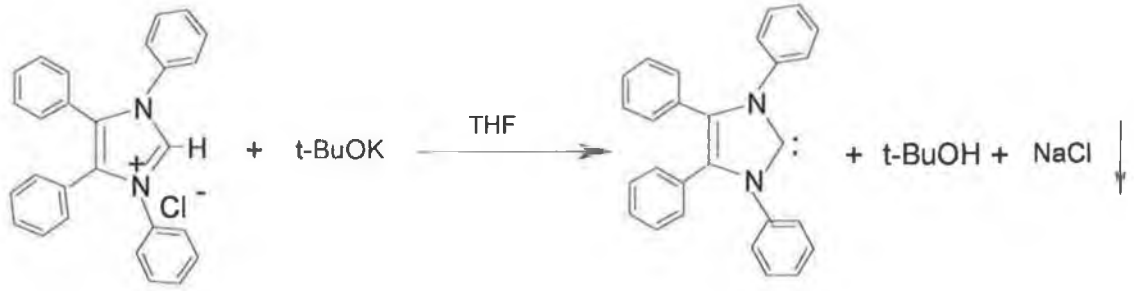

97 **98**

Scheme 1.13. Isolation of carbene **(98)**.

Carbene **(98)** was synthesised by modifying the procedure published by Wanzlick making it possible to isolate the carbene [86]. The ^{1}H NMR spectrum of **(98)** shows a collection of multiplets at δ = 6.90-7.40, but this provides little information about the compound. A signal at δ 219.60 in the ^{13}C NMR spectrum (THF-d_8) of **(98)** clearly identifies the compound as a carbene.

Recently Arduengo and co-workers [99] have prepared new imidazol and imidazolin-2-ylidenes by introducing new sterically demanding substituent groups at the ring nitrogen atoms **(100$_{a,b}$)**, **(102$_{a,b}$)** and **(103$_{a,b}$)** which are essential in the imidazoline-2-ylidine series to prevent dimerization with formation of an electronicly rich olefin [100-102]. Arduengo et al. has synthesised various imidazolidine carbenes using different pathways, in good yields, Scheme 1.14.

1-

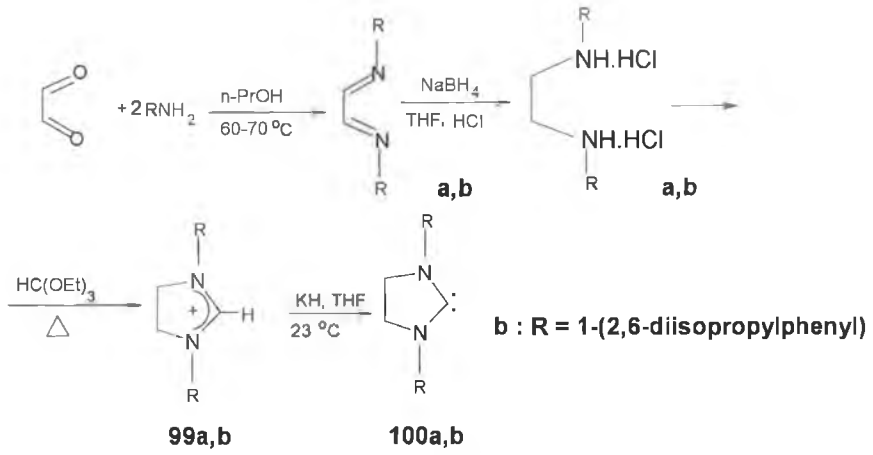

2-

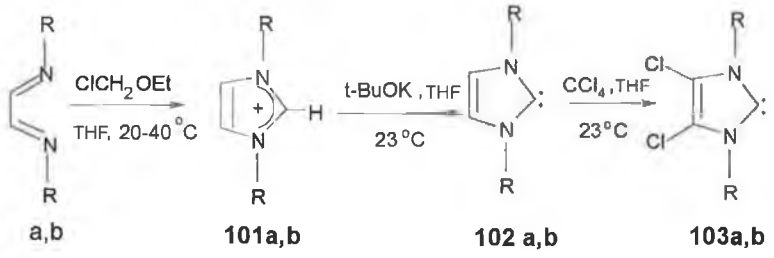

Scheme 1.14. The preparation of **(100a,b-103a,b)** by different pathways; (1) via **(99a,b)**, (2) via **(101a,b)** imidazolium salts.

The ^{13}C NMR spectrum (benzene-d_6) of **(100$_{a,b}$)** revealed a strong downfield shift of ca. 80 ppm for the C-2 carbon in the imidazole ring at δ 243.77, δ 244.01 ppm, respectively, an indication of carbene formation, whereas, the ^{13}C NMR

spectrum of (benzene-d_6) **($102_{a,b}$)** and **($103_{a,b}$)** have shown a signal for the carbene centre at δ (**102_a**: 219.70; **102_b**: 220.60 ; **103_a**: 219.90; **103_b**:220.60). These differences can be attributed to ring saturation and an aromaticity effect for **($100_{a,b}$)**.

1.4.1.2 Triazole-based nucleophilic carbenes

The first crystalline triazole-derived carbene, 1,3,4-triphenyl-4,5-dihydro-1H-1,2,4-triazol-5-ylide **(106)**, was prepared by Enders et al. [103]. This carbene was prepared by deprotonation of the highly protic triazolium salt. Carbene **(106)** was synthesised by the reaction of **(104)** with sodium methoxide in methanol, affording **(105)**, where the later was heated to 80 °C revealing decomposition endothermically with concomitant elimination of methanol to form**(106)**, Scheme 1.15.

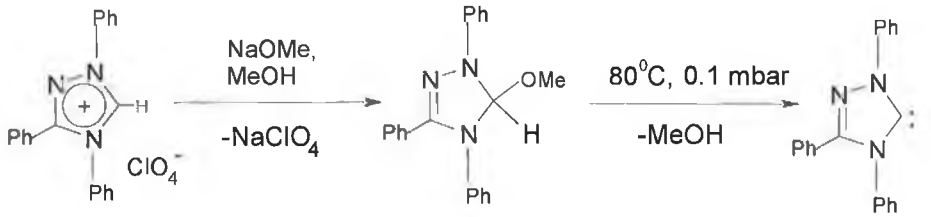

104 **105** **106**

Scheme 1.15. Carbene **(106)** was prepared using NaOMe as base under reduced pressure.

Carbene **(106)** shows no indication of dimer formation and also decomposes above 150 °C. ^{13}C NMR spectroscopy of this ylidine afforded a signal at 214.60 ppm which is an indication of carbene formation. This carbene is commercially available.

1.4.1.3 Multidentate based nucleophilic carbene

Polyfunctional derivatives have also been investigated with the synthesis of the tris carbene **(108)** which was reported by Dias [104] et al., Scheme 1.16. Carbene **(108)** shows no intermolecular interactions, even when sterically less demanding substituents are present on the imidazole ring nitrogens [90]. The ^{13}C NMR spectrum (benzene-d_6) of carbene **(108)** shows signals at δ 215.25 ppm corresponding to the C-2 carbons and signals at δ 115.29 and δ 117.07 ppm which can be assigned to the C-4 and C-5 carbons. These values are typical for imidazol-2-ylidenes [89]. The product has been isolated as a solid in 56% yield.

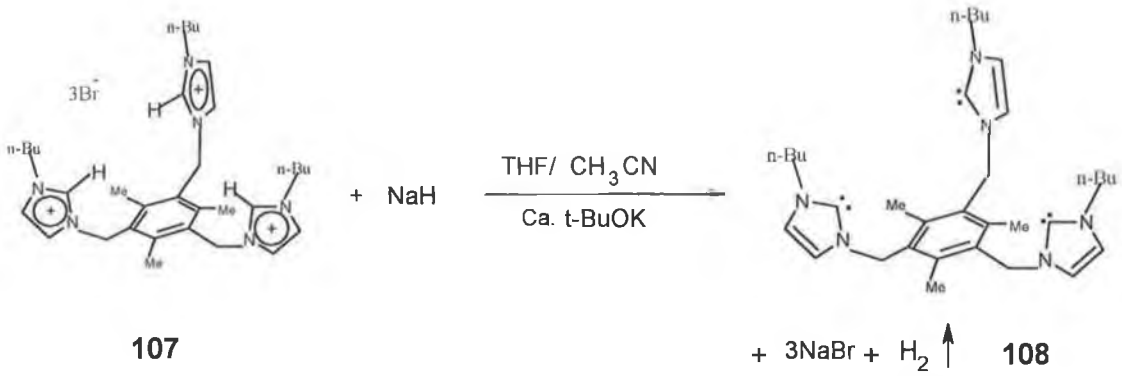

Scheme 1.16. First tridentate carbene **(108)**.

Another polyfunctional carbene **(109)** was prepared by Hermman et al.. This carbene is stable and accessible as was **(108)** but was prepared using liquid ammonia as the deprotonating agent [95], Figure 1.44.

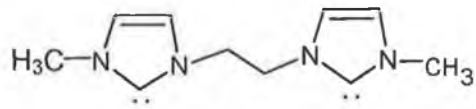

109

Figure 1.44. Bi-functional carbene **(109)**.

1.4.2 *N*-Heterocyclic carbene-metal complexes

These nucleophilic carbenes have been employed as ligands, producing carbene metal complexes that would act as controlling ligands in organometallic homogeneous catalysis [105,106]. Moreover, these ligands are excellent σ-donors and form rather strong metal-carbon bonds; therefore, catalysts containing these ligands often have better air and thermal stability than complexes containing phosphine ligands [107,108].

Arduengo et al. was able to isolate and characterize the homoleptic bis(carbene)-silver(I) **(110)** and copper(I) **(111)** complexes [109]. These carbene metal complexes were prepared by the reaction from the stable nucleophilic carbene 1,3-dimesitylimidazol-2-ylidene **(86)** and the corresponding metal triflate, as outlined in Scheme 1.17 below.

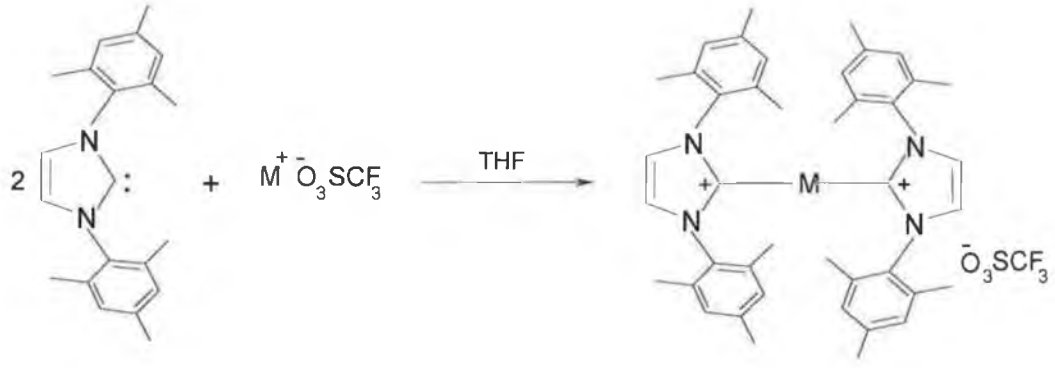

86

110 M = Ag
111 M = Cu

Scheme 1.17. Two different homoleptic bis-carbene-metal **(110,111)** were prepared by Dias et al.

The NMR data was consistent with the bis (carbene) metal structures and suggests a level of delocalisation in the imidazole ring which is intermediate between those of the free carbene and imidazolium ions.

Hermann and co-workers have successfully incorporated functional chirality into a 1,3-imidazolium salt, using it as a controlling ligand in homogenous asymmetric catalysis [96,110]. Compound **(113)** and **(114a)** were prepared from the reaction of transition metal carbonyls or rhodium salts and chiral hetrocyclic carbene ligands **(112)** Scheme 1.18.

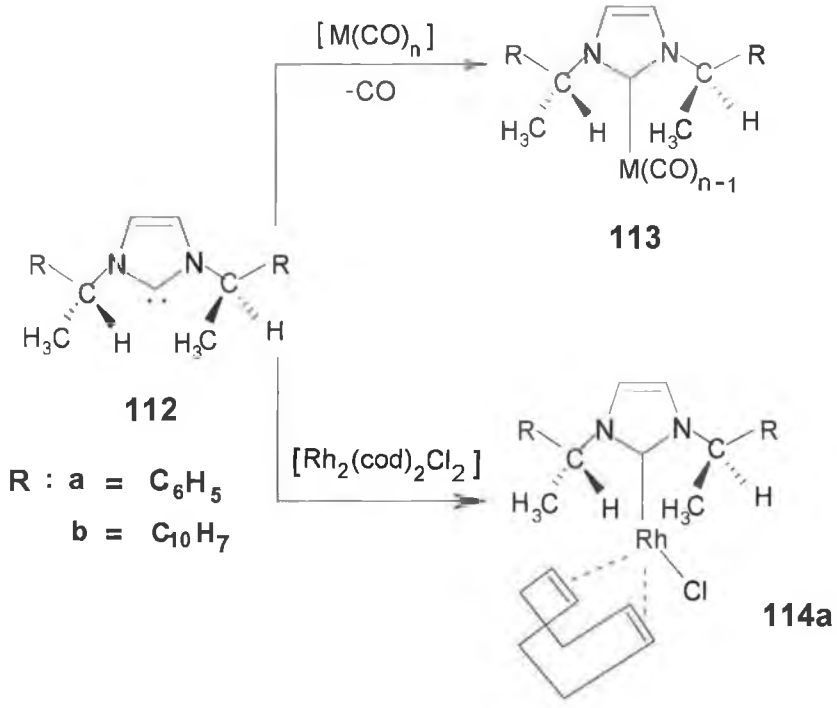

Scheme 1.18. Homogenous asymmetric catalysts **(113,114a)** synthesised from homochiral precursor **(112)**.

These complexes have shown a higher degree of thermal stability and air sensitivity, making them good candidates for asymmetric catalysis. Ligand **(114b)** was used in the asymmetric hydrosilylation of acetophenone, resulting in a quantitative yield with a 30% enantiomeric excess, Scheme 1.19.

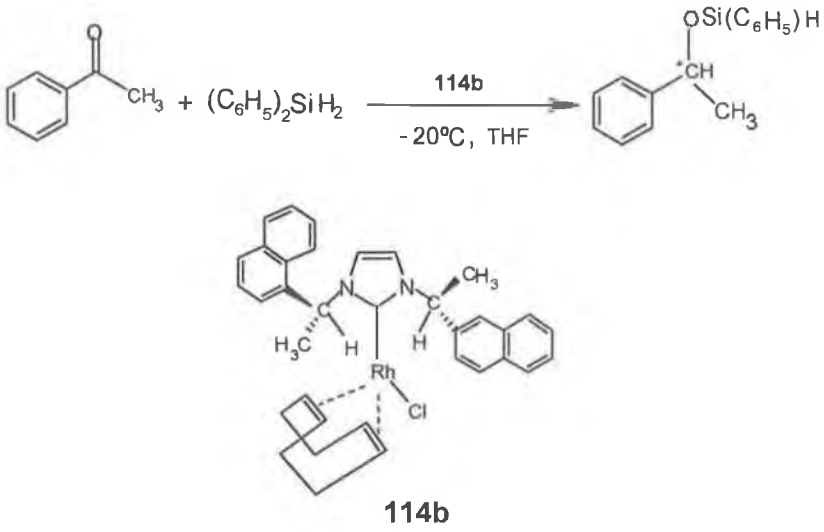

114b

Scheme 1.19. Catalyst **(114b)** is able to catalyse asymmetric hydrosilylation reaction of acetophenone.

Other attempts to prepare tris-carbene ligands based on the topology of Trofirmenko's tris(pyrazolyl) borate [111], were carried out by Fehlommer et al. [112]. This work yielded the novel chelate-like poly- and precarbene complexes, to give the first hexacarbene complex **(116)**. A tripodal carbene ligand of the Trofimenko type, tris(2,3-di-hydro-1H-imidazol-2-ylidene) borate **(116)** resulted from deprotonation of the corresponding salts **(115)** with nBuLi and subsequently treated with $FeCl_2$ (Iron dichloride) to form **(116)**, Scheme 1.20.

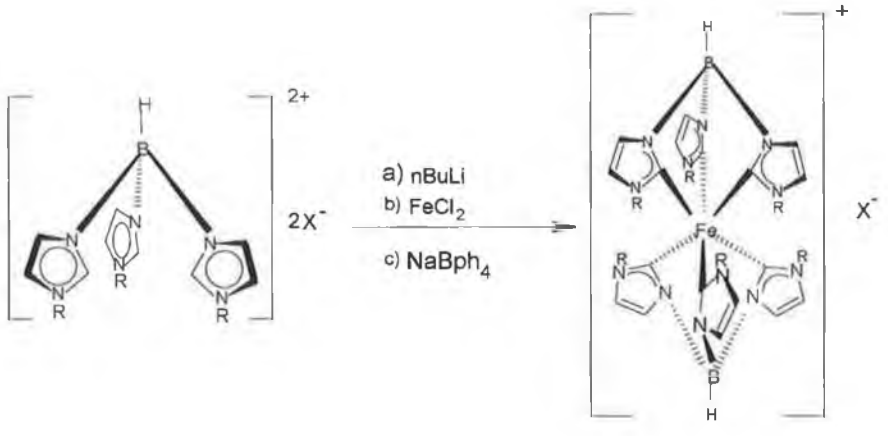

115 ($X = BF_4^-$, R = Me)

116 ($X^- = Bph_4^-$)

Scheme 1.20. Synthesis of bis-tripodal carbene-Fe(III) complex **(116)**.

The X-ray crystal structure of **(116)** shows an iron atom which is spherically surrounded by six five-membered heterocycles. Later on Fehlhammer et al. chelated **(116)** with cobalt [113].

Recently Crabtree and co-workers were able to demonstrate metallation of the different imidazolium precursors system **(117)**, **(118)** to give [Rh(Bis-carbene)-I_2(OAc)] **(119a-c)** [114], Scheme 1.21.

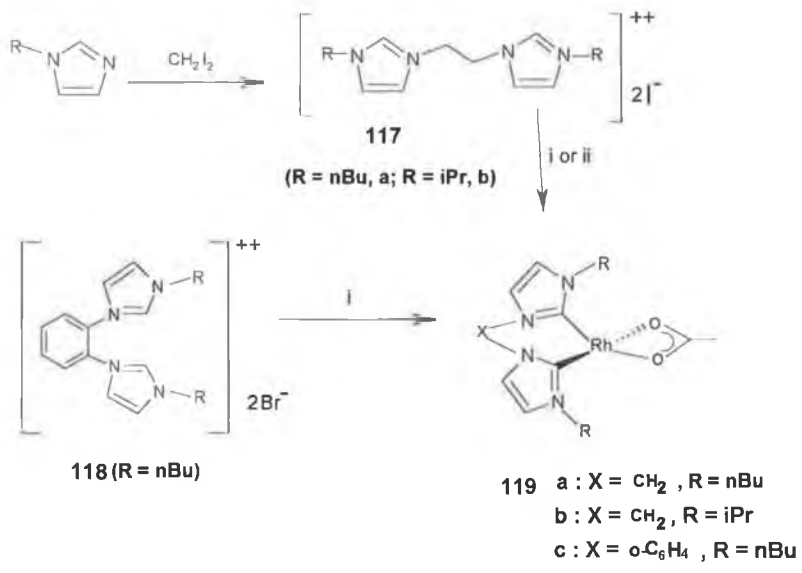

Scheme 1.21. Synthetic reagents employed; i, $[(cod)RhCl]_2$, NaOAc, KI, EtCN; ii, $[Rh(OAc)_2]_2$, MeCN.

1.4.2.1 *N*-Heterocyclic carbene complexes of Silver

As a result of the difficulties in preparing and isolating free *N*-heterocyclic carbenes an alternative method was sought to stabilize these ligands. One method is to trap the carbene with Ag_2O to give a stable silver carbene complex [115]. The silver carbene complex can then be used to transfer the carbene to another metal by a transfer reaction [115-117].

Silver-carbene complexes derived from imidazolium salts were first synthesised and characterized by Ardoengo et al. in 1993 [109], and were obtained by the

reaction of the free carbene with silver triflate. Wang and Lin et al. were able to prepare carbene-silver complexes, and use them as carbene transfer agents for different metals such as gold and palladium producing two new carbene-metal complexes **(123)** and **(124)** [115].

The carbene-silver(I) complexes **(121)** and **(123)** were prepared from 1,3-diethylbenzene imidazolium bromide **(120)** and Ag_2O in DCM in a 2:1 ratio [115], (see Scheme 1.22). Complex **(122)** was obtained from the reaction of **(120)** with Ag_2O in a 4:1 ratio under basic PTC (phase transfer catalyst) conditions, yielding **(122)** in 89%. In this reaction solvent pre-treatment was not required and a simple base NaOH was used. Subsequently complex **(122)** was treated with $Au(SMe_2)Cl$ producing **(124)** in quantitive yield.

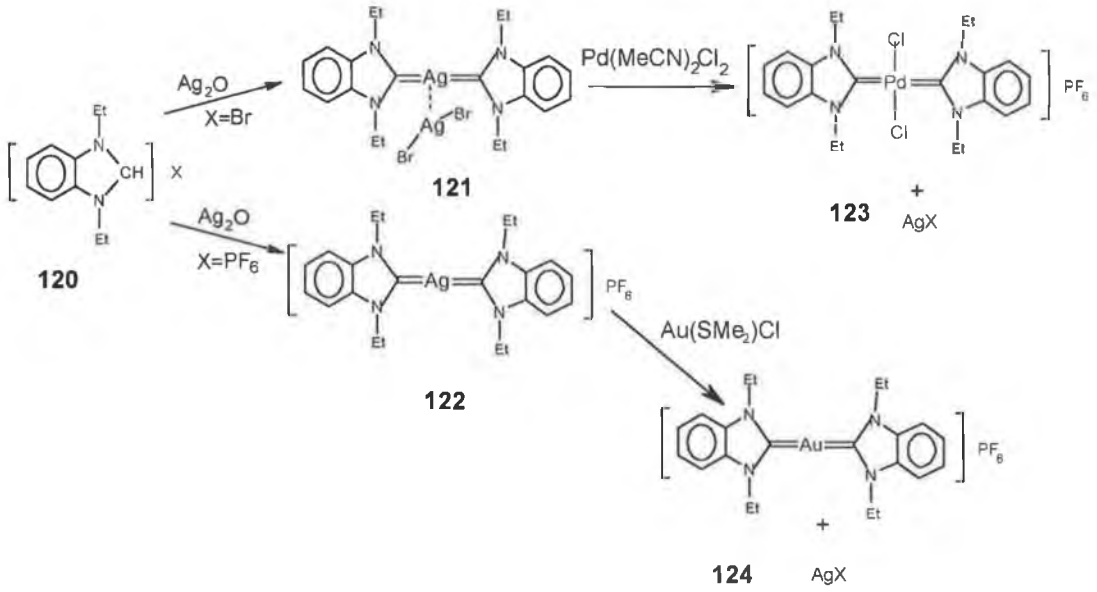

Scheme 1.22. Carbene-palladium and gold complexes **(123,124)** prepared from **(120)** and Ag_2O.

^{13}C NMR studies for compound **(121)** showed only one sharp signal at 188.90 ppm and no indication of ^{13}C-$^{107,109}Ag$ coupling, whereas in contrast, compound **(122)** showed two signals for ^{13}C-^{107}Ag and ^{13}C-^{109}Ag with coupling constants of 180 and 204 Hz, respectively.

A series of mixed donor *N*-functional imidazolium salts and their conversion into silver(I) carbene complexes **(125-130)** was carried out by Danopoulos et al. [118]. They were able to prepare the silver carbene adducts based on a modification to the product of Wang and Lin by using Ag_2O or Ag_2CO_3 as shown in Scheme 1.23.

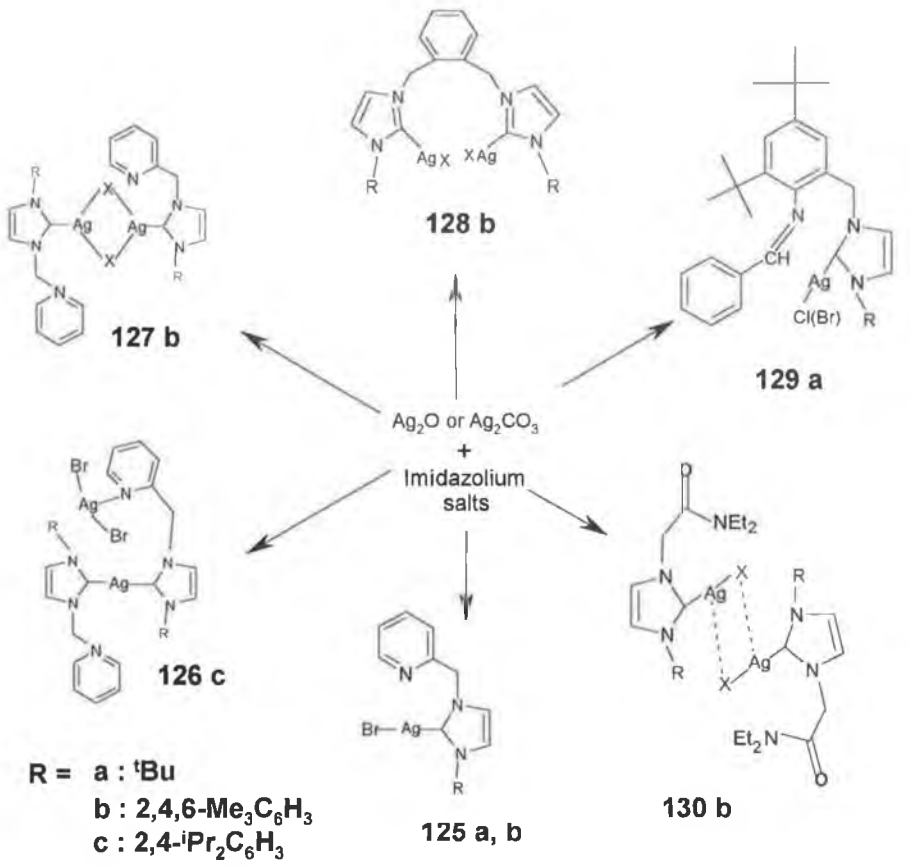

Scheme 1.23. The synthesis of silver complexes **(125-130)**.

They found that: (i) with relatively unreactive bulky imidazolium salts which are precursors for **(128a-c)**, the reaction took place only in refluxing DCE and other non-bulky imidazolium salts were faster; (ii) when complexes **(126c)** and **(125)** were synthesised at higher temperature in DCE the formation of by-products was increased; (iii) the purity of products would be increased by adding 4 Å molecular sieves to the reaction medium.

The formation of the carbene complexes was concluded by the appearance of a signal at 165 ppm in the ^{13}C NMR spectrum which can be assigned to the C-2

imidazol-2-ylidene (carbene) carbon. Also the H-2 proton is absent in the ^{1}H NMR spectrum. X-ray crystallography, indicates that the carbene ligand co-ordinates in a monodentate fashion from the carbene end or as a bridge between two different metal atoms. In one case the silver is co-ordinated by two carbene ligands, but in the majority of the structurally characterised complexes the metal centres adopt linear geometries with M-C (metal-carbene) bond lengths in the range of 207-210 pm which is typical for single bonds.

Carbene-silver complexes have been further developed by incorporating functional chirality into the carbene ligands, the synthesis of chiral diamino carbene complexes remains an important challenge for organic chemists and only a few ligands have been reported to date [119]. Roland et al. were able to synthesise and characterise a chiral *N*-heterocyclic carbene-silver(I) complex **(132a-e)**, Scheme 1.24.

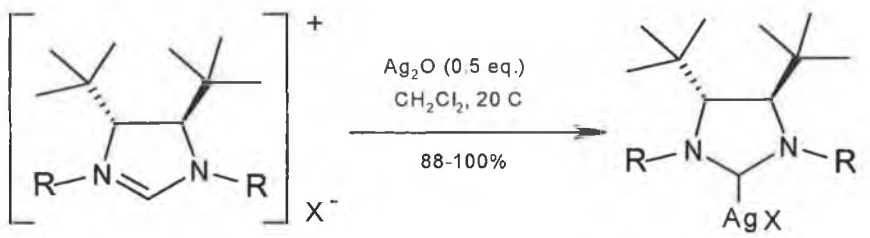

131 a-e

132

a : R = Me, X = I
b : R = Bn, X = Br
c : R = picolyl, X = Cl
d : R = (S)-1-phenylethyl, X = OAc
e : R = (S)-1-phenylethyl, X = I

Scheme 1.24. Synthesis of silver(I) carbene complexes.

Absent in the ^{1}H NMR was the H-2-imidazolium proton, the ^{13}C NMR spectrum revealed signals at 213.70 ppm for **(132a)**, 206 ppm **(132b)**, 197.20 ppm **(132c)**, 194.60 ppm **(132d)**. No ^{13}C-$^{107,109}Ag$ coupling was observed in the ^{13}C NMR studies of carbenes **(132a-c)** and **(132e)**, but in **(113d)**, two doublets centred at 194.60 ppm were observed for the carbene signal, and this multiplicity is

probably due to the ^{13}C-$^{109}Ag/^{107}Ag$ coupling with coupling constants of 268 and 232 Hz.

The chiral silver(I) diaminocarbene **(132a)** was used as a carbene transfer agent with copper(II) triflate LAC (ligand accelerate catalysis) [120], in the conjugate addition of diethyl zinc to cyclohexenone, [124]. Scheme1.25.

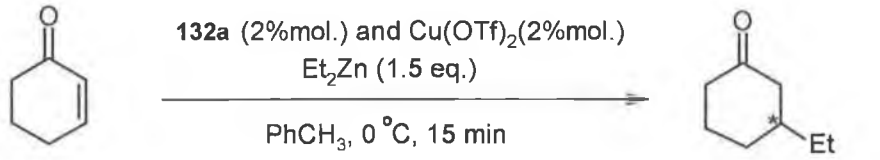

98% ; ee = 23%

Scheme 1.25. Conjugate addition using **132a** and $Cu(OTf)_2$

The conjugate adduct was obtained in less than 30 minutes with 98% conversion, giving a moderate %ee. of 23%. A solvent-dependency study was also investigated, showing higher conversions in the following order; toluene, ether and hexane over THF and DCM, respectively.

Recently a new mono carbene silver dinuclear complex, $[m\text{-}C_6H_4\text{-}(CH_2ImMeAgCl)_2]$ **(134)** was prepared by Matsumoto et al. [123], and was obtained by treating **(133)** and Ag_2O in CH_2Cl_2, Scheme1.26.

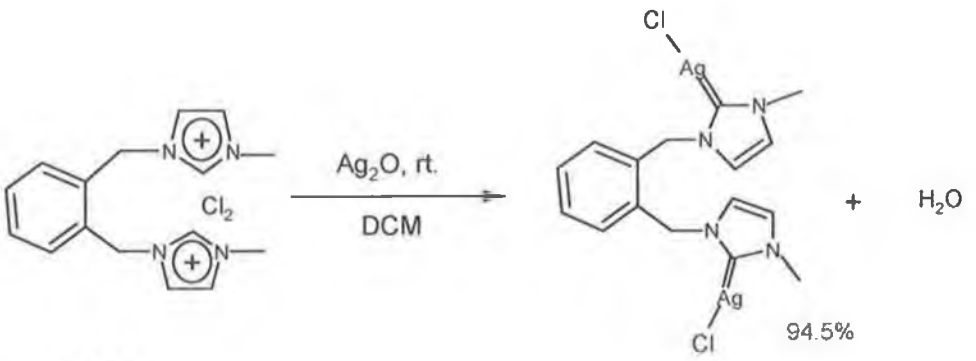

133 134

Scheme 1.26. Recent bidentate Carbene-Silver(I) **(134)** was synthesised by Matasumoto et al.

They attempted to prepare the free carbene by deprotonation of the imidazolium **(133)** with *tert*-BuOK or KH, but were not successful. Absent in the ^{1}H NMR spectrum was the H-2 proton of the imidazolium salt **(133)**. X-ray crystallography showed the geometry around the Ag atoms in **(134)** to be linear, and each Ag atom is bi-coordinated by a carbon and chloride ion. This result is quite typical when compared to the corresponding values of other silver-carbene and silver-chloride complexes [115,124].

1.5 Heck reaction

The Heck reaction is the palladium mediated coupling of aryl or vinyl iodides, bromides or triflates with alkenes in the presence of base Scheme 1.27. It has been known to synthetic chemists since the late 1960s [125-128] and was pioneered by Mizoroki [125] and Heck [126]. The substrate can be a simple olefin (with ethylene being the most reactive one), or it can contain a variety of functional groups, such as esters, ethers, carboxyl, phenolic, or cyano groups Scheme 1.27. At present it is one of the simplest methods to prepare various substituted olefins, dienes and other unsaturated compounds.

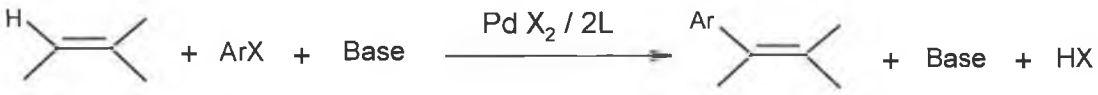

Scheme 1.27. The general reaction of Heck reaction

The electrophiles in the Heck reaction could be an aryl, heterocyclic, benzylic or vinylic halide/triflate. Pd(II) salts such as palladium acetate or dichloride are the most widely used type of catalyst. It has been shown that the reaction is accelerated in the presence of ligands. The most common ligands used are triaryl phosphines.

Mono-or disubstituted alkenes are usually used as nucleophiles as they are highly reactive, in the Heck reaction. The usual aprotic solvents used in the Heck reaction are DMF, DMSO or acetonitrile, and bases used are either secondary or tertiary amines or sodium/ potassium acetate carbonate or bicarbonate salts.

1.5.1 *N*-Heterocyclic carbene ligands in palladium catalysed Heck reactions

N-Heterocyclic carbene (NHC) [88], based on the imidazole ring system have been found to make excellent ligands for a variety of transition [129,130] and main group elements [131]. A number of transition metal-NHC complexes have given rise to active catalytic systems for a range of reactions [132-136], most notably the Heck reaction. Many reports investigated the Azolium-Palladium catalyst in the Heck reaction. Herrmann et al. were the first to use such systems in the Heck reaction presenting by catalyst **(135)** and **(136)**. These complexes were able to couple aryl chlorides and bromides to alkenes in yields of 99% [137]. These catalysts (palladium-complexes) were prepared and then used in the coupling.

Alternatively, they introduced a ligand **(137)**, 1,3-dimethyl- imidazolium iodide, and base ($Pd(OAc)_2$) to generate the catalyst *in-situ.*, demonstrating a new pathway with comparable yield to **(135)** and **(136)**, Scheme 1.28 below.

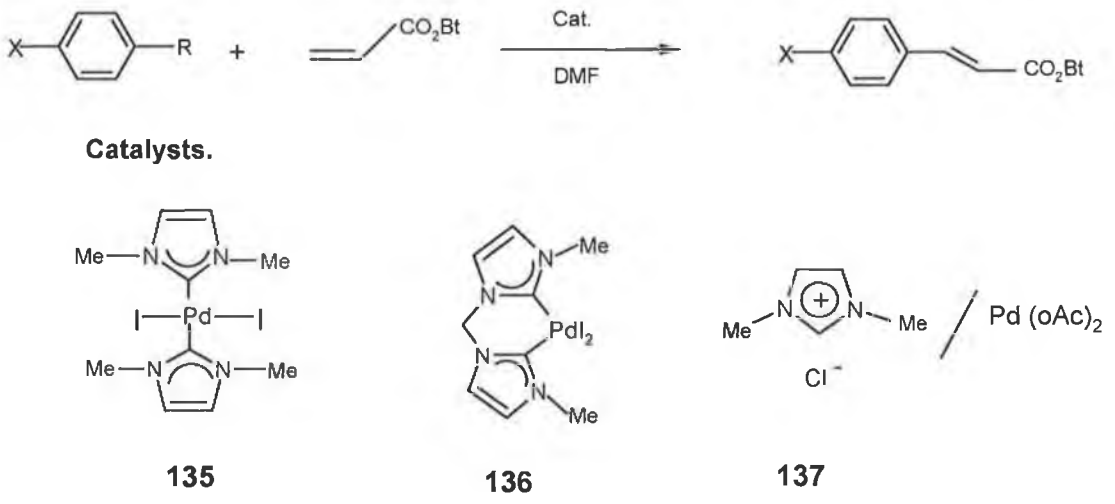

Scheme 1.28. Catalysts used in the Heck reaction.

Nolan et al. have applied imidazolium salts with base to generate the carbene-palladium complexes in-situ., Scheme 1.29 [137,138]. They also found that 1,3-substituted imidazolium chloride in the *N*-aryl ortho positions gave higher

activity when used with palladium acetate. They also investigated the electronic and steric effects of the imidazolium **(138a-141a)** precursors and imidazol-ylidene **(138b-141b)** analogues and it was found that **(140a)** gave the highest yields over other ligands in the coupling of aryl bromides with alkenes.

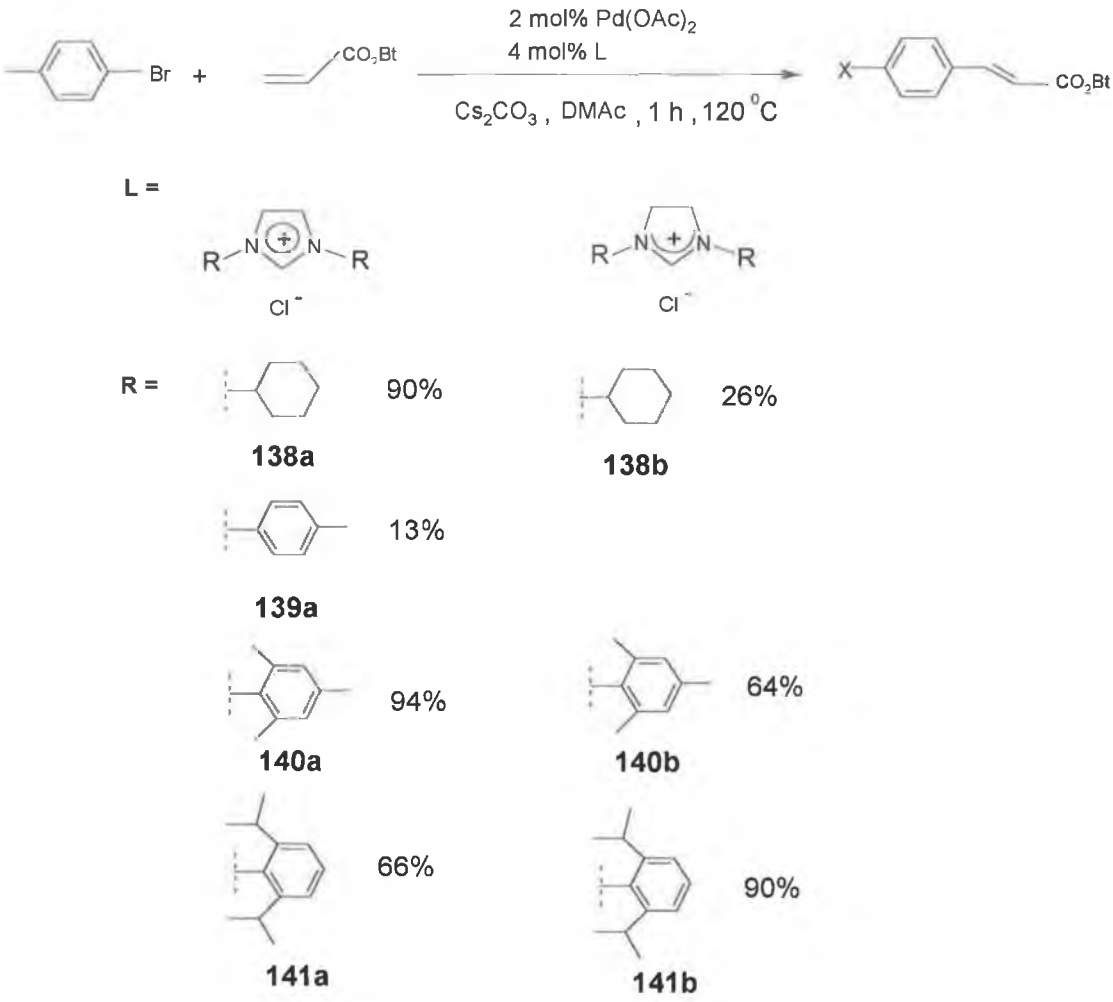

Scheme 1.29. The investigation of electronic and steric effects of the imidazolium ligand on reaction rate.

Recently numerous and various reports present different types of azolium/palladium or carbene-palladium complexes catalyst **(142-147)**, which is based on mono, bi and tridentate carbene ligands, where also using a mixture of carbene/nitrogen and phosphine donor functional system showing its application in Heck reaction [116,117,139,140] Figure 1.45.

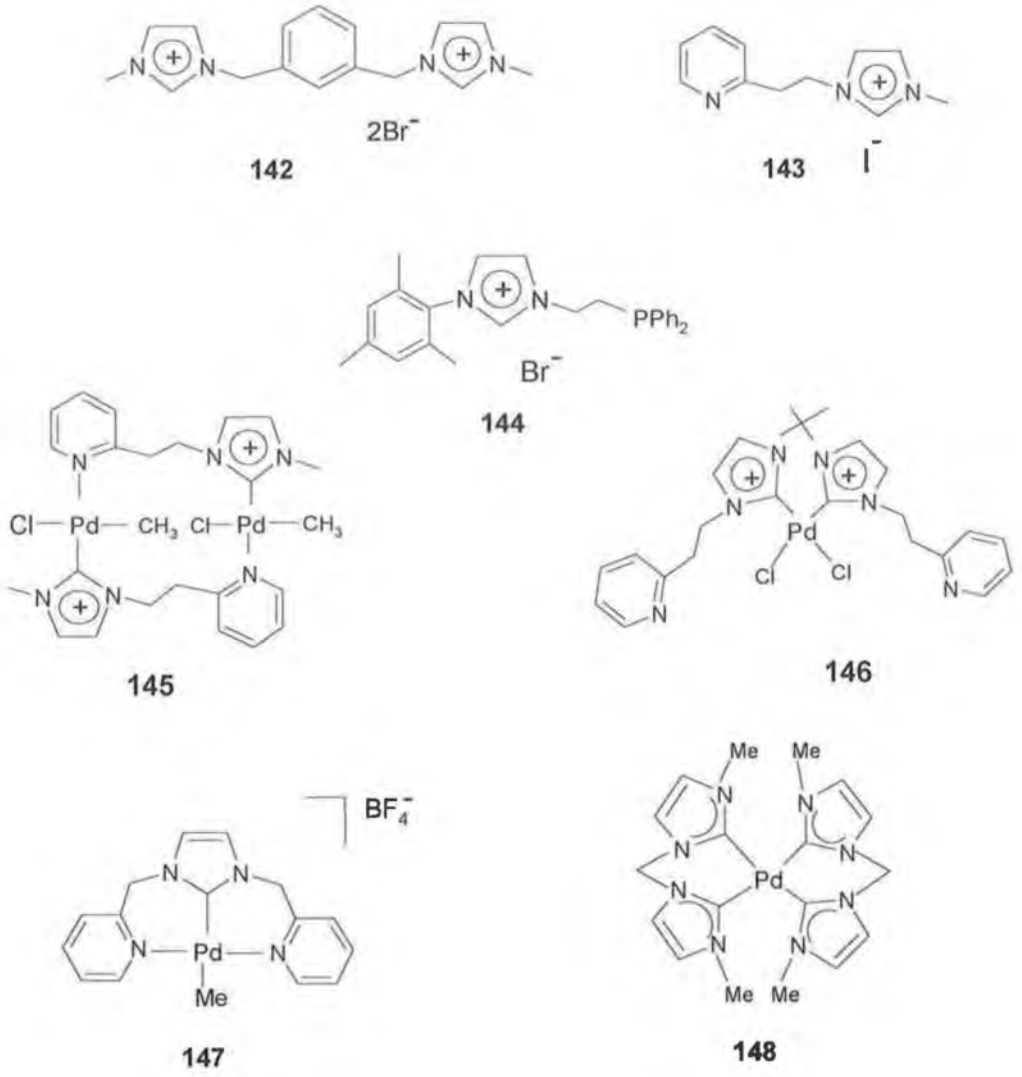

Figure 1.45. Different types of azolium and carbene-palladium complexes used in the Heck reaction.

1.6 Design of new homochiral tripodal receptors.

The aim of our research was to design a series of new homochiral tripodal azolium salts which possess the following properties:

1– Three cationic centres with H-bonding properties. This will be achieved by incorporating three imidazolium groups into our proposed receptor. Each imidazolium carries a positive charge and an electron deficient hydrogen on the C-2 carbon atom which is capable of H-bonding with various anions [141-144], Scheme 1.30 below.

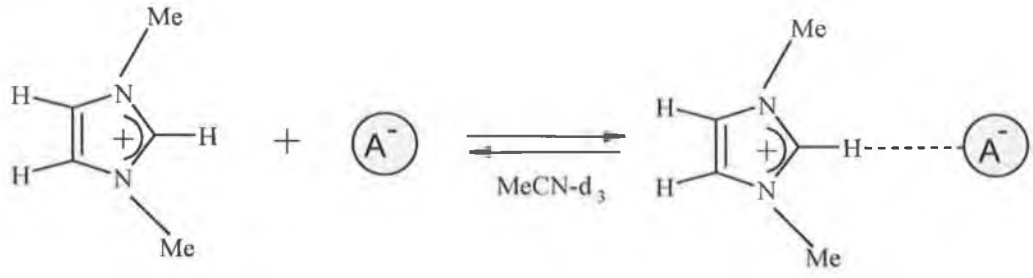

Scheme 1.30. The ability of imidazolium salts to interact with anions through electrostatic force and hydrogen bonding.

2- We were interested to prepare a new receptor which would incorporate a chiral imidazolium group. We envisaged that such a receptor could be used in both enantioselective recognition and anion recognition, Figure 1.46.

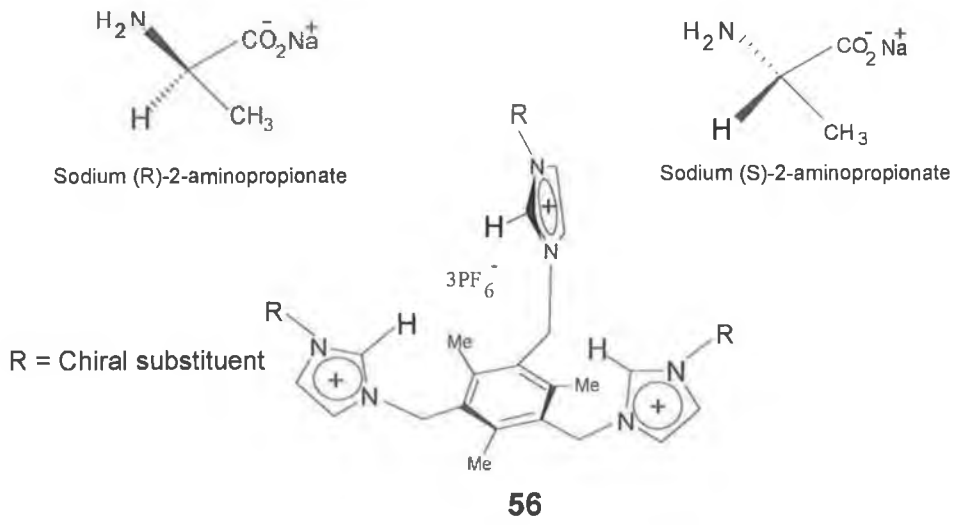

Figure 1.46. The possibility of receptor **(56)** to be modified by possessing functional chiral group to discriminate between two enantiomers.

3- Treatment of the tripodal imidazolium salts **(107)** with an appropriate base could generate the corresponding carbene **(108)**, Scheme 1.31, which could subsequently complex various metals leading to the formation of stable metal-carbene complexes.

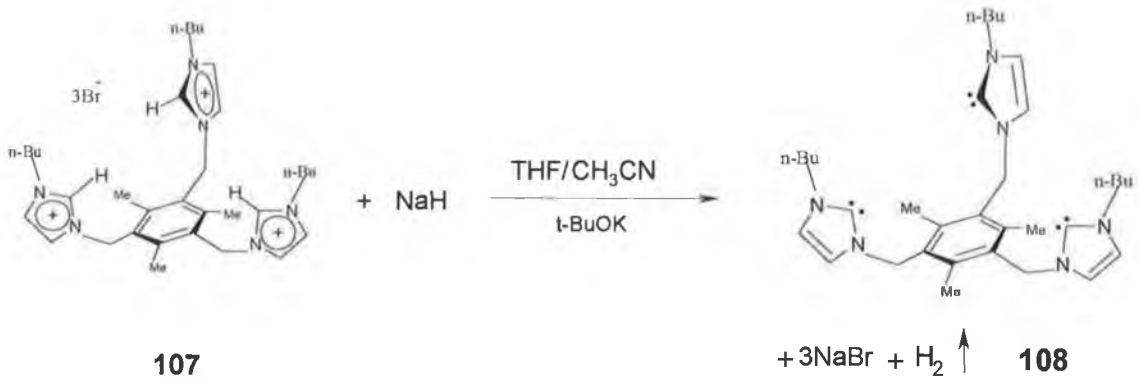

Scheme 1.31. The possibility of receptor **(107)** to be converted to tridentate carbene.

Chapter 2

Synthesis of Homochiral Tripodal Imidazolium Salts

2.1 Introduction

Previous work by Howarth et al. led to the synthesis of di(ferrocenylmethyl) imidazolium salt **(47)**, Scheme 2.1, which was formed by heating **(149)** in MeCN with two equivalents of imidazole, in the presence of sodium carbonate. Alternatively compound **(47)** could be prepared from 1-ferrocenylmethyl imidazole **(150)** in MeCN under reflux for 16 h followed by treatment with NH_4PF_6.

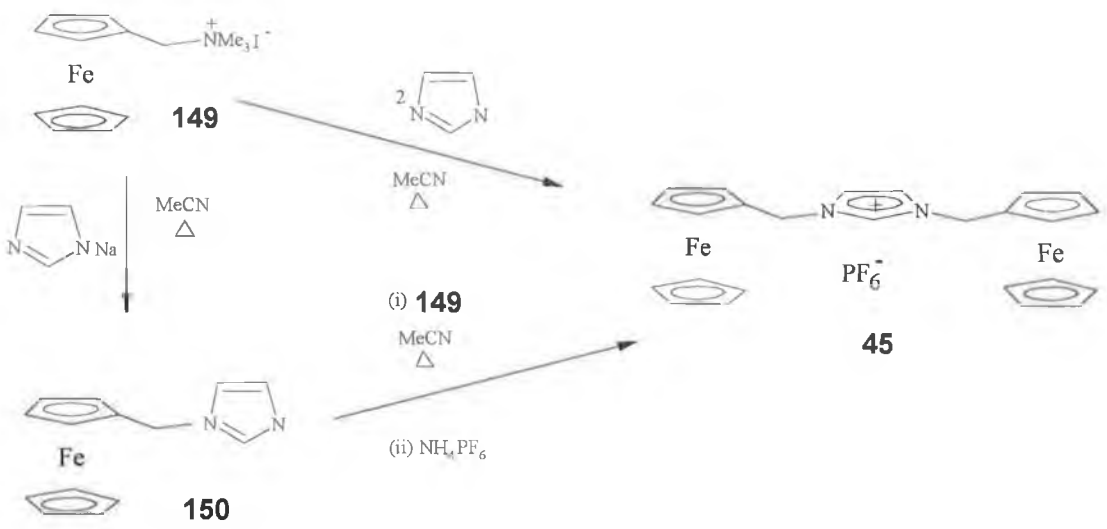

Scheme 2.1. Two pathways used by Howarth and co-workers to generate receptor **(45)**.

Sato and co-workers prepared a new tripodal anion receptor 1,3,5-tris[(3-n-butyl imidazolium)methyl]2,4,6-trimethylbenzene **(56)**, Scheme 2.2, which possesses three imidazolium groups connected through a 1,3,5-trimethyl benzene scaffold. Receptor **(56)** was synthesised by the treatment of 1,3,5-tris(bromomethyl)-2,4,6-trimethyl benzene **(154)** with 3 equivs. of 1-*n*-butylimidazole in acetonitrile to give bromide salt in 96% yield. The bromide salts were then converted into a hexafluorophosphate salt by ion exchange. Recrystallization of the PF_6 salt **(56)** from Acetonitrile:Ethanol (1:4) gave **(56)** as colourless needles in 58% yield.

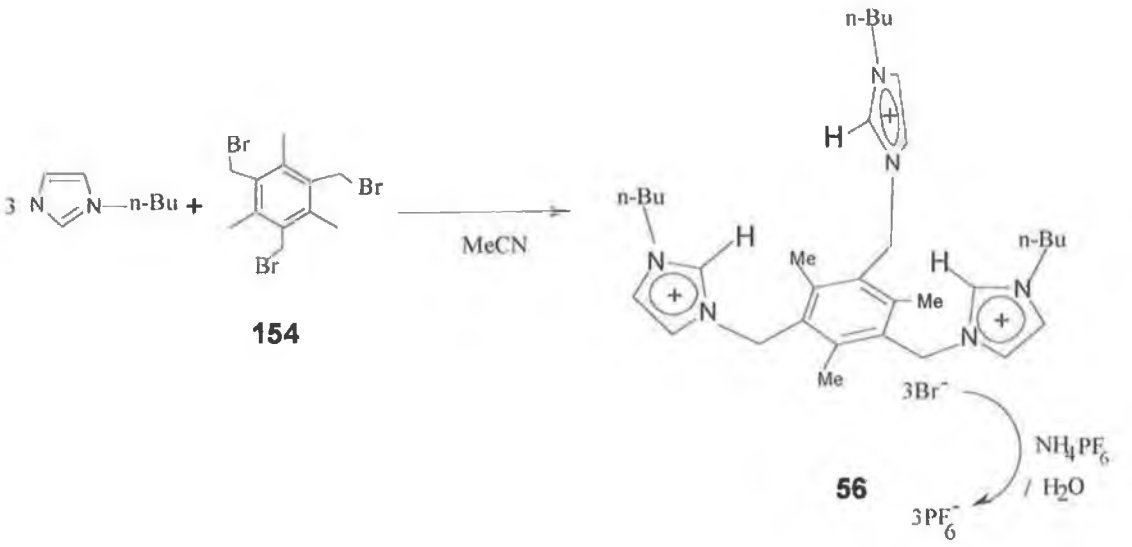

Scheme 2.2. Pathway used by Sato to prepare **(56)**.

We decided to prepare our target homochiral tripodal receptor, using the above pathways.

2.2 Synthesis of homochiral imidazolium tripodal receptors

We prepared four homochiral anion receptors **(156a-d)** according to a similar procedure used by Sato [36] and Dias [104], Scheme 2.3.

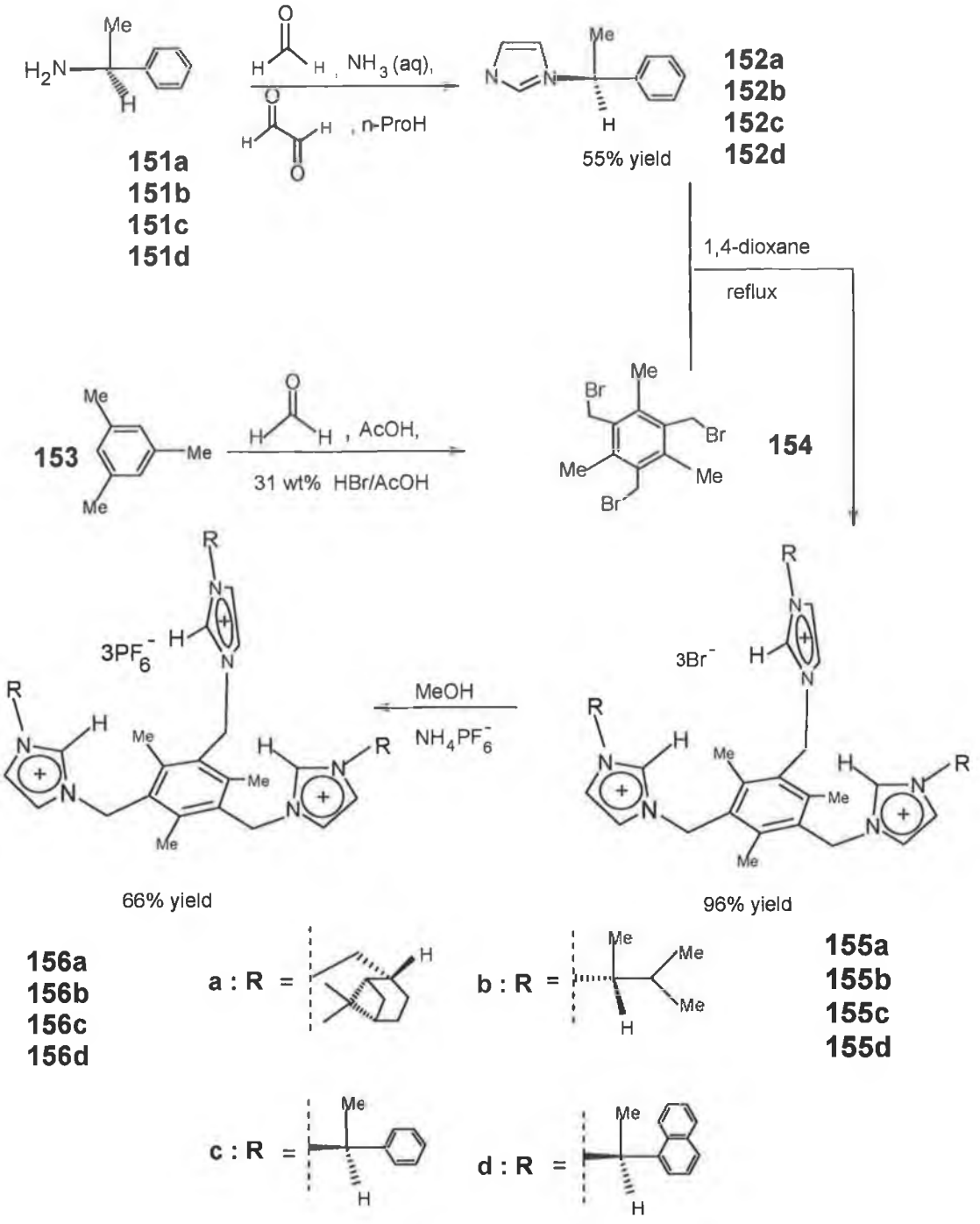

Scheme 2.3. Synthetic pathway to receptors **(156a-d)**.

2.2.1 Synthesis of (S)-1-(2-phenyl)ethyl imidazole (156c) (ring closure)

The first step in the preparation of 1,3,5-tris[((S)-1-(2-phenyl)ethylimidazolium) methyl]2,4,6-trimethylbenzene tri(hexafluorophosphate) **(156c)** was to prepare (S)-1-(2-phenyl)ethyl imidazole **(152c)** using a modified Arduengo [144] protocol, where (S)-1-(2-phenyl)ethyl amine **(151c)** is condensed with aqueous formaldehyde, glyoxal and aqueous ammonia to effect a ring closure and produce the target *N*-substituted imidazole, Scheme 2.4.

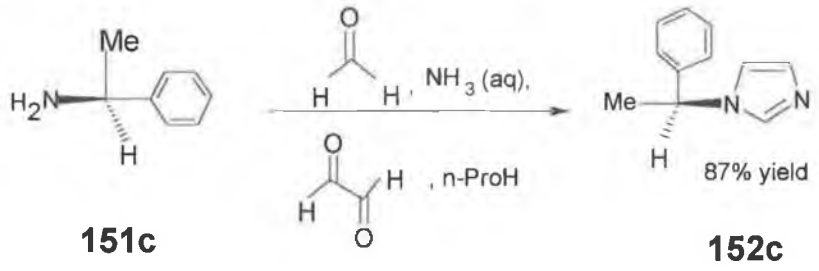

Scheme 2.4. Synthesis of (S)-1-(2-phenyl)ethyl imidazole **(152c)**.

The (S)-1-(2-phenyl)ethyl imidazole **(152c)**, was prepared by adding dropwise a solution of glyoxal and aqueous formaldehyde in 1-propanol to a solution of (S)-1-(2-phenyl)ethyl amine **(151)** and aqueous ammonia in 1-propanol. The solution was heated to 80 °C and left stirring for 2 h. The reaction mixture was purified using flash chromatography, to give **(152c)** in a 55% yield. **(152c)** was characterised by ^{1}H NMR, ^{13}C NMR and IR.

2.2.2 Synthesis of tris(bromomethyl) mesitylene

Based on Van der Made's procedure [145] we attempted to prepare a second starting material tris(bromomethyl)mesitylene **(154)** as shown in Scheme 2.5. This reaction was carried out by adding a 31wt% HBr/acetic acid solution to a mixture of mesitylene **(153)**, paraformaldehyde and glacial acetic acid. The mixture was kept for 8 h at 95-100 °C and the colour of the reaction mixture turned clear.

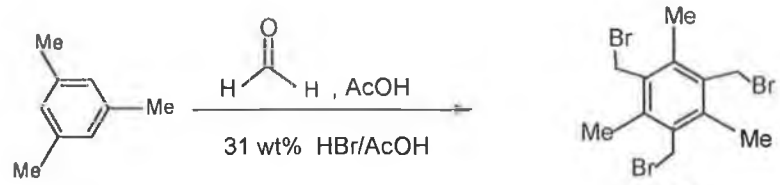

153 **154**

Scheme 2.5. Synthesis of tris(bromomethyl) mesitylene **(154)**.

Purification was accomplished by recrystallization of the crude product from chloroform, yielding large colourless crystals. In this reaction the bromo-methylation agent has an attractive feature since it allows precise control over the number of ----CH_2Br groups to be introduced by simply adjusting the reaction temperature. In other words selectivity can be controlled by temperature. The pure product was analysed and characterized by ^{1}H ,^{13}C NMR and IR.

2.2.3 Synthesis of homochiral tripodal imidazolium bromide salts

The first attempt to prepare receptor **(155c)**, is outlined in Scheme 2.6 below.

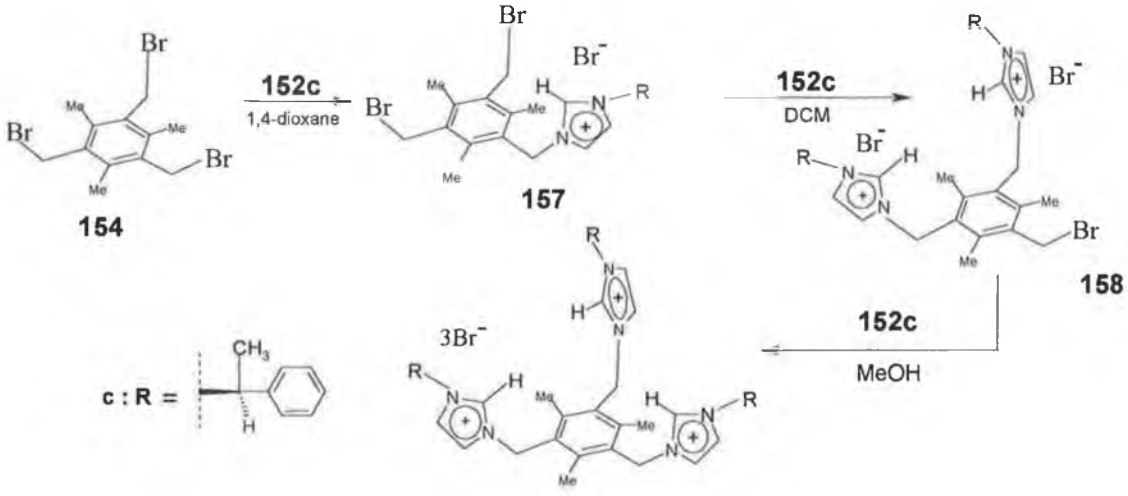

155c

Scheme 2.6. First attempt to prepare receptor **(155c)**.

This reaction was carried out by dissolving tris(bromomethyl)mesitylene in 1,4-dioxane and (S)-1-(2-phenyl)ethyl imidazole was added to the mixture. The reaction was stirred under reflux for 4 h and a brown precipitate formed. This brown compound **(157)** was then isolated and dissolved in DCM. Another stoichiometric amount of (S)-1-(2-phenyl)ethyl imidazole was added to the mixture and the reaction was stirred under reflux for 4 h. A dark brown precipitate formed and was collected **(158)**. The final step was carried out under the same reaction conditions. The product from this step was collected and analysed by TLC and ^{1}H NMR. It was found this compound was not pure and more than five spots was observed by TLC.

This reaction was unsuccessful, we believe that it's failure may have resulted due to the solvent being incompatible with an S_N2 reaction type.

Another attempt was carried out based on the procedure of Dias [104], by preparing receptors **(155c)** using a one pot synthesis. Consequently, we were able to achieve a high yield of pure receptor **(155c)** with excellent ^{1}H, ^{13}C NMR and IR spectral data. The method employed is outlined in Scheme 2.7.

This reaction was carried out by mixing compounds **(152c)** and **(154)** in 1,4-dioxane and heated to 100 °C for 24 h. The resulting cream solid was collected in 96% yield. Recrystallization gave colourless needles.

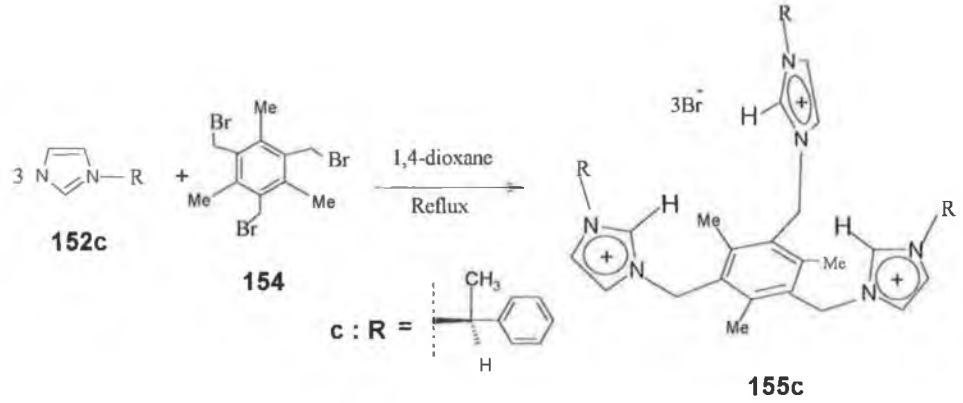

Scheme 2.7. Successful synthesis of homochiral tripodal receptor **(155c)**.

We believe this reaction goes under an S_N2 mechanism, leading to a quaternary salt of **(155c)**, Scheme 2.8.

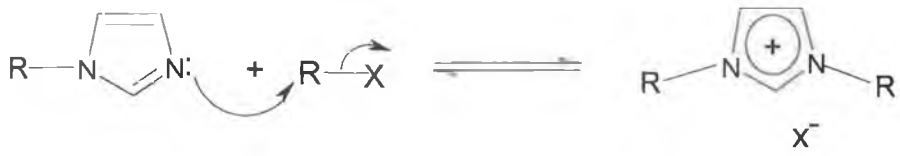

Scheme 2.8. Proposed mechanism for the formation of a quaternary tripodal salt.

2.2.4 Conversion of the bromide salt to PF_6^- salts

The final step was to convert the bromide salt **(155c)** to the hexafluorophosphate receptor **(156c)**, (Scheme 2.9). The receptor **(155c)** was dissolved in methanol and a saturated aqueous solution of ammonia hexafluorophosphate was added until no further precipitation was observed. The precipitate was filtered and washed with methanol and dried. Recrystallization was carried out using a 1:4 mixture of Acetonitrile:Ethanol, to give colourless needles (yield 66%). The resulting product was fully characterised by ^1H , ^{13}C NMR, IR and elemental microanalysis.

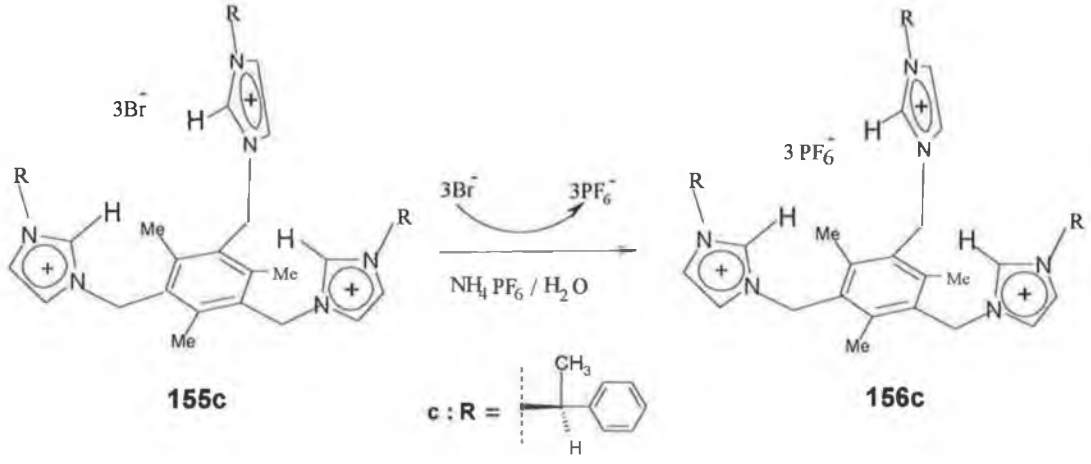

Scheme 2.9. Conversion of receptor **(155c)** to receptor **(156c)** by ion exchange reaction,

The other homochiral imidazole, homochiral tripodal bromide and hexafluoro-phosphate salts were prepared using these methods and the results are outlined in Table 2.1.

Ligands	Yield%	Bromide salts	Yield %	PF_6^- salts	Yield %
152a	87	**155a**	95	**156a**	82
152b	60	**155b**	92	**156b**	72
152d	65	**155d**	96	**156d**	80

Table 2.1. The yields from the synthesis of homochiral tripodal bromides and hexafluorophosphate salts.

The reason for converting the bromide salts to the PF_6^- salts are listed as follows:

- This process would improve purity of the receptor, and column chromatography would be avoided.
- Hexafluorophosphate anion is considered to be a weak anion in terms of its electronegativity, making it ideal for ^1H NMR titration experiments.

2.3 Spectroscopic studies

Receptors **(156a-d)** were fully characterized by ^1H, ^{13}C NMR, I.R, and elemental microanalysis.

The ^1H NMR spectra of receptors **(152c)**, **(155c)** and **(156c)**, are shown in Fig. 2.2. The respective H-2, H-4 and H-5 protons, Fig. 2.1, of the imidazolium ring show different chemical shifts. In the case of compound **(152c)** the observed peaks for H-4, H-5 and the H-2 proton appear at 6.90, 7.21 and 7.82 ppm respectively, Fig. 2.2(a), while compound **(155c)** shows different absorptions for the same protons at 7.56, 7.80 and 9.28 ppm respectively, Fig. 2.2(b). The PF_6 salts **(156c)** show different peaks at 7.34, 7.76 and 9.12, respectively, Fig.2.2(c).

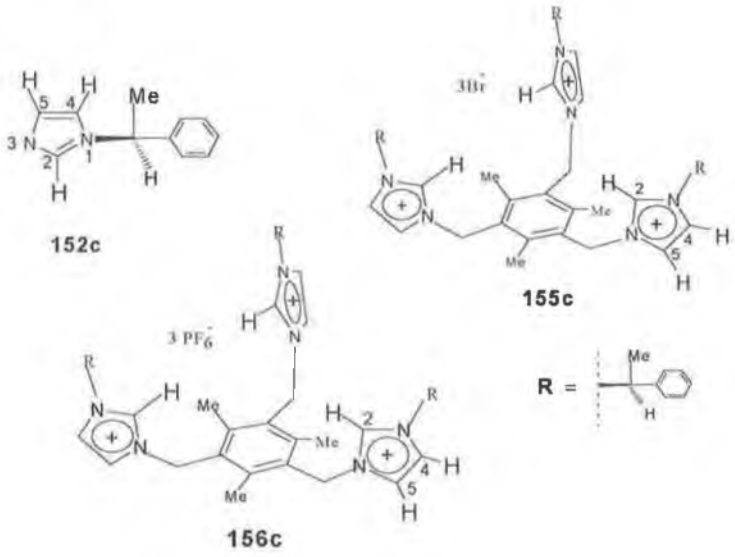

Figure 2.1. The H-2, H-4 and H-5 protons of compounds **(152c)**, **(155c)** and **(156c)**

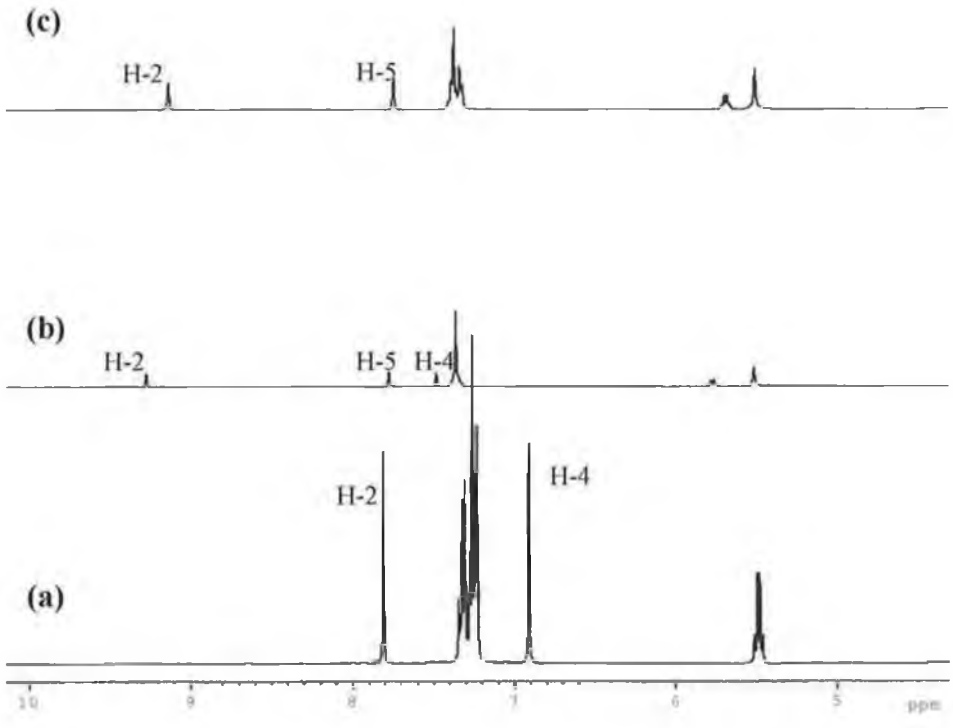

Figure 2.2. ^{1}H NMR spectra of, (a) **(152c)**, (b) **(155c)** and (c) **(156c)** compounds, showing H-2, H-4 and H-5.

The ^{1}H, and ^{13}C NMR spectra of receptor **(156c)** are shown in, Figure 2.3. and 2.4. The appearance of a doublet at 1.87 ppm is assigned to the methyl group of the chiral centre, where the proton on the same chiral centre shows up as a quartet at 5.70 ppm. Two other singlets appear at 2.24 ppm and 5.44 ppm relating to the methyl and methylene groups of the phenyl ring, while the H-4 and H-2 of the imidazolium ring give two singlets at 7.19, and 8.45 ppm respectively. The H-5 proton of the imidazolium ring overlaps with the phenyl protons. The H-2 proton is further downfield from the other protons of the imidazolium ring which can be attributed to the effect of the anion [35], [36].

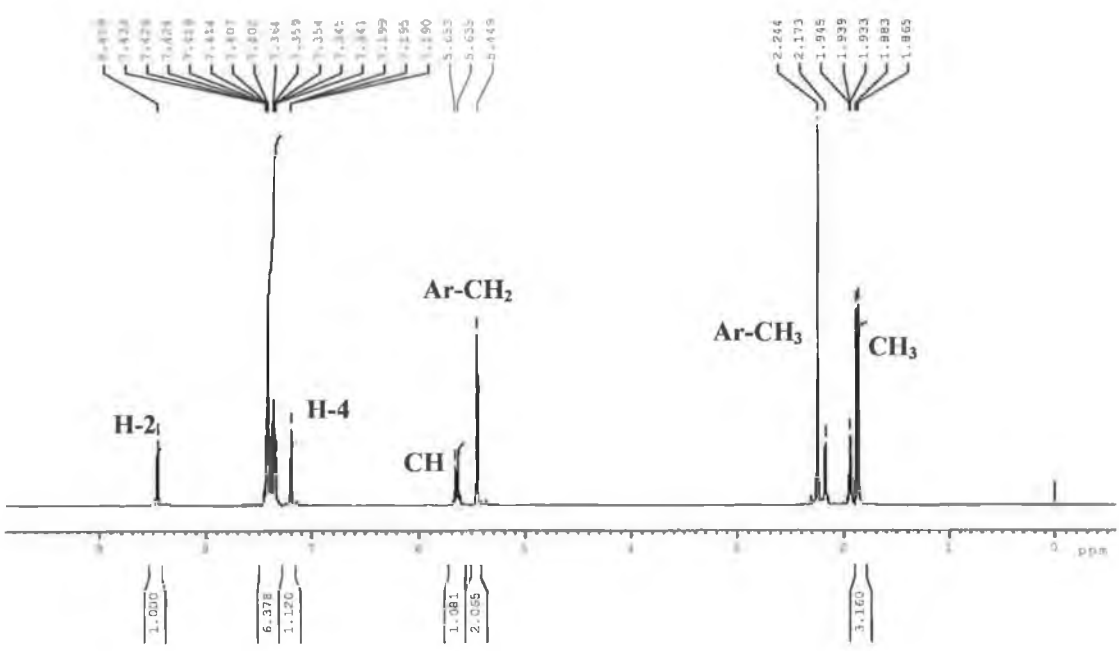

Figure 2.3. ^{1}H NMR spectrum of receptor **(156c)**

The HMQC of **(156c)** is shown in Figure 2.4.

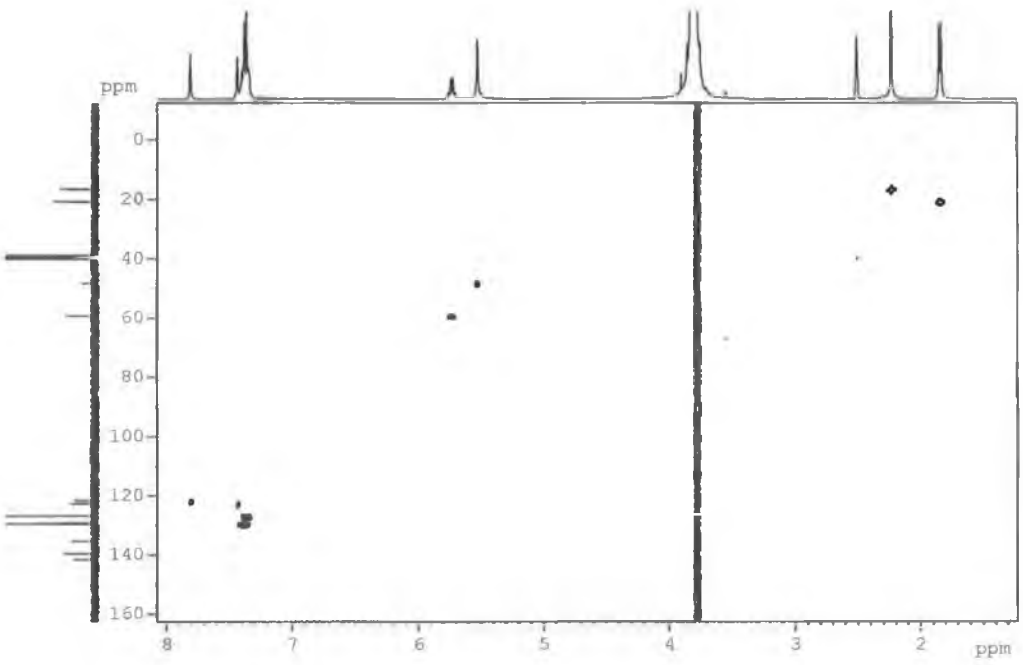

Figure 2.4. HMQC for receptor **(156c)**

2.5 Conclusion

In this work we prepared a series of homochiral tripodal imidazolium salts. These imidazolium salts were synthesised from two different starting materials **(154)** and **(152)**, where both of them were prepared in different procedures and purified by crystallisation and column chromatography. To prepare homochiral tripodal azolium bromide salts, these starting materials were applied to the reaction in different pathways; first was to react **(152)** with **(154)** in three steps. Each step employed the chiral ligand **(152)** linked with scaffold **(154)** in a 1:1 stoichiometric. But unfortunately this route was not successful. A second method was to react **(154)** with a three fold excess of **(152)**. This reaction gave the target product in good yield and high purity. Final purification for the tripodal imidazolium salts could be achieved by ion exchange. All compounds were completely characterised.

Chapter 3

Anion Recognition

3.1 Introduction

As mentioned earlier, work carried out by Sato has demonstrated that tripodal imidazolium salts act as effective anion receptors. We were interested in further developing this work by generating a new tripodal receptor containing chiral imidazolium moieties. We hoped that such a structure could not only act as an ion receptor but also be able to demonstrate enantioselective binding, Figure 3.1.

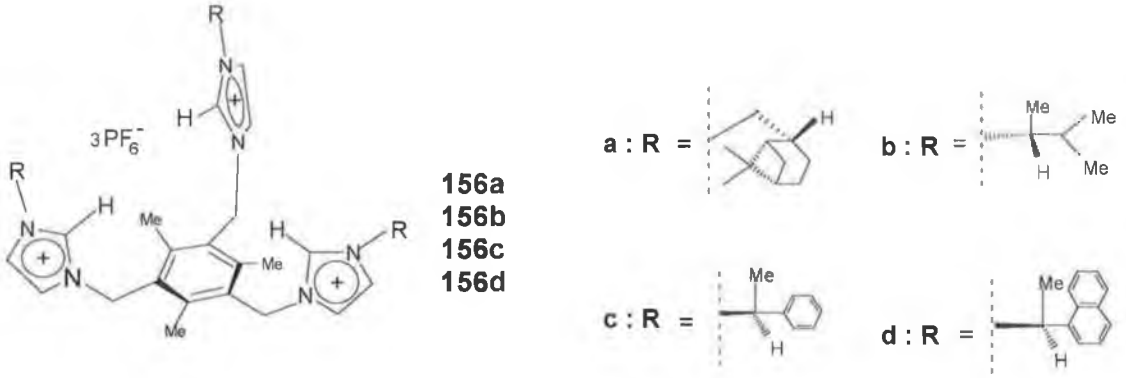

Figure 3.1 New chiral tripodal imidazolium receptor.

3.2 Results and discussion

3.2.1 ^{1}H NMR titration studies

^{1}H NMR titration studies were carried out with compounds **(156a-d)**. The H-2 protons of the imidazoluim handles were monitored with respect to change in chemical shift of the 1,3-dialkylazolium salts [35, 36, 146-153].

The addition of stoichiometric amounts of various anions as their tetraethyl or tetra butyl ammonium salts, [NEt_4] or [NBu_4] X [X = Cl^-, Br^-, I^-, NO_3^- and HSO_4^-] to a CD_3CN solution containing **(156a-d)** resulted in significant downfield shifts of the H-2 proton of the imidazolium rings.

In the case of receptor **(156a)**, the resulting titration curves (Figure 3.2) suggest a stoichiometry of 1:1 imidazolium salt:anion for all anions studied (X)[X: Cl^-, Br^-, I^-, NO_3^- and HSO_4^-]. Broadening of the H-2 proton peak of imidazolium ring was observed when chloride anion was added to receptor **(156a)** [from 0.2 to 1 equivalent]. In this case the quantitative interpretation of the experiments should be viewed with some caution as the fast-exchange criteria are not strictly met.

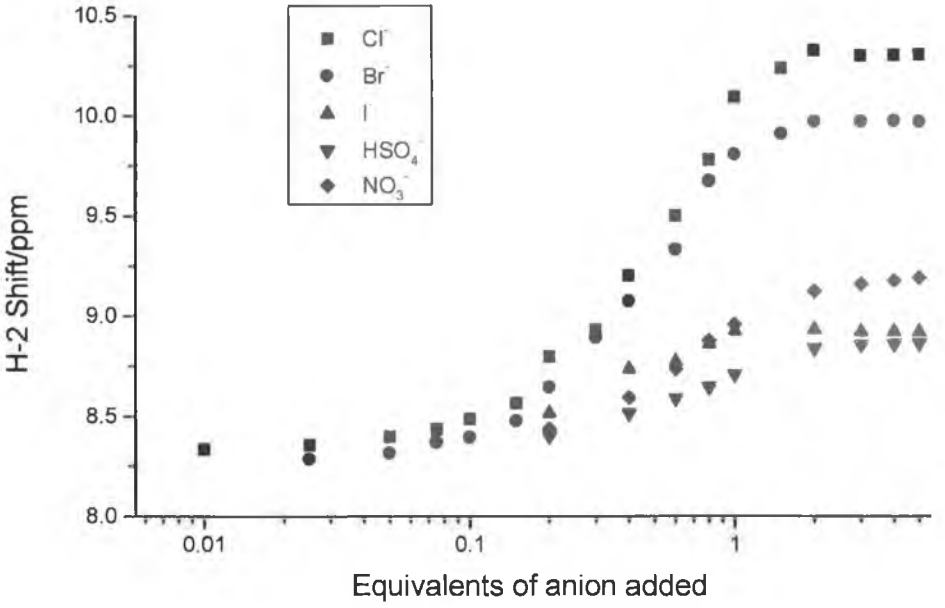

Figure 3.2 ^1H NMR titration curve of myrtanyl tripodal imidazolium salt **(156a)** with various anions added as their tetra butyl or ethylammonium salts in CD_3CN.

Very clear perturbations were observed for the H-4 and H-5 protons of the imidazolium ring which may suggest that hydrogen bonding is occurring between the anions and the H-4 and H-5 protons. This is in agreement with previous findings of hydrogen bonding between all three ring protons of the imidazolium cation and anions [142]. We also observed a downfield shift for one of the methylene protons (diastereotopic); which is adjacent to the nitrogen of the imidazolium ring in this receptor **(156a)** especially in the case of Cl^- and Br^-, giving a shift downfield of about 0.2 ppm.

In the case of **(156b)**, the resulting titration curves (Figure 3.3) again suggest a stoichiometry of 1:1 receptor:anions X (X = Cl^-, Br^-, I^-, NO_3^- and HSO_4^-). The results are similar to that of receptor **(156a)**, and this observation could be attributed to the steric hindrance caused by the alkyl group substituents bond to the imidazolium ring. This may suggest the formation of a similar anion complex for this ligand.

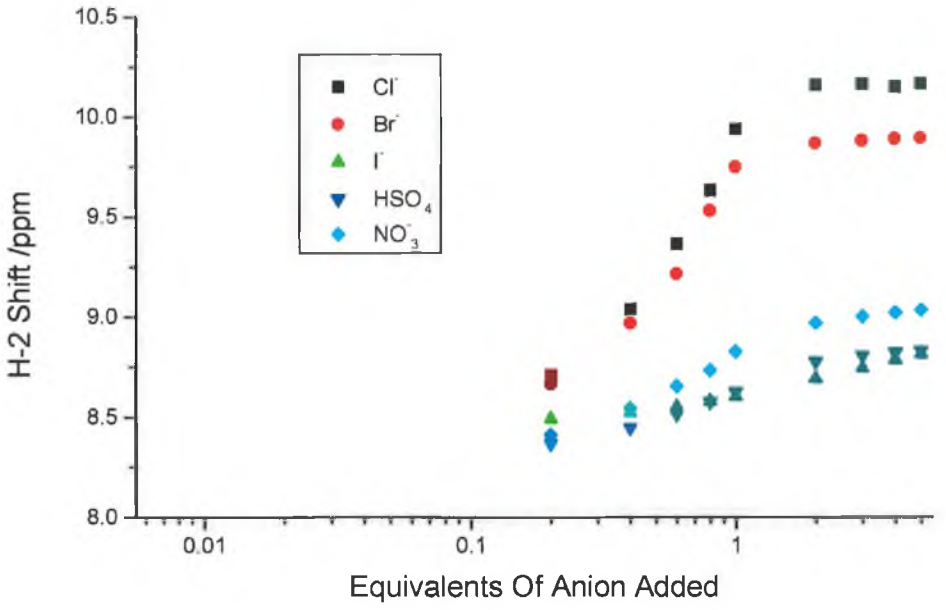

Figure 3.3 ^1H NMR titration curve of butyl tripodal imidazolium salt **(156b)** with various anions added as their tetra butyl or ethyl ammonium salts in CD_3CN.

Broadening of the H-2 proton peak of the imidazolium ring was again observed when chloride anion was added to receptor **(156b)** [from 0.2 to 1 equivalent]. Also observed was a perturbation of the H-4 and H-5 protons of the imidazolium ring of **(156b)** with all anions (Cl^-, Br^-, I^-, NO_3^- and HSO_4^-), with Cl^- and Br^- being the largest. The proton at the chiral centre of the imidazolium ring was shifted downfield with Cl^- and Br^-.

For comparison to the above results, receptors **(156c)** and **(156d)** have also been investigated and they showed similar behaviour, but different than the previous two ligands **(156a, 156b)**.

In the case of receptor **(156c)**, the resulting titration curves (Figure 3.4) indicate a stiochoimetry of 1:1 imidazolium salt:anion in all cases, but it shows a smaller downfield shift for Cl^- and Br^-, 1.5 and 1.18 ppm respectively, while I^- and NO_3^- show very small chemical shift changes of 0.26 and 0.27 ppm, respectively.

Data for HSO_4^- are not included as this anion precipitated during the titration with **(156c)**.

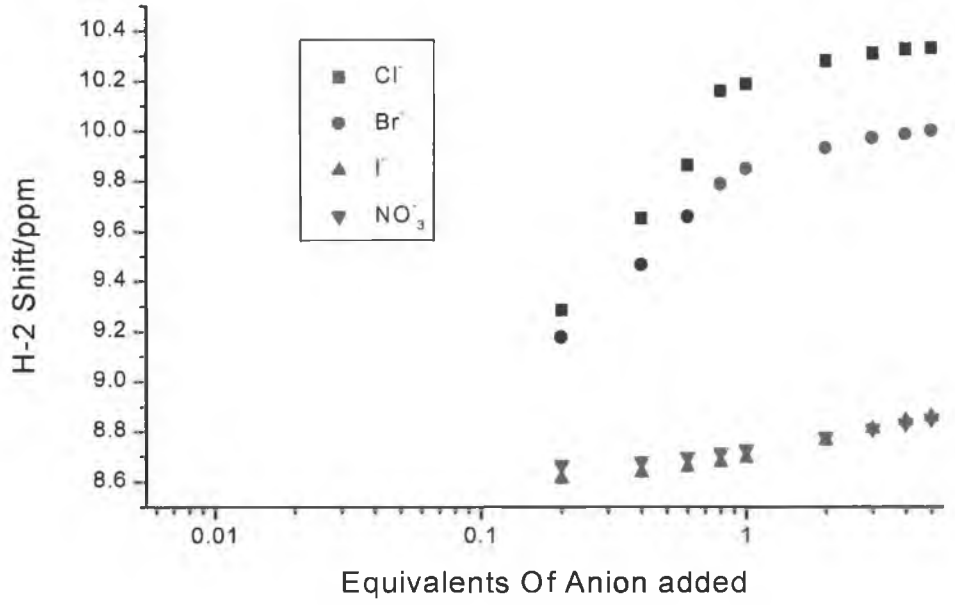

Figure 3.4 ^1H NMR titration curve of phenyl tripodal imidazolium salt **(156c)** with various anions added as their tetra butyl or ethyl ammonium salts in CD_3CN.

The final receptor to be investigated by NMR titration studies, **(156d)** displayed similar behaviour to the previous receptor **(156c)**, but different than the first two receptors **(156a)** and **(156b)**. The resulting titration curves (Figure 3.5) indicate a 1:1 stoichiometry of imidazolium salt:anion in all cases (Cl^-, Br^-, I^-, NO_3^-). Data for HSO_4^- anion was not recorded again due to precipitation.

Perturbation of the H-4 and H-5 protons also occurred upon anion addition. Also the proton at the chiral centre in the imidazolium ring was shifted downfield as was the case with receptors **(156b)** and **(156c)**.

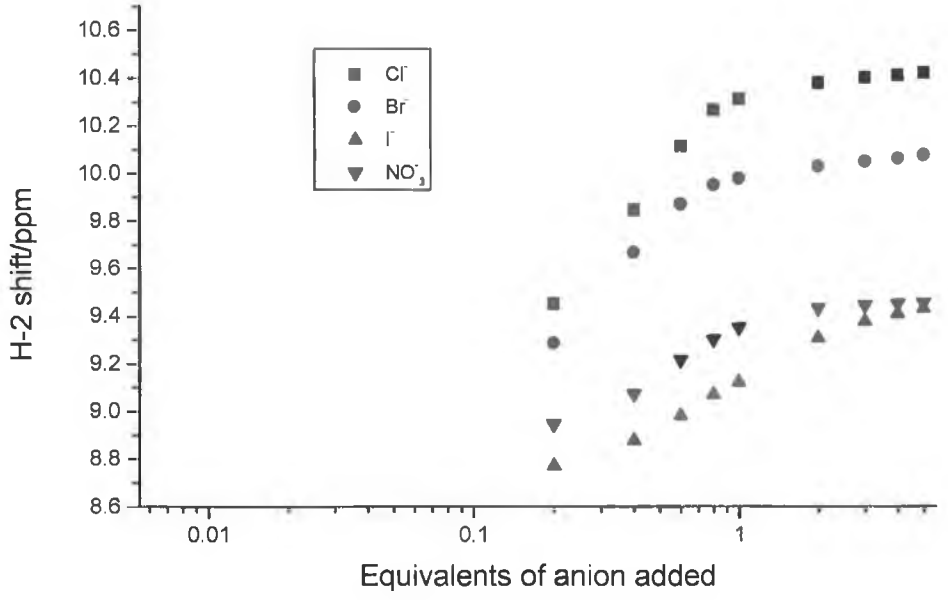

Figure 3.5. ^{1}H NMR titration curve of naphthyl tripodal imidazolium salt **(156d)** with various anions added as their tetra butyl or ethyl ammonium salts in CD_3CN.

3.2.2 K values of homochiral tripodal receptor

In order to evaluate these receptors **(156a-d)** in terms of binding strength and selectivity toward anions, we calculated the association constant **K** values by using a non-linear curve-fit to the function of the chemical shift dependence vs the equivalent of anion [154-157] in Excel, Figure 3.6.

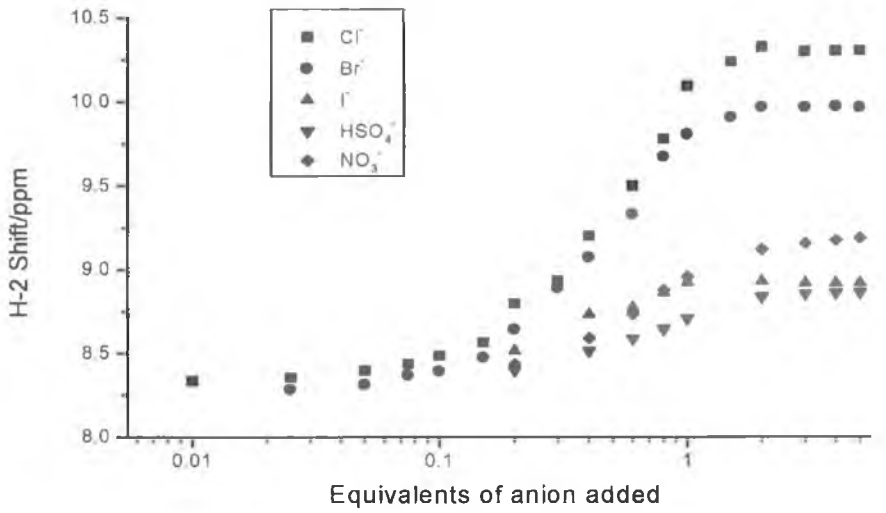

Figure 3.6 Log plot curve of myrtanyl tripodal imidazolium salt **(156b)**.

This calculation was carried out by initially estimating the **K** value. The δ_{calc} was calculated using Equation (1) [158] below, at a given data point. By using the obtained δ_{calc} and **K** values, the δ_{calc} at each experimental point is calculated. Then the difference (residual) between δ_{obs} and δ_{calc}, is computed for each data point. The **K** value is then adjusted to minimise the sum of the squared residuals. Then the entire process is repeated until convergence (see Figure 3.7). The estimated error is 10%.

$$\delta_{obs} = \delta_{Host} + (\Delta_o/2[Host^o]) \{[Host^o]+[Guest^o]+ 1/K- \sqrt{(([Host^o]+[Guest^o]+1/K)^2 - 4[Host^o][Guest^o])}\} \quad \ldots\ldots\ldots\ldots\ldots\ldots(1)$$

Where δ_{obs}, δ_{Host} are the observed and host chemical shift; Δ_o is the difference between the free and complexed chemical shift.

The calculated **K** value of Receptor **(156b)** with different anions is shown on the next page.

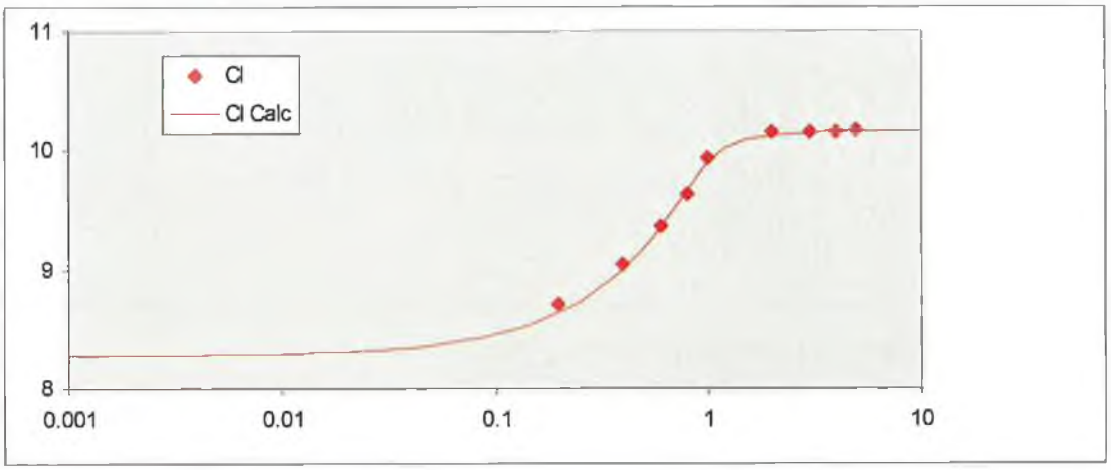
11
10
9
8
0.001
0.01
0.1
1
10
Cl
Cl Calc

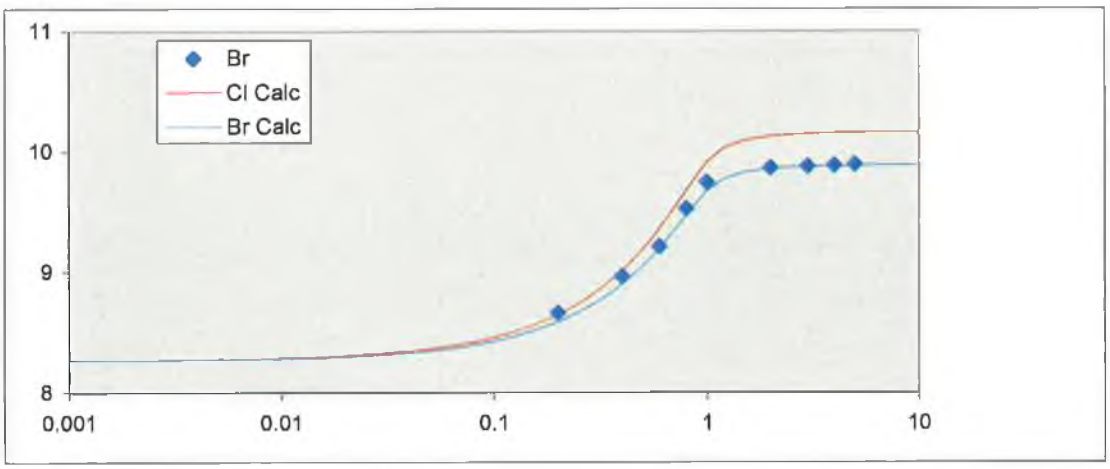
11
10
9
8
0.001
0.01
0.1
1
10
Br
Cl Calc
Br Calc

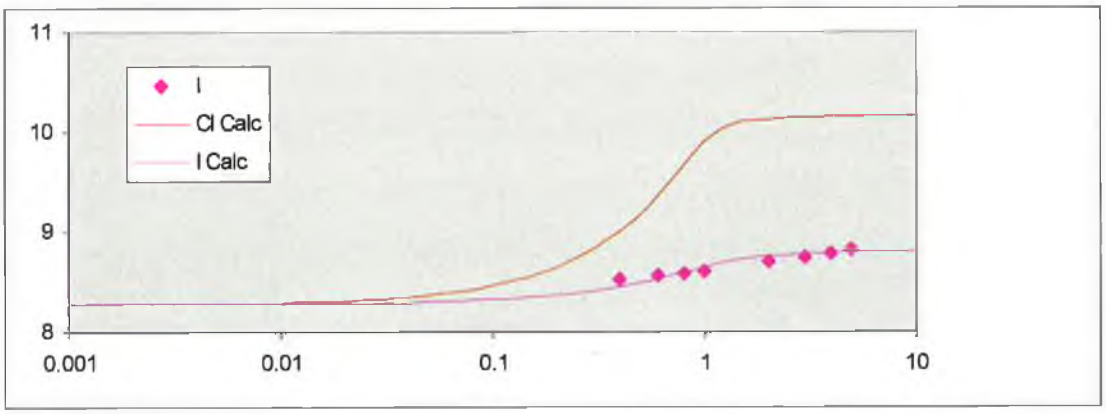
11
10
9
8
0.001
0.01
0.1
1
10
I
Cl Calc
I Calc

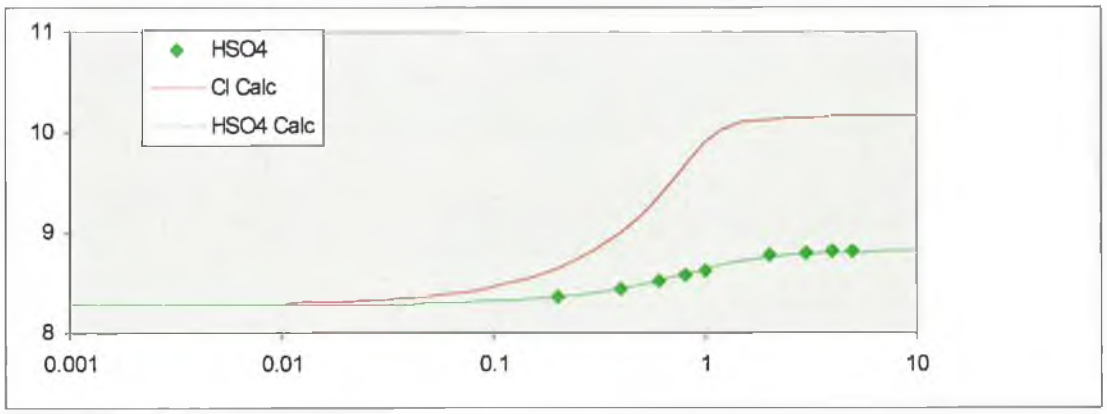

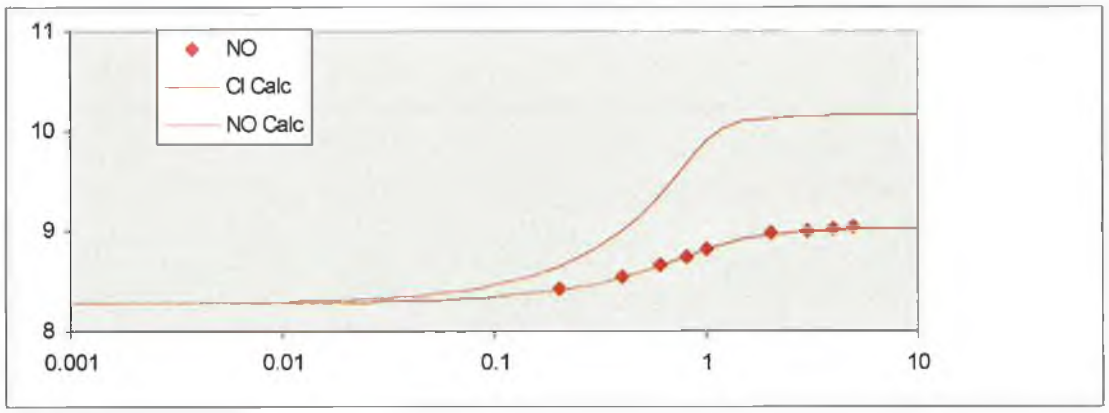

Figure 3.7. Experimental data and Calculated curves for receptor **(156b)**.

The **K** values obtained in this way are presented in, Table3.1

Anions	*156a*	*156b*	*156c*	*156d*
Cl^-	16000>	10000>	12000>	12000>
Br^-	16000>	10000>	12000	11500
I^-	-	1600	200	340
NO_3^-	1473	2647	280	2500
HSO_4^-	2780	1163	-	-

Table 3.1. K value (association constant) in M^{-1} for receptors **(156a-d)** (estimated errors; 10%).

From Table 3.1 it can be seen that these receptors **(156a-d)** were able to bind strongly with anions such as Cl^- and Br^-. Receptor **(156b)** is showing a selectivity toward Cl^- and Br^- over I^-, NO_3^- and HSO_4^-, whereas receptor **(156a)** shows a selectivity toward Cl^- and Br^- over NO_3^- and HSO_4^- (I^- was rejected because it was not possible to fit the data properly). Receptors **(156c)** and **(156d)** showed selectivity toward Cl^- and Br^- over I^- and NO_3^-. But receptors **(156c)** particularly shows some increase in selectivity compared to the others and this may be attributed to a flexible rotation of the phenyl groups which will reduce the effective size of the cavity. This would have an effect on the binding of large anions such as NO_3^- and I^- in particular. This is supported from molecular modelling studies of **(156c)** and the other receptors.

3.2.3 Selectivity and binding at low concentration

We were also interested in determining whether self-association occurs between individual receptor molecules in solution [159,160]. If such a phenomenon where to occur this would affect our interpretation of the above results. A dilution experiment was designed to determine if self-association was occurring. If no change on the chemical shift occurs on dilution then self-association can be eliminated.

Shown in Figure 3.8 are the results for the dilution study. The chemical shift change between 10^{-3}-10^{-4} M is equivalent for the shift change observed for the Cl^- titration of the same receptor. We realised that Cl^- might be present at very low concentration in CD_3CN, and what we were observing was an inverse titration. We tested the purity of CD_3CN by ion chromatography (carried out by Leon Barron in DCU) and found both Cl^- and NO_3^- present (Figure 3.9). Thus receptor **(156a)** is binding Cl^- at low concentration, and it seems to selectively bind chloride over nitrate based on the observed chemical shift.

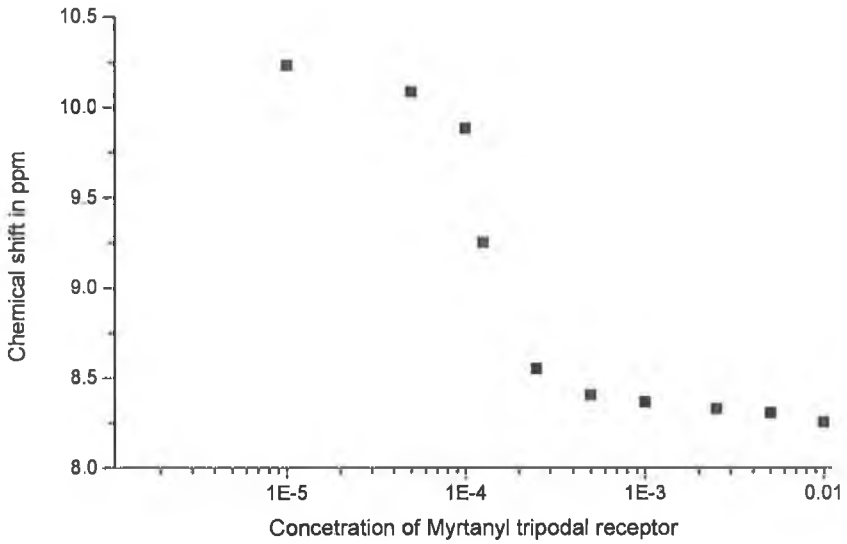

Figure 3.8. Chemical shift of H-2 resonance in **(156a)** as a function of concentration.

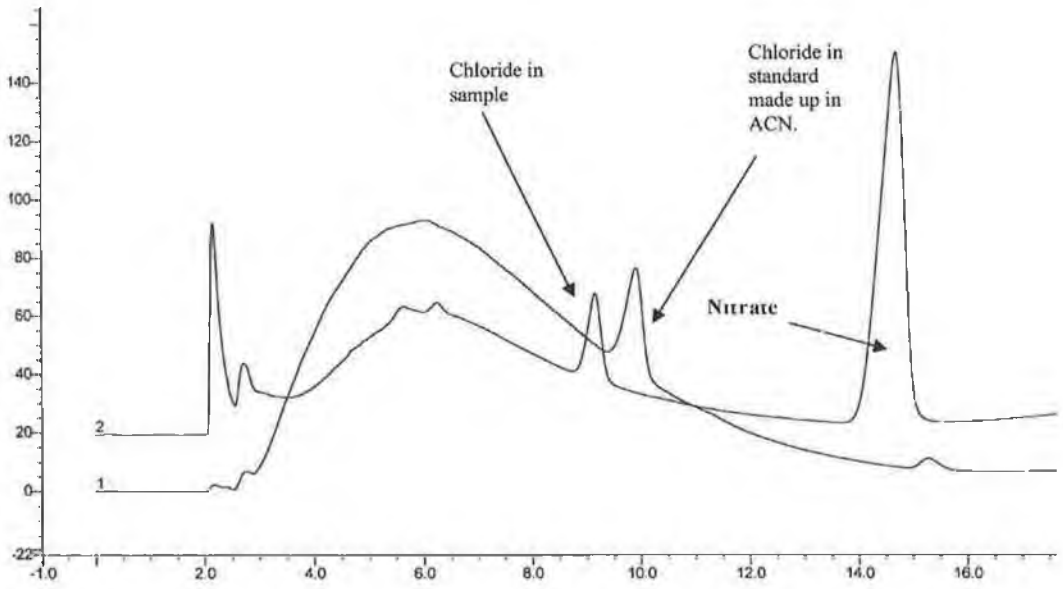

Figure 3.9. Ion chromatograph showing that CD_3CN solvent has chloride and nitrate anions present.

We found receptor **(156c)** was able to detect Cl^- anion with a downfield shift of 1.1 ppm at a concentration of 1×10^{-4} M in CD_3CN. These results demonstrate that this receptor is able to bind Cl^- selectively even at low concentrations in polar aprotic solvent such as CD_3CN.

We also titrated receptors **(156b-d)** under the same conditions (i.e. dilution experiment) and the results are outlined in table 3.2. It would appear that all receptors show the same behaviour as **(156a)** on dilution

Receptors	δ (ppm)at 10^{-2} M	δ (ppm) at 10^{-4}M
156c	8.80	9.90
156b	8.25	9.86
156d	8.58	9.98

Table 3.2. ^{1}H NMR experiments of receptors **(156b-d)** binding chloride anion in different concentration.

3.2.4 Computer modelling

In order to obtain a better understanding of these receptors in terms of binding and selectivity with different anions, it was decided to carry out computer modelling experiments. These will allow us to assess the size of the receptor's cavity and also the fitness of the anions for this cavity. Receptor **(156a)** is given a model structure using MM^+ optimisation in both stick and space-filling model [161] Figure 3.10.

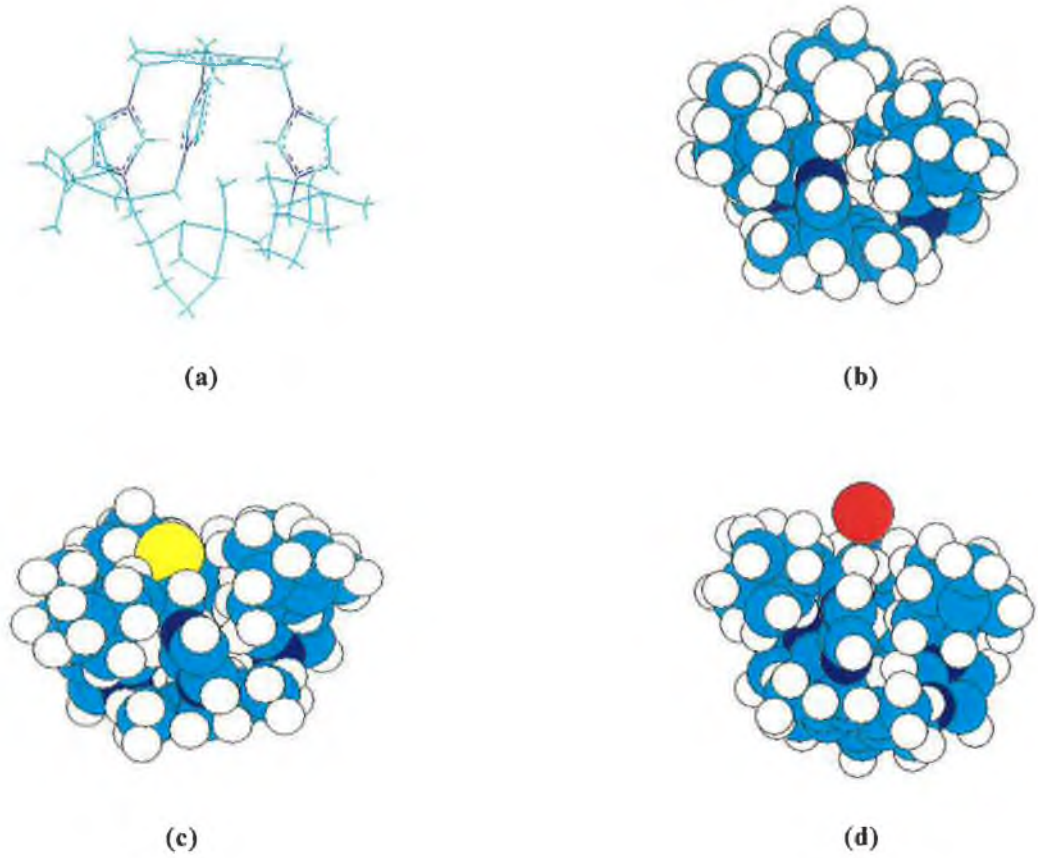

Figure 3.10 MM^+ optimisation model (using no constraints and the cavity size; 4.64 Å) for compound **(156a)**; (a) In stick model; (b) in space-filling model with Cl^- bonding; (c) in space-filling model with Br^- bonding; (d) in space-filling model with I^- bonding.

From Fig. 3.10 a-d, we can see that receptor **(156a)** has more affinity toward Cl^- and Br^- over I^- anions due to the steric hindrance of the myrtanyl handle. It would appear that I^- is too large to fit into the receptor cavity.

Also three different projected geometries for receptors **(156b-d)** were obtained using MM^+ optimisation, Figure 3.11-13.

(a) (b)

Figure 3.11. MM^+ optimisation model (no constraints and the cavity size; 4.26 Å) for compound **(156b)**; (a) stick model; (b) space-filling model.

(a) (b)

Figure 3.12. MM^+ optimisation model (no constraints and the cavity size; 4.08 Å) for compound **(156c)**; (a) stick model; (b) space-filling model.

(a) (b)

Figure 3.13. MM^+ optimisation model (no constraints and the cavity size; 4.00Å) for compound **(156d)**; (a) stick model; (b) space-filling model.

From Fig. 3.11-13, it can be seen that receptors **(156b-d)** have similar cavity sizes which may explain why receptor **(156c)** shows higher selectivity for anion binding than the others and that may be (as it is already mentioned) attributed to the flexible rotation of the phenyl groups. This will reduce the size of its cavity and therefore will enhance the capability for anion selectivity.

3.3 Conclusion

Four homochiral tripodal imidazolium salts **(156a-d)** have been investigated by ^{1}H NMR titration studies and they all demonstrate an excellent affinity and selectivity toward Cl^- and Br^- over I^-, NO_3^- and HSO_4^- in polar aprotic solvent. All receptors **(156a-d)** showed significant strong binding toward Cl^- and Br^- anions as demonstrated by the **K** (M^{-1}) value which is from 10000> to 16000> M^{-1}. Receptor **(156b)** showed selectivity towards Cl^- and Br^- over I^-, NO_3^- and HSO_4^-, respectively, while receptor **(156a)** showed similar selectivity. Receptors **(156c)** and **(156d)** showed selectivity for Cl^- and Br^- over NO_3^- and I^-. This was based on **K** (M^{-1}) value measurements. Receptor **(156c)** showed strong selectivity compared to the others and this may be attributed to the flexible rotation of the phenyl groups attached to the imidazolium ring.

In order to examine these receptors in terms of binding and selectivity at low concentration, ^{1}H NMR titration results suggest a good affinity for all these receptors with Cl^- anion, while **(156a)** showed a selectivity for Cl^- over NO_3^- in polar aprotic solvent.

Chapter 4

Enantiomeric Discrimination and Antimicrobial Activity of Homochiral Tripodal Receptors

4.1 Results and discussion

The second goal of our research was to employ compounds **(156a-d)**, Figure 4.1, as potential enantiomeric selective receptors for the enantioselective discrimination of enantiomers. We focussed on, sodium (S)-2-aminopropionate and sodium (R)-2-aminopropionate as the target guests, which we believed to be ideal since they possess the potential to both H-bond and electrostatically interact with our receptors. These factors should play an important role toward complexation between host and enantiomer guest to form a diastereomeric complex.

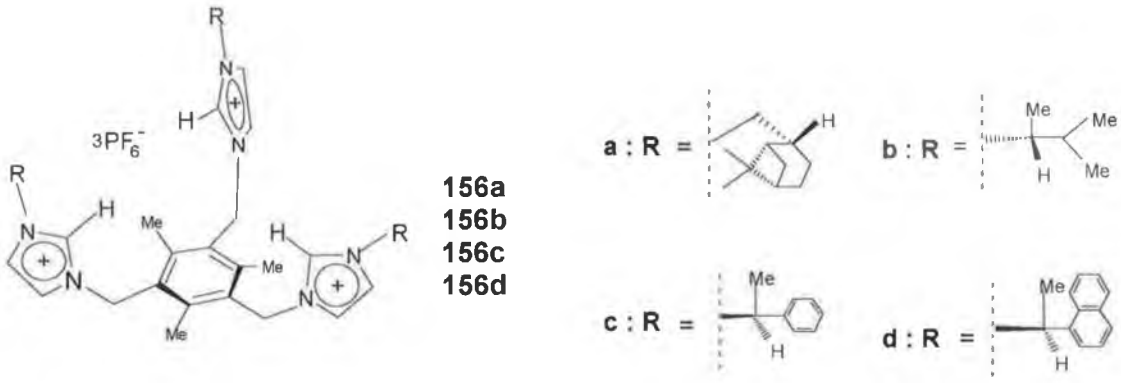

Figure 4.1. Four homochiral tripodal imidazoluim salts with different chiral substituted groups.

Receptors **(156a-d)** were screened for enantiomeric selectivity using ^{1}H NMR experiments. The rational behind these experiments was that if the tripodal molecule acts as a receptor for the anionic enantiomers, a diastereomeric complex would be formed. The formation of a distereomeric complex would lead to an observable change in the ^{1}H NMR spectra for either the anionic enantiomer or that of the tripodal molecule component of the complex. Should the potential receptor distinguish between anionic enantiomers we might see a shift difference in the δ value for a particular proton in the complex, and the magnitude of the

shift could depend on which one of the two diastereomeric complexes is formed. If this were the case, we can establish which complex is formed preferentially.

A stock solution of each of the four homochiral imidazolium hexafluoro-phosphate salts in deuterated acetonitrile solvent were prepared and titrated with the appropriate chiral salt dissolved in D_2O, a series of control experiments were also carried out in order to investigate any solvation effect as a result of using two different solvents. To equal aliquots of the stock solution, (S)-2-amino-propionate anion and (R)-2-aminopropionate anions were added in a 1:1 ratio (1:1:1 for the racemic mixture). The results from these experiments were very interesting. For our tripodal compounds **(156b-d)**, we observed no changes in the ^1H NMR spectra when titrated with either of the anionic enantiomers or the racemic mixture. On the other hand receptor **(156a)** demonstrated discrimination toward (R)-2-aminopropionate over (S)-2-aminopropionate, Figure 4.2.

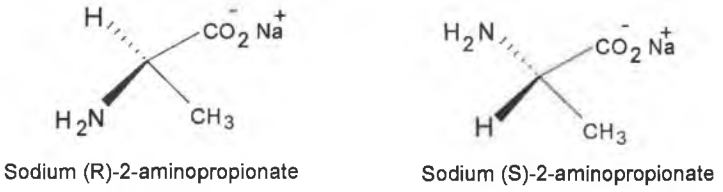

Figure 4.2. Two chiral anions which were discriminated by receptor **(156a)**.

A ^1H NMR spectrum of **(156a)** is shown in Figure 4.3 next page.

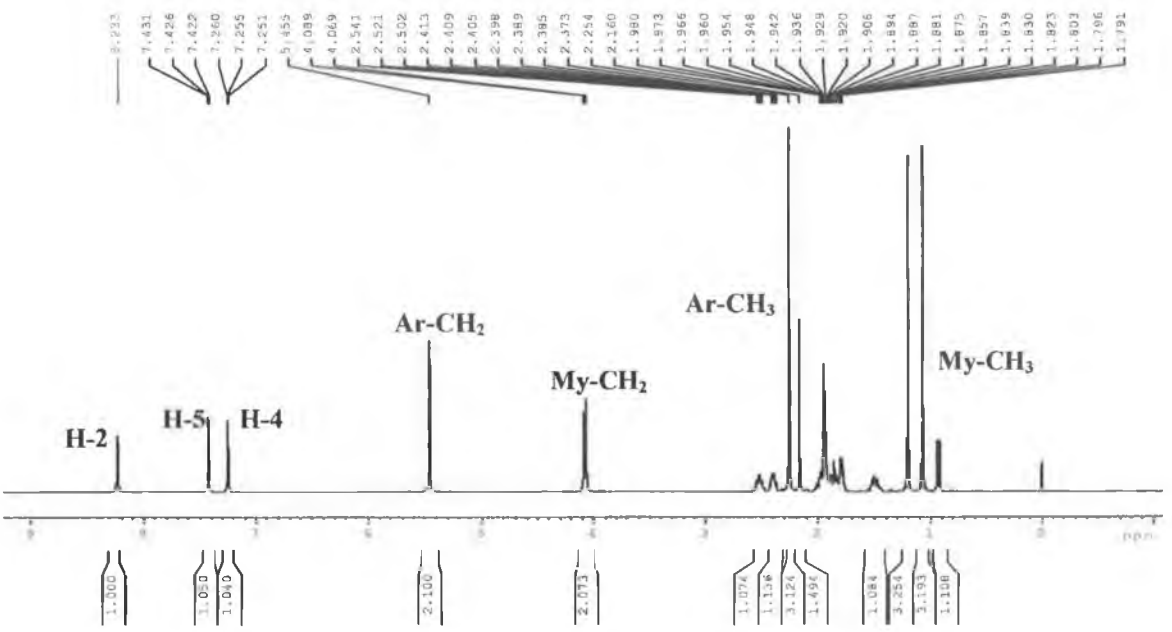

Figure 4.3 ^{1}H NMR spectrum (CD_3CN) of **(156a)**.

The α-proton of **(R)/(S)** anions show a distinct quartet at 3.62 ppm, Fig 4.4 (a). When **(156a)** was titrated with **(R)**, the α-proton shifted downfield to 4.42 ppm and there was an observed broadening of the signal, Fig. 4.4 (c). This change indicates the presence of a diastereomeric complex. Receptor **(156a)** was also titrated with **(S)** but no change was observed in the ^{1}H NMR spectrum, Fig. 4.4 (b). When the experiment was carried out with receptor and racemic mixture two signals were observed at 4.42 and 3.62 ppm. indicating that the (R)-anionic enantiomer has been complexed and the (S)-anionic enantiomer remained uncomplexed, Fig. 4.4 (d).

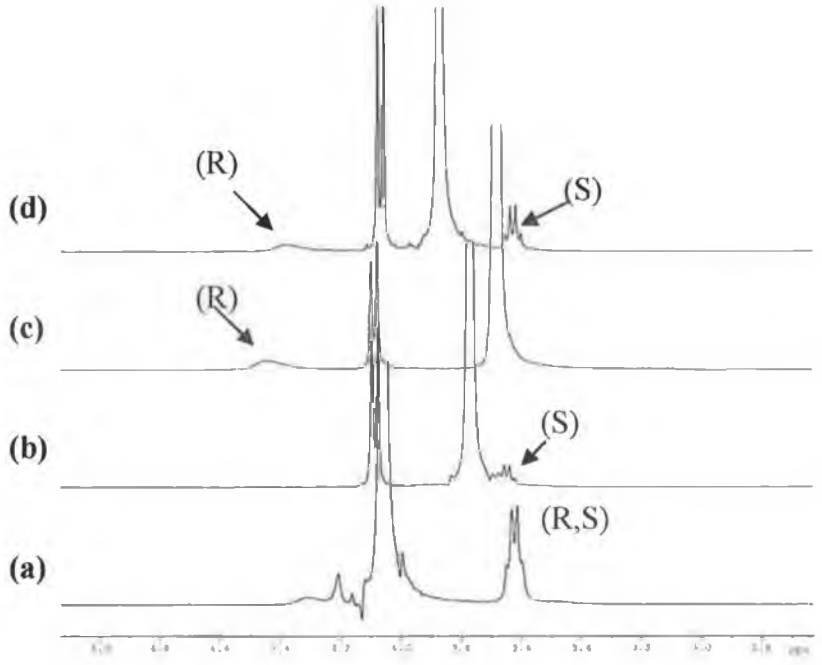

Figure 4.4 ^{1}H NMR titration spectroscopy (CD_3CN/D_2O) of host-guest complex between, (a) racemic mixture only of **(R)** and **(S)**, (b) **(156a)** and **(R)**, (c) **(156a)** and **(S)**, (d) **(156a)**, **(R)** and **(S)** respectively.

Attempts were also made to complex different chiral anions such as L, D propionate and L, D lactate with others homochiral tripodal receptors **(156a-d)**, but there was no complexation.

4.2 Control experiments

The idea of complexation between chiral host and guest was based on two factors; first, hydrogen bonding and electrostatic attraction, and second the chirality of the chiral host could selectively discriminate enantiomers (as is observed with **156a**). Three of our receptors did not demonstrate any complexation with enantiomers **(R,S)**, this could be attributed to:

1- The solvation effect: water and acetonitrile are competitively solvating the chiral anion [9,10], and this situation has been observed by ^{1}H NMR.

2- Steric hindrance: the naphthyl, phenyl and butyl groups of **156b**, **c** and **d** could prevent the chiral anion from reaching both the hydrogen bonding and positive centre of the imidazolium rings, Figure 3.11-13 (chapter 3). Receptor **(156a)** possesses an extra methylene spacer, creating more space within the receptor, allowing anions to enter the cavity for binding.

To explain the first point that the water is solvating with the receptor, we observed in previous experiments the acidic H-2 proton of the imidazolium rings completely disappearing. In order to determined whether this phenomena was occurring, we ran a series of ^{1}H NMR control experiments with just the chiral host **(156a)**, in the same ratio and volume of acetonitrile and water (same solvent ratio used in the titration experiments), Figure 4.5.

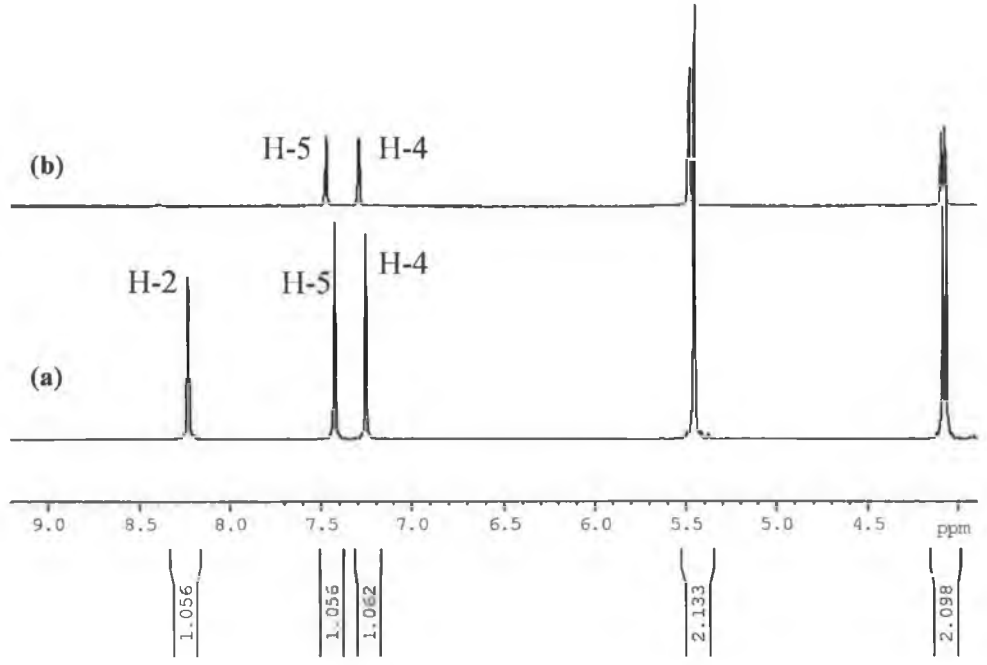

Figure 4.5 ^{1}H NMR spectra of **(156a)**; (a) in CD_3CN, (b) in a 1:1 of CN_3CN:D_2O.

The results of the control experiments showed the disappearance of the H-2 proton signal. We believe an equilibrium could be established between deuterated water and the imidazolium ligand leading to proton exchange, presumably as shown in Scheme 4.1 below:

Scheme 4.1. Homochiral receptors **(156b-d)** react with deuterated water in equilibrium situation.

Alternatively it is possible that D_2O is interfering with binding as shown in Fig. 4.6 below.

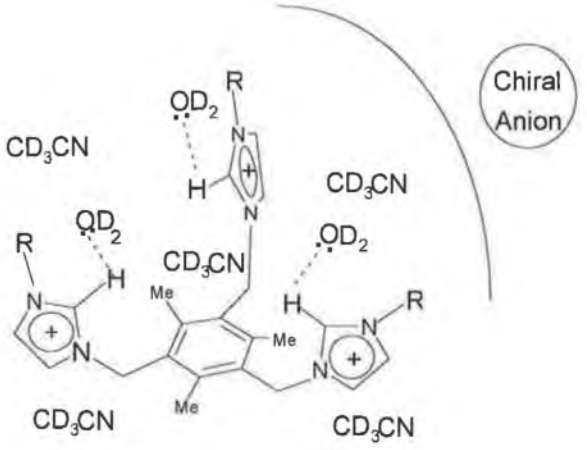

Figure 4.6. Solvation effect of D_2O on receptors **(156b-d)**.

We decided to carry out a ^1H NMR experiment for compound **(159)** in the same ratio of co-solvent (CD_3CN-D_2O) in order to examine water interference and to compare with compound **(156a)**, Figure 4.7.

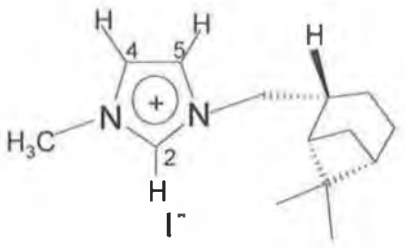

159

Figure 4.7. The H-2 proton of compound **(159)** showed sensitivity to D_2O.

The results revealed a 50% lowering of intensity of the H-2 proton signal of the imidazolium ring, Figure 4.8 (b), and when the ratio of D_2O was increased the intensity of the H-2 proton decreased by 75%, Figure 4.8 (c), but it did not completely disappear as was the case with receptor **(156a)**. This could be attributed to the structure of receptor **(156a)** preferably binding D_2O rather than compound **(159)**. The decreasing of the intensity of H-2 proton signal may be attributed to water interference, and this supports our conclusion of water interference with compound **(156a)**.

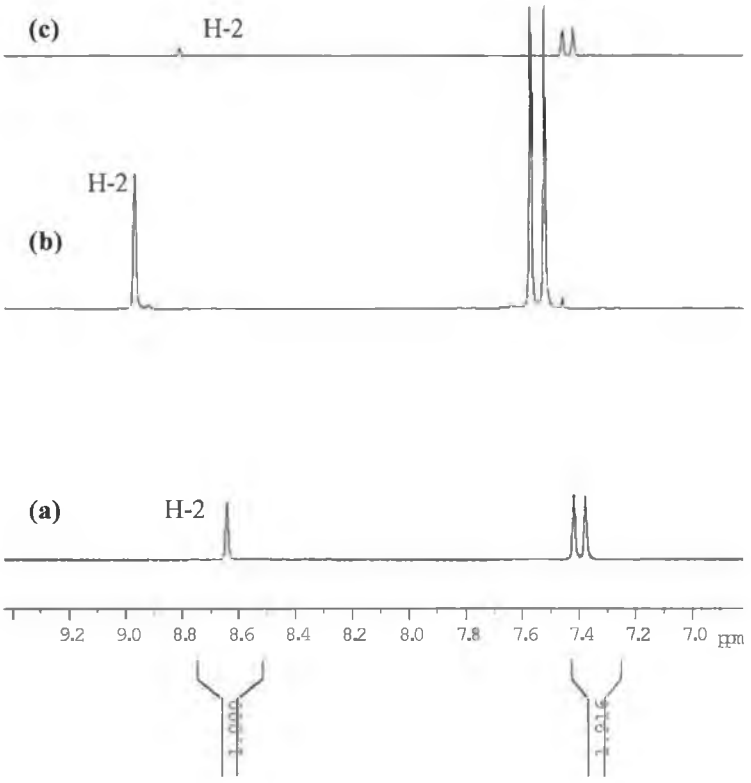

Figure 4.8. The effect of addition of D_2O solvent on the H-2 proton of compound **(159)**; (a) compound **(159)** only (CD_3CN); (b) compound **(159)** and CD_3CN: D2O (1:3); (c) Compound **(159)** and CD_3CN:D_2O (1:6).

A suggestion for future work may be to increase the number of methylene spacer groups (CH_2) between the imidazolium ring and the chiral handles of the receptors **(156b-d)**. This could reduce the steric hindrance effect, and may enhance chiral discrimination. Alternatively enlargement of the cavity by replacing the benzene ring with prophyrin or any subunit which is larger than benzene will allow for a larger pocket which may improve the performance of these receptors.

4.3 Antimicrobial activities of homochiral tripodal azolium salts

4.3.1 Introduction

We were interested in screening imidazolium receptors **(156a-d)** against a *yeast*, *candida albicans*, and a *Gram-negative bacterium*; *Pseudomonas aeruginosa*. These microbes are able to form biofilms that are resistant to antimicrobial agents [162], and have been recognised as opportunistic pathogens that infect immuncompromised human hosts [163,164]. The candida species are the etiological agents of nosocomical fungal infections, where *C. albicans* is the most significant [165]. *C. albicans* can form biofilms in vitro on various inert surfaces under different nutrient conditions, and subsequently, can cause infections associated with biomedical implants [166-169].

P. aeroginosa has a great ability to adopt to various environments and it is one of the most nosocomial acquired pathogens, and thus it is found in hospitals, where it is nearly impossible to eliminate from hospital atmospheres [170].

4.3.2 Results and discussion

The first series of homochiral imidazolium salts **(156a-d)** were screened for their antibiotic capability against *P. aeruginosa* and *C. albicans*, where also other series of compounds **(156a)**, **(159)** and **(152a)** were screened on the same test. The results are given in Table (4.1) and (4.2) for *P. aeruginosa* and *C. albicans*, respectively.

The antibiotic activities were calculated as reduction in cell growth calculated using the following formula:

Reduction in growth = [((C-B)-(T-B)) / C-B]] * 100

where C is the average absorbance per well for control wells (organism with no compound), B is the average absorbance per well for blank wells (no organism with no broth) and T is the average absorbance per well for treated wells (organism and compound).

	Percentage reduction in growth (%age)					
	25μg/ml	50μg/ml	75 μg/ml	100μg/ml	250μg/ml	500μg/ml
156c	12.97	20.48	19.46	21.45	19.40	31.56
156d	10.00	6.11	18.75	55.99	58.47	69.77
156a	18.91	0.00	50.37	93.12	81.17	90.95
156b	0.00	0.00	6.27	0.00	19.89	0.22

Table 4.1. The antimicrobial activity of homochiral tripodal azolium compounds against *P. aeruginosa*.

	Percentage reduction in growth (%age)					
	25 μg/ml	50 μg/ml	75 μg/ml	100μg/ml	250μg/ml	500μg/ml
156c	2.20	0.00	0.81	0.72	0.00	0.25
156d	2.20	2.85	18.78	54.05	90.00	89.66
156a	2.79	5.38	17.24	73.67	91.51	91.26
156b	0.28	0.38	0.00	0.00	1.00	1.06

Table 4.2. The antimicrobial activity of homochiral tripodal azolium compounds against *C. albicans*.

From the data in Table (4.1) and (4.2) it can be seen that these two homochiral tripodal receptors **(156a)** and **(156d)** show antifungal activity in both P. *aeruginosa* and C. *albicans*, where other receptors did not.

4.2.3 Antimicrobial activity of the subunits of homochiral tripodal receptors.

An investigation was carried out to better understand the observed bioactivities. It was decide to test related compounds **(156a)**, **(159)** and **(152a)** and to examine their activity for comparison purposes. For example compound **(156a)** has three positive charges and hydrogen bonding where compound **(159)** has a single charge and compound **(152a)** is neutral. Therefore the three compounds were tested for antifungal activity and the results are given in Table (4.3) and (4.4), respectively.

	Percentage reduction in growth (%age)					
	25μg/ml	50μg/ml	75μg/ml	100μg/ml	250μg/ml	500μg/ml
152a	0.00	6.01	19.20	8.82	6.58	0.00
159	0.95	10.91	11.53	1.21	7.99	7.52
156a	4.13	35.46	34.94	79.56	83.53	87.70

Table 4.3. The antimicrobial activities of compounds **(152a)**, **(159)** and **(156a)** against *P. aeruginosa*.

	Percentage reduction in growth (%age)					
	25µg/ml	50µg/ml	75µg/ml	100µg/ml	250µg/ml	500µg/ml
152a	0.00	0.00	0.21	0.00	10.87	80.42
159	0.0	0.00	0.53	0.00	2.07	10.33
156a	0.00	6.12	3.74	22.88	23.23	87.51

Table 4.4. The antimicrobial activities of compounds **(152a)**, **(159)** and **(156a)** against *C. albicans.*

From Table (4.3) and (4.4) it would appear that compound **(156a)** has an excellent antifungal activity. Compound **(159)** has no antifungal activity (has one positive imidazolium ring), whereas **(152a)** shows activity toward *C. albicans* but not *P. aeruginosa*,

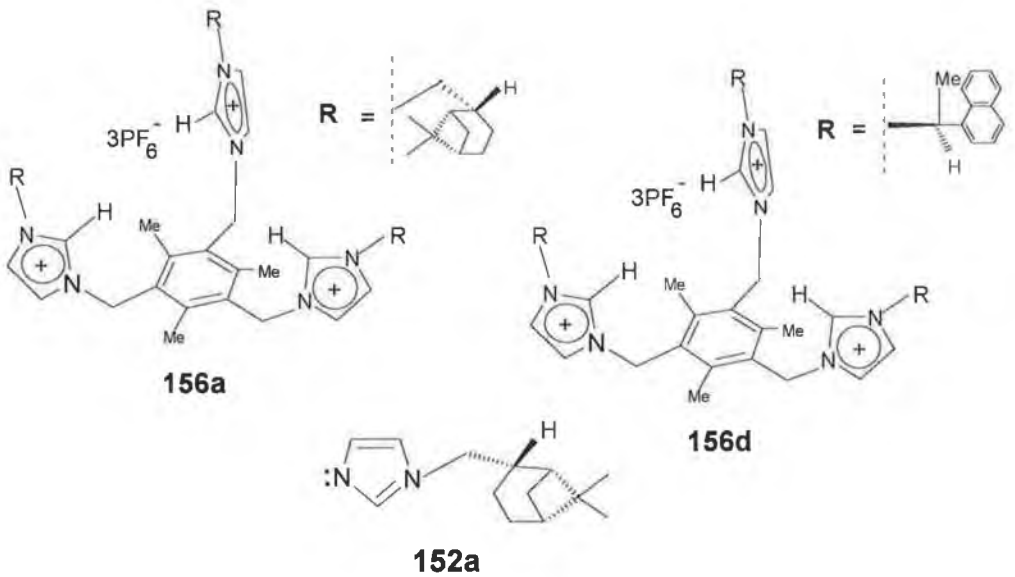

Figure 4.9. Three imidazole compounds **(156a)**, **(156d)** and **(152a)** showing their activities for antimicrobial.

For the future work we would introduce compounds **(160-163)** to be antimicrobially active (Figure 4.10).

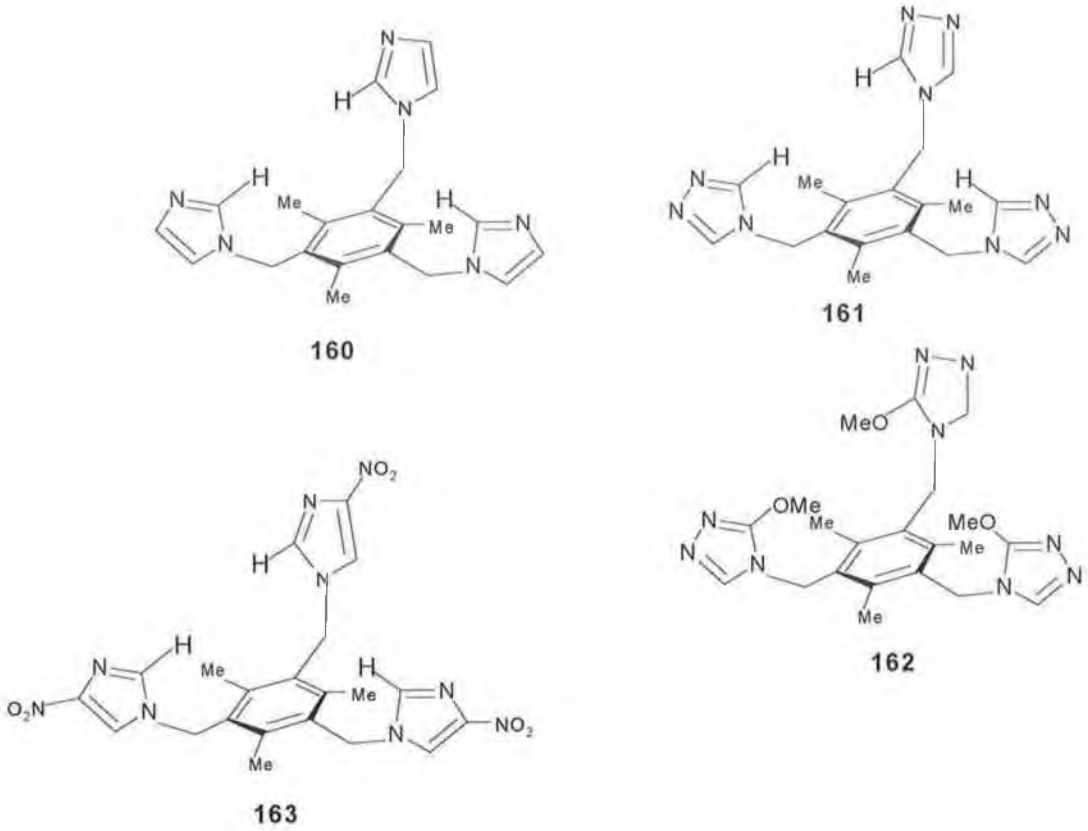

Figure 4.10. Four proposal tripodal azolium compounds based on different functionalities to enhance antimicrobial.

4.4 Conclusion

The imidazolium salt **(156a)** has been able to distinguish between two enantiomers, by complexing with sodium (R)-2-aminopropionate but not with sodium(S)-2-aminopropionate. The complexation was based on a chemical shift of α-proton in (R)-configuration anion from 3.62 to 4.42 ppm with broadening of signal, while same proton with (S)-configuration anion has no difference in chemical shift. The other three imidazolium salts **(156b-d)** was not able to discriminate between them, presumably due to effects of solvation, steric hindrance, cavity size or shape.

Future work, includes: planning to modify these receptors in terms of size and shape; or introduce one methylene groups or more between the chiral handle and imidazolium ring in order to enhance its selectivity for different enantiomers.

Homochiral tripodal receptors **(156a-156d)** have been screened for antimicrobial activities. Receptors **(156a)** and **(156d)** showed an excellent activity of antifungal with *P. aeruginosa and C. albican*, where the other two receptors did not. For comparison purposes, compounds **(156a)**, **(159)** and **(152a)** were also screened as antifungals. Compound **(156a)** showed its activity against *P. aeruginosa C. albican,* where **(159)** did not. Compound **(152a)** revealed its activity against *C. albican* but not with *P. aeruginosa.*

For future work compounds **(160-163)** have been designed to work as antimicrobial agents.

Chapter 5

Synthesis of Carbene Complexes

5.1 Results and discussion

5.1.1 Attempted synthesis of tridentate carbenes

The first report of the conversion of imidazolium salts to carbenes was by Dias, where he used NaH as a base and *tert*-BuOK as catalyst [104], Scheme 5.1.

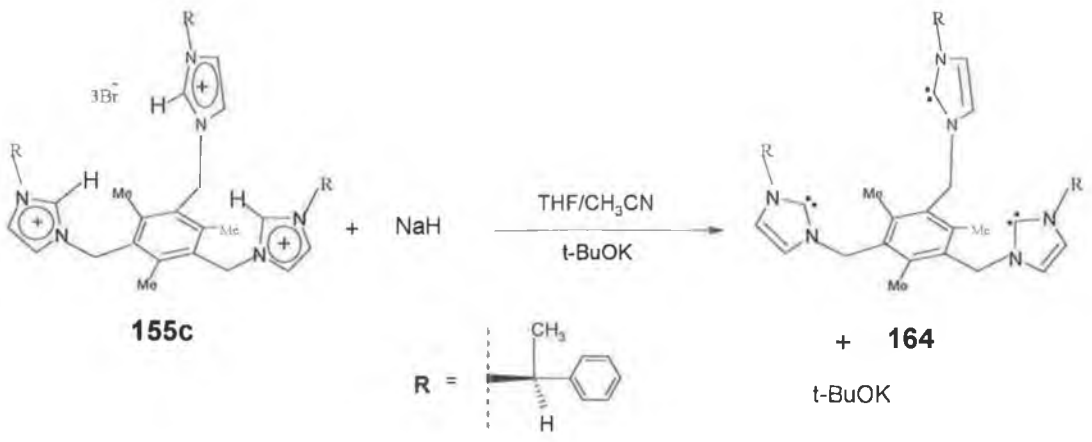

Scheme 5.1. Synthesis of phenylethyl homochiral tridentate carbene via sodium hydride.

We reproduced this reaction with imidazolium salt **(155c)** and sodium hydride in THF solvent. The reaction mixture was stirred for 5 minutes and potassium *tert*-butoxide was added at room temperature. After 30 minutes the reaction mixture was filtered and washed with THF and allowed to dry.
The ^{1}H NMR spectrum of **(164)** showed the disappearance of the H-2 protons of the imidazolium and the ^{13}C NMR of the C-2 carbon gave a signal at 160.56 ppm which may not indicate carbene formation.

Another attempt was carried out to synthesise the carbene using a procedure reported by Arduengo et al. [90]. This procedure uses potassium *tert*-butoxide instead of sodium hydride, Scheme 5.2.

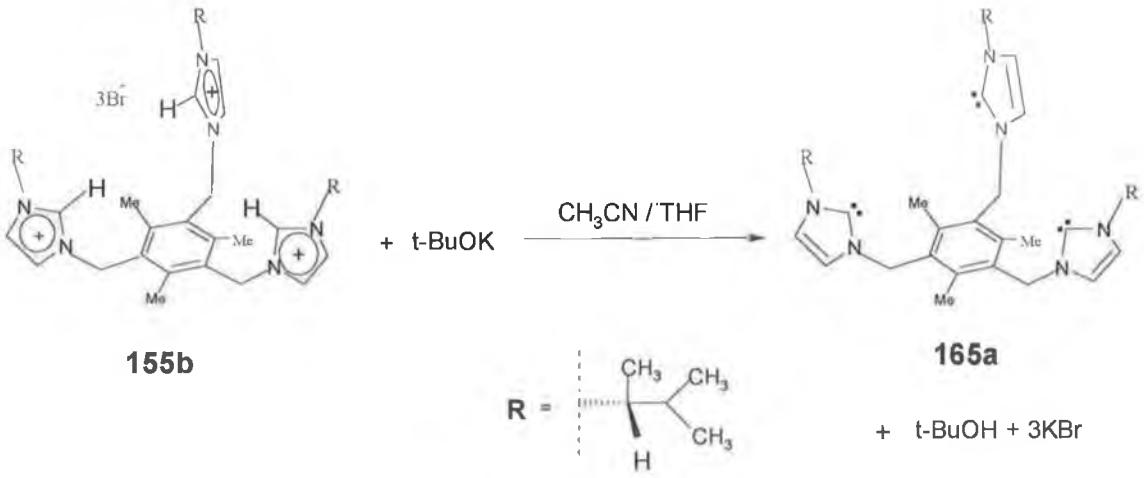

Scheme 5.2. Synthesis of isopropyl ethyl homochiral tridentate carbene via potassium *tert*-butoxide.

This reaction was carried out by adding imidazolium salts **(155b)** in Acetonitrile/THF solvent in 1:1.2 ratio followed by potassium *tert*-butoxide in a single portion. The reaction mixture was stirred for 2 h then washed with toluene and filtered through celite®, to give a yellow-orange product.

The ^{1}H, and ^{13}C NMR spectra of the resulting product indicate the formation of a carbene. The H-4 and H-5 protons of the imidazolium ring have shifted from 7.40, 8.57 ppm to 6.75, 6.95 ppm, respectively and the H-2 proton at 8.85 ppm disappeared, whereas the C-2 carbon peak in the ^{13}C NMR is shifted downfield from 135 to 162.62 ppm. Although these protons have shifted protons, we were still not completely convinced of carbene formation since the C-2 carbon did not shift to the standard carbene absorption which is around 205-230 ppm, and also the impurity attendance.

We realised that these bases, sodium hydride and potassium tert-butoxide, are not suitable to generate the carbenes.

5.1.2 Synthesis of tridentate carbenes via mild base

After many attempts to synthesise the carbene using strong bases, it was decided to explore more mild conditions using NaOMe to prepare the carbene using a

procedure reported by Ender [103]. We carried out Ender's procedure by dissolving sodium methoxide in dry methanol, this mixture was slowly added to a solution of imidazolium salt **(155b)** in methanol. The reaction mixture was stirred overnight. Volatiles were removed under reduced pressure at ambient temperature, and the crude product of the homochiral carbene tridentate **(165b)** was obtained as a dark brown oil in 80% yield, Scheme 5.3.

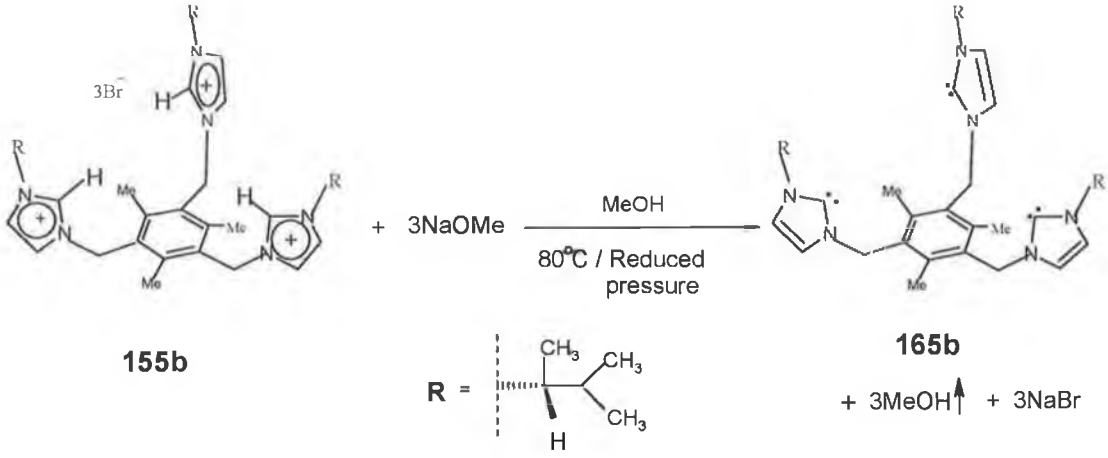

Scheme 5.3. Synthesis of isopropyl ethyl homochiral tridentate carbene **(165b)** via sodium methoxide.

The ^{1}H, and ^{13}C NMR spectra of compound **(165b)** showed the disappearance of the acidic H-2 proton signal at 10.10 ppm and a peak appeared in the ^{13}C NMR at 207.37 ppm which is highly characteristic for a carbene. We believe that the pathway for this reaction is proceeding as outlined in Scheme 5.4.

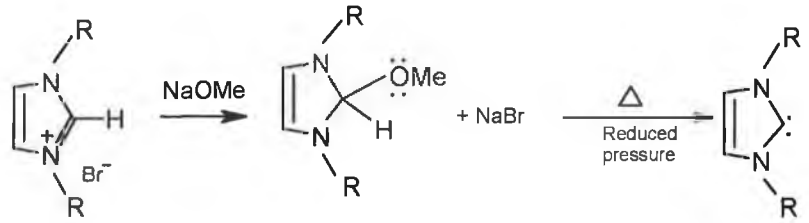

Scheme 5.4. Proposed mechanism for synthesis of homochiral tridentate carbene [103].

After successfully preparing the tripodal carbene **(165b)** we started to investigate its potential to form metal complexes. We first attempted to co-ordinate zinc metal with the tripodal carbene. The carbene is prepared in solution and was then treated *in-situ* with ZnBr, Scheme 5.5.

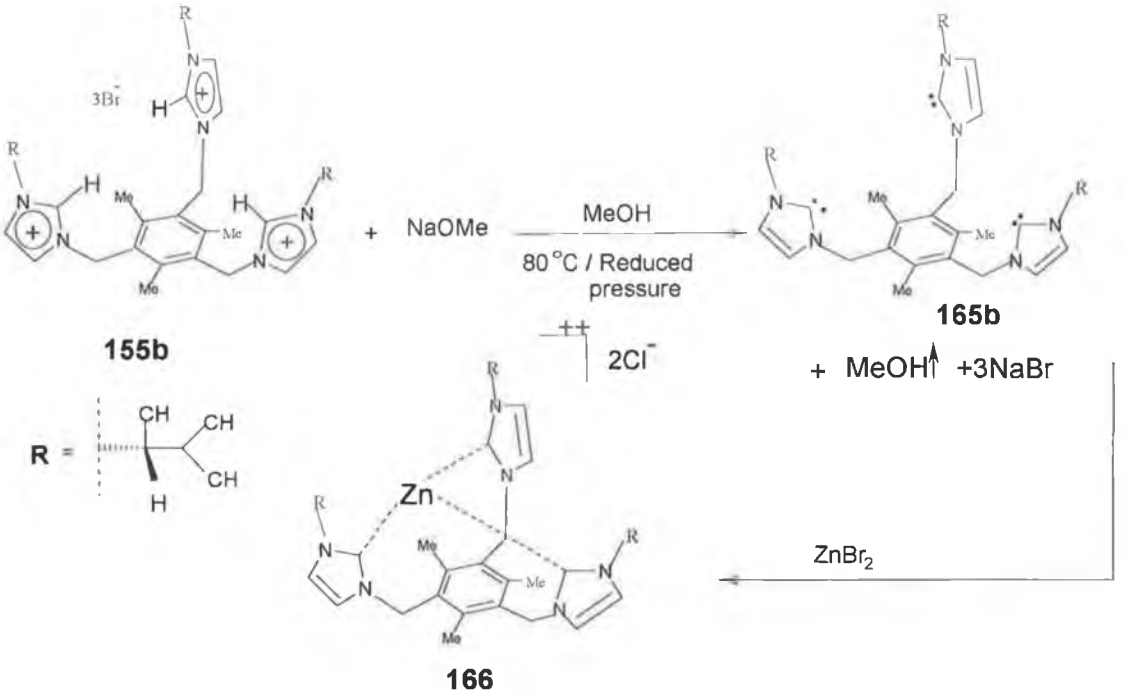

Scheme 5.5. Synthesis of myrtanyl homochiral tridentate carbene-zinc complex **(166)**.

One equivalent of zinc bromide was added to a solution of **(165b)** in methanol with stirring over 2 h. A white crude product was collected **(166)** in 55% yield.

The ^{13}C NMR spectrum revealed a peak at 170.42 ppm indicative of a Zn-complex, also present was starting material. Isolation of the Zn-complex was attempted using column chromatography and crystallization, but was unsuccessful. Complexation was also attempted using iron tribromide, Scheme 5.6.

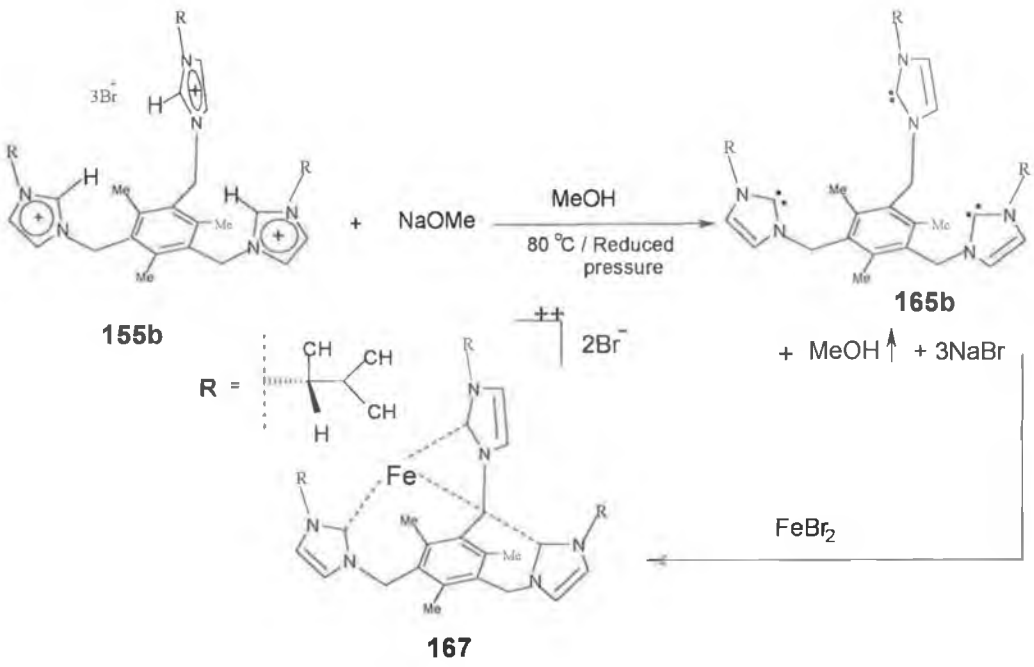

Scheme 5.6. Synthesis of isopropylethyl homochiral tridentate carbene-Fe(II) complex **(167)**.

This reaction was carried out using the same procedure used for zinc bromide. A crude red product was collected in 65% yield. The ^{13}C NMR spectrum revealed one peak at 168.87 ppm indicating an Iron-complex, but the same purification problems found with the the Zn-complex was also found with the iron and complete purification could not be achieved. Due to the purification problems an alternative procedure was attempted.

5.1.3 Synthesis of carbene-metal complexes via silver oxide

To improve purity, we decided to use Lin's methods [115], involving the use of Ag_2O which acts both as base and metal (Scheme 5.7). This method normally generates the silver carbene in high purity.

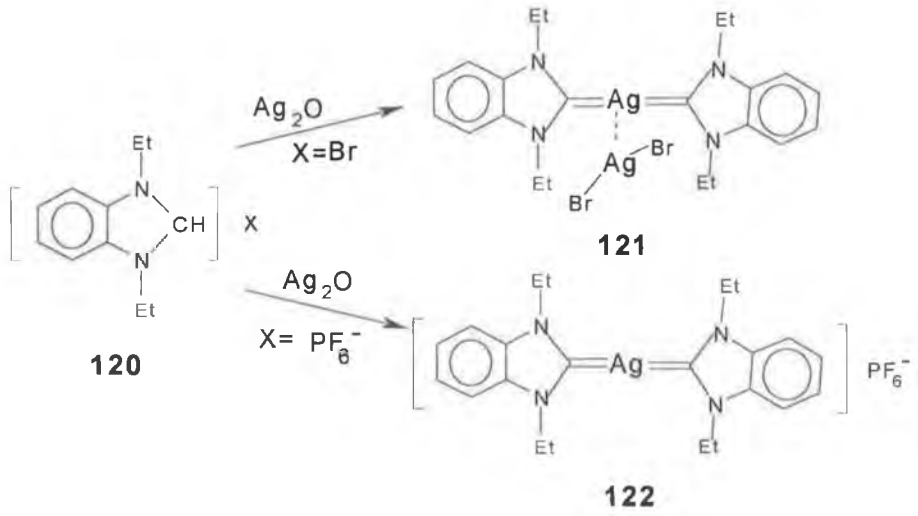

Scheme 5.7. Efficient pathway to generate carbene-silver(I) complex in quantitative yield.

Based on the procedure of Lin et al., we prepared five different silver homochiral tripodal imidazol-2-ylidene complexes by adding 1.5 equivalents of silver oxide to a solution of imidazolium salts in dichloromethane solvent. The complexes were produced in yields of 81-94%, Scheme 5.8.

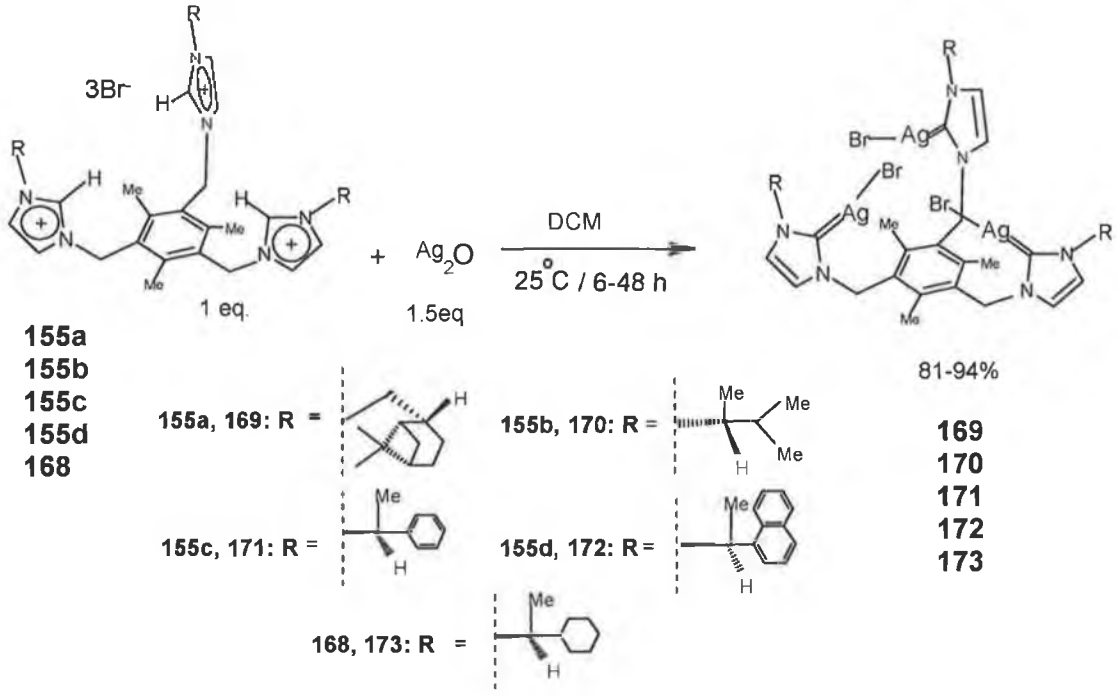

Scheme 5.8. Synthesis of homochiral tridentate carbene-Ag(I) complex **(169-173)**.

These silver carbene complexes dissolve in DMSO and DCM with moderate solubility in chloroform. The naphthyl silver carbene complex is only soluble in DMSO and it seemed to polymerise on standing.

5.1.4 Spectroscopic studies

The silver homochiral carbene tridentate complexes **(169-173)** were fully characterised by ^{1}H, ^{13}C NMR spectroscopy and mass spectrometry. The ^{1}H NMR spectrum revealed the disappearance of the H-2 imidazolium proton while the H-4, H-5-imidazolium protons were shifted upfield, indicating the loss of aromaticity within the imidazolium ring, (Figure 5.1). Other observations afforded by the ^{13}C NMR spectrum showed a downfield shift of the C-2 carbene in imidazole-2-ylidene, which is indicative of complexation between silver metal and the imidazol-2-ylidene ligand, Figure 5.2.

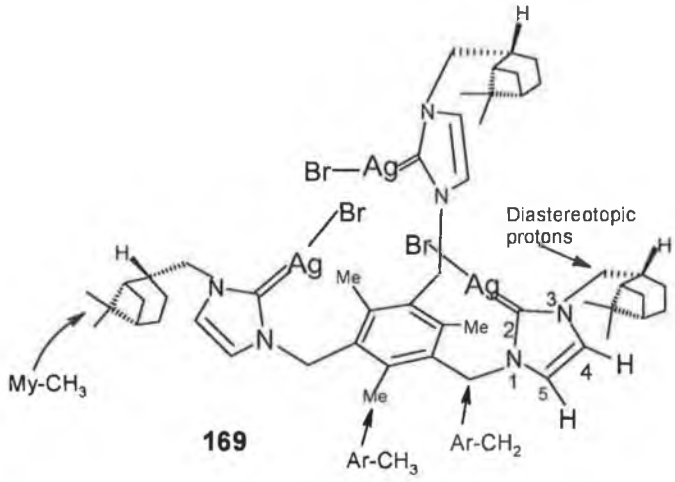

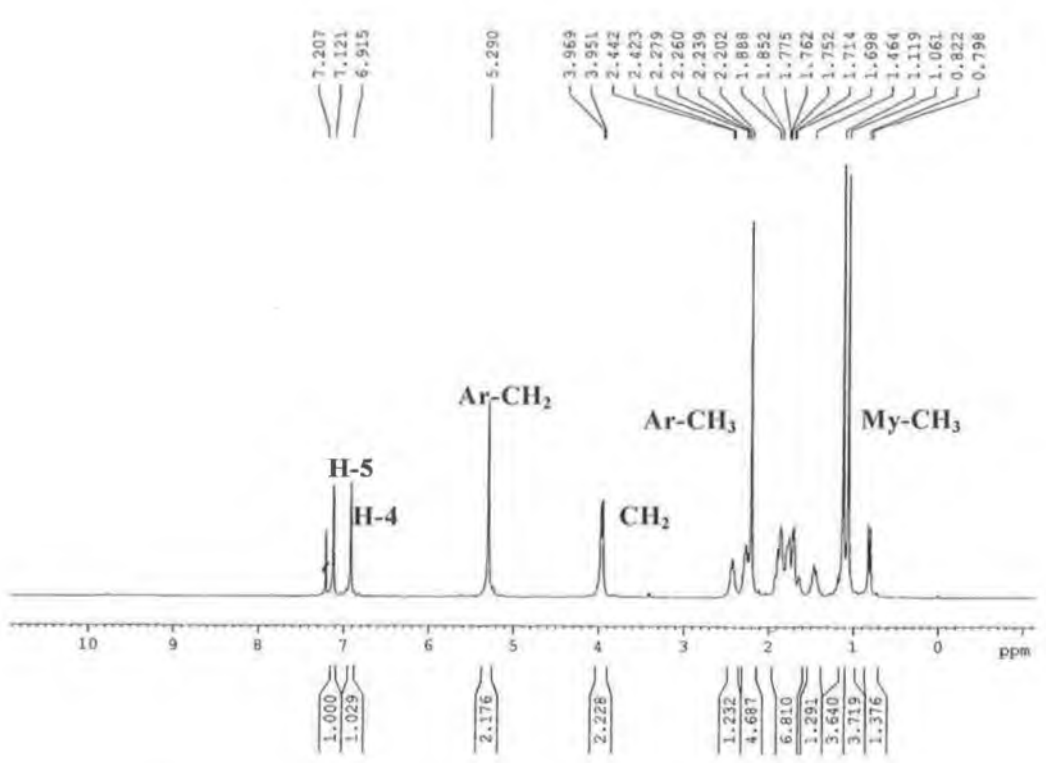

Figure 5.1 ^{1}H NMR spectrum ($CDCl_3$) of silver(I)-carbene **(169)** showing the full disappearance of H-2 proton, while H-4 and H-5 are shifting upfield.

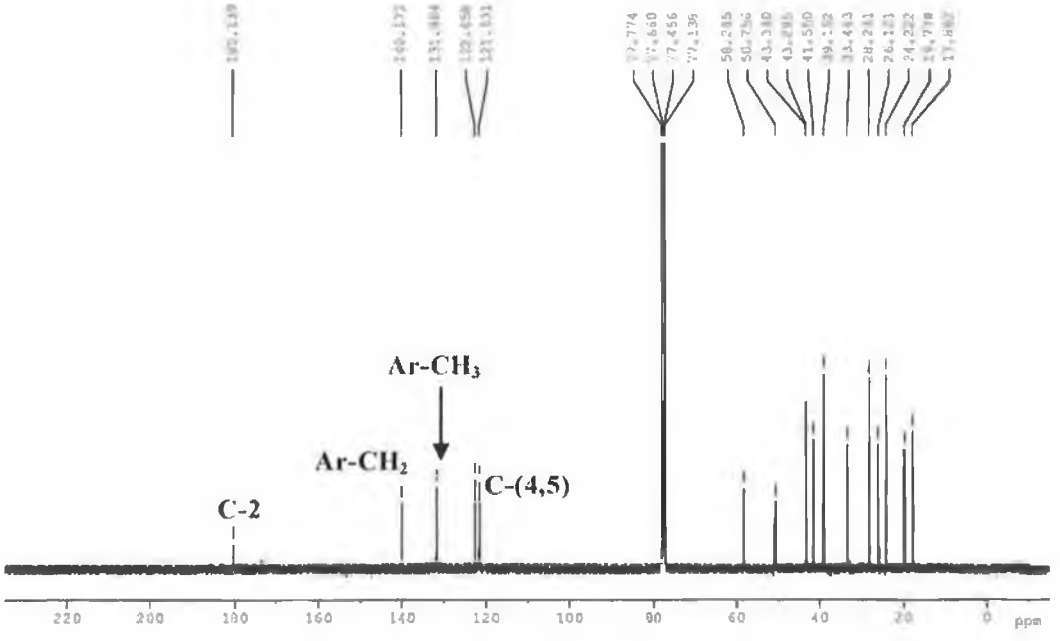

Figure 5.2 ^{13}C NMR spectrum ($CDCl_3$) of silver(I)-carbene **(169)**, showing the peak for complexation between silver and imidazol-2-ylidene ligands at 180.13 ppm.

Figure 5.1 shows the disappearance of the H-2 imidazol-2-ylidene proton at 10.09 ppm while H-4, H-5 of the imidazol-2-ylidene are shifted downfield to 7.12 and 6.91 ppm, respectively. Also it can be seen from Figure 5.2 that the C-2 carbon of imidzol-2-ylidene is at 180.14 ppm, which is downfield from 136.42 ppm in the imidazolium salt **(155a)**, all these observations indicate the formation of an imidazol-2-ylidene-silver complex.

5.1.5 Application of silver-carbenes

It was hoped to convert the silver carbene complexes to the Pd, Au and Ru complexes via a carbene transfer reaction [115,116,117].

The initial step to prepare the Ruthenium complex was to prepare $Ru(DMSO)Cl_2$ **(174)**. This was accomplished by adding Ruthenium dichloride in 3 ml of DMSO solvent [171,172]. The reaction mixture was stirred at 145 °C over 5 minutes until the colour turned to bright red. The volume was reduced to half under vacuum, and acetone was added to precipitate the product. A yellow solid was collected in 60% yield. Scheme 5.9.

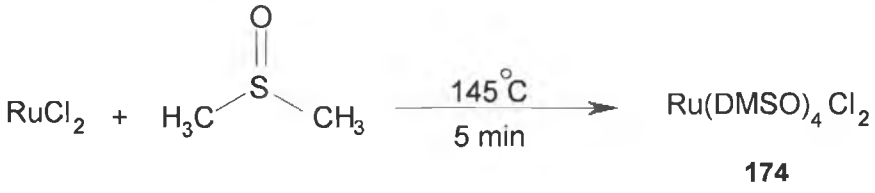

Scheme 5.9. Synthesis of ruthenium complex **(174)**.

This starting material $Ru(DMSO)_4Cl_2$ was then treated with the silver carbene complex **(170)** in a 1:1 stoichiometry in DCM. The solution was stirred over 24 h at room temperature. A silver bromide precipitate appeared and was filtered off. Volatiles were removed under vacuum. A brown solid was collected in 75% yield, Scheme 5.10.

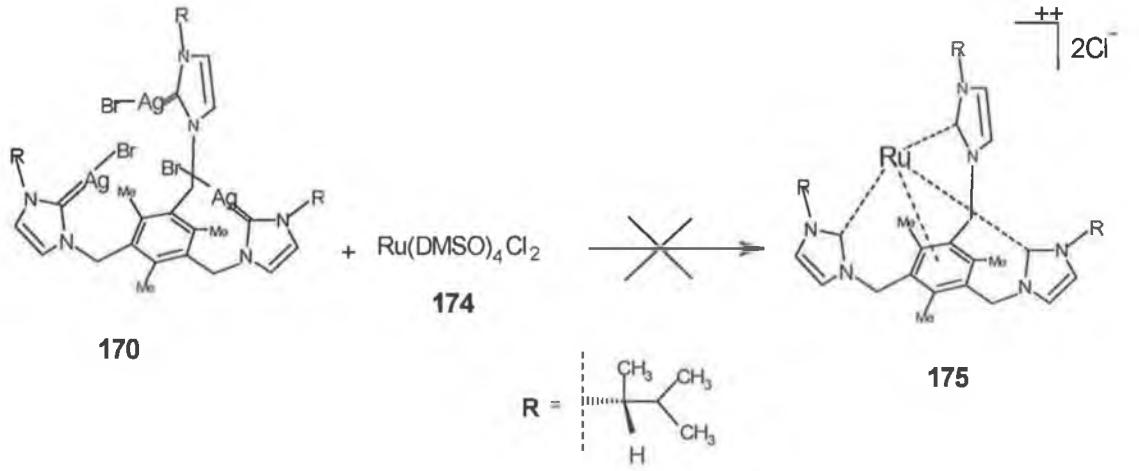

Scheme 5.10. Synthesis of isopropyl ethyl homochiral carbene-Ru(II) complex **(175)**.

Compound **(175)** was investigated by ^{13}C NMR spectroscopy and mass spectrometry which afforded no evidence for the Ruthenium complex being formed. This was attributed to the steric hindrance of the substituents in the imidazol-2-ylidene. Also the Ruthenium metal may not be able to complex with the three imidazol-2-ylidenes and the benzene ring, thus preventing formation of a stable 18 e^- complex.

5.1.5.1 Synthetic applications

We attempted to use the silver carbene complex as a ligand accelerate catalyst (LAC) [121,122] in a Michael addition reaction according to the procedure of Roland et al.. This reaction was carried out by mixing the silver carbene compound **(170)** and copper triflate in a 1:1 ratio of toluene and DCM for 5 minutes at 20 °C. To this diethylzinc was added and then the reaction was cooled to 0 °C and cyclohexanone was added. The reaction was hydrolyzed with hydrochloric acid and extracted with ether and dried. The crude product was purified by silica gel chromatography, Scheme 5.11.

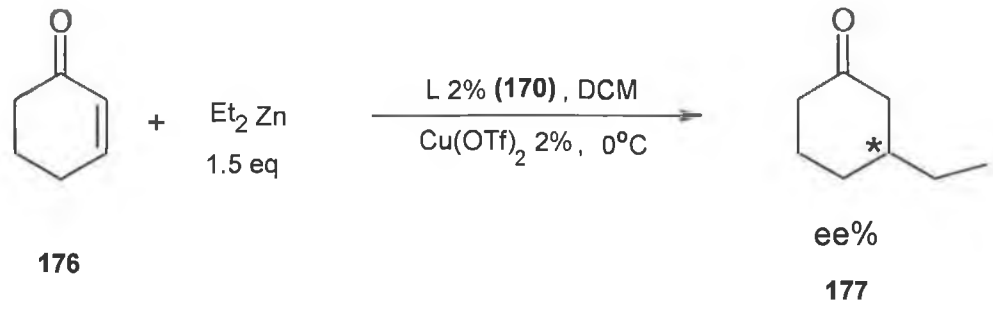

176 **177**

Scheme 5.11. Conjugate addition reaction catalized by LAC as auxiliary ligand, represented by **(170)**.

Through out the investigation of compound **(177)** by TLC and ^1H NMR spectroscopy we have found that compound **(177)** was not pure and over seven spots were observed by TLC, including a base line spot. The fractions were separated by column chromatography. Compound **(177)** was not present in the obtained fractions as determined by ^1H, and ^{13}C NMR.

It would appear, that compound **(170)** is not able to work as a LAC for conjugate addition reaction and this could be attributed to the bulkiness of compound **(170)**, and as a result copper is not able to complex with the ligands.

5.1.6 Synthesis of 1,3-myrtanyl methyl imidazol-2-ylidene-silver(I) complex

As a result of the failure of **(169-173)** as a LAC and carbene transfer agent, we decided to prepare a new imidazolium salt (**159**). This compound would be converted to the imidazolium-2-ylidene-silver complex **(178)** and would then be used as a carbene transfer agent, and applied as a LAC in conjugate addition reactions (Michael addition reaction), Figure. 5.3.

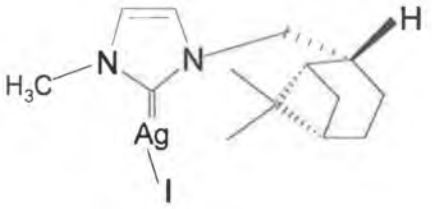

178

Figure 5.3. 1,3-myrtanylmethylimidazol-2-ylidene-silver(I) complex **(178)**.

The 1,3-myrtanylimidazolium-2-ylidene-silver(I) complex was prepared by the reaction of 1,3-myrtanylmethylimidazolium iodide **(159)** and silver dioxide in DCM at room temperature over 2 h.

The characterisation of complex **(178)** was based on ^{1}H, and ^{13}C NMR spectroscopy. ^{1}H NMR spectra showed the disappearance of the H-2 signal at 9.97 ppm (Fig.6.2, chapter 6), H-4 and H-5 were shifted downfield from 7.37 and 7.56 ppm (Fig. 6.2, chapter 6) to 6.93 and 7.04 ppm, respectively (Fig 5.4). The ^{13}C NMR spectra showed a downfield shift of the C-2 carbon from 137.24 ppm (Fig 6.3, chapter 6) to 182.52 (Fig. 5.5) ppm which is a clear indication of the formation of a silver-carbene complex. The methylene and methyl substituents of the imidazol-ylidene ring resonate at 4.03 and 3.83 ppm respectively.

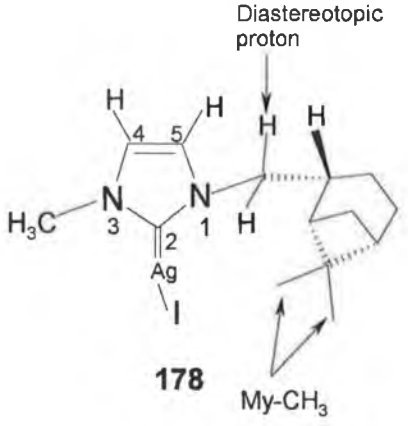

178

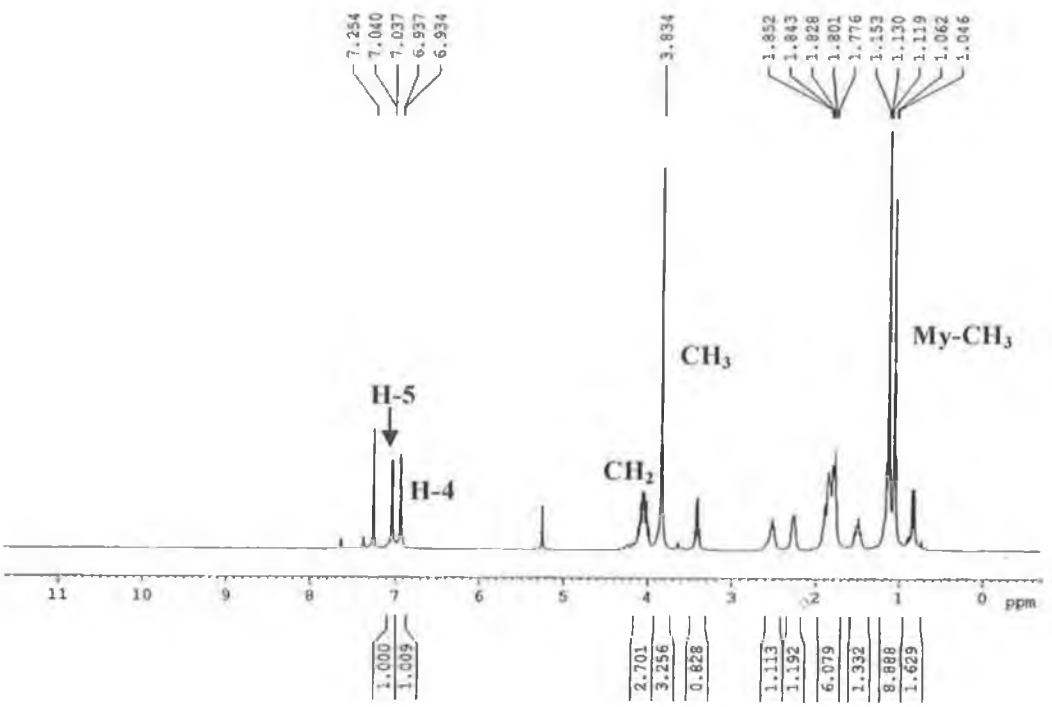

Figure 5.4. ^{1}H NMR spectrum ($CDCl_3$) of 1,3-myrtanylmethylimidazol-2-ylidene-silver(I) complex **(178)**.

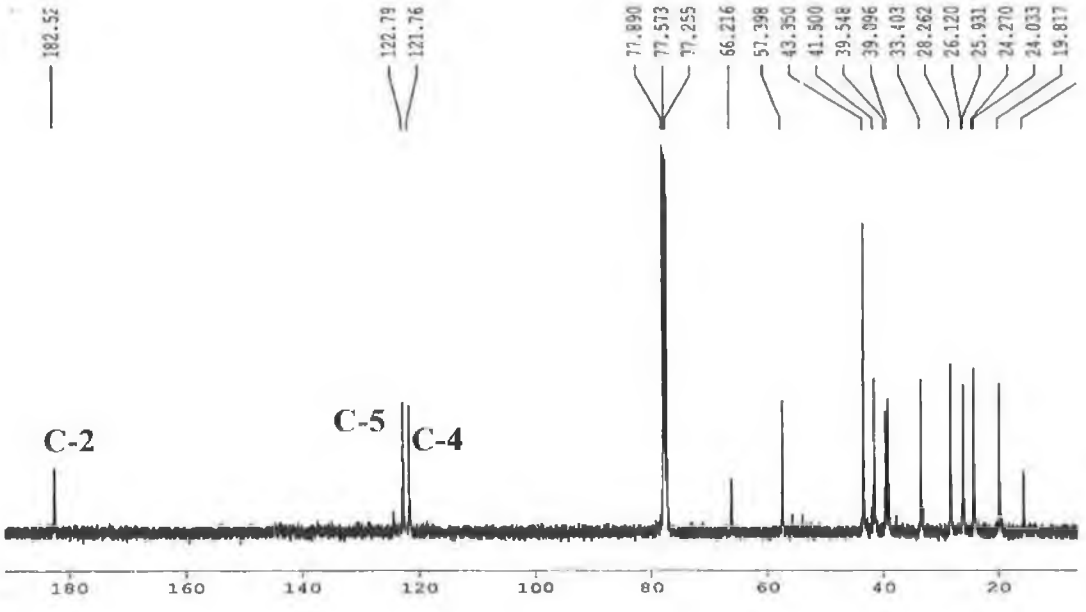

Figure 5.5. ^{13}C NMR spectrum ($CDCl_3$) of 1,3-myrtanylmethylimidazol-2-ylidene-silver(II) complex **(178)**.

It was expected that complex **(178)**, based on its low bulk character, would work effectively as a LAC in conjugate addition reactions, or as a carbene transfer agent for metals such as (Pd) and (Au) [115,116,117].

5.2 Conclusion

Silver homochiral tridentate carbene complexes have been successfully synthesised and characterised in good yields. These silver carbene complexes failed to act as ligand accelerate catalysts and carbene transfer agents which could be due to steric hinderance. Butyl homochiral tridentate carbene was synthesised from sodium methoxide and characterised. This carbene was able to complex with zinc and iron metal, but the resulting complexes could not be isolated from the reaction crudes. To reduce the bulkiness of our ligands, complex **(178)** was synthesised and characterised and would expect to perform effectively in terms of LAC in conjugate addition reactions and carbene transfer agents.

Chapter 6

Synthesis of (1,3-homochiral myrtanyl methyl imidazole-2-ylidene)$_2$-palladium(II) I_2 complex and its application in the Heck reaction

6.1 Introduction

N-Heterocyclic carbenes (NHC) have emerged as an important family of ligands with strong electronic donor properties [173-175], and are now commonly used as ligands in catalytic systems.

The first use of palladium (II) NHC complexes was reported by Herrmann (as mentioned earlier in Chapter 1) in 1995, where they were applied as ligands in the Heck reaction. The palladium (II) NHC complex is similar in structure to our palladium complex **(179)**.

We planned to apply our NHC as potential ligands in the Heck reaction. We attempted to synthesise and characterise a new series of Pd(II) NHC complexes **(179)** based on the NHC (*N*-Heterocyclic Carbene) ligand containing a myrtanyl and methyl group in the imidazolylidene ring, Figure 6.1.

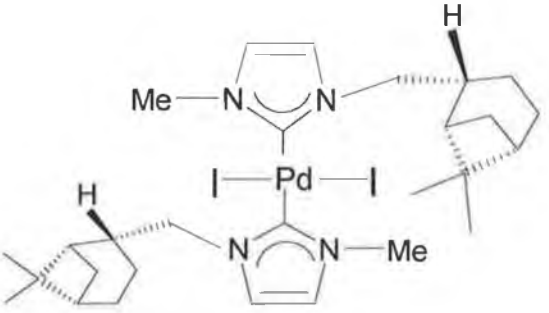

179

Figure 6.1. 1,3-Myrtanylmethylimidazol-2-ylidene-Palladium(II) complex **(179)**.

6.2 Results and discussion

6.2.1 Synthesis of 1,3-myrtanylmethylimidazolium iodide salts (159)

The first step in the preparation of 1,3-myrtanylmethylimidazol-2-ylidene-Pd(II) complex **(179)** was to prepare the required starting material 1,3-myrtanylmethyl imidazolium iodide salts **(159)**. These salts can be prepared by the reaction between myratanyl imidazole **(152a)** and methyl iodide, Scheme 6.1.

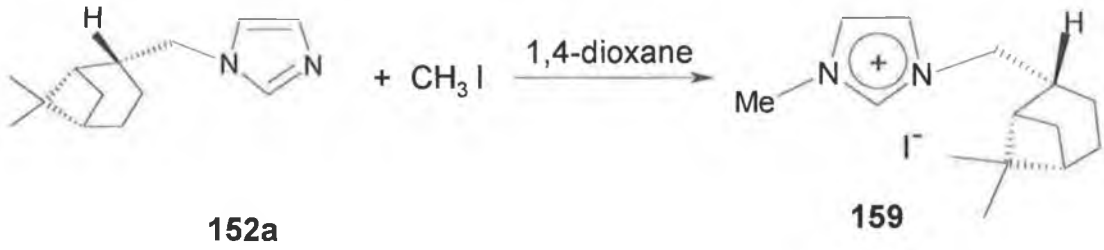

152a **159**

Scheme 6.1. The synthesis of 1,3-myratanylmethylimidazolium iodide salts **(159)**.

This reaction was carried out at reflux for two hours in 1,4-dioxane. A precipitate appeared and was isolated and washed with ether and dried. The yield was as high as 98%.

Compound **(159)** was fully characterised by ^{1}H, and ^{13}C NMR spectroscopy, Figure 6.2. The protons of the imidazolium ring (quarternization) absorb at 7.38, 7.56 and 9.97 ppm respectively. The methyl group at position-3 in the imidazolium ring is at 4.10 ppm and is a singlet. In our system the methylenes at position-1 absorb as a multiplet at 4.25 ppm which is to be expected for these diastereotopic protons.

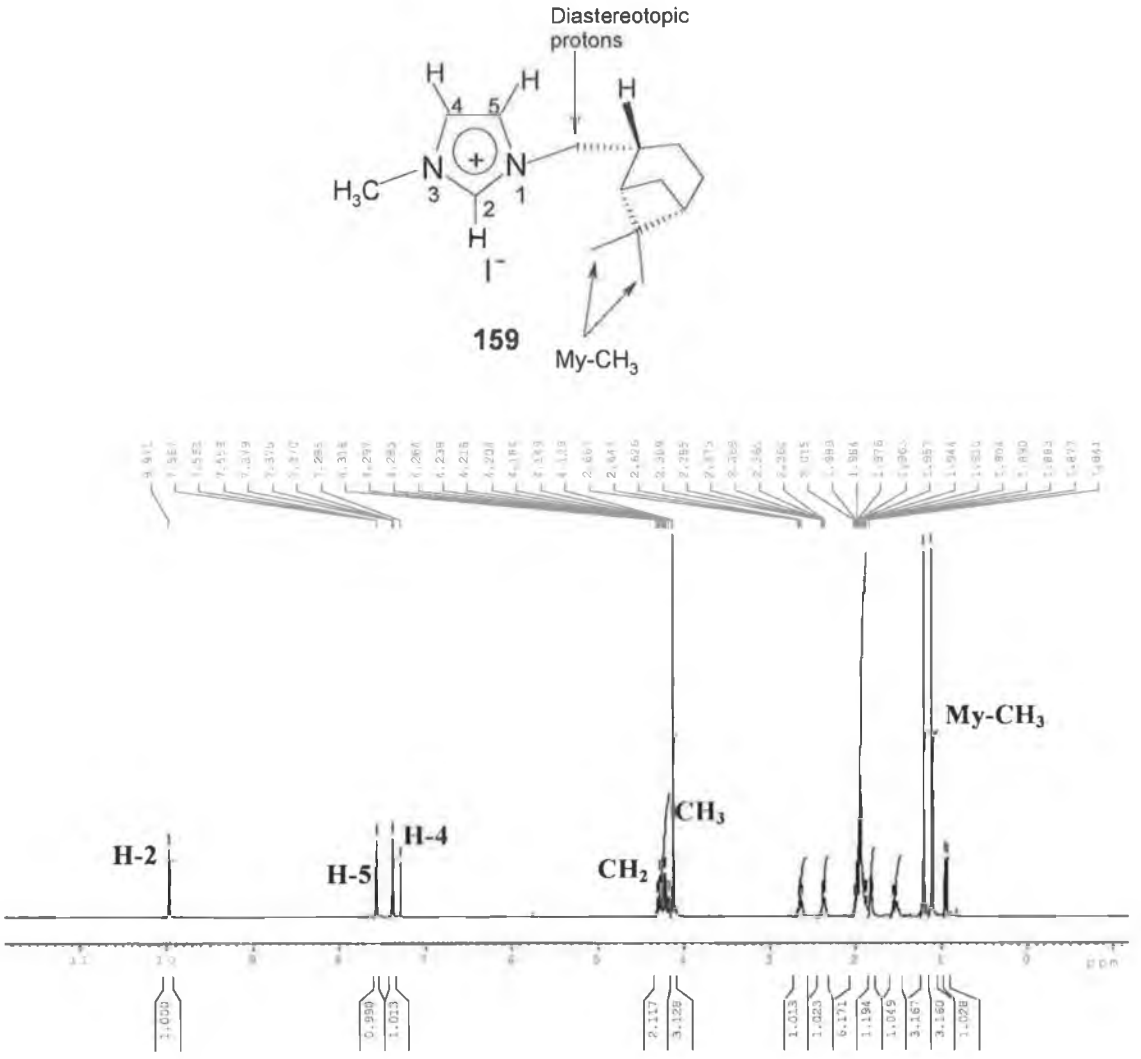

Figure 6.2. ^{1}H NMR spectrum ($CDCl_3$) of 1,3-myrtanylmethylimidazolium iodide salt **(159)**.

The ^{13}C NMR spectrum revealed the expected 14 peaks for **(159)**, (Figure 6.3). Three peaks positioned at 19.64, 24.01 and 25.84 ppm can be assigned to three different methyl groups, where two of them are bond to the myrtanyl group, and the other at position-3 of the imidazolium ring. Carbons C-2, C-4 and C-5 in the imidazolium ring appear at 137.24, 122.71 and 124.11 ppm respectively.

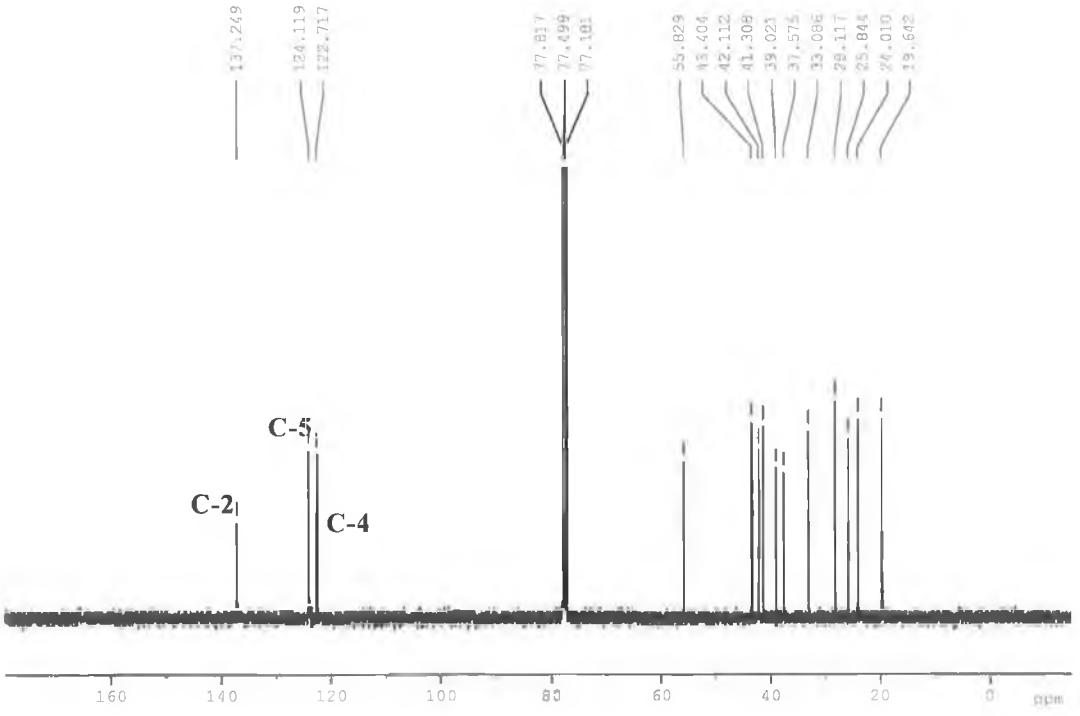

Figure 6.3. ^{13}C NMR spectrum ($CDCl_3$) of 1,3-myratanylmethyl imidazolium iodide salt **(159)**.

6.2.2 Synthesis of imidazolylidene-Pd(II) complex

We then attempted to prepare the carbene-Pd(II) complex, using a procedure developed by Herrmann [173], from the reaction of $[Pd(OAc)_2]$ and 1,3-myrtanyl methylimidazolium iodide **(159)**, Scheme 6.2.

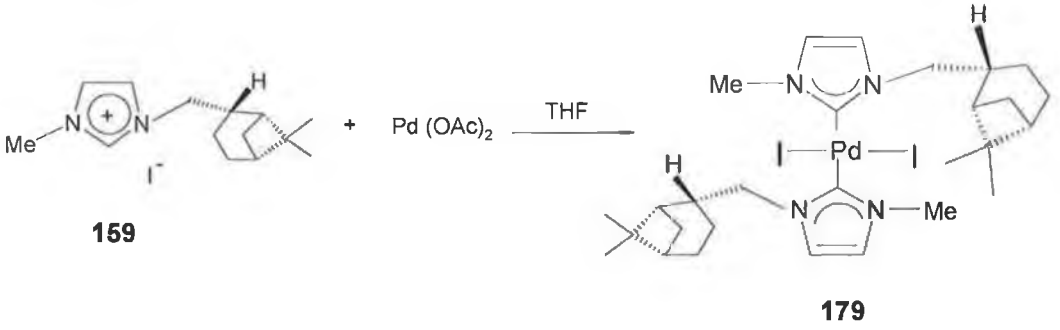

Scheme 6.2. The synthesis of (1,3-myratanylmethylimidazol-2-ylidene)$_2$-Pd(II) I_2 complex **(179)**.

In this reaction THF was used as solvent and the reaction mixture was refluxed for 3-4 h. Compound **(179)** was collected as a yellow solid in 50% yield, and was found to be oxygen, moisture and heat stable.

Compound **(179)** has been extensively investigated by ^{1}H and ^{13}C NMR. The ^{1}H NMR of **(179)** (Figure 6.4) shows, the H-2 signal of the imidazolium ring has disappeared and the H-4 and H-5 protons are shifted upfield which can be attributed to a loss of aromaticity. The disappearance of the H-2 proton in the imidazolium ring indicates the formation of a carbene bound to Pd(II).

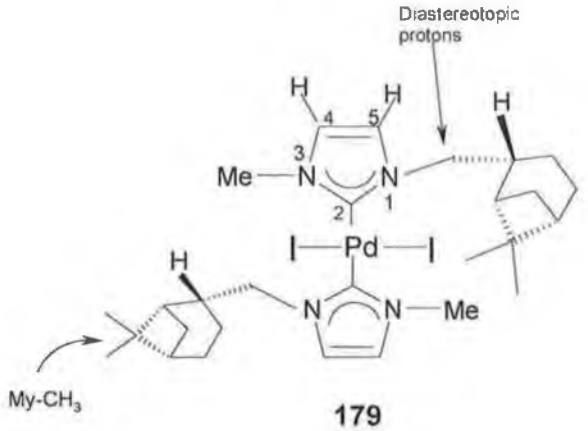

179

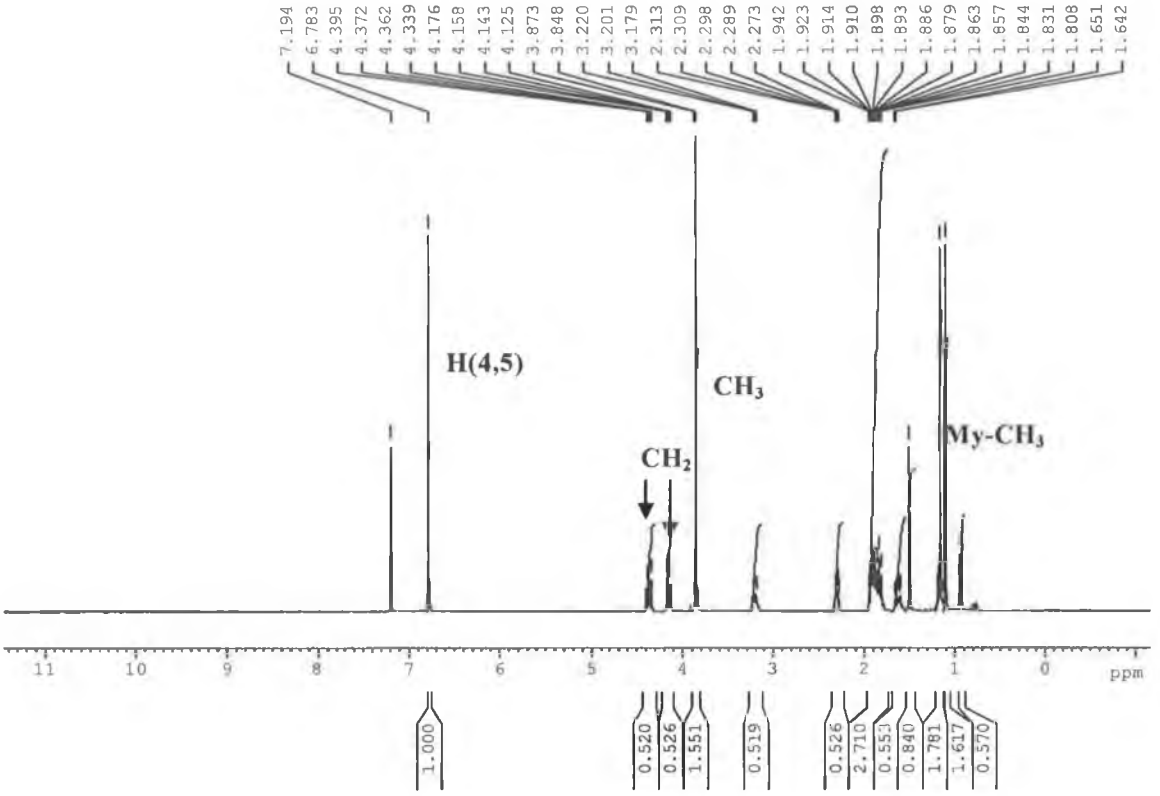

Figure 6.4. ^{1}H NMR spectrum ($CDCl_3$) of (1,3-myrtanylmethylimidazol-2-ylidene)$_2$-Pd(II) I_2 complex **(179)**.

The ^{13}C NMR spectrum further supports complex formation, Figure 6.5. The C-2 carbon in the imidazolylidene ring is at 168.01 ppm, which is very indicative of complex formation [139,176,177]. The C-4 and C-5 carbons absorb at 121.90 and 122.30 ppm respectively, and are shifted slightly upfield which can be attributed to complexation.

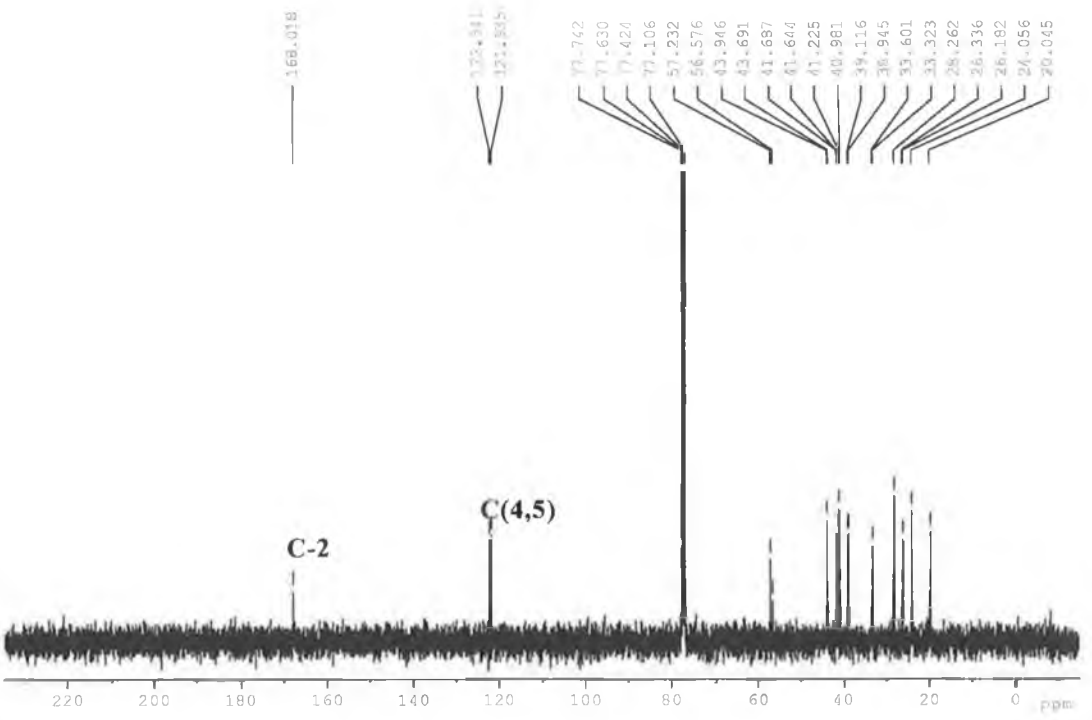

Figure 6.5. ^{13}C NMR spectrum ($CDCl_3$) of (1,3-myrtanylmethylimidazol-2-ylidene)$_2$- Pd(II) I_2 complex **(179)**.

6.3 Application of Imidazolium salts as effective ligands in the Heck reaction

In order to investigate the effectiveness of the imidazolylidene-Pd(II) complex **(179)** as a catalyst in the Heck reaction, we carried out a simple Heck reaction with different alkene substrates as starting materials.

Generally the Heck reaction is carried out with ethyl acrylate and a substituted bromobenzene together with sodium acetate as base, DMF or *N*,*N*-dimethyl acetamide as solvent, and the catalyst $Pd(OAc)_2$ with triphenylphosphine as an auxiliary ligand, Scheme 6.3.

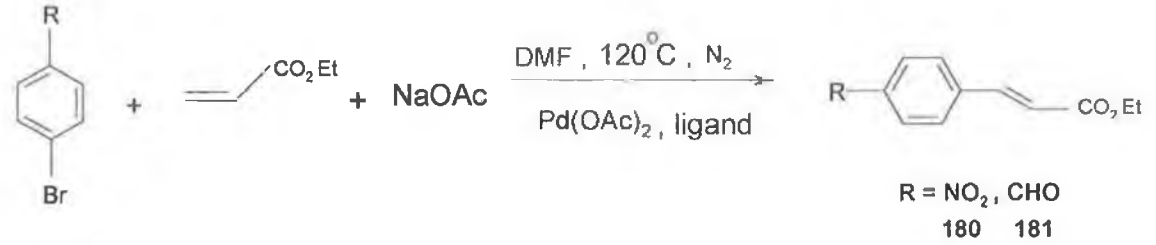

Scheme 6.3. The general Heck reaction

We first attempted to carry out the Heck reaction with bromobenzaldehyde and butyl acrylate in *N,N*-dimethylacetamide using 0.5% Pd-ligand **(179)** as catalyst Scheme 6.4.

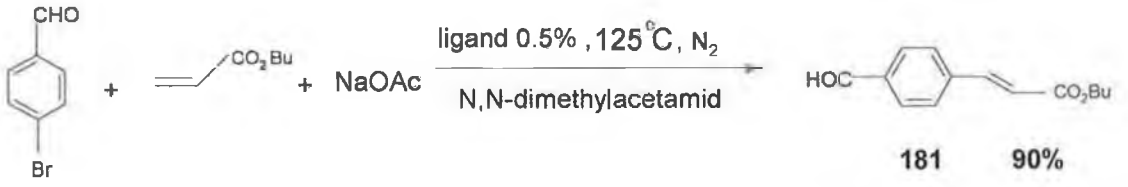

Scheme 6.4. The application of ligand **(179)** in the Heck reaction.

This reaction yielded product **(181)** in 90% yield, which is about the same as Herrmann's findings.

We believe the mechanism of this reaction is outlined in Scheme 6.5 [35b].

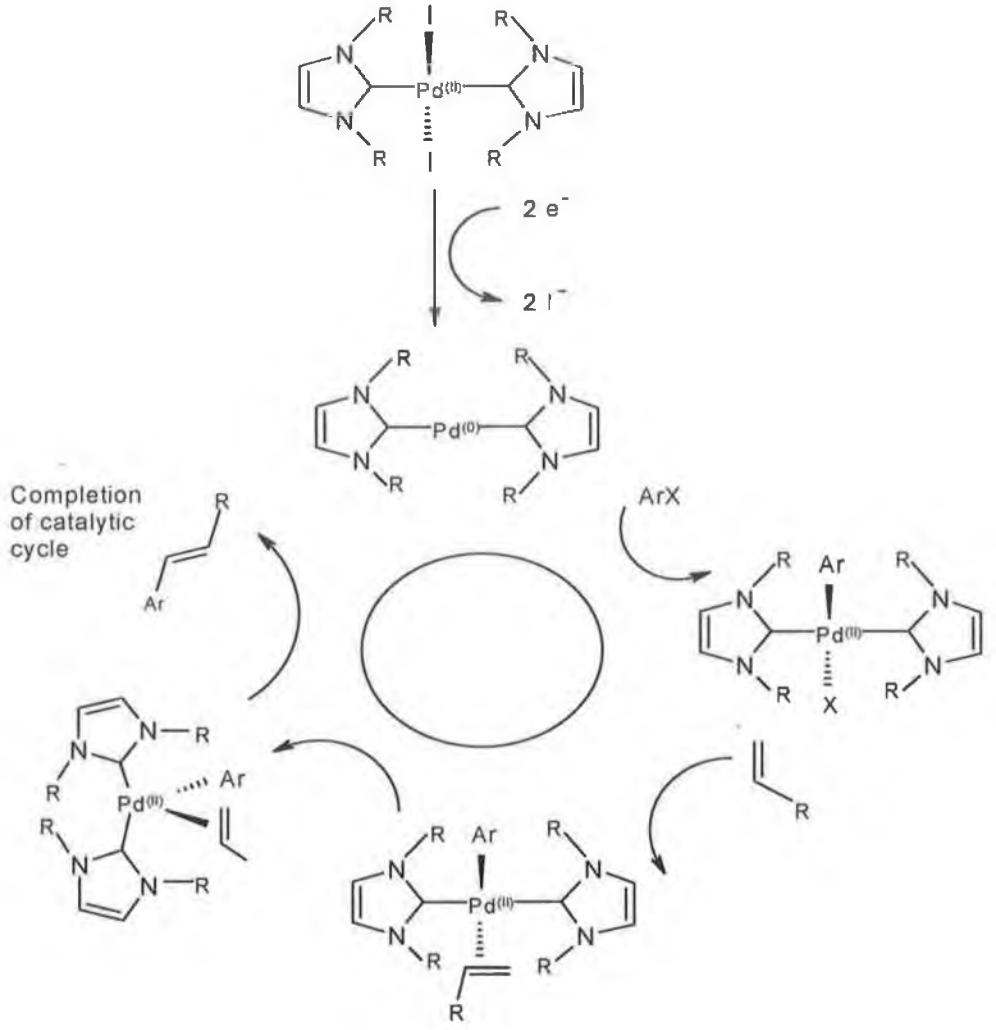

Scheme 6.5. The proposed mechanism for the Heck reaction.

It was decided to use our catalyst with different alkenes to examine it's reactivity order. The first involved the reaction of *n*-heptene. The reaction conditions were kept the same as the previous example except with *n*-heptene as the alkene, Scheme 6.6.

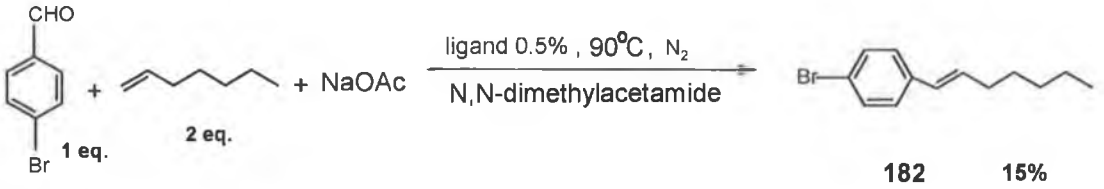

Scheme 6.6. Catalyst **(179)** in the Heck reaction with *n*-heptene and aryl halide.

This reaction was carried out with 2 equivalents of *n*-heptene as a result of *n*-heptene's low b.p. 95 °C. Unfortunately, we could not control the reaction at 125 °C, so we lowered the temperature to 90 °C and the final yield was only 15%. The catalyst **(179)** did catalyse this reaction to produce compound **(182)**, but the ^{1}H NMR spectrum was not sufficiently clear since the integration ratio's were slightly off. We also believe that low yield of product resulted from the volatility of *n*-heptene.

A third reaction using 2,3-dihydrofuran as the alkene gave the same problem as the previous reaction with *n*-heptene. As a result of it's low b.p. (55 °C) we increased the mole ratio of 2,3-dihydrofuran to 3 eq., NaOAc was kept in the same ratio, and the temperature was changed to 80 °C to try and minimize evaporation of 2,3-dihydrofuran, Scheme 6.7.

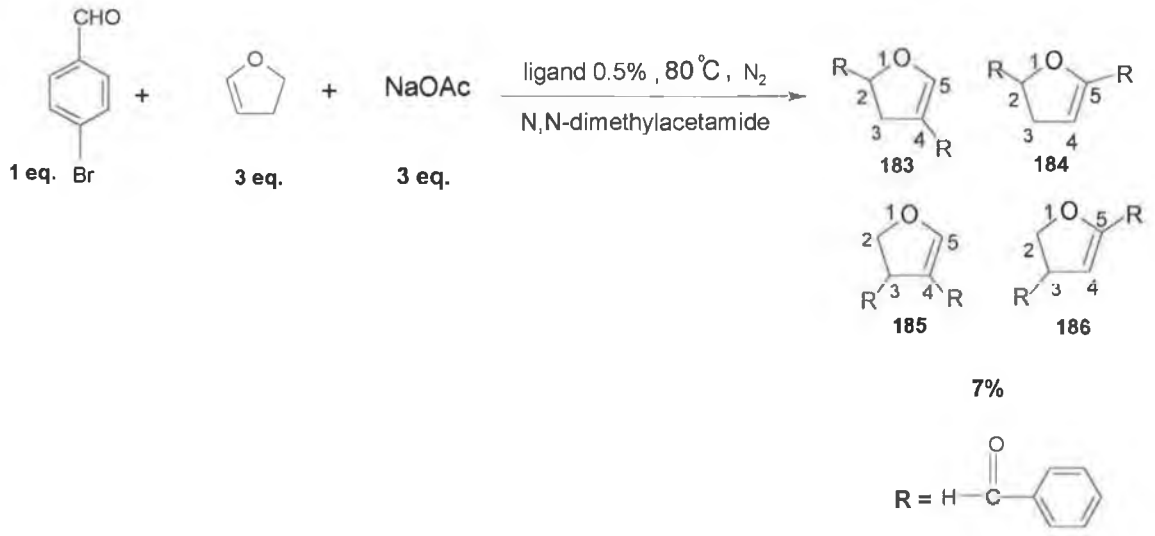

Scheme 6.7. Catalyst **(179)** showing a promising ability to couple 2,3-dihydrofuran and aryl halide.

This reaction gave a product which we believe to be one of **(183-186)** as determined by ^{1}H NMR and HMQC. We believe this resulted from the volatility of 2,3-dihydrofuran. As the reaction progresses 2,3-dihydrofuran is lost thereby increasing the stoichiometric ratio of aryl halide to 2,3-dihydrofuran. This allow the possibility for multiple substitutions of the dihydrofuran.

Two other attempts were carried out, but with modified reaction conditions and using different aromatic starting materials. We wished to see the effect of the absence of CHO (carboxyaldehyde) group at the benzene ring on the reaction with dihydrofuran, Scheme 6.8.

These two reactions were carried out between 2,3-dihydrofuran and iodo benzene and phenyl triflate, respectively, where the solvent was CH_3CN and the base was triethyl amine at 80 °C in 3% mole of catalyst **(179)** [178-182].

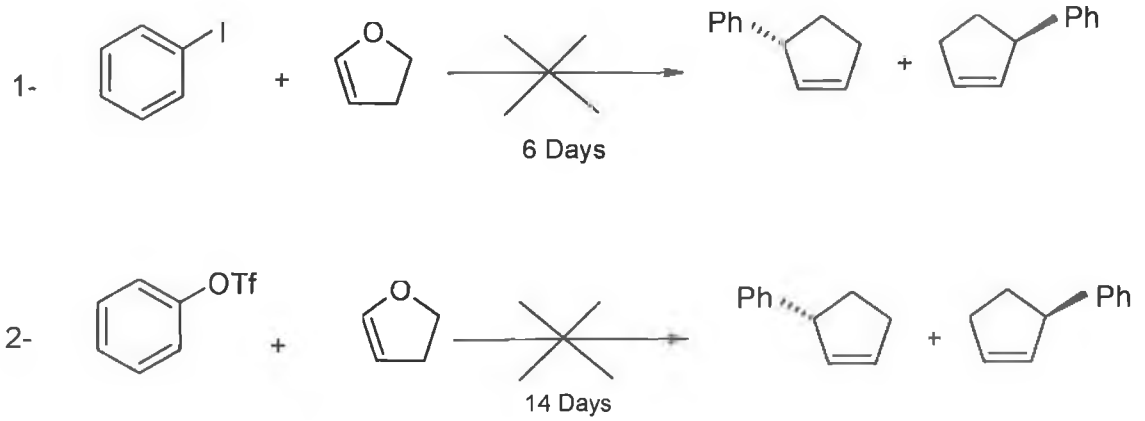

Scheme 6.8. Failure of catalyst **(179)** to couple 2,3-dihydrofuran and iodo, triflate benzene, respectively.

The catalyst **(179)** was not able to catalyse these two reactions which could be due to the absence of an efficient electron withdrawing group such as CHO. The temperature of reaction may have also been too low, since we used CH_3CN as solvent. This solvent was used as it is included in literature [178].

Results for all reactions are outlined in Table 6.1 below.

Substrate (1)	Substrate (2)	Base	Cat. [mol%]	T[h]	Turnover[%]
4-BrC_6H_4CHO	Bu-acrylate	NaOAc	0.5	125	90
4-BrC_6H_4CHO	1,2-heptene	NaOAc	0.5	90	15
4-BrC_6H_4CHO	2,3-dihydrofuran	NaOAc	0.5	80	7
C_6H_5 I	2,3-dihydrofuran	Et_3N	3	80	0
C_6H_5 OTf	2,3-dihydrofuran	Et_3N	3	80	0
PPh_3	Bu-acrylate	NaOAc			100

Table 6.1 Heck olefination of bromoarenes with *N*-heterocycliccarbene-palladium catalyst **(179)**.

6.4 Conclusion

A new Heck reaction catalyst **(179)** has been synthesised and fully characterised. This catalyst has been applied in the Heck reaction with different substrates, showing an excellent result in the reaction between bromobenzaldehyde and butyl acrylate in up to 90% yield. The same reaction but with different alkene such as heptene or 2,3-dihydrofuran gave lower yields, we believed this to be a result of volatility of the alkene and a lower reaction temperature being used. We also found that our catalyst was ineffective with aromatics lacking electron withdrawing groups. We believe that this catalyst would work effectively in the Heck reaction if: used with aryl halides containing electron withdrawing groups; if the reaction is carried out at higher temperature, about 120 °C.

Chapter 7

Crystallographic studies

7.1 Introduction

An understanding of the interactions present in the crystal structure of a potential anion receptor can provide valuable information on the bonding mode and binding sites in solution studies; whereas the crystallographic analysis of therapeutic compounds has proved invaluable to chemists and biologists in understanding the key binding sites and modes of action of these therapeutic agents.

7.2 Structural studies of homochiral tripodal imidazolium salts.

Crystals suitable for X-ray crystallographic determination of 1,3,5-tris[N-((-)cis-myrtanylimidazolium)methyl]2,4,6-trimethylbenezene tri(hexafluorophosphate) **(156a)** (code kno01) were grown from an ethanol-acetonitrile solution, yielding a cluster of needles. All pertinent crystallographic information is summarised in Table 7.1, selected bond distances and angles of the non hydrogen atoms are given in Table 7.2 and selected torsional angles in Table 7.3. Figure 7.1 shows a perspective view of the molecule with the atomic numbering scheme assigned, whereas Figure 7.2 shows a perspective view of packing molecules.

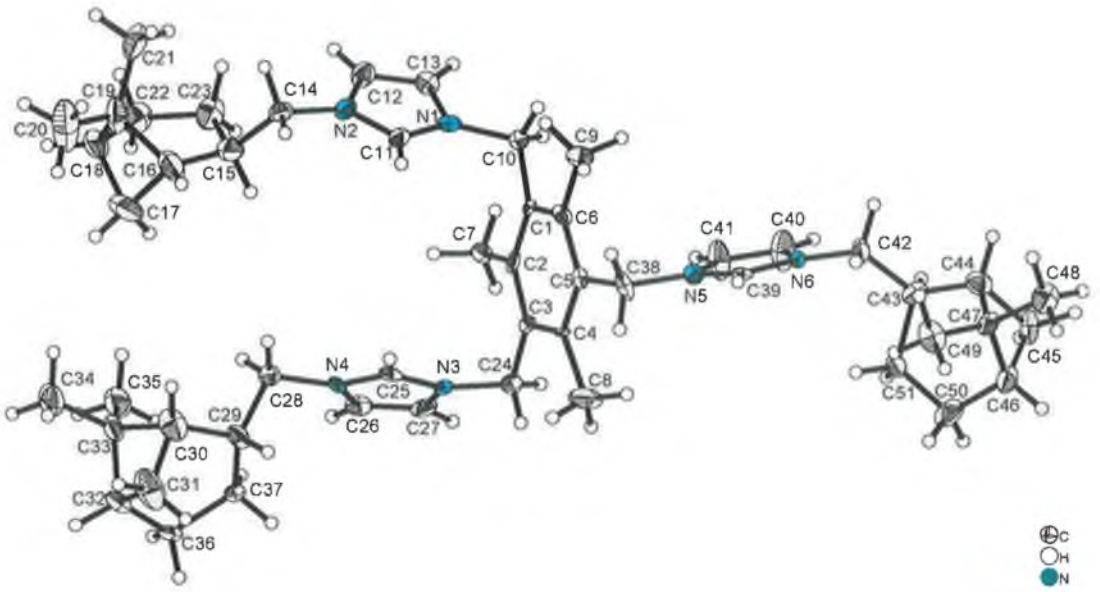

Figure 7.1. ORTEP drawing of the crystal structures of **(156a)** (code ko01).

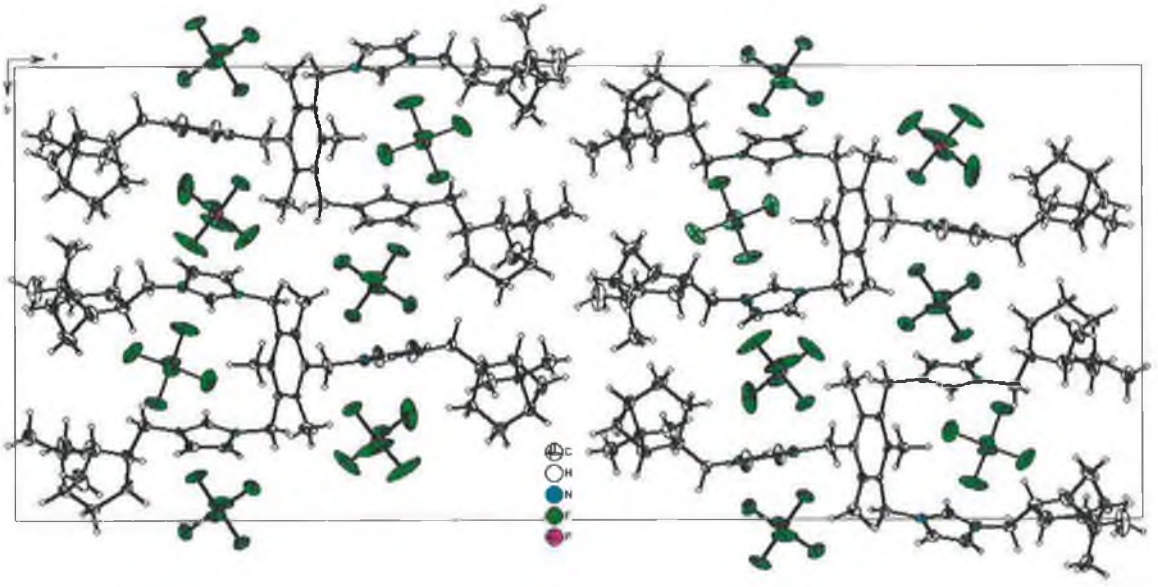

Figure 7.2. ORTEP drawing of the packing crystal structures of **(156a)** (code ko01).

Identification code	kno01
Empirical formula	$C_{51}\ H_{75}\ N_6\ F_{18}\ P_3$
Molecular formula	$[C_{51}\ H_{75}\ N_6]^{3+}\ \{[PF_6]^-\}_3$
Formula weight	1207.08
Temperature	100(2) K
Wavelength	0.71073 Å
Crystal system	Orthorhombic
Space group	$P2_12_12_1$ (#19)
Unit cell dimensions	a = 7.0442(10) Å α= 90°.
	b = 17.927(3) Å β= 90°.
	c = 43.952(6) Å γ = 90°.
Volume	5550.1(14) $Å^3$
Z	4
Density (calculated)	1.445 Mg/m^3
Absorption coefficient	0.210 mm^{-1}
F(000)	2520
Crystal size	0.40 x 0.20 x 0.10 mm^3
Theta range for data collection	1.23 to 23.00°.
Index ranges	−7<=h<=7, −19<=k<=19, −48<=l<=48
Reflections collected	30043
Independent reflections	7740 [R(int) = 0.0854]
Completeness to theta = 23.00°	100.0 %
Absorption correction	Semi−empirical from equivalents
Max. and min. transmission	0.9793 and 0.6122
Refinement method	Full−matrix least−squares on F^2
Data / restraints / parameters	7740 / 0 / 712
Goodness−of−fit on F^2	1.055
Final R indices [I>2sigma(I)]	R1 = 0.0711, wR2 = 0.1466
R indices (all data)	R1 = 0.0948, wR2 = 0.1579
Absolute structure parameter	-0.04(17)
Largest diff. peak and hole	0.739 and −0.457 $e.Å^{-3}$

Table 7.1. Crystal data and structure refinement for **(156a)**.

C(24)-N(24) (Å)	1.468(7)
C(3)-C(24) (Å)	1.526(8)
N(3)-C(24)-C(3) (°)	114.6(5)
C(25)-N(3) (Å)	1.316(7)
C(25)-N(4) (Å)	1.345(7)
N(3)-C(25)-N(4) (°)	108.6(5)
N(4)-C(28) (Å)	1.477(7)
C(28)-C(29) (Å)	1.513(8)
N(4)-C(28)-C(29) (°)	112.7(5)
C(1)-C(10) (Å)	1.513(8)
C(10)-N(1) (Å)	1.486(7)
N(1)-C(10)-C(1) (°)	113.9(5)
C(11)-N(1) (Å)	1.333(7)
C(11)-N(2) (Å)	1.327(7)
N(2)-C(11)-N(1) (°)	108.1(5)
C(14)-N(2) (Å)	1.485(7)
C(14)-C(15) (Å)	1.533(9)
N(2)-C(14)-C(15) (°)	112.4(5)
C(5)-C(38) (Å)	1.517(8)
C(38)-N(5) (Å)	1.493(7)
N(5)-C(38)-C(5) (°)	110.2(5)
C(39)-N(6) (Å)	1.321(7)
C(39)-N(5) (Å)	1.324(7)
N(6)-C(39)-N(5) (°)	109.6(5)
N(42)-N(6) (Å)	1.463(7)
C(42)-C(43) (Å)	1.524(8)
N(6)-C(42)-C(43) (°)	113.1(5)

Table 7.2. Selected bond distance (Å) and bond angles (°) for **(156a)**.

The bond lengths for imidazolium nucleus: N(1)-C(11) is 1.333 Å and C(11)-N(2) is 1.327 Å. The bond angle of N(1)-C(11)-N(2) is 108.1(°). The other two imidazolium rings have similar results.

For the methylene spacer the N(4)-C(28) bond length is slightly shorter at 1.477 and the C(28)-C(29) bond length at 1.513(8) Å which is similar to those of the two other methylene spacers. The angle of N(4)-C(28)-C(29) is 112.7 (°) which is also similar with the other two bond angles of the methylene spacers.

The torsional angles C(3)-C(24)-N(3)-C(25) and C(1)-C(10)-N(1)-C(11) are -42.6(8)° and 41.2(9)°, respectively, whereas C(5)-C(38)-N(5)-C(39) is 175.7(6)°. The torsional angles of the methylene spacer linking the myrtanyl groups to the imidazolium nucleus: C(29)-C(28)-N(4)-C(25) is –93.5(7)°, C(15)-C(14)-N(2)-C(11) is –114.2(7)° and C(43)-C(42)-N(6)-C(39) is 129.9(6)°. This gives an indication that compound **(156a)** is not completely symmetrical in the solid state.

C(3)-C(24)-N(3)-C(25) (°)	-42.6(8)
C(29)-C(28)-N(4)-C(25) (°)	-93.5(7)
N(4)-C(26)-C(27)-N(3)) (°)	-1.3(7)
C(1)-C(10)-N(1)-C(11) (°)	41.2(9)
C(15)-C(14)-N(2)-C(11) (°)	-114.2(7)
N(2)-C(12)-C(13)-N(1) (°)	1.3(7)
C(5)-C(38)-N(5)-C(39) (°)	175.7(6)
C(43)-C(42)-N(6)-C(39) (°)	126.9(6)
C(4)-C(5)-C(38)-N(5) (°)	94.3(7)
N(6)-C(40)-C(41)-N(5) (°)	0.8(9)

Table 7.3. Torsion angles (°) for **(156a)**.

The crystal structures of 1,3,5-tris[((R)-3-methyl-2-butylimidazolium)methyl]-2,4,6-trimethylbenzene tri(hexafluorophosphate) **(156b)** (code kno02) has also been determined. This compound was crystallised from a Methanol:Acetonitrile solution yielding clusters of block shaped crystals. All pertinent crystallographic data are listed in Table 7.4, selected bond lengths and angles of the non-hydrogen atoms in Table 7.5 and selected torsional angles in Table 7.6. Figure 7.3 shows a perspective view of the molecule with the atomic numbering scheme assigned. whereas Figure 7.4 shows a perspective view of packing molecules.

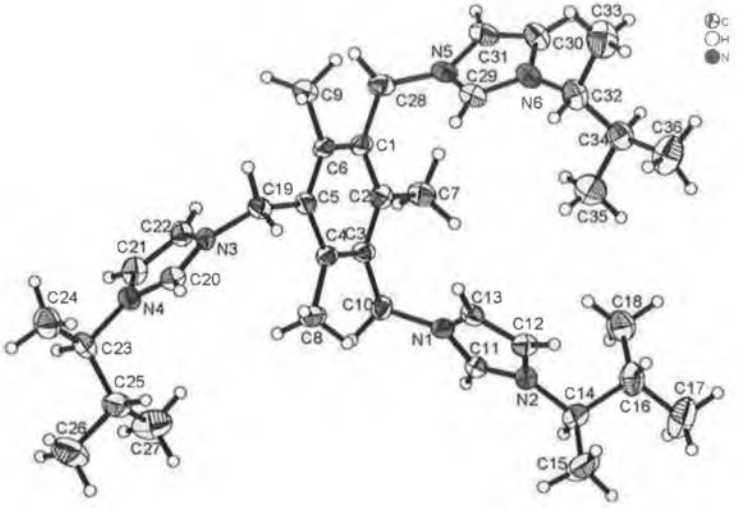

Figure 7.3. ORTEP drawing of the crystal structural of **(156b)** (code kno02).

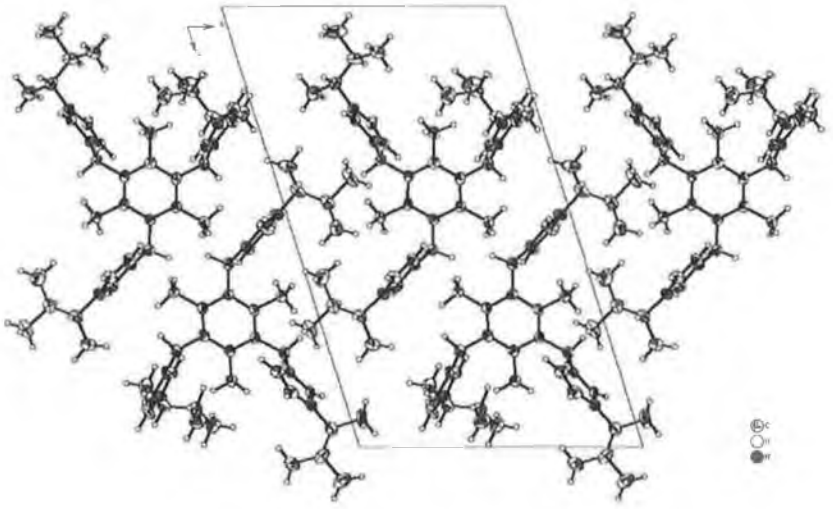

Figure7.4. ORTEP drawing of the packing crystal structures of **(156b)** (code ko02).

Identification code	kno02	
Empirical formula	$C_{76}\ H_{123}\ N_{13}\ O\ F_{36}\ P_6$	
Molecular formula	$2\ \{[C_{36}\ H_{57}\ N_6]^{3+}\ 3\ ([F_6\ P]^-)\}\ x\ C_2\ H_3\ N\ x\ C_2\ H_6\ O$	
Formula weight	2104.69	
Temperature	100(2) K	
Wavelength	0.71073 Å	
Crystal system	Triclinic	
Space group	P 1 (#1)	
Unit cell dimensions	a = 9.0263(6) Å	α= 72.834(1)°.
	b = 13.1480(9) Å	β= 82.686(1)°.
	c = 21.8139(15) Å	γ = 89.558(1)°.
Volume	2452.2(3) $Å^3$	
Z	1	
Density (calculated)	1.425 Mg/m^3	
Absorption coefficient	0.226 mm^{-1}	
F(000)	1092	
Crystal size	0.80 x 0.35 x 0.30 mm^3	
Theta range for data collection	1.97 to 25.00°.	
Index ranges	–10<=h<=10, –15<=k<=15, –25<=l<=25	
Reflections collected	17668	
Independent reflections	15499 [R(int) = 0.0126]	
Completeness to theta = 25.00°	99.2 %	
Absorption correction	Semi–empirical from equivalents	
Max. and min. transmission	0.9352 and 0.7773	
Refinement method	Full–matrix least–squares on F^2	
Data / restraints / parameters	15499 / 3 / 1215	
Goodness–of–fit on F^2	1.023	
Final R indices [I>2sigma(I)]	R1 = 0.0580, wR2 = 0.1511	
R indices (all data)	R1 = 0.0627, wR2 = 0.1562	
Absolute structure parameter	0.03(8)	
Largest diff. peak and hole	1.105 and –0.525 $e.Å^{-3}$	

Table 7.4. Crystal data and structure refinement for **(156b)** (code kno02).

C(1)-C(28) (Å)	1.517(6)
N(5)-C(28) (Å)	1.479(6)
N(5)-C(28)-C(1) (°)	110.8(3)
N(5)-C(29) (Å)	1.329(5)
N(6)-C(29) (Å)	1.324(6)
N(6)-C(29)-N(5) (°)	109.3(4)
N(6)-C(32) (Å)	1.479(6)
C(32)-C(34) (Å)	1.532(7)
N(6)-C(32)-C(34) (°)	110.0(4)
C(5)-C(19) (Å)	1.518(6)
N(3)-C(19) (Å)	1.481(5)
N(3)-C(19)-C(5) (°)	109.2(3)
N(3)-C(20) (Å)	1.321(5)
N(4)-C(20) (Å)	1.326(6)
N(3)-C(20)-N(4) (°)	109.5(5)
N(4)-C(23) (Å)	1.495(5)
C(23)-C(25) (Å)	1.530(6)
N(4)-C(23)-C(24) (°)	108.8(4)
C(3)-C(10) (Å)	1.511(60)
N(1)-C(10) (Å)	1.481(5)
N(1)-C(10)-C(3) (°)	111.5(3)
N(1)-C(11) (Å)	1.325(5)
N(2)-C(11) (Å)	1.335(5)
N(1)-C(11)-N(2) (°)	108.7(4)
N(2)-C(14) (Å)	1.465(6)
C(14)-C(16) (Å)	1.523(7)
N(2)-C(14)-C(16) (°)	110.7(4)

Table7.5. Selected bond distance (Å) and bond angles(°) for **(156b)**.

For the compound **(156b)** the bond length for imidazolium nucleus: N(1)-N(11) is 1.325(5)Å and N(2)-C(11) is 1.335(5)Å, are similar to the other imidazolium rings. The bond angle of N(1)-C(11)-N(2) is 108.7(4)Å is slightly narrower than the bond angles in the other two imidazolium rings.
The bond length between imidazolium ring and chiral centre: N(6)-C(32) is 1.479(6)Å which is slightly different with the other chiral centres, N(4)-C(23) is 1.495(5)Å and N(2)-N(14) is 1.465(6)Å.

The torsional angles of C(11)-N(1)-C(10)-C(3) and C(20)-N(3)-C(19)-C(5) are –162.3(4) (°)and 140.2(4)(°) respectively, whereas C(29)-N(5)-C(28)-C(11) is –23.1(6)(°).

C(29)-N(5)-C(28)-C(11) (°)	-23.1(6)
N(6)-C(30)-C(31)-N(5) (°)	-0.1(5)
C(11)-N(1)-C(10)-C(3) (°)	-162.3(4)
N(4)-C(21)-C(22)-N(3) (°)	0.7(5)
C(20)-N(3)-C(19)-C(5) (°)	140.2(4)
N(2)-C(12)-C(13)-N(1) (°)	-1.1(5)

Table 7.6. Torsion angles (°) for **(156b)**.

7.3 Structural studies of Palladium-complex (179)

Other crystals suitable for X-ray crystallographic determination of the imidazolylidene-Pd(II) complex **(179)** were grown from an acetonitrile solution yielding clusters of needle shaped crystals. All pertinent crystallographic data are shown in Table 7.7, selected bond lengths and angles of the non-hydrogen atoms in Table 7.8 and selected torsion angles are in Table 7.9. Figure 7.5 shows a perspective view of the molecule with the atomic numbering scheme assigned, whereas Figure 7.6 shows a perspective view of packing molecules.

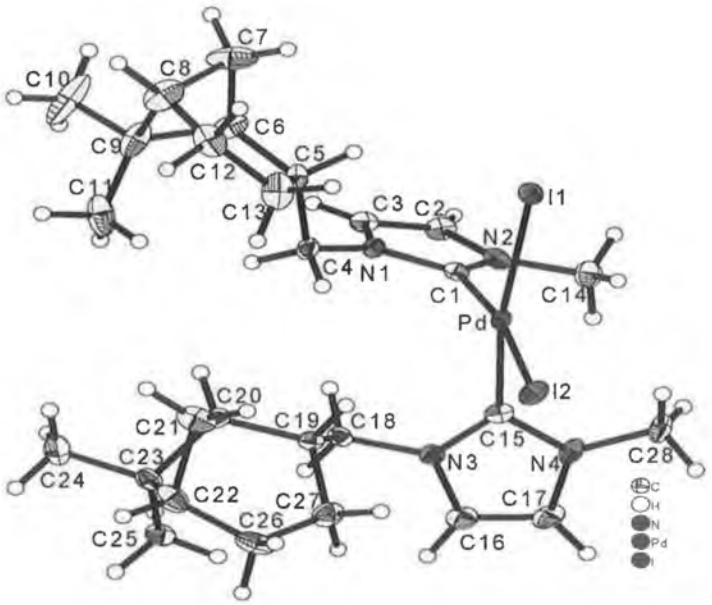

Figure 7.5. ORTEP drawing of the crystal structural of **(179)** (code kno03).

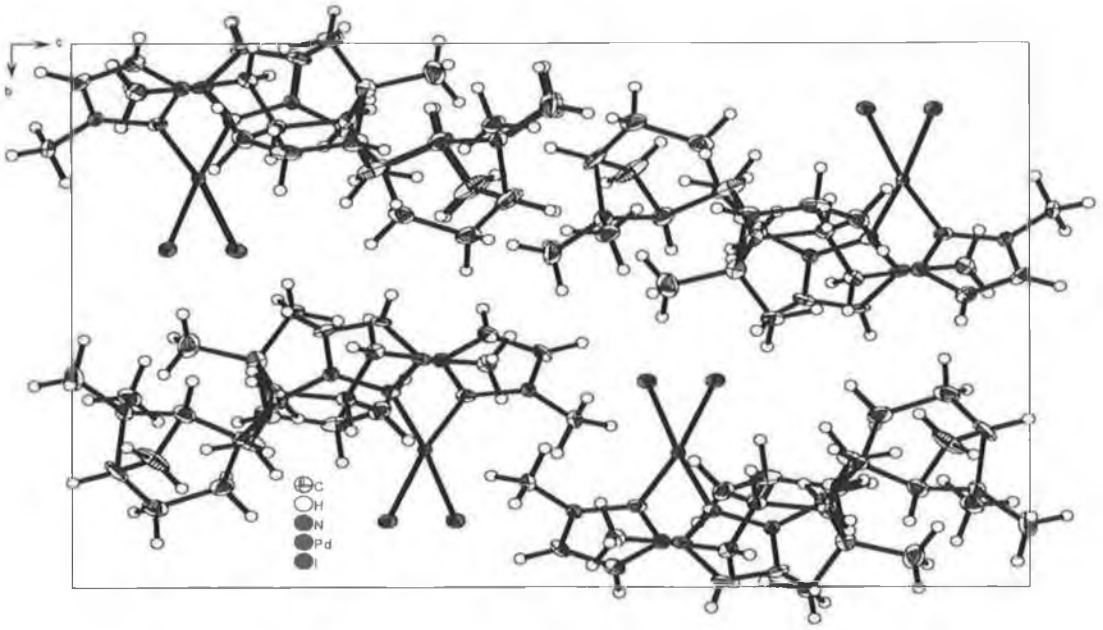

Figure7.6. ORTEP drawing of the packing crystal structures of **(179)** (code kno03).

Identification code	kno03	
mpirical formula	$C_{28}H_{44}N_4Pd I_2$	
Formula weight	796.87	
Temperature	100(2) K	
Wavelength	0.71073 Å	
Crystal system	Orthorhombic	
Space group	P21 21 21	
Unit cell dimensions	a = 10.6316(7) Å	α= 90°.
	b = 13.6965(9) Å	β= 90°.
	c = 20.6279(14) Å	γ = 90°.
Volume	3003.7(3) $Å^3$	
Z	4	
Density (calculated)	1.762 Mg/m^3	
Absorption coefficient	2.696 mm^{-1}	
F(000)	1568	
Crystal size	0.20 x 0.10 x 0.10 mm^3	
Theta range for data collection	1.78 to 28.28°.	
Index ranges	–14<=h<=14, –18<=k<=18, –26<=l<=26	
Reflections collected	51800	
Independent reflections	7257 [R(int) = 0.0527]	
Completeness to theta = 28.28°	98.4 %	
Absorption correction	Semi–empirical from equivalents	
Max. and min. transmission	0.7743 and 0.6845	
Refinement method	Full–matrix least–squares on F^2	
Data / restraints / parameters	7257 / 0 / 322	
Goodness–of–fit on F^2	1.134	
Final R indices [I>2sigma(I)]	R1 = 0.0360, wR2 = 0.0811	
R indices (all data)	R1 = 0.0389, wR2 = 0.0823	
Absolute structure parameter	0.01(2)	
Largest diff. peak and hole	2.054 and –0.586 $e.Å^{-3}$	

Table 7.7. Crystal data and structure refinement for **(179)** (code kno03).

I(1)-Pd	2.6595(4)
I(2)-Pd	2.6533(5)
I(2)-Pd-I(1)	94.415(14)
Pd-C(1)	1.989(5)
Pd-C(15)	1.999(5)
C(1)-Pd-C(15)	90.47(18)
C(1)-N(2)	1.352(6)
C(1)-N(1)	1.360(6)
N(2)-C(1)-N(1)	104.9(4)
C(15)-N(3)	1.355(6)
C(15)-N(4)	1.361(6)
N(3)-C(15)-N(4)	104.7(4)
N(3)-C(18)	1.472(6)
C(18)-C(19)	1.539(6)
N(3)-C(18)-C(19)	111.7(4)
N(1)-C(4)	1.463(6)
C(4)-C(5)	1.539(7)
N(1)-C(4)-C(5)	113.8(4)
C(1)-Pd-I(1)	90.19(12)
C(15)-Pd-I(2)	86.38(13)
C(1)-Pd-I(2)	170.43(13)
C(15)-Pd-I(1)	170.45(14)

Table 7.8. Selected bond distance (Å) and bond angles(°) for **(179)**.

The crystal structure analysis of compound **(179)** shows that the square-planar core geometry of two carbene ligands are in a cis arrangement, and twisted relative to the PdI_2; the bond length of Pd-C(1) is 1.989(5) Å and Pd-C(5) is 1.999(5) Å. Whereas the bond angle of C(1)-Pd-C(5) is 90.47(18) (°). The bond length of I(1)-Pd is 2.6595(4) Å and I(2)-Pd is 2.6533(5). The bond angle of I(2)-Pd-I(1) is 94.415(14) (°). These results are similar to those reported previously [183-188] and in agreement with expected values, showing the heterocyclic carbenes of the imidazole type have donor properties similar to the electron-rich phosphanes [139]. The bond angle of N(2)-C(1)-N(1) is 104-9(4) (°) which is similar to previous reported [139]. The methylene spacer bond angle of N(1)-C(4)-C(5) is 113.8(4) (°).

The torsional angles of C(1)-N(1)-C(4)-C(5) and C(15)-N(3)-C(18)-C(19) are 96.9(5) and –70.9(6) (°), respectively. The other two torsional angles of N(3)-C(16)-C(170-N(4) and N(20-C(2)-C(3)-N(1) are –0.3(6) and 0.2(5) (°), respectively.

Pd-C(1)-N(1)-C(4)	6.3(6)
Pd-C(15)-N(3)-C(18)	2.2(7)
C(1)-N(1)-C(4)-C(5)	96.9(5)
C(15)-N(3)-C(18)-C(19)	-70.9(6)
N(3)-C(16)-C(17)-N(4)	-0.3(6)
N(2)-C(2)-C(3)-N(1)	0.2(5)

Table 7.9. Torsion angles (°) for **(179)**.

7.4 Conclusion

In the case of 1,3,5-tris[N-((-)-cis-myrtanylimidazolium)methyl]2,4,6-trimethyl-benzene tri(hexafluorophosphate) **(156a)**, the crystallographic studies shows that the PF_6^- counter anion is positioned nearby the H-2 proton in the imidazolium ring, where this would suggest hydrogen bonding. Also this anion is in close proximity to the cation centre of the imidazolium ring.

Also the crystallographic studies for the Pd-complex **(179)** shows this complex is in a cis conformation.

Chapter 8

Experimental

Introduction

NMR spectra were carried out on a Bruker AVANCE instrument using XWINMR software processed on a Silicon Graphics O2 workstation. The instrument operated at 400 MHz for ^{1}H NMR and 100 MHz for ^{13}C NMR. Infra red (IR) spectra were recorded using a Nicolet 405 FTIR spectrophotometer. Melting point determinations were carried out on a Stuart Scientific melting point apparatus. Specific rotations $[\alpha]_D^{25}$ were performed on a Perkin Elmer 341 polarimeter operating at 589 nm and 25 °C.

Elemental analysis were carried out by the Microanalytical Laboratory at University College, Dublin. Mass spectra were recorded on Bruker ESQUIRE LCMS instrument at Dublin City University.

Flash chromatography was performed using Riedel de Haën or Matrix silica gel 60. All chemicals were purchased from the Sigma / Aldrich chemical company and used without further purification, unless otherwise stated.

Acetonitrile was dried over potassium carbonate and distilled. DCM was distilled directly and stored over 3Å sieves. Methanol was refluxed for 0.5 h with protection from the atmosphere and then distilled. Toluene was distilled with rejection of the first fore-run fraction (ca.-5%). Finally THF was refluxed over sodium and benzophenone. All reactions were performed under a nitrogen atmosphere unless otherwise stated.

General procedure of substituted imidazole synthesis

To a solution of (-)-cis-myrtanylamine (2.86 g, 18.6 mmol) and aqueous ammonia (1ml, 18.60 mmol) in propan-1-ol (10 ml), a solution of glyoxal (2.34 ml, 20 mmol) and aqueous formaldehyde (37%, 1.45 ml, 20.0 mmol) in propan-1-ol (20 ml) were added dropwise. The solution was then cooled to room temperature and water was added. Subsequently, the mixture was extracted with dichloromethane (3×30 ml) and the combined extracts were washed with water (2×20 ml), dried (anhydrous $MgSO_4$), filtered and dichloromethane was removed under vacuum to give **(152a)** as a brown oil. This was used without further purification in the following step. A small sample of (-)-cis-myrtanyl imidazole **(152a)** was purified (flash chromatography, silica gel, 10:1 Ethylacetate: Methanol) to give the following analytical data :

(-)-cis-myrtanyl imidazole (152a)

Yield 3.20g (87%) yellow oil, $[\alpha]_D^{25}$ = +12° (EtOH)

^{1}H NMR ($CDCl_3$) δ (ppm): 0.83 (d, 1H , *J*=9.6 Hz, CH), 1.02 (s, 3H, CH_3), 1.13 (s, 3H, CH_3), 1.45 (m, 1H, CH), 1.70 (m, 1H, CH), 1.84 (m, 4H, $2CH_2$), 2.27 (m, 1H, CH), 2.39 (m, 1H, CH), 3.83 (q, 1H, *J*=3.2 Hz, CH), 6.81 (s, 1H, NCHCH), 6.97 (s, 1H, NCHCH), 7.36(s, 1H, NCHN).

^{13}C NMR ($CDCl_3$) δ (ppm): 19.84 (CH_3), 23.83 (CH_3), 26.10 (CH_2), 28.21 (CH_2), 33.23 (CH_2), 38.96 (CH_2), 41.48 (CH), 43.06 (CH), 43.41 (CH), 52.94 (C), 119.37 (NCC), 129.58 (NCC), 137.63 (NCN).

IR (neat) *v* (cm^{-1}): 2985, 2940, 2919, 2871, 1678, 1472, 145,1389, 1366, 736.

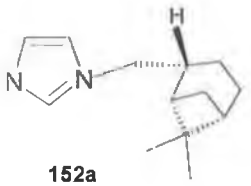

152a

(R)-3-Methyl-2-butyl imidazole (152b)

The general procedure was used with starting material of (R)-3-Methyl-2-butyl-amine (1.62 g, 18.6 mmol) to give 1.69g brown oil of (60% yield); $[\alpha]_D^{25}$ = +64° (EtOH).

^{1}H NMR ($CDCl_3$) δ (ppm): 0.51 (d, 3H, *J*=6.4 Hz, CH_3), 0.70 (d, 3H, *J*=6.8 Hz, CH_3), 1.21 (d, 3H, *J*=7.2 Hz, CH_3), 1.65 (m, 1H, CH), 3.58 (m, 1H, CH), 6.66 (s, 1H, NCHCH), 6.80 (s, 1H , NCHCH), 7.23 (s, 1H , NCHN).

^{13}C NMR ($CDCl_3$) δ (ppm): 19.14 (CH_3), 19.35 (CH_3), 19.54 (CH_3), 35.21 (CH), 59.85 (CH), 117.45 (NCC), 129.17 (NCC), 136.50 (NCN).

IR (neat) *v* (cm^{-1}): 3112, 2968, 2880, 1674, 1494, 1459, 1415, 1380, 1112, 915, 731.

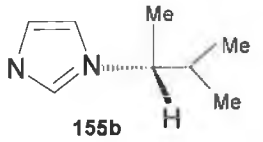

155b

(S)-1-(2-phenyl)ethyl imidazole (152c)

The general procedure was used with starting material of (S)-1-(2-phenyl)ethyl-amine (2.24 g, 18.6 mmol) to give 1.58g brown oil of (55% yield).

^{1}H NMR ($CDCl_3$) δ (ppm): 1.83 (d, 3H, *J*=7.2 Hz, CH_3), 5.32 (m, 1H, *J*=6.8 Hz, CH), 6.91 (s, 1H, NCHCH), 7.06 (s, 1H, NCHCH), 7.13 (d, 2H, Ar-CH), 7.29 (m, 3H, Ar-CH), 7.58 (s, 1H, NCHN).

^{13}C NMR ($CDCl_3$) δ (ppm): 22.40 (CH_3), 56.93 (CH), 118.36 (NCC), (126.36, 128.46, 129.28, 129.64) (Ar-C), 136.42 (NCC), 141.91(NCN).

IR (neat) ν (cm^{-1}): 3109, 2983, 2914, 1678, 1508, 1468, 1452, 1384, 1110, 1060, 730, 664.

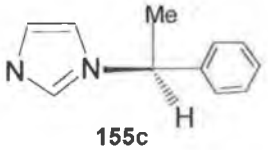

155c

(S)-1-(2-Naphthyl)ethyl imidazole (152d)

The general procedure was used with starting material of (S)-1-(2-Naphthyl)ethyl-amine (3.18 g, 18.6 mmol) to give 2.60 g brown oil of (65% yield).

^{1}H NMR ($CDCl_3$) δ (ppm): 1.87 (d, 3H, J=7.2 Hz, CH_3), 5.70 (q, 1H, J=7.2 Hz, CH), 6.92 (s, 1H, NCHCH), 7.30 (s, 1H, NCHCH), 7.42 (d, 1H, J=8 Hz, Ar-CH), 7.51 (m, 2H, Ar-CH), 7.78 (s, 1H, NCHN), 7.87 (m, 4H, Ar-CH).

^{13}C NMR ($CDCl_3$) δ (ppm): 22.36 (CH), 57.03 (CH), 118.50 (NCC), (124.37, 125.16, 126.83, 127.22, 128.09, 128.39, 129.28, 129.89, 133.30, 133.59) (Ar-C), 136.56 (NCC), 139.29 (NCN).

IR (neat) ν (cm^{-1}): 3110, 3070, 3980, 3910, 1610, 1500, 1480, 1410, 1310, 1300, 820, 740.

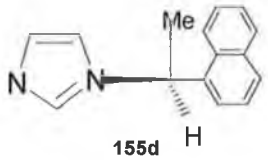

155d

(S)-1-(2-hexyl)ethyl imidazole (152e)

The general procedure was used with starting material of (S)-1-(2-hexyl)ethyl amine (2.36 g, 18.6 mmol) to give 2.15g brown oil of (65% yield).

^{1}H NMR ($CDCl_3$) δ (ppm): Overlapping 0.65-1.60 (m, 11H, hexyl-H), 1.26 (d, 3H, J=6.8 Hz, CH_3), 3.66 (m, 1H, CH), 6.70 (s, H, NCHCH), 6.86 (s, H, NCHCH), 7.28 (s, 1H, NCHN).

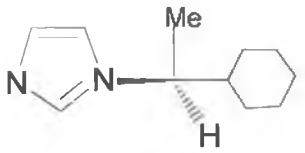

155e

1,3,5-Tris(bromomethyl)-2,4,6-trimethylbenzene (154)

To a mixture of mesitylene (3.6 g, 29 mmol), paraformaldehyde (3.08 g, 100 mmol), and (50 ml) of glacial acitic acid (20 ml) of 31 wt % HBr/acetic acid solution was added rapidly. The mixture was kept for 8 h at 95-100 °C and the colour was turned to a clear orange. The reaction mixture was then poured onto (100 ml) of water to give a white solid precipitate. The crude product was recrystalized by slow evaporation from chloroform.

Yield 11.28g (95 %) white crystals, m.p. 184-186 °C.

^{1}H NMR ($CDCl_3$) δ (ppm): 2.50 (s, 9H, CH_3), 4.60 (s, 6H, CH_2Br)

^{13}C NMR ($CDCl_3$) δ (ppm): 15.80 (Ar-CH_3), 30.25 (Ar-CH_2Br), 133.65 (Ar-CH_3), 138.30 (Ar-CH_2).

IR (KBr) ν (cm^{-1}): 3041, 3010, 1565, 1444, 1408, 1376, 1080, 786, 759, 683, 571.

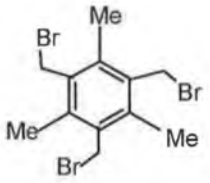

154

1,3,5-Tris[N-((-)-cis-myrtanylimidazolium)methyl]2,4,6-trimethylbenzene-tribromide (155a)

1,3,5,-Tris(bromomethyl)-2,4,6-trimethyl benzene (0.50 g, 1.35 mmol) and (-)-cis-myrtanyl imidazole (1.00 g, 4.80 mmol) in 1,4-dioxane (15 ml) were heated to 100 °C for 24 h. The resulting solid, 1,3,5-tris[N-((-)-cis-myrtanyl-

imidazolium)methyl]-2,4,6-trimethylbenzene tribromide, was collected, washed with diethylether (3×100 ml) and dried.

Yield 0.678g (95%) creamy solid, m.p. 284-286 °C, $[\alpha]_D^{25}$ = +50° (EtOH).

^{1}H NMR (CD_3CN) δ (ppm): 0.83 (d, 3H, *J*=9.6 Hz, CH), 1.01 (s, 9H, CH_3), 1.11 (s, 9H, CH_3), 1.46 (m, 3H, CH), overlapping 1.75-1.87 (m, 15H, CH_2CH_2CH), 2.26 (s, 9H, CH_3), 2.44 (m, 3H, CH), 4.12 (m, 3H, CH), 4.29 (m, 3H, CH), 5.75 (s, 6H, CH_2), 7.21 (d, 3H, *J*=6.8 Hz, NCHCH), 8.44 (s, 3H, NCHCH), 10.09 (s, 3H, NCHN)

^{13}C NMR ($CDCl_3$) δ (ppm): 17.89 (CH_3), 19.48 (CH_3), 24.04 (CH_3), 25.92 (CH_2), 28.14 (CH_2), 33.19 (CH_2), 38.89 (CH_2), 41.28 (CH_2), 42.61 (CH), 43.81 (CH), 49.50 (CH), 55.54 (C), 122.38 (NCC), 124.36 (NCC), 129.28 (Ar-CH_3), 136.42 (NCN), 142.29 (Ar-CH_2).

IR (KBr) *v* (cm^{-1}): 3100, 3075, 2945, 2890, 1630, 1590, 1480, 1420, 1485, 1350, 1300, 1160, 840, 720, 560.

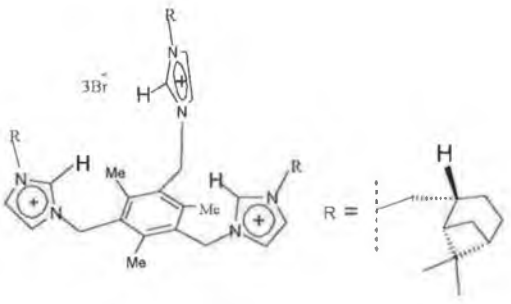

155a

1,3,5-Tris[((R)-3-methyl-2-butylimidazolium)methyl]2,4,5-trimethylbenzene-tribromide (155b)

The general procedure was used with starting materials of 1,3,5-tris(bromo-methyl)-2,4,6-trimethylbenezene **(154)** (0.36 g, 0.91 mmol) and (R)-3-Methyl-2-butyl imidazol **(152b)** (0.50 g, 3.28 mmol) to give 0.68g creamy powder of (92% yield), m.p. 253-255 °C, $[\alpha]_D^{25}$ = +37° (EtOH).

^{1}H NMR (CD_3CN) δ (ppm): 0.71 (d, 9H, *J*=6.4 Hz, CH_3), 0.95 (d, 9H, *J*=6.4 Hz, CH_3), 1.52 (d, 34, *J*=6.8 Hz, CH_3), 2.00 (q, 3H, *J*=7.2 Hz, CH), 2.33 (s, 9H, CH_3), 4.70 (q, 3H, *J*=7.6 Hz, CH), 5.85 (q, 6H, *J*=8.4 Hz, CH_2), 7.46 (s, 3H, NCHCH), 8.57 (s, 3H, NCHCH), 10.09 (s, 3H, NCHN).

^{13}C NMR ($CDCl_3$) δ (ppm): 17.73 (CH_3), 18.74 (CH_3), 19.14 (CH_3), 19.28 (CH_3), 34.64 (CH), 49.50 (CH_2), 62.32 (CH), 120.11 (NCC), 124.68 (NCC), 129.26 (Ar-CH_3), 135.70 (NCN), 142.33 (Ar-CH_2).

IR (KBr) *v* (cm^{-1}): 3123, 3064, 2967, 2877, 2340, 1636, 1570, 1551, 1460, 1385, 1334, 1155, 879, 834, 623.

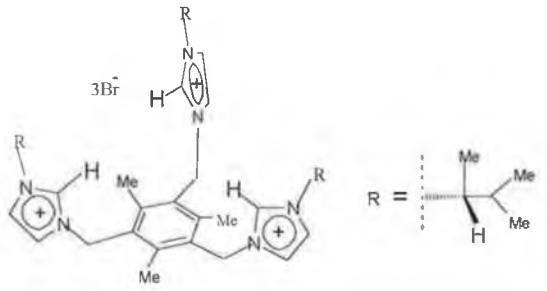

155b

1,3,5-Tris[((S)-1-(2-phenyl)ethylimidazolium)methyl]2,4,6-trimethylbenzene-tribromide (155c)

The general procedure was used with starting materials of 1,3,5-tris(bromo-methyl)-2,4,6-trimethylbenezene **(154)** (0.66 g, 1.66 mmol) and (S)-1-(2-phenyl) ethyl imidazole (1.10 g, 6.39 mmol) **(152c)** to give 1.46g brownish yellow powder of (96% yield), m.p. 120-122 °C, $[\alpha]_D^{25}$ = - 78° (CH_2Cl_2).

^{1}H NMR (CD_3CN) δ (ppm): 1.82 (d, 9H, *J*=12 Hz, CH_3), 2.25 (s, 9H, CH_3), 5.75 (q, 6H, *J*=8 Hz, CH_2), 6.03 (q, H, *J*=7.2 Hz, CH), 7.06 (s, 3H, NCHCH), 7.25 (m, 15H, Ar-H), 8.31 (s, 3H, NCHCH), 10.21 (s, 3H, NCHN).

^{13}C NMR (CD_3CN) δ (ppm): 18.01 (CH_3), 21.55 (CH_3), 49.54 (CH_2), 59.44 (CH), 120.16 (NCC), 124.53 (NCC), (127.30, 129.30, 129.64, 129.69) (Ar-C), 135.78 (Ar-CH_3), 138.27 (NCN), 142.41 (Ar-CH_2).

IR (KBr) ν (cm^{-1}): 3100, 3050, 3980, 3900, 3880, 1630, 1550, 1500, 1470, 1450, 1410, 1320, 1260, 1200, 1150, 1110, 820, 720, 630, 520.

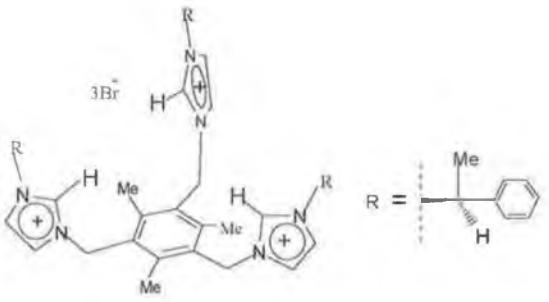

155c

1,3,5-Tris[((S)-1-(2-Naphthyl)ethylimidazolium)methyl]2,4,6-trimethyl-benzene tribromide (155d)

The general procedure was used with starting materials of 1,3,5-tris(bromo-methyl)-2,4,6-trimethylbenezene **(154)** (0.26 g, 0.65 mmol) and (S)-1-(2-Naphthyl)ethyl imidazole **(152d)** (0.52 g, 2.34 mmol) to give 0.66g brownish yellow powder of (96% yield), m.p: 182-184°C, $[\alpha]_D^{25}$ = -160° (EtOH).

^{1}H NMR (CD_3CN) δ (ppm): 1.95 (d, 9H, *J*=6.4 Hz, CH_3), 2.29 (s, 9H, CH_3), 5.60 (s, 6H, CH_2), 6.16 (q, 3H, *J*=6.8 Hz, CH), 7.58 (m, 9H, Ar-H), 7.79 (s, 3H, NCHCH), overlapping 7.91-8.03 (m, 15H, (Ar-H), (NCHCH)), 9.69 (s, 3H, NCHN).

^{13}C NMR (CD_3CN) δ (ppm); 16.78 (CH_3), 20.57 (CH_3), 48.36 (CH_2), 58.74 (CH), 121.32 (NCC), 123.30 (NCC), (124.73, 126.07, 127.09, 127.13, 127.94, 128.37, 129.04, 129.64, 132.96, 133.00) (Ar-C), 135.64 (Ar-CH_3), 137.05 (NCN), 141.53 (Ar-CH_2).

IR (KBr) ν (cm^{-1}): 3120, 3053, 2982, 2960, 2340, 1601, 1508, 1546, 1453, 1420, 1388, 1147, 1019, 866, 826, 756, 723, 620.

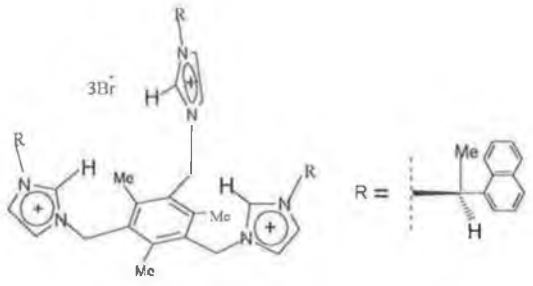

155d

1,3,5-Tris[((S)-1-(2-hexyl)ethylimidazolium)methyl]2,4,6-trimethylbenzene-tribromide (155e)

The general procedure was used with starting materials of 1,3,5-tris(bromo-methyl)-2,4,6-trimethylbenezene **(154)** (1.84 g, 10.4 mmol) and (S)-1-(2-hexyl)ethyl imidazole (1.14 g, 2.88 mmol) to give 2.48g brown solid of (92% yield), m.p. 108-110 °C, $[\alpha]_D^{25}$ = -53° (EtOH).

^{1}H NMR (CD_3CN) δ (ppm): overlapping 0.88-1.19 (m, 18H, hexyl-CH), 1.45 (d, 9H, *J*=6.8 Hz, CH_3), overlapping 1.48-177 (m, 15H, hexyl-CH), 2.30 (s, 9H, CH_3), 4.67 (m, 3H, CH), 5.81 (d, 6H, *J*=5.6 Hz, CH_2), 7.26 (s, 3H, NCHCH), 8.52 (s, 3H, NCHCH), 10.05 (s, 3H, NCHN).

^{13}C NMR (CD_3CN) δ (ppm): 17.80 (CH_3), 18.80 (CH_3), (25.98, 29.17, 29.47, 43.68) (hexyl-C), 49.44 (CH_2), 61.57 (CH), 119.67 (NCC), 124.77 (NCC), 129.16 (Ar-CH_3), 135.816 (NCN), 142.4 (Ar-CH_2).

IR (KBr) *v* (cm^{-1}): 3118, 3054, 2995, 2927, 2853, 1628, 1556, 1445, 1381, 1338, 1300, 1152, 1120, 892, 872, 766, 664.

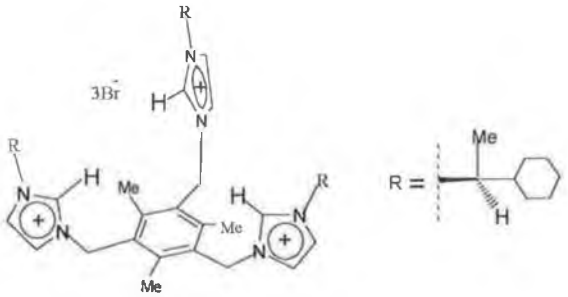

155e

Conversion to hexafluorophosphate salt

1,3,5-Tris[N-((-)-cis-myrtanylimidazolium)methyl]2,4,6-trimethylbenzene-tri(hexafluorophosphate) (156a)

General procedure:

The trisbromide salt was converted to the trihexafluorophosphate salt by dissolving the trisbromide salt (0.50 g, 0.49 mmol) in methanol (ca.5% w/v) and adding a saturated aqueous solution of ammonium hexafluorophosphate (0.24 g, 1.48 mmol) until no further precipitation occurred. The precipitate was filtered, washed with methanol and dried, to yield **(156a)**, 0.48g (82%) white powder and m.p. 260-262 °C, $[\alpha]_D^{25}$ = +60° (CH_3CN).

^1H NMR (CD_3CN) δ (ppm): 0.94 (d, 3H, *J*=9.6 Hz, CH), 1.07 (s, 9H, CH_3), 1.20 (s, 9H, CH_3), 1.50 (m, 3H, CH), overlapping 1.78-2.0 (m, 15H, CH_2CH_2CH), 2.25 (s, 9H, CH_3), 2.40 (m, 3H, CH), 2.52 (m, 3H, CH), 4.08 (d, 6H, *J*=8 Hz, CH_2), 5.45 (s, 6H, CH_2), 7.25 (s, 3H, NCHCH), 7.42 (s, 3H, NCHCH), 8.23 (s, 3H, NCHN).

^{13}C NMR (CD_3CN) δ (ppm): 15.56 (CH_3), 18.19 (CH_3), 22.05 (CH_3), 24.89 (CH_2), 26.62 (CH_2), 32.03 (CH_2), 37.87 (CH_2), 40.64 (CH_2), 41.13 (CH), 42.76 (CH), 47.86 (CH), 54.67 (C), 121.80 (NCC), 122.55 (NCC), 128.85 (Ar-CH_3), 134.50 (NCN), 141.41 (Ar-CH_2).

^{31}P (DMSO-d_6) δ (ppm): -134.27, -138.66, -143.05, -147.44, -151.84.

^{19}F (DMSO-d_6) δ (ppm): -69.55, -71.44.

IR (KBr) *v* (cm^{-1}): 3162, 3105, 2988, 2916, 2874, 2370, 1630, 1560, 1459, 1425, 1387, 1156, 1109, 841, 740.

Elemental analysis: calcd. for $C_{51}H_{75}N_6P_3F_{18}$ (1207.10): C, 50.75; H, 6.26; N, 6.96%. Found: C, 50.50; H, 6.14; N, 6.90%.

1,3,5-Tris[((R)-3-methyl-2-butylimidazolium)methyl]2,4,5-trimethylbenzene-tri(hexafluorophosphate) (156b)

The general procedure was used with starting materials of trisbromide salt **(155b)** (0.5 g, 0.16 mmol) and hexafluorophosphate salt (0.30 g, 1.84 mmol) to give 0.44g white powder of (72% yield), m.p. 203-205 °C, $[\alpha]_D^{25}$ = + 56° (CH_3CN).

^1H NMR ($CDCl_3$) δ (ppm): 0.74 (d, 9H, *J*=6.4 Hz , CH_3), 0.94 (d, 9H, *J*=6.4 Hz, CH_3), 1.49 (d, 9H, *J*=6.8 Hz, CH_3), 2.00 (m, 3H, CH), 2.25 (s, 9H, CH_3), 4.15 (m, 3H, CH), 5.46 (m, 6H, Ar-CH_2), 7.26 (s, 3H, NC<u>H</u>CH), 7.46 (s, 3H, NCHC<u>H</u>), 8.23 (s, 3H, NCHN).

^{13}C NMR ($CDCl_3$) δ (ppm): 15.54 (Ar-CH_3), 16.64 (CH_3), 17.41 (CH_3), 17.60 (CH_3), 33.50 (CH), 47.90 (CH_2), 62.71 (CH), 120.68 (N<u>C</u>C), 121.97 (NC<u>C</u>), 128.84 (Ar-CH_3), 133.70 (N<u>C</u>N), 141.40 (Ar-CH_2).

^{31}P (DMSO-d_6) δ (ppm): -130.00, -134.27, -138.66, -143.05, -147.44, -151.83, -156.20.

^{19}F (DMSO-d_6) δ (ppm): -69.54, -71.43.

IR (KBr) *v* (cm^{-1}): 3163, 3109, 2972, 3950, 2884, 2373, 1625, 1556, 1432, 1388, 1332, 1153, 1110, 843, 740.

Elemental analysis: calcd. for $C_{36}H_{57}N_6P_3F_{18}$ (1008.80): C, 42.86; H, 5.69; N, 8.33%. Found: C, 42.56; H, 5.55; N, 8.30%.

1,3,5-Tris[((S)-1-(2-phenyl)ethylimidazolium)methyl]2,4,6-trimethylbenzene-tri(hexafluorophosphate) (156c)

The general procedure was used with starting materials of trisbromide salt **(155c)** (0.50 g, 0.54 mmol) and hexafluorophosphate salt (0.26 g, 1.64 mmol) to give 0.4g brown solid of (66% yield), m.p.118-120 °C, $[\alpha]_D^{25}$ = -143° (CH_3CN).

^{1}H NMR (CD_3CN) δ (ppm): 1.84 (d, 9H, *J*=7.2 Hz, CH_3), 2.23 (s, 9H, Ar-CH_3), 5.52 (s, 6H, Ar-CH_2), 5.73 (q, 3H, *J*=6.8 Hz, CH), 7.34-7.41 (m, 15H, Ar-H), 7.43 (s, 3H, NCHCH), 7.81 (s, 3H, NCHCH), 9.19 (s, 3H, NCHN).

^{13}C NMR (DMSO-d_6) δ (ppm): 16.46 (Ar-CH_3), 20.64 (CH_3), 48.13 (Ar-CH_2), 59.15 (CH), 121.55 (NCC), 122.58 (NCC), (126.71, 129.17, 129.42, 129.51) (Ar-C), 135.28 (Ar-CH_3), 139.54 (NCN), 141.43 (Ar-CH_2).

^{31}P (DMSO-d_6) δ (ppm): -129.86, -134.25, -138.65, -143.04, -147.43, -151.83, -156.25.

^{19}F (DMSO-d_6) δ (ppm): -69.54, -71.43.

IR (KBr) *v* (cm^{-1}), 3160, 3104, 3036, 2991, 2947, 2892, 2366, 1605, 1552, 1498, 1425, 1389, 1148, 1111, 838, 777, 741, 705.

Elemental analysis: calcd. For $C_{45}H_{51}N_6P_3F_{18}$ (1110.84): C, 48.65; H, 4.63; N, 7.56%. Found: C, 48.10; H, 4.54; N, 7.51%.

1,3,5-Tris[((S)-1-(2-Naphthyl)ethylimidazolium)methyl]2,4,6-trimethyl-benzene tri(hexafluorophosphate) (156d)

The general procedure was used with starting materials of trisbromide salt **(155d)** (50 g, 0.46 mmol) and hexafluorophosphate salt (0.22 g, 1.40 mmol) to give 0.47g white powder of (80% yield), m.p. 190-192 °C, $[\alpha]_D^{25}$ = -165° (CH_3CN).

^{1}H NMR (CD_3CN) δ (ppm): 1.94 (d, 9H, *J*=10.4 Hz, CH_3), 2.16 (s, 9H, Ar-CH_3), 5.43 (s, 6H, Ar-CH_2), 5.87 (q, 3H, *J*=6.8 Hz, CH), 7.25 (s, 3H, NCHCH), overlapping (7.41, 7.54, 7.90) (m, 24H, Ar-H, NCHCH), 8.70 (s, 3H, NCHN).

^{13}C NMR (CD_3CN) δ (ppm): 15.63 (Ar-CH_3), 19.69 (CH_3), 48.00 (Ar-CH_2), 59.40 (CH), 120.96 (NCC), 122.09 (NCC), (123.87, 125.83, 126.63, 126.72, 12.34, 127.75, 128.68, 132.75, 132.86) (Ar-C), 134.32 (Ar-CH_3), 135.58 (NCN), 141.59 (Ar-CH_2).

^{32}P (DMSO-d_6) δ (ppm): -134.25, -138.65, -143.04, -147.43, -151.82.

^{19}F (DMSO-d_6) δ (ppm): -69.53, -71.42

IR (KBr) ν (cm^{-1}): 3158, 3103, 3058, 2990, 2946, 2856, 2370, 1603, 1551, 1509, 1454, 1421, 1389, 1146, 1109, 843, 774, 755, 741.

Elemental analysis: calcd.for $C_{57}H_{57}N_6P_3F_{18}$ (1261.02): C, 54.28; H, 4.56; N, 6.66%. Found: C, 54.04; H, 4.52; N, 6.65%.

1,3,5-Tris[((S)-1-(2-hexyl)ethylimidazolium)methyl]2,4,6-trimethylbenzene-tri(hexafluorophosphate) (156e)

The general procedure was used with starting materials of trisbromide salt **(155e)** (0.50 g, 0.53 mmol) and hexafluorophosphate salt (0.26 g, 1.60 mmol) to give 0.33g white powder of (55% yield), m.p. 182-184 °C, $[\alpha]_D^{25}$ = - 81° (CH_3CN).

^1H NMR (CD_3CN) δ (ppm): overlapping 0.72-1.15 (m, 18H, hexyl-CH), 1.45 (d, 9H, J=6.8 Hz, CH_3), 1.52 (s(broad), 6H, hexyl-CH), 1.68 (m, 9H, hexyl-CH), 2.32 (s, 9H, Ar-CH_3), 4.25 (q, 3H, J=8 Hz, CH), 5.65 (5, 6H, Ar-CH_2), 7.55 (s, 3H, NCHCH), 7.73 (s, 3H, NCHCH), 8.66 (s, 3H, NCHN).

^{13}C NMR (CD_3CN) δ (ppm): 16.03 (Ar-CH_3), 17.68 (CH_3), (25.64, 25.74, 25.92, 43.13) (hexyl-C), 48.66 (Ar-CH_2), 62.38 (CH), 121.24 (NCC), 123.12 (NCC), 129.68 (Ar-CH_3), 134.87 (NCN), 142.12 (Ar-CH_2).

^{19}F NMR (CD_3CN) δ (ppm): -71.66, -73.54.

^{31}P NMR (CD_3CN) δ (ppm): -134.49, -138.87, -143.24, -147.62, -151.99.

IR (KBr), ν (cm^{-1}): 3160, 3109, 2988, 2933, 2858, 2340, 1617, 1555, 1425, 1337, 1150, 827, 740, 662.

NMR Titration procedure:

A- Anion recognition

A 5×10^{-3} molar stock solution of each imidazolium hexafuolorophosphate salt was prepared by weighing out an accurate amount salt on an analytical balance and diluting to a volume of (10 ml) using deuterated acetonitrile. In to a series of clean glass NMR tubes approximately (0.50 ml) aliquots of these receptor stock solutions was transferred with the aid of a micropipette. Each aliquot was then subsequently treated with zero to five mole equivalents of the solid tetra ethyl or butylammonium salt of the anion being studied.

^{1}H NMR titration results of host (156a) with anions (Cl^-, Br^-, I^-, HSO_4^-, NO_3^-)

The first and second figure refer to host-guest ratio in moles, where the third figure would refer to chemical shift in (ppm) of the C-2 proton of the imidazolium ring.

Titration between host **(156a)** and chloride anion; ^{1}H NMR (CD_3CN) δ (ppm): NCHN; 1:0;8.30, 1:0.2;8.79, 1:0.4;9.20, 1:0.6;9.50, 1:0.80;9.78, 1:1;10.09, 1:2;10.32, 1:3;10.30, 1:4;10.30, 1:5;10.30.

Titration between host **(156a)** and bromide anion; ^{1}H NMR (CD_3CN) δ (ppm): NCHN; 1:0;8.30, 1:0.2;8.64, 1:0.4;9.07, 1:0.6;9.33, 1:0.8;9.67, 1:1;9.80, 1:2;9.96, 1:3;9.96, 1:4;9.97, 1:5;9.96.

Titration between host **(156a)** and iodide anion; ^{1}H NMR (CD_3CN) δ (ppm): NCHN: 1:0;8.30, 1:0.2;8.51, 1:0.4;8.73, 1:0.6;8.77, 1:0.8;8.86, 1:1;8.92, 1:2;8.93, 1:3;8.92, 1:4;8.92, 1:5;8.92.

Titration between host **(156a)** and hydrogen sulfate anion; ^{1}H NMR (CD_3CN) δ (ppm); NCHN; 1:0;8.30, 1:0.2;8.39, 1:0.4;8.51, 1:0.6;8.58; 1:0.8;8.64, 1:1;8.70, 1:2;8.83, 1:3;8.85, 1:4;8.85, 1:5;8.86.

Titration between host **(156a)** and nitrate anion; ^{1}H NMR (CD_3CN) δ (ppm); NCHN; 1:0;8.30, 1:0.2;8.43, 1:0.4;8.59, 1:0.6;8.73, 1:0.8;8.87, 1:1;8.95, 1:2;9.12, 1:3;9.15, 1:4;9.17, 1:5;9.18.

^{1}H NMR titration results of host (156b) with anions (Cl^-, Br^-, I^-, HSO_4^-, NO_3^-)

Titration between host **(156b)** and chloride anion; ^{1}H NMR (CD_3CN) δ (ppm); NCHN; 1:0;8.27, 1:0.2;8.70, 1:0.4;9.03, 1:0.6;9.36, 1:0.8;9.63, 1:1;9.93, 1:2;10.15, 1:3;10.16, 1:4;10.15, 1:5;10.16.

Titration between host **(156b)** and bromide anion; ^{1}H NMR (CD_3CN) δ (ppm); NCHN; 1:0;8.26, 1:0.2;8.66, 1:0.4;8.96, 1:0.6;9.21, 1:0.8;9.52, 1:1;9.74, 1:2;9.86, 1:3;9.87, 1:4;9.88, 1:5;9.89.

Titration between host **(156b)** and iodide anion; ^{1}H NMR (CD_3CN) δ (ppm); NCHN; 1:0;8.27, 1:0.2;8.49, 1:0.4;8.52, 1:0.6;8.55, 1:0.8;8.57, 1:1;8.60, 1:2;8.69, 1:3;8.74, 1:4;8.78, 1:5;8.81.

Titration between host **(156b)** and sulfate anion; ^{1}H NMR (CD_3CN) δ (ppm); NCHN; 1:0;8.27, 1:0.2;8.36, 1:0.4;8.44, 1:0.6;8.51, 1:0.8;8.73, 1:1;8.82, 1:2;8.97, 1:3;9.00, 1:4;9.02, 1:5;9.03.

Titration between host **(156b)** and nitrate anion; ^{1}H NMR (CD_3CN) δ (ppm); NCHN; 1:0;8.27, 1:0.2;8.41, 1:0.4;8.54, 1:0.6;8.65, 1:0.8;8.73, 1:1;8.82, 1:2;8.97, 1:3;9.00, 1:4;9.02, 1:5;9.03.

^{1}H NMR titration results of host (156c) with anions (Cl^-, Br^-, I^-, NO_3^-)

Titration between host **(156c)** and chloride anion; ^{1}H NMR (CD_3CN) δ (ppm); NCHN; 1:0;8.58, 1:0.2;9.28, 1:0.4;9.65, 1:0.6;9.86, 1:0.8;10.16, 1:1;10.18, 1:2;10.28, 1:3;10.30, 1:4;10.32, 1:5;10.33.

Titration between host **(156c)** and bromide anion; ^{1}H NMR (CD_3CN) δ (ppm); NCHN; 1:0;8.58, 1:0.2;9.17, 1:0.4;9.46, 1:0.6;9.65, 1:0.8;9.78, 1:1;9.84, 1:2;9.93, 1:3;9.97, 1:4;9.98; 1:5;9.99.

Titration between host **(156c)** and iodide anion; ^{1}H NMR (CD_3CN) δ (ppm); NCHN; 1:0;8.58, 1:0.2;8.61, 1:0.4;8.63, 1:0.6;8.65, 1:0.8;8.67, 1:1;8.69, 1:2;8.76, 1:3;8.81, 1:4;8.84, 1:5;8.86.

Titration between host **(156c)** and nitrate anion: ^{1}H NMR (CD_3CN) δ (ppm); NCHN; 1:0;8.58, 1:0.2;8.66, 1;0.4;8.68, 1:0.6;8.69, 1:0.8;8.71, 1:1;8.72, 1:2;8.77, 1:3;8.80, 1:4;8.83, 1:5;8.84.

^{1}H NMR titration results of host (156d) with anions (Cl^-, Br^-, I^-, NO_3^-)

Titration between host **(156d)** and chloride anion; ^{1}H NMR (CD_3CN) δ (ppm); NCHN; 1:0;8.73, 1:0.2;9.45, 1:0.4;9.84, 1:0.6;10.11, 1:0.8;10.26, 1:1;10.31, 1:2;10.37, 1:3;10.4, 1:4;10.41, 1:5;10.42.

Titration between host **(156d)** and bromide anion; ^{1}H NMR (CD_3CN) δ (ppm); NCHN; 1:0;8.73, 1:0.2;9.28, 1:0.4;9.66, 1:0.6;9.86, 1:0.8;9.94, 1:1;9.97, 1:2;10.02, 1:3;10.04, 1:4;10.05, 1:5;10.07.

Titration between host **(156d)** and iodide anion; ^{1}H NMR (CD_3CN) δ (ppm); NCHN; 1:0;8.73, 1:0.2;8.77, 1:0.4;8.87, 1:0.6;8.98, 1:0.8;9.07, 1:1;9.12, 1:2;9.30, 1:3;9.37, 1:4;9.40, 1:5;9.43.

Titration between host **(156d)** and nitrate anion; ^{1}H NMR (CD_3CN) δ (ppm); NCHN; 1:0;8.73, 1:0.2;8.94, 1:0.4;9.07, 1:0.6;9.21, 1:0.8;9.29, 1:1;9.35, 1:2;9.43, 1:3;9.44, 1:4;9.44, 1:5;9.45.

B- Enantiomeric selectivity

A 2×10^{-2} molar stock solution for each of the four homochiral imidazolium hexafluorophosphate salts **(156a-d)** in deuterated acetonitrile was prepared. For each salt four ^{1}H NMR experiments were run. To four equal aliquots of the stock solution, no chiral anion, (R)-2-aminopropionate anion, (S)-2-aminopropionate anion, and both (R) and (S)-2-aminopropionate anion were added in 1:1 ratio (1:1:1 for the racemic mixture), the anions being dissolved in deuterated water.

2-Aminopropionate: ^{1}H NMR ($CDCl_3$) δ (ppm): 1.36 (d, 3H, *J*=7.2 Hz), 3.62 (q, 1H, *J*=7.2 Hz).

(S)-2-Aminopropionate in host **(156a)**: ^{1}H NMR ($CDCl_3$) δ (ppm): 1.40 (d, 3H, *J*=7.2, CH_3), 3.64 (q, 1H, *J*=7.2, CH)

(R)-2-Aminopropionate in host **(156a)**: ^{1}H NMR ($CDCl_3$) δ (ppm): 1.40 (d, 3H, *J*=7.2, CH_3), 4.40 (broad, 1H, CH).

(S) and (R)-2-Aminopropionate in Host **(156a)**: ^{1}H NMR ($CDCl_3$) δ (ppm): 1.40 (d, 3H, *J*=7.2, CH_3), 3.64 (q, 1H, *J*=7.2, CH), 4.40 (broad, 1H, CH).

Antimicrobial activities experimental procedure [189]

A number of homochiral imidazolium salts **(156a-d)** and compound **(152a)** and **(159)** were screened for its antibiotic capabilities against a *Pseudomonas aeruginosa* strain (Gram-negative bacterium) and a *Candida albicans* strain (yeast). The Compounds were dissolved in MeOH or DMSO and were then added to the wells of microtiter plates at a range of concentrations (25 μg/ml, 50 μg/ml, 75 μg/ml, 100 μg/ml, 250 μg/ml and 500 μg/ml). The microtiter plates used were polystyrene with round bottoms. Microbial strain were grown overnight in Mueller-Hinton broth (bacterial strains) or Sabouraud Liquid medium (fungal strains) and (2 ml) of the overnight cultures added to 98 mls of sterile medium. 200μl of the resultant broths was added to the wells of the plates and plates inoculated for 24 h at 37 °C (*P. aeruginosa*) and 25 °C (*Y. lypolytica, C. albicans*). Growth of the organism was measured at OD 595nm using a plate reader.

1,3,5-Tris[((S)-1-(2-phenyl)ethylimidazole-2-ylidene)methyl]2,4,6-trimethyl-benzene(164)

The imidazolium salt **(155c)** (0.10 g, 0.10 mmol) and NaH (0.07 g, 0.30 mmol) were mixed in THF (15 ml) and stirred for 5 minutes to ensure good mixing. Then *tert*-BuOK (0.02 g, 0.16 mmol) was added to the reaction mixture at room temperature. The colour became gradually pale yellow. After 45 minutes the reaction mixture was filtered through celite® and washed with toluene under nitrogen. The volatiles were removed under vacuum to give a yellow solid.

Yield 0.04g (55%).

^{1}H NMR (DMSO-d_6) δ (ppm): 2.32 (d, H, J=7.2 Hz, CH_3), 2.69 (s, H, Ar-CH_3), 3.01 (s, 6H, Ar-CH_2), 4.36 (q, 3H, J=5.2 Hz, CH), overlapping 7.12-7.44 (m, 17H, Ar-CH, NC<u>H</u>CH, NCHC<u>H</u>).

^{13}C NMR (DMSO-d_6) δ (ppm): 15.73 (Ar-CH_3), 21.05 (CH_3), 41.41 (Ar-CH_2), 61.00 (CH), 125.31 (N<u>C</u>C), (128.15, 128.64, 130.2, 132.90) (Ar-C), 136.18 (Ar-CH_3), 137.33 (NC<u>C</u>), 160.56 (NCN).

1,3,5-Tris[((R)-3-methyl-2-butylimidazole-2-ylidene)methyl]2,4,6,-trimethyl-benzene (165a)

To a solution of **(155b)** salt (0.15 g, 0.18 mmol) in THF:Acetonitrile (4 ml), was added potassium *tert*-BuOK (0.06 g, 0.58 mmol) in a single portion under argon for 2 h at room temperature and the colour changed to orange with time. The reaction mixture was then washed with dried toluene (2×10 ml) and filtered through celite®, under nitrogen. The solvent was removed and 0.52g (50%) of a yellow solid was collected.

^{1}H NMR (CD_3CN) δ (ppm): 0.62 (d, 9H, CH_3), 0.82 (d, 9H, CH_3), 1.18 (s, 9H, Ar-CH_3), 1.36 (d, 9H, CH_3), 1.65 (m, 3H, CH), 4.60 (m, 3H, CH), 5.62 (m, 6H, Ar-CH_2), 6.78 (s, 3H, NC<u>H</u>CH), 6.97 (s, 3H, NCHC<u>H</u>).

^{13}C NMR (CD_3CN) δ (ppm): overlapping 16.71-18.64 (Ar-CH_3, CH_3, CH_3, CH_3), 33.50 (CH), 48.06 (Ar-CH_2), 59.93 (CH), 124.90 (NCC), 127.86 (NCC), 128.55 (Ar-CH_3), 158.34 (Ar-CH_2), 162.62 (NCN).

1,3,5-Tris[((R)-3-methyl-2-butylimidazole-2-ylidene)methyl]2,4,6-trimetyl-benzene via NaOMe (165b)

Sodium methoxide (0.030 g, 0.58 mmol) dissolved in dried methanol (3 ml) and was slowly added to a solution of homochiral tripodal imidazolium salt **(155b)** (0.11 g, 0.18 mmol) in methanol (5 ml). The reaction mixture was stirred overnight. Methanol was removed under reduced pressure at ambient temperature. A brown oil was collected (0.04 g, 63 %), and stored under N_2.

^1H NMR ($CDCl_3$) δ (ppm): 0.65 (d, 9H, *J*=6.4 Hz, CH_3), 0.89 (d, 9H, *J*=6.4 Hz, CH_3), 1.44 (d, 9H, *J*=6.8 Hz, CH_3), 1.90 (m, 3H, CH), 2.26 (s, (H, Ar-CH_3), 4.60 (q, 3H, *J*=7.2 Hz, CH), 5.80 (s, 6H, Ar-CH_2), 8.51 (s, 3H, NCHCH).

^{13}C NMR ($CDCl_3$) δ (ppm): 17.82 (Ar-CH_3), 18.69 (CH_3), 19.14 (CH_3), 19.24 (CH_3), 34.73 (CH), 49.48 (Ar-CH_2), 62.36 (CH), 119.69 (NCC), 124.82 (NCC), 135.93 (Ar-CH_2), 142.39 (Ar-CH_3), 207.37 (NCN).

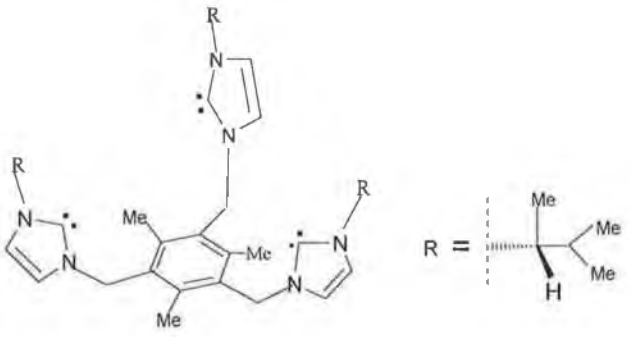

165b

1,3,5-Tris[((R)-3-methyl-2-butylimidazole-2-ylidene)methyl]2,4,6-trimethyl benzene-Zinc(II) complex (166)

To a solution of homochiral tridentate carbene **(165b)** (0.02g, 0.024 mmol) and sodium methoxide (4.20×10^{-2} g, 0.078 mmol) in methanol, zinc bromide solution (6.60×10^{-3}g, 0.03 mmol) was added and a white turbid colour formed immediately. The reaction was allowed to stir for an additional 2 h and the reaction mixture was filtered under nitrogen and dried, leaving a white precipitate, yield 0.04g (55%).

^{1}H NMR (Acetone-d_6) δ (ppm): 0.75 (d, 9H, *J*=6.4 Hz, CH_3), 0.98 (d, 9H, *J*=6.4 Hz, CH_3), 1.56 (d, 9H, *J*=6.8 Hz, CH_3), 2.12 (m, 3H, CH), 2.41 (s, 9H, Ar-CH_3), 4.65 (m, 3H, CH), 5.78 (s, 6H, Ar-CH_2), 7.88 (s, 3H, NC<u>H</u>CH), 7.94 (s, 3H, NCHC<u>H</u>).

^{13}C NMR (Acetone-d_6) δ (ppm): 17.24 (Ar-CH_3), 18.67 (CH_3), 19.41 (CH_3), 19.47 (CH_3), 35.27 (CH), 48.40 (Ar-CH_2), 63.50 (CH), 121.95 (N<u>C</u>C), 124.51 (NC<u>C</u>), 130.53 (Ar-CH_3), 143.30 (Ar-CH_2), 170.42 (N-C-Zn).

1,3,5-Tris[((R)-3-methyl-2-butylimidazole-2-ylidene)methyl]2,4,6-trimethyl-benzene-Furious(II) complex (167)

Same procedure as that used for the preparation of **(166)** with starting material of trisbromide salt **(155b)** (0.06 g, 0.073 mmol), sodium methoxide (1.19×10^{-2} g, 0.22 mmol) and iron bromide (1.59×10^{-2} g, 0.073 mmol) to give 0.05g red solid of (65 % yield).

^{1}H NMR (Acetone-d_6) δ (ppm): 0.85 (d, 9H, CH_3), 1.10 (d, 9H, CH_3), 1.31 (s, 9H, Ar-CH_3), 1.65 (d, 9H, CH_3), 4.68 (m, 3H, CH), 5.75 (s, 6H, Ar-CH_2), 7.89 (s, 3H, NC<u>H</u>CH), 7.90 (s, 3H, NCHC<u>H</u>).

^{13}C NMR (Acetone-d_6) δ (ppm): 16.04 (Ar-CH_3), 17.66 (CH_3), 18.44 (CH_3), 34.35 (CH), 53.07 (Ar-CH_2), 63.50 (CH), 117.43 (NCC), 121.06 (NCC), 129.53 (Ar-CH_3), 135.61 (Ar-CH_2), 168.87 (N-C-Fe).

General procedure of the synthesis of *N*-Heterocyclic-2-ylidene-silver compounds

To a solution of a homochiral tripodal imidazolium salt **(155a)** (0.03g, 1 mmol) in DCM (5 ml) was added Ag_2O (0.013 g, 1.5 mmol). The reaction mixture was stirred at 20 °C until the precipitate disappeared (8-20 h), the reaction mixture was then filtered through celite® and the filtrate was concentrated to (3 ml). Addition of (20 ml) ether afforeded a creamy white solid, which was then washed with (3×10 ml) ether and dried under vacuum.

1,3,5-Tris[N-((-)-cis-myrtanylimidazol-2-ylidene-silverbromide)methyl]2,4,6-trimethylbenzene complex (169)

The general procedure was used to give 0.05g of a creamy powder (94% yield).

^{1}H NMR ($CDCl_3$) δ (ppm): 0.79 (d, H, *J*=9.6 Hz, CH), 1.06 (s, 9H, CH_3), 1.11 (s, 9H, CH_3), 1.46 (m, 3H, CH), overlapping 1.69-1.88 (m, 15H, 2CH_2, CH), 2.20 (s, 9H, Ar-CH_3), 2.42 (m, 3H, CH), 2.45 (m, 3H, CH), 3.96 (d, 6H, *J*=7.2 Hz, CH_2), 5.29 (s, 6H, Ar-CH_2), 6.91 (s, 3H, NCHCH), 7.12 (s, 3H, NCHCH).

^{13}C NMR (DMSO-d_6) δ (ppm): 17.88 (CH_3), 19.77 (CH_3), 24.22 (CH_3), 26.12 (CH_2), 28.23 (CH_2), 33.44 (CH_2), 39.15 (CH_2), 41.55 (CH_2), 43.29 (CH), 50.75 (CH), 58.24 (CH), 121.53 (NCC), 122.45 (NCC), 131.88 (Ar-CH_3), 140.17 (Ar-CH_2), 180.13 (N-C=Ag).

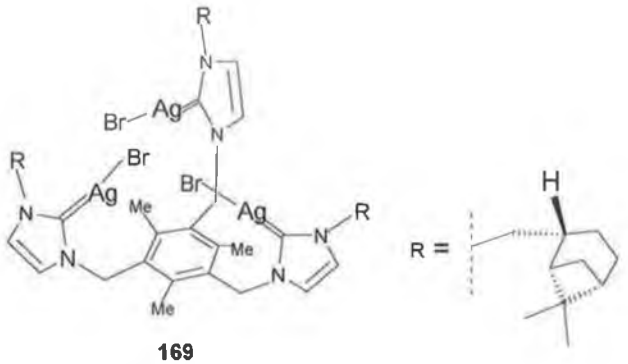

169

1,3,5-Tris[((R)-3-methyl-2-butylimidazol-2-ylidene-silverbromide)methyl]-2,4,6-trimethylbenzene complex (170)

The general procedure was used with starting materials of trisbromide salt **(155b)** (0.20 g, 0.24 mmol) and Ag_2O (8.54×10^{-2} g, 0.36 mmol) to give 2.26g of a creamy powder (81% yield).

^{1}H NMR (DMSO-d_6) δ (ppm): 0.55 (d, 9H, J= 6.4 Hz, CH_3), 0.95 (d, 9H, J=6.4 Hz, CH_3), 1.40 (d, 9H, J=6.8 Hz, CH_3), 1.98 (m, 3H, CH), 2.25 (s, 9H, Ar-CH3), 4.00 (m, 3H, CH), 5.48 (s, 6H, Ar-CH_2), 7.37 (s, 3H, NCHCH), 7.54 (s, 3H, NCHCH).

^{13}C NMR (DMSO-d_6) δ (ppm): 16.90 (Ar-CH_3), 19.51 (CH_3), 19.68 (CH_3), 19.82 (CH_3), 35.10 (CH), 49.50 (Ar-CH_2), 65.25 (CH), 119.88 (NCC), 123.91 (NCC), 133.25 (Ar-CH_3), 139.10 (Ar-CH_2), 178.82 (N-C=Ag).

M.S. (m/z ion); (m/z 1135.40-H^+, Na), (m/z 1004-H_2O) and (m/z 929).

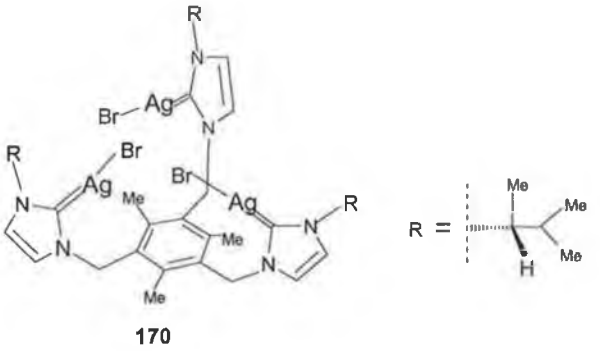

170

1,3,5-Tris[((S)-1-(2-phenyl)ethylimidazol-2-ylidene-silverbromide)methyl] 2,4,6-trimethylbenzene complex (171)

The general procedure was used with starting material of trisbromide salt **(155c)** (0.10 g, 0.10 mmol) and Ag_2O (3.81×10^{-2} g, 0.16 mmol) to give 0.11g of a creamy powder (81% yield).

^{1}H NMR ($CDCl_3$) δ (ppm): 1.74 (d, 9H, *J*=13.6 Hz, CH_3), 2.21 (d, 9H, *J*=14.4 Hz, Ar-CH_3), 5.28 (s, 6H, Ar-CH_2), 5.63 (q, 3H, *J*=6.8 Hz, CH), 6.88 (s, 3H, NCHCH), 7.09 (s, 3H, NCHCH), overlapping 7.14-7.25 (m, 15H, Ar-CH).

^{13}C NMR ($CDCl_3$) δ (ppm): 18.01 (Ar-CH_3), 21.90 (CH_3), 50.84 (Ar-CH_2), 61.69 (CH), 118.87 (NCC), 122.71 (NCC), (126.91, 128.79, 129.38, 131.86) (Ar-C), 140.16 (Ar-CH_3), 140.44 (Ar-CH_2), 180.52 (N-C=Ag).

M.S. (m/z ion); (1235.90-H^+).

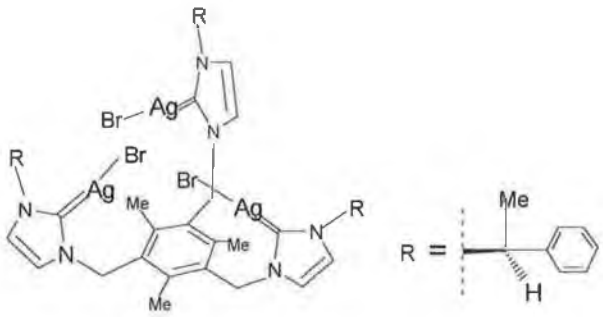

171

1,3,5-Tris[((S)-1-(2-hexyl)ethylimidazol-2-ylidene-silver(I)bromide)methyl]-2,4,6-trimethylbenzene complex (173)

The general procedure was used with starting material of trisbromide salt **(168)** (0.10 g, 0.10 mmol) and Ag_2O (3.72×10^{-2} g, 0.16 mmol) to give 0.11g of a creamy powder (81% yield).

^{1}H NMR ($CDCl_3$) δ(ppm): overlapping 0.70-1.80 (m, 33H, hexyl-CH), 1.33 (d, 9H, *J*=6.8 Hz, CH_3), 2.20 (s, 9H, Ar-CH_3), 4.10 (m, 3H, CH), 5.29 (s, 6H, Ar-CH_2), 6.89 (s, 3H, NCHCH), 7.14 (s, 3H, NCHCH).

^{13}C NMR ($CDCl_3$) δ (ppm): 17.83 (Ar-CH_3), 19.95 (CH_3), (26.12, 26.21, 26.26, 30.21) (hexyl-C), 50.75 (Ar-CH_2), 64.67 (CH), 118.33 (Ar-CH_3), 122.70 (Ar-CH_2), 131.86 (NCC), 140.14 (NCC), 179.45 (NCN).

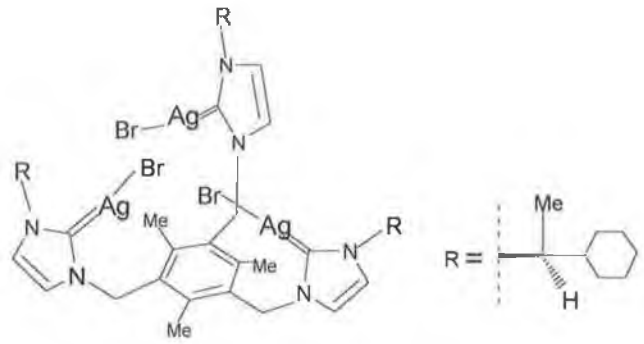

173

Preparation of ruthenium tetra-dimethyl sulfoxide dibromide (174)

Ruthenium tribromide (0.2 g, 0.58 mmol) was placed in a one neck round bottom flask in DMSO (2 ml) and the colour turned dark red. The reaction mixture was heated to 160 °C for 5 minutes until the reaction mixture turned to a clear red solution. The resulting solution was cooled down to 50 °C and higher vacuum was applied to reduce the volume by half. Acetone was then added which yielded a yellow precipitate. This was washed several times with acetone and dried under vacuum, yield 0.17g (60%).

^{1}H NMR ($CDCl_3$) δ (ppm): 2.74 (s, 6H, $2CH_3$), 3.33 (s, 6H, $2CH_3$), 3.50 (s, 6H, $2CH_3$), 3.53 (s, 6H, $2CH_3$).

^{13}C NMR ($CDCl_3$) δ (ppm): 39.25 ($2CH_3$), 44.69 (CH_3), 44.84 (CH_3), 47.05 ($2CH_3$), 48.07 ($2CH_3$).

1,3-Myratanyl methyl imidazolium iodide salt (159)

To a solution of myratanyl imidazole (0.15 g, 0.73 mmol) in 1,4-dioxane (5 ml), methyl iodide (0.114 g, 0.80 mmol) was added. The reaction mixture was stirred for 2 h and a precipitate appeared. The precipitate was collected and washed with ether (3×10 ml) to removed any remaning starting material. Solvent was removed by vacuum, leaving a dark brown oil, yield 0.245g (98%), $[\alpha]_D^{25}$ = - 24° (CH_2Cl_2).

^{1}H NMR ($CDCl_3$) δ (ppm): 0.95 (d, 3H, *J*=9.60 Hz, CH), 1.10 (s, 9H, CH_3), 1.21 (s, 9H, CH_3), 1.55 (m, 3H, CH), overlapping 1.84-2.01 (m, 5H, CH_2CH_2CH), 2.37 (m, 3H, CH), 2.62 (m, 3H, CH), 4.13 (s, 9H, CH_3), 4.20 (m, 6H, CH_2), 7.37 (s, 3H, NCHCH), 7.56 (s, 3H, NCHCH), 9.97 (s, 3H, NCHN).

^{13}C NMR ($CDCl_3$) δ (ppm): 19.64 (CH_3), 24.01 (CH_3), 25.84 (CH_3), 28.11 (CH_2), 33.08 (CH_2), 37.57 (CH_2), 39.02 (CH_2), 41.30 (CH), 42.11 (CH), 43.4 (CH), 55.82 (C), 122.71 (NCC), 124.12 (NCC), 137.24 (NCN).

IR (neat) *v* (cm^{-1}): 3140, 3100, 2990, 2950, 2910, 2340, 1630, 1610, 1500, 1470, 1450, 1410, 1380, 1200, 710.

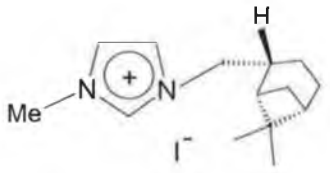

159

1,3-myrtanylmethylimidazole-2-ylidene-silver(II) complex (178)

To a solution of 1,3-myratanylmethylimidazolium iodide salt (0.10 g, 0.28 mmol) in DCM (5 ml), was added Ag_2O (0.334 g, 0.14 mmol). The mixture was stirred until all the Ag_2O dissolved. The colourless solution was then filtered and concentrated to (3 ml). The white creamy solid was afforded by the addition of ether (20 ml) and then dried under vacuum, yielding 0.122g (90%).

^{1}H NMR ($CDCl_3$) δ (ppm): 0.84 (d, H, *J*=9.60 Hz, CH), overlapping 1.77-1.85 (m, 5H, CH_2CH_2CH), 2.25 (m, H, CH), 2.52 (m, H, CH), 3.83 (s, 3H, CH_3), 4.05 (m, 2H, CH_2), 6.93 (s, H, NCHCH), 7.04 (s, H, NCHCH).

^{13}C NMR ($CDCl_3$) δ (ppm): 17.20 (CH_3), 19.81 (CH_3), 24.03 (CH_3), 26.12 (CH_2), 28.26 (CH_2), 33.40 (CH_2), 39.10 (CH_2), 39.54 (CH), 41.50 (CH), 43.35 (CH), 57.93 (C), 121.76 (NCC), 122.97 (NCC), 182.52 (NCN).

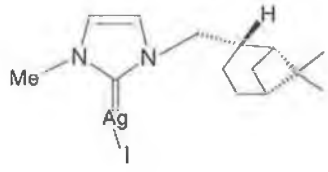

178

[1,3-mratanylmethylimidazol-2-ylidene]$_2$-Pd(II) di-iodide complex (179)

To a solution of 1,3-myratanylmethylimidazolium iodide salt **(159)** in (20 ml) THF (0.1 g, 0.28 mmol), palladium acetate was added (0.032 g, 0.14 mmol) and the reaction mixture turned dark brown immediately. The solution was stirred under reflux until which time the colour turned a light brown. The solvent was removed under vacuum and the residue was washed (2×10 ml) with ether and (3×10 ml) with acetonitrile to leave a very clear yellow solid palladium complex. Yield 0.57g (50%).

^{1}H NMR ($CDCl_3$) δ (ppm): 0.92 (d, 2H, *J*=9.6 Hz, CH), 1.10 (s, 6H, CH_3), 1.18 (s, 6H, CH_3), 1.64 (m, 2H, CH), overlapping 1.80-1.94 (m, 10H, CH_2CH_2CH), 2.30 (m, 2H, CH), 3.20 (m, 2H, CH), 3.87 (s, 6H, CH_3), 4.15 (m, 2H, CH(geminal)), 4.36 (m, 2H, CH(geminal)), 6.78 (s, 4H, NCHCH).

^{13}C NMR ($CDCl_3$) δ (ppm): 20.04 (CH_3), 24.05 (CH_3), 26.18 (CH_3), 28.26 (CH_2), 33.60, (CH_2), 38.94 (CH_2), 39.11 (CH_2), 41.22 (CH), 41.68 (CH), 43.94 (CH), 57.23 (C), 121.93 (NCC), 122.34 (NCC), 168.01 (NCN).

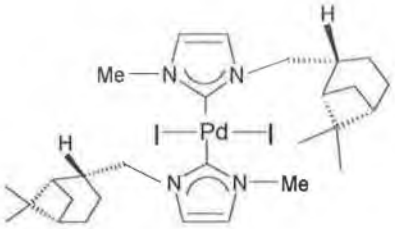

179

Cross coupling (Heck-olefination) between bromo benzaldehyd and butyl acrylate producing (181)

General procedure :

In a (100 ml) three-necked round bottom flask fitted with a reflux condenser was placed aryl halide (5.40 mmol, 1 g), anhydrous sodium acetate (0.57 g, 7.02 mmol), diethyleneglycol di-*n*-butyl ether (0.15g), *N*,*N*-butylacrylate (11.08 ml, 7.50 mmol). The reaction mixture was vigorously stirred and heated to the appropriate reaction temperature (100 °C in this case) and catalyst was added (0.02 g, 0.50 % mol). The reaction mixture was then heated to 125 °C for 12 h and was then cooled to room temperature. The product was poured onto water and extracted with DCM (10×50 ml) and dried over magnesium sulphate. After removal of the DCM and *N*,*N*-dimethyl acetamide by vacuum pump, the crude products was purified by column chromatography (1:4) Ether:Petroleum ether as eluant, giving white crystals, yield 1.13g (90%).

^{1}H NMR ($CDCl_3$) δ (ppm): 0.98 (m, 3H, CH_3), 1.45 (m, 2H, CH_2), 1.71 (m, 2H, CH_2), 4.24 (m, 2H, CH_2), 6.57 (d, H, *J*=16.4 H, CH), 7.68-7.73 (m, 3H, Ar-CH, CH), 7.91 (d, 2H, *J*=6.8 Hz, Ar-CH), 10.04 (s, H, CHO).

^{13}C NMR ($CDCl_3$) δ (ppm): 14.13 (CH_3), 19.57 (CH_2), 31.10 (CH_2), 65.15 (CH_2), (121.88, 128.89, 130.56, 143.19) (Ar-C), 137.50 (CH=C<u>H</u>), 140.53 (C<u>H</u>=CH), 166.85 (COH), 191.86 (CO_2).

Cross coupling (Heck-olefination) between bromobenzaldehyde and 1,2-heptene producing (182)

Same as the general procedure but 1,2-heptene (1.06g, 10.80 mmol) was used in 2 molar ratio for 14 h, at 125 °C, yield 0.175g (15%).

^{1}H NMR ($CDCl_3$) δ (ppm): 0.83 (CH_3), overlapping 1.15-1.51 (m, 6H, CH_2CH_2 CH_2), 2.19 (s, 2H, CH_2), 6.38 (s, H, CH), 7.40 (d, 2H, Ar-CH_2), 7.52 (d, 2H, Ar-CH), 9.98 (s, H, CHO).

^{13}C NMR ($CDCl_3$) δ (ppm): 14.44 (CH_3), 22.93 (CH_2), 29.17 (CH_2), 31.83 (CH_2), 33.59 (CH_2), 53.87 (CH), (126.72, 129.28, 130.20, 135.84) (Ar-C), 144.47 (CH), 192.28 (CHO).

Cross coupling (Heck-olefination) between bromo benzaldehyde and 2,3-di-hydrofuran

Same general procedure was used with a 3 molar excess of 2,3-dihydrofuran (1.13g,16.20 mmol) for 12 h at 80°C. Compounds **(183-186)** yield 0.10g (7%). ^{1}H NMR ($CDCl_3$) δ (ppm): 2.77 (m, *J*=2.80 Hz, CH (geminal)), 3.34 (m, H, *J*= 2.80 Hz, CH (geminal)), 5.52 (t, 1H, CH), 5.75 (m, 1H, CH), (7.50, 7.72, 7.84) (Ar-CH), 9.98 (s, H, CHO).

^{13}C NMR ($CDCl_3$) δ (ppm): 40.04 (CH_2), 82.25 (CH), 98.59 (CH), (126.01, 126.32, 130.30, 130.59) (Ar-C), 136.34 (Ar-(C)), 150.10 (Ar-(C)), 154.96 (Ar-(C)), 192.15 (CHO).

Bibliography

[1] H. Debus, *Liebigs Ann. Chem.*, **1858**, 107, 199.

[2] A. Hantzsch, *Liebigs Ann. Chem.*, **1888**, 249, 1.

[3] G. Wyss, *Ber.*, **1877**, 10, 1365.

[4] Reviews: *Nitroimidazoles*; *Chemistry, Pharmacology and Clinical Applications*, eds A. Breccia, B. Cavalleri, and G.E. Adams, Plenum Press, New York, **1982**; J. H. Boyer, *Nitrazoles*, VCH, Deerfield Beach, Florida, 1986.

[5] D.F. Shriver, M.J. Ballais, *J. Am. Chem. Soc.*, **1967**, 89, 1078.

[6] C.H. Park, H.E. Simmons, *J. Am. Chem. Soc.*, **1968**, 90, 2431.

[7] P.M. Quinton, *FASEB J.*, **1990**, 4, 2709.

[8] K. Renkawek, *Pollution*: *Causes, Effects and Control*, RSC, London, **1983**.

[9] P.D. Beer, P.A. Gale, *Angew. Chem. Int. Ed. Engl.* 2001, 40, 486.

[10] A. Bianchi, K. Bowman-James, E. Garcia-Espana, *Supramolecular Chemistry of Anions*, Wiley VCH, New York, **1997**.

[11] T.S. Snowden, E.V. Anslyn, *Curr. Opin. Chem. Biol*, **1999**, 3, 740.

[12] M.T. Reetz, C.M. Niemeyer, and K. Harms, *Angew. Chem. Int. Ed. Engl.*, **1991**, 30/11, 1472.

[13] S. Shinoda, M. Tadokoro, H. Tsukube, and R. Arkawa, *Chem. Commun.*, **1998**, 181.

[14] B. Dietrich, T.M. Fyles, J. M. Lehn, L.G. Pease, and D.L. Fyles, *Chem. Commun.*, **1978**, 934.

[15] B. Dietrich, M.W. Hosseini, J.M. Lehn, and R.B. Sessions, *J. Am. Chem. Soc.*, **1981**, 103, 1282.

[16] P.D. Beer and A.D. Keefe, *J. Organomet. Chem.*, **1989**, 375, C40.

[17] P.D. Beer, D. Hesek, J. Hodacova, S-E. Stokes, *J. Chem. Soc., Chem. Commun.*, **1992**, 270.

[18] P.D. Beer, D. Hesek, J.E. Kingston, D.K. Smith, S.E. Stokes, M.G.B. Drew, *Organometallics*, **1995**, 14, 3288.

[19] P.D. Beer, M.G.B. Drew, A. R. Graydon, D.K. Smith, S.E. Stokes, *J. Chem. Soc., Dalton Trans.*, **1995**, 403.

[20] P.D. Beer, A.R. Graydon, *J. Organomet. Chem.*, **1994**, 446. 241.

[21] M. Uno, N. Komatsuzaki, K. Shirai, S. Takahashi, *J. Organomet. Chem.*, **1993**, 462, 343.

[22] P.D. Beer, M.G.B. Drew, J. Hodacova, S.E. Stokes, *J. Chem. Soc., Dalton Trans.*, **1995**, 3447.

[23] P.D. Beer, S.E. Stokes, *Polyhedron*, **1995**, 14, 2631.

[24] P.D. Beer, M.G.B. Drew, D. Hesek, R. Jagessar, *J. Chem. Soc., Chem. Commun.*, **1995**, 1187.

[25] P.D. Beer, M.G.B. Drew, C. Hazlewood, D. Hesek, J. Hodocova, S.E. Stokes, *J. Chem. Soc., Chem Commun.*, **1993**, 229.

[26] P.D. Beer, M.G.B. Drew, D. Hesek, M. Shade, F. Szemes, *J. Chem. Soc., Chem. Commun.*, **1996**, 2161.

[27] P.D. Beer, *Acc. Chem. Res.*, **1998**, 31, 71.

[28] P.D. Beer, A.R. Graydon, A.O.M. Johnson, D.K. Smith, *Inorg. Chem.*, **1997**, 36, 2112.

[29] Z. Chen, A.R. Graydon, P.D. Beer, *J. Chem.* Soc., *Faraday Trans.*, **1996**, 92, 97.

[30] P.D. Beer, Z. Chen, A.R. Graydon, S.E. Stokes, T. Weer, *J. Chem. Soc., Chem. Commun.*, **1993**, 1834.

[31] P.A. Gale, Z. Chen, M.G.B. Drew, J.A. Heath, P.D. Beer, *Polyhedron*, **1998**, 17, 404.

[32] J.E. Kingston, L. Ashford, P.D. Beer, M.G.B. Drew, *J. Chem. Soc., Dalton Trans.*, **1999**, 251.

[33] P.D. Beer, Z. Chem, M.G.B. Drew, J. Kingston, M. Ogden, P. Spencer, *J. Chem. Soc., Chem. Commun.*, **1993**, 1046.

[34] P.D. Beer, Z. Chen, M.G.B. Drew, A.O.M, Johnson, D. K. Smith, P. Spencer, *Inorg. Chim. Acta*, **1996**, 246, 143.

[35] (a) J.-L. Thomas, J. Howarth, K. Hanlon, D. McGuirk, *Tetrahedron Lett.*, **2000**, 41, 413; (b) A. Dallas, Ph.D. Thesis, Dublin City University, Ireland, **2003**.

[36] K. Sato, S. Arai, T. Yamagishi, *Tetrahedron Lett.*, **1999**, 40, 5219.

[37] "AGRNMRL" programmed by Professor Emeritus M. Hida (T.M.U.).

[38] A.G. Avent, P.A. Chaloner, M.P. Day, K.R. Seddon, T. Welton, *J. Chem. Soc., Dalton Trans.*, **1994**, 3405-3413.

[39] A. Metzger, V.M. Lynch, E.V. Anslyn, *Angew. Chem. Int. Ed. Engl.*, **1997**, 36, 862.

[40] P.D. Beer, N.C. Fletcher, A. Grieve, J.W. Wheeler, C.P. Moore, T. Wear, *J. Chem. Soc. Perkin Trans. 2*, **1996**, 2, 1545.

[41] J.,Jr. Rebek, *Angew. Chem. Int. Ed. Engl.* 1990, 29, 245. and *Acc. Chem. Res.* **1990**, 23, 399.

[42] a) D.M. Kneeland, K. Ariga, V.M. Lynch, C.Y. Huang, E.V. Anslyn, *J. Am. Chem. Soc.* **1993**, 115, 10042; b) J. DeMendoza, A. Galan, C. Seel, *Top. Curr. Chem.* **1995**, 175, 101.

[43] K.A. Conners, *Binding constants, The Measurment of Molecular Complex Stability*, Wiley, New York, **1987**.

[44] P.N. Kale, P.G. Adsule in *Handbook of Fruit Science And Technology: Production, Composition, Storage, and Processing* (Eds: D.K. Salunke, S.S. Kadam), Marcel Dekker, New York, **1995**, Chapter 3.

[45] B.D. Dietrich, D.L. Fyles, T.M. Fyles, J.M. Lehn, *Helv. Chim. Acta.*, **1979**, 62, 2763.

[46] L.O. Abouderbala, W.J. Belcher, M.G. Boutelle, P.J. Cragg, J. Dhaliwal, M. Fabre, J.W. Steed, D.R. Turner, K.J. Wallace, *Chem. Commun.*, **2002**, 358.

[47] E.E. Simanek, S. Qiao, I.S. Choi, G.M. Whitesides, *J. Org. Chem.*, **1997**, 62, 2619.

[48] J. Sanchez-Quesada, C. Seel, P. Prados, J. deMendoza, I. Dalcol, E. Giralt, *J. Am. Chem. Soc.*, **1996**, 118, 277.

[49] J.,Jr. Rebek, C. Nuckolls, F. Hof, T. Martin, *J. Am. Chem. Soc.*, **1999**, 121, 10281.

[50] T. Martín, U. Obst, J.,Jr. Rebek, *Science*, **1998**, 281, 1842.

[51] S. Saito, C. Nuckolls, J.,Jr. Rebek, *J. Am. Chem. Soc.*, **2000**, 122, 9628.

[52] D.M. Rudkevich, J.,Jr. Rebek, *Eur. J. Org. Chem.*, **1999**, 1991.

[53] Y. Kikuchi, Y. Kato, Y. Tanaka, H. Toi, Y. Aoyama, *J. Am. Chem.* Soc., **1991**, 113, 1349.

[54] M. Vincenti, E. Dalcanale, P. Soncini, G. Guglielmetti, *J. Am. Chem.* Soc., **1990**, 112, 445.

[55] A. Shivanyuk, K. Rissanen, S. K. Konner, D. M. Rudkevich, J.,Jr. Rebek, *Helv. Chim. Acta,* In Press.

[56] J.M. Rivera, T. Martín, J.,Jr. Rebek, *Science,* **1998**, 279, 1021.

[57] C. Nuckolls, F. Hof, T. Martín, J.,Jr. Rebek, *J. Am. Chem. Soc.*, **1999**, 121, 10281.

[58] L. Pu, *Chem. Rev.*, **1998**, 98, 2405.

[59] *Comprehensive Asymmetric Catalysis*, E.N. Jacobesn, A. *Pfalts*, H. Yamamoto, Eds.; Springer: Heidelberg, **1999**.

[60] K. Tsubaki, H. Tanaka, T. Kinoshita, K. Fuji, *Tetrahedron*, **2002**, 58, 1679.

[61] K. Hu, J.S. Bradshaw, V.N. Pastushok, K.E. Krakowiak, N.K. Dalley, X.X. Zhang, R.M. Izatt, *J. Org. Chem.*, **1998**, 63, 4786.

[62] X.X. Zhang, J.S. Bradshaw, R. M. Izatt, *Chem. Rev.*, **1997**, 97, 3313.

[63] S. Nagayama, S. Kobayashi, *J. Am. Chem. Soc.*, **2000**, 122, 11531.

[64] Y. Kubo, S. Maeda, S. Tokita, M. Kubo. *Nature*, **1996**, 382, 522.

[65] R. Warmuth, J.-L. Kerdelhuè, S. Sànchez Carrera, K.J. Langenwalter, N. Brown, *Angew. Chem., Int. Ed.*, **2002**, 41, 96.

[66] H. Singh, R. Warmuth, *Tetrahedron*, **2002**, 58, 1257.

[67] J. Yoon, D.J. Cram, *Chem. Commun.*, **1998**, 497.

[68] E.L. Piatnitski, R.A. Flowers II, K. Deshayes, *Chem. Eur. J.*, **2000**, 6, 999.

[69] J.M. Rivera, T. Martin, J.,Jr. Rebek, *J. Am. Chem. Soc.*, **2001**, 123, 5213.

[70] J.K. Judice, D.J. Cram, *J. Am. Chem. Soc.* **1991**, 113, 2790.

[71] J.Yoon, D.J. Cram, *J. Am. Chem. Soc.*, **1997**, 119, 11796.

[72] B.S. Park, C. B. Knobler, Jr.,C.N. Eid, R. Warmuth, D.J. Cram, *Chem. Commun.*, **1998**, 55.

[73] S. Tsuzuki, K. Honda, T. Uchimaru, M. Mikami, K. Tanabe, *J. Am. Chem. Soc.*, **2000**, 122, 3746.

[74] R. Warmuth, *J. Am. Chem. Soc.*, **2001**, 123, 6955.

[75] C. Lynam, K. Jennings, K. Nolan, P. Kane, M. McKervey, D. Diamond, *Anal. Chem.*, **2002**, 74, 59.

[76] P.S. Skell, S.R. Sandler, *J. Am. Chem. Soc.*, **1958**, 80, 2024.

[77] a) E.O. Fischer, A. Maasböl, *Angew. Chem.*, **1964**, 76, 645; *Angew. Chem. Int. Ed. Engl.*, **1964**, 580; b) E.O. Fischer, *ibid.*, **1974**, 86. 651.

[78] *Applied Homogeneous Catalysis with Organometallic Complexes* (Eds.: B. Cornils, W.A. Herrmann), VCH, Weinheim, **1996**.

[79] R.H. Grubbs in *Comprehensive Organometallic Chemistry, Vol.* 8 (Eds.: G. Wilkinson, F.G.A. Stone, E. W. Abel), *Pergamon, Oxford*, **1982**, p. 499.

[80] M. Brookhart, W.B. Studabaker, *Chem. Rev.* **1987**, 87, 411.

[81] K.H. Dötz in *Organometallics in Organic synthesis* (Eds.: A. de Meijere, H. tom Dieck), Springer, Berlin, **1988**.

[82] a) Reviews: H.-W. Wanzlick, *Angew. Chem.*, **1962**, 74, 129; *Angew. Chem. Int. Ed . Engl.*, **1962**, 1, 75.

[83] R.W. Hoffmann, *ibid.*, **1968**, 80, 823; **1968**, 7, 754.

[84] N. Wiberg, *Angew. ibid.*, **1968**, 80, 809; *Angew. Chem. Int. Ed. Engl.*, **1968**, 7, 766.

[85] D.M. Lemal, R.A. Lovald, K.J. Kawano, *J. Am. Chem. Soc.*, **1964**, 86, 2518; W. Krasuski, D. Nikolaus, M. Regitz, *Liebigs Ann. Chem.*, **1982**, 1451.

[86] H.-W. Wanzlick, H. J. Schönherr, *Liebigs Ann. Chem.*, **1970**, 731, 176.

[87] H.J. Schönherr, H. W. Wanzlick, *Chem. Ber.*, **1970**, 103, 1037.

[88] A.J. Arduengo, III, R.L. Harlow, M. Kline, *J. Am. Chem. Soc.*, **1991**, 113, 361.

[89] D.A. Dixon, A.J. Arduengo, III, *J. Phys. Chem.*, **1991**, 95, 4180.

[90] A.J. Arduengo, III, H.V.R. Dias, R. L. Harlow, M. Kline, *J. Am. Chem. Soc.*, **1992**, 114, 5530.

[91] H.-W. Wanzlick, *Angew. Chem, Int. Ed. Engl.*, **1962**, 1, 75.

[92] K.K. Irikura, W.A. Goddard, J.L. Beauchamp, *J. Am. Chem. Soc.*, **1992**, 114, 48.

[93] A.J. Arduengo, III, R. Goerlich, W. J. Marshall, *J. Am. Chem.* Soc., **1995**, 17, 11027

[94] A.J. Arduengo, III, H.V.R. Dias, J.C. Calabrese, F. Davidson, *Inorg. Chem.*, **1993**, 32, 1541.

[95] W.A. Herrmann, C. Köcher, L. Goossen, G.R.J. Artus, *Chem, Eur. J.* **1996**, 2, 1627.

[96] W.A. Herrmann, L.J. Goossen, G.R.J. Artus, C. Kocher, *Organometallics*, **1997**, 16, 2472.

[97] C. Köcher, Dissertation, Technische Universität München, **1997**.

[98] A.J. Arduengo, III, J.R. Goerlich, R. Krafczyk, W. J. Marshall, *Angew. Chem. Int. Ed.*, **1998**, 37, 1963.

[99] A.J. Arduengo, III, R. KrafczyK, R. Schmutzler, *Tetrahedron*, 55, **1999**, 14523.

[100] A.J. Arduengo, III, *Acc. Chem. Res.* **1999**, 23, 399-404.

[101] A.J. Arduengo, III, F. Davidson, R. Krafczyk, W.J. Marshall, M. Tamm, *Organometal.*, **1998**, 17, 3375.

[102] R.W. Alder, P.R. Allen, M. Murray, A.G. Orpen, *Angew. Chem. Int. Ed. Engl.* **1996**, 32. 1121.

[103] D. Enders, K. Brever, G. Raabe, J. Runsink, J. Teles, J.,-P Melder, K. Ebel, S. Brode, *Angew. Chem. Int. Ed. Engl.* **1995**, 34, 1021.

[104] H.V. R. Dias, W. Jin, *Tetrahedron Lett.*, **1994**. 35, 1365.

[105] P.B. Hitchcock, M.F. Lappert, P. Terrenos, K.P. Wain-wright, *J. Chem. Soc. Chem. Commun.*, **1980**, 1180.

[106] W.A. Herrmann, *Angew. Chem. Int. Ed.*, **2002**, 41, 1290.

[107] E. Peris, J.A. Loch, J. Mata, R.H. Crabtree, *Chem. Commun.*, **2001**, 201.

[108] A. Briot, M. Bujard, V. Gouverneur, S.P. Nolan, C. Mioskowski, *Org. Lett.*, **2000**, 2, 1517.

[109] A.J. Arduengo, III, H.V. Dias, J.C. Calabrese, F. Davidson, *Organomet.*, **1993**, 12, 3405.

[110] W.A. Herrmann, L.J. Goossen, C. Köcher, G.R.J. Artus, *Angew. Chem. Int. Ed. Engl.*, **1996**, 35, 2805.

[111] S. Trofimenko, *Prog. Inorg. Chem.*, **1986**, 34, 115.

[112] U. Kernbach, M. Ramm, P. Luger, W.P. Fehlhammer, *Amgew. Chem. Int. Ed. Engl.*, **1996**, 35, 310.

[113] R. Fränkel, U. Kernbach, M. Bakola-christianopoulou, U. Plaia, M. Suter, W. Ponikwar, H. Nöth, C. Moinet, W.P. Fehlhammer, *J. Organomet. Chem.*, **2001**, 530, 617.

[114] M. Albrecht, R. H. Crabtree, J. Mata, E. Peris, *Chem. Comm.*, **2002**, 32.

[115] H.M.J. Wang, I.J.B. Lin, *Organometallics*, **1998**, 17, 972.

[116] A.M. Magill, D.S. McGuiness, K.J. Cavell, G.J.P. Britovesek, V.C. GiBson, A.J.P. White, D.J. Williams, A.H. White, B.W. Skelton, *J. Organomet. Chem.*, **2001**, 546, 617.

[117] D.S. McGuiness, K.J. Cavell, *Organometallics*, **2000**, 19, 741.

[118] A.A.D. Tulloch, A.A. Danopoulos, S. Winston, S. Kleinhenz, G. Eastham, *J. Chem. Soc., Dalton Trans.*, **2000**, 4499.

[119] J. Pytkowicz, S. Roland, P. Mangeney, *J. Organomet. Chem.*, 2001, 631, 157.

[120] J. Pytkowicz, S. Roland, P.J. Mangeney, *Tetrahedron Asymmetry*, **2001**, 12, 2087.

[121] D.J. Berrisford, C. Bolm, K.B. Sharpless, *Reviews, Angew. Chem. Int. Ed. Engl.*, **1995**, 34, 1059.

[122] K. P. Fraser, S. Woodward, *Tetrahedron Lett.*, **2001**, 42, 2747.

[123] W. Chen, B. Wu, K. Matsumoto, *J. Organomet. Chem.*, **2002**, 654, 233.

[124] S. Liu, T. Hsieh, G. Lee, S. Peng, *Organomet.*, **1998**, 17, 993.

[125] R.F. Heck, *J. Am. Chem.* Soc., **1968**, 90, 5518.

[126] T. Mizoroki, K. Mori, A. Ozaki, *Bull. Chem. Soc. Jap.*, **1971**, 44, 581.

[127] R.F. Heck, J.P. Nolley Jr., *J. Org. Chem.* 37, **1972**, 2320.

[128] R.F. Heck, *J. Am. Chem. Soc.*, **1986**, 90, 4546.

[129] T. Weskamp, V.P.W. Bohm, W.A. Herrmann, *J. Organomet. Chem.*, **2000**, 600, 12.

[130] W.A. Herrmann, M. Elison, J. Fischer, C. Köcher, G.R.J. Artus, *J. Chem. Eur.*, **1996**, 2, 772.

[131] C.J. Carmalt, A.H. Cowley, *Adv. Inorg. Chem.: Main group Chem.*, **2000**, 50, 1.

[132] D.S. McGuinness, M.J. Green, K.J. Cavell, B.W. Skelton, A.H. White, *J. Organomet. Chem.*, **1998**, 565, 165.

[133] A. Furstner, O.R. Thiel, L. Ackermann, H.-J. Schanz, S.P. Nolan, *J. Org. Chem.*, **2000**, 65, 2204.

[134] M.G. Gardiner, W.A. Herrmann, C.-P. Reisiveger, J. Schwarz, M. Spiegler, *J. Organomet. Chem.*, **1999**, 572, 239.

[135] W.A. Herrmann, C.-P. Reisinger, M. Spiegler, *J. Organomet. Chem.*, **1998**, 557, 93.

[136] T. Weskamp, V.P.W. Bohm, W.A. Herrmann, *J. Organomet. Chem.*, **1999**, 585, 348.

[137] A.C. Hillier, G.A. Grasa, M.S. Viciu, H.M. Lee, C.Y.S.P. Nolan, *J. Organomet. Chem.*, **2002**, 653, 69.

[138] C. Yang, S.P. Nolan, *Synlett*, **2001**, 10, 1539.

[139] W.A. Herrmann, M. Elison, J. Fischer, C. Köcher, G.R.J. Artus, *Angew. Chem. Int. Ed. Engl.*, **1995**, 34, 2371.

[140] W. P. Fehlhammer, T. Bliss, U. Kernbach, I. Brüdgam, *J. Organomet. Chem.*, **1995**, 490, 149.

[141] J. Howarth, K. Hanlon, D. Fayne, P. MaCormac, *Tetrahedron Lett.*, **1997**, 17, 3097.

[142] A. Elaiwi, P.B. Hitchcock, K.R. Seddon, N. Srinivasan, Y. Tan, T. Welton, J.A. Zora, *J. Chem. Soc., Dalton Trans.*, **1995**, 3467.

[143] K.M. Dieter, C.J. Dymek, N.E. Heimer, J.W. Rovang, J.S. Wilkes, *J. Am. Chem. Soc.*, **1988**, 110, 2722.

[144] A.J. Areduengo , III, Us Patent 5, 077, 414, **1991**.

[145] A.W. Van der Made, R. H. Van der Made, *J. Org. Chem.*, **1993**, 58, 1262.

[146] C.J. Dymek, J.J.P. Stewart, *Inorg. Chem.*, **1989**, 28, 1472.

[147] S.A. Lapshin, A. Yu. Chervinskii, L.M. Litvinento, V.A. Dadali, L.M. Kapkan, A.N. Zh. Vdovichenko, *Zh. Org. Khim.*, **1985**, 21, 357.

[148] A.G. Avent, P.A. Chaloner, M.P. Day, K.R. Seddon, T.J. Welton, *J. Chem. Soc. Dalton Trans.*, **1994**, 3405.

[149] J. Howarth, N.A. AL-Hashimy, *Tetrahedron Lett.*, **2001**, 42, 5777.

[150] E.Alcalde, C. Alavarez-Rúa, S. García-Granda, E. García-Rodrigvez, N. Mesquida, L. Perez-Gareía, *Chem. Commun.*, **1999**, 295.

[151] Y. Yuan, G. Gao, Z.-L. Jiang, J.-S. you, Z.-Y., Zhou, D.-Q. Yuan, R.-G. Xie, *Tetrahedron Lett.*, 58, **2002**, 8993.

[152] K. Hanlon, Ph.D. Thesis, Dublin City University, Ireland, **2000**.

[153] D.J.M. McGuirk, MSc. Thesis, Dublin City University, Ireland, **2000**.

[154] W.H. Press, B.H. Flannery, S.A. Teukolsky, WT. Vettreling, "Numerical Recipes; *The Art of Scientific Computing*", Cambridge University Press, Cambridge, **1987**, Chap.9.

[155] J.H. Noggle, *Physical Chemistry on a Microcomputer*, Little Brown, Boston, **1985**, pp. 145.

[156] D.J. Leggett (ed), *Computational Methods for the Determination of Formation Constant*, Plenum, New York, **1985**.

[157] C.L. Shavers, M.L. Persons, S.N. Deming, *J. Chem. Educ.*, **1979**, 56, 307.

[158] J.L. Atwood, J.E.D. Davies, D.D Macnicol, F. Vögtle, *Comprehensive Supramolecular Chemistry*, New York, *Pergamon*, 1996, pp. 425.

[159] J.-S. Chen, F. Rosenberger, *Tetrahedron Lett.*, **1990**, 31, 3975.

[160] J.-S. Chen, R.B. Shirts, *J. Phys. Chem.*, **1985**, 89, 1643.

[161] N.L. Allinger, *J. Am. Chem. Soc.*, **1977**, 99, 8127.

[162] P.S. Stewart, J.W. Costerton, *Lancet*, **2001**, 358, 135.

[163] P.A. Suci, B.J. Tyler, *J. Microbiol. Methods*, **1998**, 53, 313.

[164] B.H. Iglewski, C. Van Delden, *Emerg. Infect. Dis.*, **1998**, 4, 551.

[165] S.F. Fridkin, W.R. Jarvis, *Clin. Microbiol. Rev.*, **1996**, 9, 499.

[166] G.S. Baillie, L.J. Douglas, *Antimicrob. Agents Chemother.*,**1998**, 42, 1900.

[167] G.S. Baillie, L.J. Douglas, *Antimicrob. Agents Chemother.*, **1998**, 42, 2146.

[168] J. Chandra, P.K. Mukherjee, S.D. Leidich, F.F. Faddoul, L.L. Hoyer, L.J. Doulgous, M.A. Channoum, *J. Dent. Res.*, **2001**, 80, 903.

[169] S.P. Hawser, L.J. Douglas, *Infect. Immun.*, **1994**, 62, 915.

[170] K.M. Smith, Y. Bu, H. Suga, *Chem. Biol.*, **2003**, 10, 81.

[171] I.P. Evans, A. Spencer, G. Wilkinson, *J. Chem, Soc. Dalton*, **1972**, 204.

[172] B.R. James, E. Ochiai, G.L. Rempel. *Inorg. Nvel. Chem. Lett.*, **1971**, 7, 781.

[173] D. Bourrissou, O. Gverret, F.P. Gabbaï, G. Bertrand, *Chem. Rev.*, **2000**, 100, 39.

[174] W.A. Herrmann, C. Köher, *Angew. Chem. Int. Ed. Engl.*, **1997**, 36, 2162.

[175] L. Jafarpour, S.P. Nolan, *Adv. Organomet. Chem.*, **2001**, 46, 181.

[176] A.M. Magill, D.S. McGuinness, K.J. Cavell, G.J.P. Britovsek, V.C. Gibson, A.J.P. White, D.J. Williams, A.H. White, B.W. Skelton, *J. Organomet. Chem.*, **2001**, 546, 617.

[177] D.J. Nielsen, K.J. Cavell, B.W. Skelton, A.H. White. *Inorganica chimica Acta*, **2002**, 327, 116.

[178] R.C. Larock, B.E. Baker, *Tetrahedron Lett.*, **1988**, 29, 905.

[179] C. Richard, W.H. Gong, B.E. Baker, *Tetrahedron Lett.*, **1989**, 30, 2603.

[180] F. Ozawa, A. Kubo, Y. Matsumoto, T. Hayashi, *Organomet.*, **1993**, 12, 4188.

[181] F. Ozawa, Y. Kobatake, T. Hayashi, *Tetrahedron Lett.*, **1993**, 34, 2505.

[182] S. Hillers, O. Reiser, *Tetrahedron Lett.*, **1993**, 34, 5265.

[183] R.D. Wilson, Y. Kamitori, H. Ogoshi, Z.-I. Yoshida, J.A. Ibers, *J. Organomet. Chem.*, **1979**, 173, 199.

[184] A. Modinos, P. Woodward, *J. Chem. Soc. Dalton Trans.*, **1974**, 2065.

[185] P. Domaino, A. Musatti, M. Nardelli, G. Predieri, *J. Chem. Soc. Dalton Trans.*, **1975**, 2165.

[186] H.C. Clark, C.R.C. Milne, N.C. Payne, *J. Am. Chem. Soc.*, **1978**, 100, 1164.

[187] W.M. Butler, J.H. Enemark, *Inorg. Chem.*, **1971**, 10, 2416.

[188] O.P. Anderson, A.B. Packard, *ibid.*, **1978**, 17, 1333.

[189] Antimicrobial experiments were carried out by Alan Farrell and Brid Quilty at *School of Biotechnology Laboratories, Dublin City University.*

Appendix I- X-ray data.

Table 1. Bond lengths (Å) and angles (°) for **(156a)**.

P(1)–F(5)	1.577(4)	C(9)–H(9A)	0.9800
P(1)–F(6)	1.578(4)	C(9)–H(9B)	0.9800
P(1)–F(2)	1.581(4)	C(9)–H(9C)	0.9800
P(1)–F(4)	1.588(4)	C(10)–N(1)	1.486(7)
P(1)–F(3)	1.596(4)	C(10)–H(10A)	0.9900
P(1)–F(1)	1.612(4)	C(10)–H(10B)	0.9900
P(2)–F(10)	1.566(4)	C(11)–N(2)	1.327(7)
P(2)–F(12)	1.581(4)	C(11)–N(1)	1.333(7)
P(2)–F(11)	1.589(4)	C(11)–H(11)	0.9500
P(2)–F(7)	1.592(4)	C(12)–C(13)	1.332(8)
P(2)–F(8)	1.595(4)	C(12)–N(2)	1.370(8)
P(2)–F(9)	1.608(4)	C(12)–H(12)	0.9500
P(3)–F(15)	1.553(5)	C(13)–N(1)	1.366(8)
P(3)–F(18)	1.563(5)	C(13)–H(13)	0.9500
P(3)–F(16)	1.571(5)	C(14)–N(2)	1.485(7)
P(3)–F(13)	1.572(4)	C(14)–C(15)	1.533(9)
P(3)–F(14)	1.587(4)	C(14)–H(14A)	0.9900
P(3)–F(17)	1.595(5)	C(14)–H(14B)	0.9900
C(1)–C(6)	1.397(8)	C(15)–C(16)	1.542(10)
C(1)–C(2)	1.415(8)	C(15)–C(23)	1.552(10)
C(1)–C(10)	1.513(8)	C(15)–H(15)	1.0000
C(2)–C(3)	1.409(8)	C(16)–C(19)	1.534(10)
C(2)–C(7)	1.501(8)	C(16)–C(17)	1.550(11)
C(3)–C(4)	1.387(8)	C(16)–H(16)	1.0000
C(3)–C(24)	1.526(8)	C(17)–C(18)	1.535(10)
C(4)–C(5)	1.397(8)	C(17)–H(17A)	0.9900
C(4)–C(8)	1.515(8)	C(17)–H(17B)	0.9900
C(5)–C(6)	1.411(8)	C(18)–C(22)	1.516(11)
C(5)–C(38)	1.517(8)	C(18)–C(19)	1.527(11)
C(6)–C(9)	1.522(8)	C(18)–H(18)	1.0000
C(7)–H(7A)	0.9800	C(19)–C(20)	1.532(11)
C(7)–H(7B)	0.9800	C(19)–C(21)	1.542(10)
C(7)–H(7C)	0.9800	C(20)–H(20A)	0.9800
C(8)–H(8A)	0.9800	C(20)–H(20B)	0.9800
C(8)–H(8B)	0.9800	C(20)–H(20C)	0.9800
C(8)–H(8C)	0.9800	C(21)–H(21A)	0.9800

C(21)–H(21B)	0.9800	C(34)–H(34A)	0.9800
C(21)–H(21C)	0.9800	C(34)–H(34B)	0.9800
C(22)–C(23)	1.560(9)	C(34)–H(34C)	0.9800
C(22)–H(22A)	0.9900	C(35)–H(35A)	0.9800
C(22)–H(22B)	0.9900	C(35)–H(35B)	0.9800
C(23)–H(23A)	0.9900	C(35)–H(35C)	0.9800
C(23)–H(23B)	0.9900	C(36)–C(37)	1.565(8)
C(24)–N(3)	1.468(7)	C(36)–H(36A)	0.9900
C(24)–H(24A)	0.9900	C(36)–H(36B)	0.9900
C(24)–H(24B)	0.9900	C(37)–H(37A)	0.9900
C(25)–N(3)	1.316(7)	C(37)–H(37B)	0.9900
C(25)–N(4)	1.345(7)	C(38)–N(5)	1.493(7)
C(25)–H(25)	0.9500	C(38)–H(38A)	0.9900
C(26)–C(27)	1.325(8)	C(38)–H(38B)	0.9900
C(26)–N(4)	1.365(8)	C(39)–N(6)	1.321(7)
C(26)–H(26)	0.9500	C(39)–N(5)	1.324(7)
C(27)–N(3)	1.362(8)	C(39)–H(39)	0.9500
C(27)–H(27)	0.9500	C(40)–C(41)	1.329(9)
C(28)–N(4)	1.477(7)	C(40)–N(6)	1.361(8)
C(28)–C(29)	1.513(8)	C(40)–H(40)	0.9500
C(28)–H(28A)	0.9900	C(41)–N(5)	1.360(7)
C(28)–H(28B)	0.9900	C(41)–H(41)	0.9500
C(29)–C(30)	1.529(8)	C(42)–N(6)	1.463(7)
C(29)–C(37)	1.535(9)	C(42)–C(43)	1.524(8)
C(29)–H(29)	1.0000	C(42)–H(42A)	0.9900
C(30)–C(31)	1.537(10)	C(42)–H(42B)	0.9900
C(30)–C(33)	1.552(9)	C(43)–C(44)	1.523(8)
C(30)–H(30)	1.0000	C(43)–C(51)	1.554(8)
C(31)–C(32)	1.521(10)	C(43)–H(43)	1.0000
C(31)–H(31A)	0.9900	C(44)–C(45)	1.541(9)
C(31)–H(31B)	0.9900	C(44)–C(47)	1.558(9)
C(32)–C(36)	1.534(9)	C(44)–H(44)	1.0000
C(32)–C(33)	1.542(10)	C(45)–C(46)	1.552(9)
C(32)–H(32)	1.0000	C(45)–H(45A)	0.9900
C(33)–C(35)	1.515(10)	C(45)–H(45B)	0.9900
C(33)–C(34)	1.555(9)	C(46)–C(50)	1.508(9)

C(46)–C(47)	1.548(9)	F(11)–P(2)–F(7)	89.1(3)
C(46)–H(46)	1.0000	F(10)–P(2)–F(8)	90.1(2)
C(47)–C(48)	1.519(8)	F(12)–P(2)–F(8)	91.6(2)
C(47)–C(49)	1.525(8)	F(11)–P(2)–F(8)	177.8(3)
C(48)–H(48A)	0.9800	F(7)–P(2)–F(8)	89.3(2)
C(48)–H(48B)	0.9800	F(10)–P(2)–F(9)	90.5(2)
C(48)–H(48C)	0.9800	F(12)–P(2)–F(9)	178.4(3)
C(49)–H(49A)	0.9800	F(11)–P(2)–F(9)	89.3(2)
C(49)–H(49B)	0.9800	F(7)–P(2)–F(9)	89.0(2)
C(49)–H(49C)	0.9800	F(8)–P(2)–F(9)	89.2(2)
C(50)–C(51)	1.548(8)	F(15)–P(3)–F(18)	91.0(4)
C(50)–H(50A)	0.9900	F(15)–P(3)–F(16)	93.5(4)
C(50)–H(50B)	0.9900	F(18)–P(3)–F(16)	92.3(3)
C(51)–H(51A)	0.9900	F(15)–P(3)–F(13)	89.1(3)
C(51)–H(51B)	0.9900	F(18)–P(3)–F(13)	87.3(2)
		F(16)–P(3)–F(13)	177.4(4)
F(5)–P(1)–F(6)	90.5(3)	F(15)–P(3)–F(14)	90.6(3)
F(5)–P(1)–F(2)	178.2(3)	F(18)–P(3)–F(14)	177.7(3)
F(6)–P(1)–F(2)	91.1(3)	F(16)–P(3)–F(14)	89.3(2)
F(5)–P(1)–F(4)	90.7(2)	F(13)–P(3)–F(14)	91.0(2)
F(6)–P(1)–F(4)	89.1(2)	F(15)–P(3)–F(17)	176.5(4)
F(2)–P(1)–F(4)	90.2(2)	F(18)–P(3)–F(17)	91.3(4)
F(5)–P(1)–F(3)	89.2(2)	F(16)–P(3)–F(17)	89.0(4)
F(6)–P(1)–F(3)	179.6(3)	F(13)–P(3)–F(17)	88.4(3)
F(2)–P(1)–F(3)	89.2(2)	F(14)–P(3)–F(17)	87.0(3)
F(4)–P(1)–F(3)	91.2(2)	C(6)–C(1)–C(2)	121.0(5)
F(5)–P(1)–F(1)	90.0(2)	C(6)–C(1)–C(10)	119.9(5)
F(6)–P(1)–F(1)	90.1(2)	C(2)–C(1)–C(10)	118.7(6)
F(2)–P(1)–F(1)	89.2(2)	C(3)–C(2)–C(1)	118.9(5)
F(4)–P(1)–F(1)	179.0(2)	C(3)–C(2)–C(7)	120.5(6)
F(3)–P(1)–F(1)	89.5(2)	C(1)–C(2)–C(7)	120.6(6)
F(10)–P(2)–F(12)	90.8(2)	C(4)–C(3)–C(2)	120.7(5)
F(10)–P(2)–F(11)	91.5(3)	C(4)–C(3)–C(24)	118.6(5)
F(12)–P(2)–F(11)	89.8(2)	C(2)–C(3)–C(24)	120.3(6)
F(10)–P(2)–F(7)	179.3(3)	C(3)–C(4)–C(5)	119.4(5)
F(12)–P(2)–F(7)	89.7(2)	C(3)–C(4)–C(8)	121.7(5)

C(5)–C(4)–C(8)	118.8(5)	N(2)–C(12)–H(12)	125.8
C(4)–C(5)–C(6)	121.5(5)	C(12)–C(13)–N(1)	106.6(6)
C(4)–C(5)–C(38)	120.1(5)	C(12)–C(13)–H(13)	126.7
C(6)–C(5)–C(38)	118.2(5)	N(1)–C(13)–H(13)	126.7
C(1)–C(6)–C(5)	118.3(5)	N(2)–C(14)–C(15)	112.4(5)
C(1)–C(6)–C(9)	120.9(5)	N(2)–C(14)–H(14A)	109.1
C(5)–C(6)–C(9)	120.8(5)	C(15)–C(14)–H(14A)	109.1
C(2)–C(7)–H(7A)	109.5	N(2)–C(14)–H(14B)	109.1
C(2)–C(7)–H(7B)	109.5	C(15)–C(14)–H(14B)	109.1
H(7A)–C(7)–H(7B)	109.5	H(14A)–C(14)–H(14B)	107.9
C(2)–C(7)–H(7C)	109.5	C(14)–C(15)–C(16)	109.2(6)
H(7A)–C(7)–H(7C)	109.5	C(14)–C(15)–C(23)	112.8(6)
H(7B)–C(7)–H(7C)	109.5	C(16)–C(15)–C(23)	112.2(6)
C(4)–C(8)–H(8A)	109.5	C(14)–C(15)–H(15)	107.5
C(4)–C(8)–H(8B)	109.5	C(16)–C(15)–H(15)	107.5
H(8A)–C(8)–H(8B)	109.5	C(23)–C(15)–H(15)	107.5
C(4)–C(8)–H(8C)	109.5	C(19)–C(16)–C(15)	114.5(6)
H(8A)–C(8)–H(8C)	109.5	C(19)–C(16)–C(17)	86.8(6)
H(8B)–C(8)–H(8C)	109.5	C(15)–C(16)–C(17)	105.1(7)
C(6)–C(9)–H(9A)	109.5	C(19)–C(16)–H(16)	115.5
C(6)–C(9)–H(9B)	109.5	C(15)–C(16)–H(16)	115.5
H(9A)–C(9)–H(9B)	109.5	C(17)–C(16)–H(16)	115.5
C(6)–C(9)–H(9C)	109.5	C(18)–C(17)–C(16)	86.1(6)
H(9A)–C(9)–H(9C)	109.5	C(18)–C(17)–H(17A)	114.3
H(9B)–C(9)–H(9C)	109.5	C(16)–C(17)–H(17A)	114.3
N(1)–C(10)–C(1)	113.9(5)	C(18)–C(17)–H(17B)	114.3
N(1)–C(10)–H(10A)	108.8	C(16)–C(17)–H(17B)	114.3
C(1)–C(10)–H(10A)	108.8	H(17A)–C(17)–H(17B)	111.4
N(1)–C(10)–H(10B)	108.8	C(22)–C(18)–C(19)	112.1(6)
C(1)–C(10)–H(10B)	108.8	C(22)–C(18)–C(17)	108.5(7)
H(10A)–C(10)–H(10B)	107.7	C(19)–C(18)–C(17)	87.6(7)
N(2)–C(11)–N(1)	108.1(5)	C(22)–C(18)–H(18)	115.2
N(2)–C(11)–H(11)	125.9	C(19)–C(18)–H(18)	115.2
N(1)–C(11)–H(11)	125.9	C(17)–C(18)–H(18)	115.2
C(13)–C(12)–N(2)	108.3(6)	C(18)–C(19)–C(20)	112.2(7)
C(13)–C(12)–H(12)	125.8	C(18)–C(19)–C(16)	87.0(6)

C(20)–C(19)–C(16)	112.7(7)	N(4)–C(25)–H(25)	125.7
C(18)–C(19)–C(21)	120.3(7)	C(27)–C(26)–N(4)	107.0(6)
C(20)–C(19)–C(21)	104.9(7)	C(27)–C(26)–H(26)	126.5
C(16)–C(19)–C(21)	119.4(6)	N(4)–C(26)–H(26)	126.5
C(19)–C(20)–H(20A)	109.5	C(26)–C(27)–N(3)	108.7(6)
C(19)–C(20)–H(20B)	109.5	C(26)–C(27)–H(27)	125.6
H(20A)–C(20)–H(20B)	109.5	N(3)–C(27)–H(27)	125.6
C(19)–C(20)–H(20C)	109.5	N(4)–C(28)–C(29)	112.7(5)
H(20A)–C(20)–H(20C)	109.5	N(4)–C(28)–H(28A)	109.1
H(20B)–C(20)–H(20C)	109.5	C(29)–C(28)–H(28A)	109.1
C(19)–C(21)–H(21A)	109.5	N(4)–C(28)–H(28B)	109.1
C(19)–C(21)–H(21B)	109.5	C(29)–C(28)–H(28B)	109.1
H(21A)–C(21)–H(21B)	109.5	H(28A)–C(28)–H(28B)	107.8
C(19)–C(21)–H(21C)	109.5	C(28)–C(29)–C(30)	112.7(6)
H(21A)–C(21)–H(21C)	109.5	C(28)–C(29)–C(37)	114.9(5)
H(21B)–C(21)–H(21C)	109.5	C(30)–C(29)–C(37)	111.2(5)
C(18)–C(22)–C(23)	113.1(6)	C(28)–C(29)–H(29)	105.7
C(18)–C(22)–H(22A)	109.0	C(30)–C(29)–H(29)	105.7
C(23)–C(22)–H(22A)	109.0	C(37)–C(29)–H(29)	105.7
C(18)–C(22)–H(22B)	109.0	C(29)–C(30)–C(31)	107.7(6)
C(23)–C(22)–H(22B)	109.0	C(29)–C(30)–C(33)	114.3(5)
H(22A)–C(22)–H(22B)	107.8	C(31)–C(30)–C(33)	88.5(5)
C(15)–C(23)–C(22)	113.8(6)	C(29)–C(30)–H(30)	114.5
C(15)–C(23)–H(23A)	108.8	C(31)–C(30)–H(30)	114.5
C(22)–C(23)–H(23A)	108.8	C(33)–C(30)–H(30)	114.5
C(15)–C(23)–H(23B)	108.8	C(32)–C(31)–C(30)	85.5(5)
C(22)–C(23)–H(23B)	108.8	C(32)–C(31)–H(31A)	114.4
H(23A)–C(23)–H(23B)	107.7	C(30)–C(31)–H(31A)	114.4
N(3)–C(24)–C(3)	114.6(5)	C(32)–C(31)–H(31B)	114.4
N(3)–C(24)–H(24A)	108.6	C(30)–C(31)–H(31B)	114.4
C(3)–C(24)–H(24A)	108.6	H(31A)–C(31)–H(31B)	111.5
N(3)–C(24)–H(24B)	108.6	C(31)–C(32)–C(36)	107.8(6)
C(3)–C(24)–H(24B)	108.6	C(31)–C(32)–C(33)	89.5(6)
H(24A)–C(24)–H(24B)	107.6	C(36)–C(32)–C(33)	111.4(5)
N(3)–C(25)–N(4)	108.6(5)	C(31)–C(32)–H(32)	115.1
N(3)–C(25)–H(25)	125.7	C(36)–C(32)–H(32)	115.1

C(33)–C(32)–H(32)	115.1	H(38A)–C(38)–H(38B)	108.1
C(35)–C(33)–C(32)	119.1(6)	N(6)–C(39)–N(5)	109.6(5)
C(35)–C(33)–C(30)	122.0(5)	N(6)–C(39)–H(39)	125.2
C(32)–C(33)–C(30)	84.3(5)	N(5)–C(39)–H(39)	125.2
C(35)–C(33)–C(34)	108.2(6)	C(41)–C(40)–N(6)	108.1(6)
C(32)–C(33)–C(34)	111.0(6)	C(41)–C(40)–H(40)	126.0
C(30)–C(33)–C(34)	110.5(6)	N(6)–C(40)–H(40)	126.0
C(33)–C(34)–H(34A)	109.5	C(40)–C(41)–N(5)	107.5(6)
C(33)–C(34)–H(34B)	109.5	C(40)–C(41)–H(41)	126.2
H(34A)–C(34)–H(34B)	109.5	N(5)–C(41)–H(41)	126.2
C(33)–C(34)–H(34C)	109.5	N(6)–C(42)–C(43)	113.1(5)
H(34A)–C(34)–H(34C)	109.5	N(6)–C(42)–H(42A)	109.0
H(34B)–C(34)–H(34C)	109.5	C(43)–C(42)–H(42A)	109.0
C(33)–C(35)–H(35A)	109.5	N(6)–C(42)–H(42B)	109.0
C(33)–C(35)–H(35B)	109.5	C(43)–C(42)–H(42B)	109.0
H(35A)–C(35)–H(35B)	109.5	H(42A)–C(42)–H(42B)	107.8
C(33)–C(35)–H(35C)	109.5	C(44)–C(43)–C(42)	111.6(5)
H(35A)–C(35)–H(35C)	109.5	C(44)–C(43)–C(51)	111.0(5)
H(35B)–C(35)–H(35C)	109.5	C(42)–C(43)–C(51)	112.8(5)
C(32)–C(36)–C(37)	112.1(6)	C(44)–C(43)–H(43)	107.0
C(32)–C(36)–H(36A)	109.2	C(42)–C(43)–H(43)	107.0
C(37)–C(36)–H(36A)	109.2	C(51)–C(43)–H(43)	107.0
C(32)–C(36)–H(36B)	109.2	C(43)–C(44)–C(45)	107.5(5)
C(37)–C(36)–H(36B)	109.2	C(43)–C(44)–C(47)	115.6(5)
H(36A)–C(36)–H(36B)	107.9	C(45)–C(44)–C(47)	88.4(5)
C(29)–C(37)–C(36)	115.5(5)	C(43)–C(44)–H(44)	114.2
C(29)–C(37)–H(37A)	108.4	C(45)–C(44)–H(44)	114.2
C(36)–C(37)–H(37A)	108.4	C(47)–C(44)–H(44)	114.2
C(29)–C(37)–H(37B)	108.4	C(44)–C(45)–C(46)	85.1(5)
C(36)–C(37)–H(37B)	108.4	C(44)–C(45)–H(45A)	114.5
H(37A)–C(37)–H(37B)	107.5	C(46)–C(45)–H(45A)	114.5
N(5)–C(38)–C(5)	110.2(5)	C(44)–C(45)–H(45B)	114.5
N(5)–C(38)–H(38A)	109.6	C(46)–C(45)–H(45B)	114.5
C(5)–C(38)–H(38A)	109.6	H(45A)–C(45)–H(45B)	111.6
N(5)–C(38)–H(38B)	109.6	C(50)–C(46)–C(47)	112.6(5)
C(5)–C(38)–H(38B)	109.6	C(50)–C(46)–C(45)	107.6(6)

C(47)–C(46)–C(45)	88.4(5)	C(13)–N(1)–C(10)	124.2(5)
C(50)–C(46)–H(46)	115.1	C(11)–N(2)–C(12)	107.9(5)
C(47)–C(46)–H(46)	115.1	C(11)–N(2)–C(14)	123.6(5)
C(45)–C(46)–H(46)	115.1	C(12)–N(2)–C(14)	128.4(5)
C(48)–C(47)–C(49)	108.2(5)	C(25)–N(3)–C(27)	107.8(5)
C(48)–C(47)–C(46)	112.9(5)	C(25)–N(3)–C(24)	126.8(5)
C(49)–C(47)–C(46)	116.9(5)	C(27)–N(3)–C(24)	125.3(5)
C(48)–C(47)–C(44)	111.0(5)	C(25)–N(4)–C(26)	107.9(5)
C(49)–C(47)–C(44)	121.7(5)	C(25)–N(4)–C(28)	124.7(5)
C(46)–C(47)–C(44)	84.7(5)	C(26)–N(4)–C(28)	127.5(5)
C(47)–C(48)–H(48A)	109.5	C(39)–N(5)–C(41)	107.5(5)
C(47)–C(48)–H(48B)	109.5	C(39)–N(5)–C(38)	123.0(5)
H(48A)–C(48)–H(48B)	109.5	C(41)–N(5)–C(38)	129.4(5)
C(47)–C(48)–H(48C)	109.5	C(39)–N(6)–C(40)	107.2(5)
H(48A)–C(48)–H(48C)	109.5	C(39)–N(6)–C(42)	124.5(5)
H(48B)–C(48)–H(48C)	109.5	C(40)–N(6)–C(42)	128.1(5)
C(47)–C(49)–H(49A)	109.5		
C(47)–C(49)–H(49B)	109.5		
H(49A)–C(49)–H(49B)	109.5		
C(47)–C(49)–H(49C)	109.5		
H(49A)–C(49)–H(49C)	109.5		
H(49B)–C(49)–H(49C)	109.5		
C(46)–C(50)–C(51)	113.6(6)		
C(46)–C(50)–H(50A)	108.8		
C(51)–C(50)–H(50A)	108.8		
C(46)–C(50)–H(50B)	108.8		
C(51)–C(50)–H(50B)	108.8		
H(50A)–C(50)–H(50B)	107.7		
C(50)–C(51)–C(43)	115.1(5)		
C(50)–C(51)–H(51A)	108.5		
C(43)–C(51)–H(51A)	108.5		
C(50)–C(51)–H(51B)	108.5		
C(43)–C(51)–H(51B)	108.5		
H(51A)–C(51)–H(51B)	107.5		
C(11)–N(1)–C(13)	108.9(5)		
C(11)–N(1)–C(10)	126.2(6)		

Table 2. Torsion angles (°) for **(156a)**.

C(6)–C(1)–C(2)–C(3)	2.4(8)	C(16)–C(17)–C(18)–C(19)	–26.3(6)
C(10)–C(1)–C(2)–C(3)	175.2(5)	C(22)–C(18)–C(19)–C(20)	164.3(7)
C(6)–C(1)–C(2)–C(7)	–176.2(5)	C(17)–C(18)–C(19)–C(20)	-86.7(8)
C(10)–C(1)–C(2)–C(7)	–3.4(8)	C(22)–C(18)–C(19)–C(16)	–82.3(7)
C(1)–C(2)–C(3)–C(4)	–5.5(8)	C(17)–C(18)–C(19)–C(16)	26.6(6)
C(7)–C(2)–C(3)–C(4)	173.1(5)	C(22)–C(18)–C(19)–C(21)	40.2(9)
C(1)–C(2)–C(3)–C(24)	–178.8(5)	C(17)–C(18)–C(19)–C(21)	149.2(7)
C(7)–C(2)–C(3)–C(24)	–0.2(8)	C(15)–C(16)–C(19)–C(18)	78.8(7)
C(2)–C(3)–C(4)–C(5)	3.6(8)	C(17)–C(16)–C(19)–C(18)	–26.4(6)
C(24)–C(3)–C(4)–C(5)	177.1(5)	C(15)–C(16)–C(19)–C(20)	–168.4(7)
C(2)–C(3)–C(4)–C(8)	–172.9(6)	C(17)–C(16)–C(19)–C(20)	86.5(8)
C(24)–C(3)–C(4)–C(8)	0.5(8)	C(15)–C(16)–C(19)–C(21)	–44.6(10)
C(3)–C(4)–C(5)–C(6)	1.3(8)	C(17)–C(16)–C(19)–C(21)	–149.7(8)
C(8)–C(4)–C(5)–C(6)	178.0(6)	C(19)–C(18)–C(22)–C(23)	42.2(9)
C(3)–C(4)–C(5)–C(38)	–173.5(5)	C(17)–C(18)–C(22)–C(23)	–52.8(8)
C(8)–C(4)–C(5)–C(38)	3.1(8)	C(14)–C(15)–C(23)–C(22)	–140.2(6)
C(2)–C(1)–C(6)–C(5)	2.3(8)	C(16)–C(15)–C(23)–C(22)	–16.4(9)
C(10)–C(1)–C(6)–C(5)	–170.3(5)	C(18)–C(22)–C(23)–C(15)	13.0(9)
C(2)–C(1)–C(6)–C(9)	–180.0(5)	C(4)–C(3)–C(24)–N(3)	133.5(6)
C(10)–C(1)–C(6)–C(9)	7.4(8)	C(2)–C(3)–C(24)–N(3)	–53.0(8)
C(4)–C(5)–C(6)–C(1)	–4.3(8)	N(4)–C(26)–C(27)–N(3)	–1.3(7)
C(38)–C(5)–C(6)–C(1)	170.7(5)	N(4)–C(28)–C(29)–C(30)	170.5(5)
C(4)–C(5)–C(6)–C(9)	178.0(5)	N(4)–C(28)–C(29)–C(37)	–60.8(7)
C(38)–C(5)–C(6)–C(9)	–7.0(8)	C(28)–C(29)–C(30)–C(31)	–175.0(6)
C(6)–C(1)–C(10)–N(1)	–121.8(6)	C(37)–C(29)–C(30)–C(31)	54.4(7)
C(2)–C(1)–C(10)–N(1)	65.4(8)	C(28)–C(29)–C(30)–C(33)	88.5(7)
N(2)–C(12)–C(13)–N(1)	1.3(7)	C(37)–C(29)–C(30)–C(33)	–42.2(8)
N(2)–C(14)–C(15)–C(16)	165.5(5)	C(29)–C(30)–C(31)–C(32)	–89.1(6)
N(2)–C(14)–C(15)–C(23)	–69.0(7)	C(33)–C(30)–C(31)–C(32)	26.0(5)
C(14)–C(15)–C(16)–C(19)	91.2(8)	C(30)–C(31)–C(32)–C(36)	86.3(6)
C(23)–C(15)–C(16)–C(19)	–34.6(9)	C(30)–C(31)–C(32)–C(33)	–26.1(5)
C(14)–C(15)–C(16)–C(17)	–175.4(6)	C(31)–C(32)–C(33)–C(35)	149.5(6)
C(23)–C(15)–C(16)–C(17)	58.7(8)	C(36)–C(32)–C(33)–C(35)	40.6(8)
C(19)–C(16)–C(17)–C(18)	26.2(6)	C(31)–C(32)–C(33)–C(30)	25.9(5)
C(15)–C(16)–C(17)–C(18)	–88.3(7)	C(36)–C(32)–C(33)–C(30)	–83.0(6)
C(16)–C(17)–C(18)–C(22)	86.1(7)	C(31)–C(32)–C(33)–C(34)	–83.8(7)

C(36)–C(32)–C(33)–C(34)	167.2(6)	C(45)–C(44)–C(47)–C(46)	–27.3(4)
C(29)–C(30)–C(33)–C(35)	–37.8(10)	C(47)–C(46)–C(50)–C(51)	46.6(8)
C(31)–C(30)–C(33)–C(35)	–146.5(7)	C(45)–C(46)–C(50)–C(51)	–49.1(7)
C(29)–C(30)–C(33)–C(32)	83.1(7)	C(46)–C(50)–C(51)–C(43)	4.7(8)
C(31)–C(30)–C(33)–C(32)	–25.6(5)	C(44)–C(43)–C(51)–C(50)	–6.4(8)
C(29)–C(30)–C(33)–C(34)	–166.6(6)	C(42)–C(43)–C(51)–C(50)	–132.5(6)
C(31)–C(30)–C(33)–C(34)	84.7(7)	N(2)–C(11)–N(1)–C(13)	2.3(7)
C(31)–C(32)–C(36)–C(37)	–51.2(8)	N(2)–C(11)–N(1)–C(10)	173.4(5)
C(33)–C(32)–C(36)–C(37)	45.5(8)	C(12)–C(13)–N(1)–C(11)	–2.2(7)
C(28)–C(29)–C(37)–C(36)	–138.8(6)	C(12)–C(13)–N(1)–C(10)	–173.6(6)
C(30)–C(29)–C(37)–C(36)	–9.3(8)	C(1)–C(10)–N(1)–C(11)	41.2(9)
C(32)–C(36)–C(37)–C(29)	7.7(9)	C(1)–C(10)–N(1)–C(13)	–148.9(6)
C(4)–C(5)–C(38)–N(5)	94.3(7)	N(1)–C(11)–N(2)–C(12)	–1.4(7)
C(6)–C(5)–C(38)–N(5)	–80.7(7)	N(1)–C(11)–N(2)–C(14)	–177.7(5)
N(6)–C(40)–C(41)–N(5)	0.8(9)	C(13)–C(12)–N(2)–C(11)	0.0(7)
N(6)–C(42)–C(43)–C(44)	–179.7(5)	C(13)–C(12)–N(2)–C(14)	176.1(6)
N(6)–C(42)–C(43)–C(51)	–54.0(7)	C(15)–C(14)–N(2)–C(11)	–114.2(7)
C(42)–C(43)–C(44)–C(45)	–179.6(5)	C(15)–C(14)–N(2)–C(12)	70.3(8)
C(51)–C(43)–C(44)–C(45)	53.6(7)	N(4)–C(25)–N(3)–C(27)	–0.9(7)
C(42)–C(43)–C(44)–C(47)	83.6(7)	N(4)–C(25)–N(3)–C(24)	–178.4(5)
C(51)–C(43)–C(44)–C(47)	–43.1(7)	C(26)–C(27)–N(3)–C(25)	1.4(7)
C(43)–C(44)–C(45)–C(46)	–89.2(6)	C(26)–C(27)–N(3)–C(24)	179.0(6)
C(47)–C(44)–C(45)–C(46)	27.2(5)	C(3)–C(24)–N(3)–C(25)	–42.6(8)
C(44)–C(45)–C(46)–C(50)	85.8(5)	C(3)–C(24)–N(3)–C(27)	140.3(6)
C(44)–C(45)–C(46)–C(47)	–27.4(4)	N(3)–C(25)–N(4)–C(26)	0.1(7)
C(50)–C(46)–C(47)–C(48)	168.1(6)	N(3)–C(25)–N(4)–C(28)	–180.0(5)
C(45)–C(46)–C(47)–C(48)	–83.5(6)	C(27)–C(26)–N(4)–C(25)	0.8(7)
C(50)–C(46)–C(47)–C(49)	41.6(8)	C(27)–C(26)–N(4)–C(28)	–179.1(6)
C(45)–C(46)–C(47)–C(49)	150.1(5)	C(29)–C(28)–N(4)–C(25)	–93.5(7)
C(50)–C(46)–C(47)–C(44)	–81.3(6)	C(29)–C(28)–N(4)–C(26)	86.4(7)
C(45)–C(46)–C(47)–C(44)	27.1(4)	N(6)–C(39)–N(5)–C(41)	0.3(7)
C(43)–C(44)–C(47)–C(48)	–166.1(5)	N(6)–C(39)–N(5)–C(38)	–177.3(5)
C(45)–C(44)–C(47)–C(48)	85.3(5)	C(40)–C(41)–N(5)–C(39)	–0.7(8)
C(43)–C(44)–C(47)–C(49)	–37.1(8)	C(40)–C(41)–N(5)–C(38)	176.7(7)
C(45)–C(44)–C(47)–C(49)	–145.8(6)	C(5)–C(38)–N(5)–C(39)	175.7(6)
C(43)–C(44)–C(47)–C(46)	81.3(6)	C(5)–C(38)–N(5)–C(41)	–1.3(10)

N(5)–C(39)–N(6)–C(40)	0.2(7)
N(5)–C(39)–N(6)–C(42)	176.5(5)
C(41)–C(40)–N(6)–C(39)	–0.6(8)
C(41)–C(40)–N(6)–C(42)	–176.8(6)
C(43)–C(42)–N(6)–C(39)	126.9(6)
C(43)–C(42)–N(6)–C(40)	–57.6(9)

Table 3. Anisotropic displacement parameters ($Å^2 x\ 10^3$) for **(156a)**. The anisotropic displacement factor exponent takes the form: $-2\pi^2[\ h^2\ a^{*2}U^{11} + ... + 2\ h\ k\ a^*\ b^*\ U^{12}\ ]$

Atom	U^{11}	U^{22}	U^{33}	U^{23}	U^{13}	U^{12}
P(1)	23(1)	13(1)	34(1)	–2(1)	4(1)	–1(1)
F(1)	21(2)	18(2)	68(3)	–1(2)	6(2)	–2(2)
F(2)	22(2)	80(3)	40(2)	–13(2)	0(2)	–11(2)
F(3)	37(3)	28(2)	78(3)	16(2)	15(2)	–1(2)
F(4)	26(2)	26(2)	40(2)	–1(2)	–1(2)	0(2)
F(5)	49(3)	68(3)	60(3)	–38(2)	9(2)	–4(2)
F(6)	26(3)	29(3)	133(4)	28(3)	1(3)	–2(2)
P(2)	26(1)	14(1)	26(1)	–2(1)	–1(1)	–2(1)
F(7)	24(2)	20(2)	66(3)	–5(2)	12(2)	–5(2)
F(8)	50(3)	43(3)	31(2)	6(2)	5(2)	–6(2)
F(9)	53(3)	27(2)	44(2)	–11(2)	–13(2)	0(2)
F(10)	34(3)	23(2)	107(4)	–3(3)	–26(3)	1(2)
F(11)	98(4)	35(3)	43(2)	11(2)	–8(3)	–10(3)
F(12)	32(3)	28(2)	73(3)	–25(2)	0(2)	9(2)
P(3)	26(1)	20(1)	33(1)	–7(1)	–6(1)	2(1)
F(13)	32(2)	19(2)	59(3)	–4(2)	–8(2)	–6(2)
F(14)	38(3)	34(3)	55(3)	–22(2)	–11(2)	4(2)
F(15)	169(7)	94(5)	104(4)	79(4)	–86(4)	–88(5)
F(16)	42(3)	53(3)	224(7)	–75(4)	–61(4)	20(3)
F(17)	66(4)	166(6)	39(3)	17(3)	5(3)	–60(4)
F(18)	50(4)	92(4)	184(6)	–110(4)	–40(4)	32(3)
C(1)	35(4)	9(4)	8(3)	–3(2)	–3(3)	3(3)
C(2)	29(4)	21(4)	8(3)	–5(3)	–1(3)	–7(3)
C(3)	29(4)	12(4)	12(3)	–3(3)	–1(3)	–2(3)

C(4)	29(4)	4(3)	10(3)	–1(2)	0(3)	6(3)
C(5)	17(3)	20(4)	11(3)	2(3)	0(2)	–1(3)
C(6)	18(4)	16(4)	16(3)	5(3)	–3(3)	–8(3)
C(7)	26(4)	17(4)	19(3)	3(3)	–1(3)	–1(3)
C(8)	43(5)	20(4)	52(5)	6(3)	16(4)	8(4)
C(9)	36(4)	16(4)	33(4)	2(3)	1(3)	–6(3)
C(10)	46(5)	16(4)	16(3)	1(3)	7(3)	2(3)
C(11)	24(4)	17(4)	20(3)	–3(3)	0(3)	6(3)
C(12)	23(4)	28(4)	24(4)	–4(3)	0(3)	4(3)
C(13)	7(3)	22(4)	24(4)	2(3)	1(3)	–4(3)
C(14)	30(4)	18(4)	25(3)	–3(3)	–6(3)	3(3)
C(15)	61(6)	22(4)	33(4)	1(3)	12(4)	1(4)
C(16)	61(6)	44(5)	30(4)	13(4)	6(4)	18(4)
C(17)	128(9)	33(5)	52(5)	20(4)	26(6)	22(6)
C(18)	79(7)	38(5)	29(4)	12(4)	23(4)	7(5)
C(19)	44(5)	68(6)	18(4)	3(4)	6(4)	22(5)
C(20)	68(7)	132(10)	30(4)	6(5)	2(5)	34(6)
C(21)	57(6)	50(6)	25(4)	–12(4)	6(4)	–18(4)
C(22)	40(5)	42(5)	40(4)	–3(4)	16(4)	–8(4)
C(23)	44(5)	43(5)	36(4)	–5(4)	11(4)	–21(4)
C(24)	32(4)	15(4)	20(3)	–1(3)	–2(3)	–6(3)
C(25)	13(3)	9(3)	23(3)	5(3)	4(3)	–1(3)
C(26)	14(3)	16(4)	32(4)	1(3)	4(3)	–7(3)
C(27)	30(4)	14(4)	29(4)	–7(3)	–7(3)	–2(3)
C(28)	21(4)	20(4)	21(3)	1(3)	5(3)	–1(3)
C(29)	20(4)	26(4)	22(3)	9(3)	4(3)	8(3)
C(30)	31(4)	43(5)	36(4)	9(4)	–4(3)	–15(4)
C(31)	35(5)	80(7)	42(5)	22(5)	–5(4)	13(5)
C(32)	46(5)	20(4)	28(4)	10(3)	–3(4)	0(4)
C(33)	42(5)	27(4)	17(3)	6(3)	–3(3)	–13(4)
C(34)	119(8)	42(5)	26(4)	3(4)	–23(5)	–19(5)
C(35)	57(6)	43(5)	30(4)	7(4)	11(4)	11(4)
C(36)	87(6)	10(4)	28(4)	3(3)	–10(4)	6(4)
C(37)	62(5)	12(4)	19(3)	–2(3)	–2(4)	–2(4)
C(38)	20(4)	40(4)	15(3)	12(3)	–1(3)	–1(3)
C(39)	13(3)	6(3)	20(3)	3(3)	2(3)	0(3)
C(40)	24(5)	80(7)	23(4)	0(4)	–9(3)	13(4)
C(41)	17(4)	76(6)	20(4)	7(4)	–6(3)	10(4)

C(42)	30(4)	25(4)	13(3)	2(3)	–1(3)	–6(3)
C(43)	22(4)	22(4)	28(3)	–6(3)	3(3)	–1(3)
C(44)	29(4)	24(4)	31(4)	5(3)	4(3)	–5(4)
C(45)	31(4)	52(5)	13(3)	1(3)	2(3)	–7(4)
C(46)	34(4)	34(5)	20(3)	–5(3)	4(3)	0(3)
C(47)	26(4)	21(4)	20(3)	–6(3)	4(3)	–13(3)
C(48)	34(4)	39(4)	32(4)	–4(4)	5(3)	–9(4)
C(49)	16(4)	47(5)	32(4)	8(3)	0(3)	–9(3)
C(50)	45(5)	29(4)	36(4)	–13(3)	–3(4)	–11(4)
C(51)	29(4)	21(4)	18(3)	3(3)	–4(3)	–6(3)
N(1)	20(3)	12(3)	24(3)	0(2)	0(3)	1(2)
N(2)	22(3)	20(3)	20(3)	–4(2)	–1(2)	3(3)
N(3)	27(3)	9(3)	16(3)	–2(2)	–1(3)	0(3)
N(4)	29(3)	10(3)	15(3)	5(2)	0(2)	–4(2)
N(5)	21(3)	19(3)	17(3)	1(2)	–2(2)	2(3)
N(6)	28(3)	13(3)	10(3)	0(2)	–1(2)	4(2)

Table 4. Hydrogen coordinates (x 10^4) and isotropic displacement parameters ($Å^2$x 10^3) for **(156a)**.

Atom	x	y	z	U(eq)
H(7A)	–3661	7991	7803	31
H(7B)	–3628	8884	7806	31
H(7C)	–2841	8427	8093	31
H(8A)	3390	6829	7554	58
H(8B)	3173	7093	7208	58
H(8C)	1501	6634	7369	58
H(9A)	4059	9737	7420	42
H(9B)	2437	10194	7593	42
H(9C)	2217	10013	7239	42
H(10A)	–342	10240	7622	31
H(10B)	–2326	9813	7592	31
H(11)	821	9641	8259	24
H(12)	–3746	10731	8558	30

H(13)	–4120	10553	8007	22
H(14A)	–226	10699	8893	29
H(14B)	1051	9999	8798	29
H(15)	–1552	9195	8950	46
H(16)	1290	9417	9282	54
H(17A)	–2069	8689	9422	85
H(17B)	–373	8726	9676	85
H(18)	–2331	9684	9897	58
H(20A)	798	10311	10015	115
H(20B)	2386	10358	9755	115
H(20C)	1580	9564	9860	115
H(21A)	–1364	11049	9341	66
H(21B)	827	11147	9428	66
H(21C)	–777	11261	9682	66
H(22A)	–4301	10409	9557	49
H(22B)	–4785	9547	9504	49
H(23A)	–4289	9759	9015	49
H(23B)	–3330	10551	9082	49
H(24A)	–2178	6948	7594	27
H(24B)	–184	6593	7689	27
H(25)	376	7351	8304	18
H(26)	–4575	6448	8554	25
H(27)	–4352	6407	7999	29
H(28A)	–2515	7201	8978	25
H(28B)	–497	7510	8868	25
H(29)	698	6288	8867	27
H(30)	1209	7058	9321	44
H(31A)	1995	5563	9254	63
H(31B)	2560	5992	9570	63
H(32)	–228	5383	9760	37
H(34A)	–278	7383	9866	93
H(34B)	1238	6722	9895	93
H(34C)	–794	6648	10055	93
H(35A)	–3567	6432	9382	65
H(35B)	–3147	7217	9541	65
H(35C)	–3675	6506	9745	65
H(36A)	–2769	5138	9393	50
H(36B)	–861	4753	9273	50

H(37A)	–1234	5371	8843	37
H(37B)	–2957	5839	8981	37
H(38A)	5097	8811	7291	30
H(38B)	4910	7925	7249	30
H(39)	6272	8552	6703	15
H(40)	1162	8804	6339	51
H(41)	748	8567	6883	45
H(42A)	6374	8795	6157	27
H(42B)	4745	9378	6069	27
H(43)	2946	8444	5841	29
H(44)	5305	9041	5515	34
H(45A)	4706	8136	5124	38
H(45B)	3271	7775	5377	38
H(46)	6771	7121	5282	35
H(48A)	8874	8971	5335	52
H(48B)	7574	8522	5100	52
H(48C)	9497	8157	5224	52
H(49A)	9748	7720	5747	47
H(49B)	8015	7820	5979	47
H(49C)	9179	8534	5866	47
H(50A)	6505	6726	5810	44
H(50B)	4501	6631	5643	44
H(51A)	5237	7458	6151	27
H(51B)	3207	7303	6002	27

Table 5. Bond lengths (Å) and angles (°) for **(156b)**.

P(1)–F(2)	1.519(4)	N(1)–C(11)	1.325(5)
P(1)–F(6)	1.526(5)	N(1)–C(13)	1.379(5)
P(1)–F(4)	1.562(4)	N(1)–C(10)	1.481(5)
P(1)–F(1)	1.562(6)	N(2)–C(11)	1.335(5)
P(1)–F(5)	1.575(4)	N(2)–C(12)	1.380(5)
P(1)–F(3)	1.582(4)	N(2)–C(14)	1.465(6)
P(2)–F(12)	1.567(3)	N(3)–C(20)	1.321(5)
P(2)–F(7)	1.569(3)	N(3)–C(22)	1.372(6)
P(2)–F(8)	1.586(3)	N(3)–C(19)	1.481(5)
P(2)–F(11)	1.599(3)	N(4)–C(20)	1.326(6)
P(2)–F(9)	1.600(3)	N(4)–C(21)	1.363(5)
P(2)–F(10)	1.600(3)	N(4)–C(23)	1.495(5)
P(3)–F(17)	1.571(3)	N(5)–C(29)	1.329(6)
P(3)–F(15)	1.576(3)	N(5)–C(31)	1.380(6)
P(3)–F(14)	1.590(3)	N(5)–C(28)	1.479(6)
P(3)–F(16)	1.594(3)	N(6)–C(29)	1.324(6)
P(3)–F(18)	1.599(3)	N(6)–C(30)	1.373(6)
P(3)–F(13)	1.607(3)	N(6)–C(32)	1.479(6)
P(4)–F(21)	1.572(3)	C(1)–C(2)	1.400(6)
P(4)–F(24)	1.589(3)	C(1)–C(6)	1.401(6)
P(4)–F(22)	1.593(3)	C(1)–C(28)	1.517(6)
P(4)–F(23)	1.595(3)	C(2)–C(3)	1.390(6)
P(4)–F(20)	1.596(3)	C(2)–C(7)	1.510(6)
P(4)–F(19)	1.612(3)	C(3)–C(4)	1.408(6)
P(5)–F(25)	1.557(5)	C(3)–C(10)	1.511(6)
P(5)–F(27)	1.559(3)	C(4)–C(5)	1.393(6)
P(5)–F(28)	1.566(4)	C(4)–C(8)	1.518(6)
P(5)–F(26)	1.581(4)	C(5)–C(6)	1.397(6)
P(5)–F(29)	1.589(3)	C(5)–C(19)	1.518(6)
P(5)–F(30)	1.596(4)	C(6)–C(9)	1.518(6)
P(6)–F(35)	1.465(9)	C(7)–H(7A)	0.9800
P(6)–F(34)	1.509(5)	C(7)–H(7B)	0.9800
P(6)–F(31)	1.511(6)	C(7)–H(7C)	0.9800
P(6)–F(36)	1.567(5)	C(8)–H(8A)	0.9800
P(6)–F(33)	1.577(8)	C(8)–H(8B)	0.9800

P(6)–F(32)	1.581(4)	C(8)–H(8C)	0.9800
C(9)–H(9A)	0.9800	C(25)–C(27)	1.508(7)
C(9)–H(9B)	0.9800	C(25)–C(26)	1.536(7)
C(9)–H(9C)	0.9800	C(25)–H(25)	1.0000
C(10)–H(10A)	0.9900	C(26)–H(26A)	0.9800
C(10)–H(10B)	0.9900	C(26)–H(26B)	0.9800
C(11)–H(11)	0.9500	C(26)–H(26C)	0.9800
C(12)–C(13)	1.345(6)	C(27)–H(27A)	0.9800
C(12)–H(12)	0.9500	C(27)–H(27B)	0.9800
C(13)–H(13)	0.9500	C(27)–H(27C)	0.9800
C(14)–C(16)	1.523(7)	C(28)–H(28A)	0.9900
C(14)–C(15)	1.529(7)	C(28)–H(28B)	0.9900
C(14)–H(14)	1.0000	C(29)–H(29)	0.9500
C(15)–H(15A)	0.9800	C(30)–C(31)	1.360(7)
C(15)–H(15B)	0.9800	C(30)–H(30)	0.9500
C(15)–H(15C)	0.9800	C(31)–H(31)	0.9500
C(16)–C(18)	1.519(7)	C(32)–C(33)	1.523(7)
C(16)–C(17)	1.528(7)	C(32)–C(34)	1.532(7)
C(16)–H(16)	1.0000	C(32)–H(32)	1.0000
C(17)–H(17A)	0.9800	C(33)–H(33A)	0.9800
C(17)–H(17B)	0.9800	C(33)–H(33B)	0.9800
C(17)–H(17C)	0.9800	C(33)–H(33C)	0.9800
C(18)–H(18A)	0.9800	C(34)–C(35)	1.499(8)
C(18)–H(18B)	0.9800	C(34)–C(36)	1.527(7)
C(18)–H(18C)	0.9800	C(34)–H(34)	1.0000
C(19)–H(19A)	0.9900	C(35)–H(35A)	0.9800
C(19)–H(19B)	0.9900	C(35)–H(35B)	0.9800
C(20)–H(20)	0.9500	C(35)–H(35C)	0.9800
C(21)–C(22)	1.350(6)	C(36)–H(36A)	0.9800
C(21)–H(21)	0.9500	C(36)–H(36B)	0.9800
C(22)–H(22)	0.9500	C(36)–H(36C)	0.9800
C(23)–C(24)	1.508(7)		
C(23)–C(25)	1.530(6)		
C(23)–H(23)	1.0000		
C(24)–H(24A)	0.9800		
C(24)–H(24B)	0.9800		
C(24)–H(24C)	0.9800		

F(2)–P(1)–F(6)	102.3(5)	F(15)–P(3)–F(16)	179.6(2)
F(2)–P(1)–F(4)	94.3(2)	F(14)–P(3)–F(16)	89.0(2)
F(6)–P(1)–F(4)	101.2(4)	F(17)–P(3)–F(18)	90.6(2)
F(2)–P(1)–F(1)	81.9(5)	F(15)–P(3)–F(18)	89.76(18)
F(6)–P(1)–F(1)	174.2(4)	F(14)–P(3)–F(18)	89.53(18)
F(4)–P(1)–F(1)	82.3(4)	F(16)–P(3)–F(18)	90.00(17)
F(2)–P(1)–F(5)	171.4(4)	F(17)–P(3)–F(13)	90.73(19)
F(6)–P(1)–F(5)	85.5(4)	F(15)–P(3)–F(13)	90.56(17)
F(4)–P(1)–F(5)	87.7(2)	F(14)–P(3)–F(13)	89.13(16)
F(1)–P(1)–F(5)	90.1(4)	F(16)–P(3)–F(13)	89.67(15)
F(2)–P(1)–F(3)	86.8(2)	F(18)–P(3)–F(13)	178.62(18)
F(6)–P(1)–F(3)	84.7(4)	F(21)–P(4)–F(24)	179.29(19)
F(4)–P(1)–F(3)	173.7(4)	F(21)–P(4)–F(22)	90.10(17)
F(1)–P(1)–F(3)	91.6(4)	F(24)–P(4)–F(22)	90.44(19)
F(5)–P(1)–F(3)	90.4(3)	F(21)–P(4)–F(23)	89.92(18)
F(12)–P(2)–F(7)	91.1(2)	F(24)–P(4)–F(23)	89.61(17)
F(12)–P(2)–F(8)	179.3(2)	F(22)–P(4)–F(23)	89.51(15)
F(7)–P(2)–F(8)	89.6(2)	F(21)–P(4)–F(20)	91.27(17)
F(12)–P(2)–F(11)	89.9(2)	F(24)–P(4)–F(20)	89.21(15)
F(7)–P(2)–F(11)	178.6(2)	F(22)–P(4)–F(20)	89.78(15)
F(8)–P(2)–F(11)	89.4(2)	F(23)–P(4)–F(20)	178.62(19)
F(12)–P(2)–F(9)	90.58(18)	F(21)–P(4)–F(19)	89.19(18)
F(7)–P(2)–F(9)	92.28(18)	F(24)–P(4)–F(19)	90.3(2)
F(8)–P(2)–F(9)	89.24(17)	F(22)–P(4)–F(19)	179.3(2)
F(11)–P(2)–F(9)	88.73(16)	F(23)–P(4)–F(19)	90.42(16)
F(12)–P(2)–F(10)	89.69(17)	F(20)–P(4)–F(19)	90.30(16)
F(7)–P(2)–F(10)	89.15(18)	F(25)–P(5)–F(27)	93.2(3)
F(8)–P(2)–F(10)	90.47(17)	F(25)–P(5)–F(28)	176.6(3)
F(11)–P(2)–F(10)	89.85(16)	F(27)–P(5)–F(28)	90.0(2)
F(9)–P(2)–F(10)	178.55(18)	F(25)–P(5)–F(26)	89.1(3)
F(17)–P(3)–F(15)	90.0(3)	F(27)–P(5)–F(26)	89.0(2)
F(17)–P(3)–F(14)	179.3(3)	F(28)–P(5)–F(26)	89.8(3)
F(15)–P(3)–F(14)	90.7(3)	F(25)–P(5)–F(29)	91.8(3)
F(17)–P(3)–F(16)	90.4(2)	F(27)–P(5)–F(29)	92.2(2)
F(28)–P(5)–F(29)	89.3(2)	C(31)–N(5)–C(28)	126.5(4)
F(26)–P(5)–F(29)	178.5(3)	C(29)–N(6)–C(30)	108.6(4)
F(25)–P(5)–F(30)	87.9(3)	C(29)–N(6)–C(32)	125.0(4)

F(27)–P(5)–F(30)	178.2(3)	C(30)–N(6)–C(32)	126.4(4)
F(28)–P(5)–F(30)	88.8(3)	C(2)–C(1)–C(6)	121.2(4)
F(26)–P(5)–F(30)	89.6(2)	C(2)–C(1)–C(28)	118.6(4)
F(29)–P(5)–F(30)	89.2(2)	C(6)–C(1)–C(28)	120.1(4)
F(35)–P(6)–F(34)	96.0(8)	C(3)–C(2)–C(1)	118.7(4)
F(35)–P(6)–F(31)	88.5(9)	C(3)–C(2)–C(7)	119.9(4)
F(34)–P(6)–F(31)	175.3(8)	C(1)–C(2)–C(7)	121.4(4)
F(35)–P(6)–F(36)	88.6(5)	C(2)–C(3)–C(4)	121.3(4)
F(34)–P(6)–F(36)	89.1(3)	C(2)–C(3)–C(10)	119.3(4)
F(31)–P(6)–F(36)	92.3(3)	C(4)–C(3)–C(10)	119.3(4)
F(35)–P(6)–F(33)	179.3(8)	C(5)–C(4)–C(3)	118.7(4)
F(34)–P(6)–F(33)	83.3(5)	C(5)–C(4)–C(8)	120.9(4)
F(31)–P(6)–F(33)	92.1(8)	C(3)–C(4)–C(8)	120.3(4)
F(36)–P(6)–F(33)	91.1(4)	C(4)–C(5)–C(6)	121.1(4)
F(35)–P(6)–F(32)	91.7(4)	C(4)–C(5)–C(19)	118.7(4)
F(34)–P(6)–F(32)	90.3(2)	C(6)–C(5)–C(19)	120.0(4)
F(31)–P(6)–F(32)	88.2(3)	C(5)–C(6)–C(1)	118.9(4)
F(36)–P(6)–F(32)	179.4(3)	C(5)–C(6)–C(9)	120.9(4)
F(33)–P(6)–F(32)	88.6(3)	C(1)–C(6)–C(9)	120.2(4)
C(11)–N(1)–C(13)	108.5(3)	C(2)–C(7)–H(7A)	109.5
C(11)–N(1)–C(10)	124.4(3)	C(2)–C(7)–H(7B)	109.5
C(13)–N(1)–C(10)	127.0(3)	H(7A)–C(7)–H(7B)	109.5
C(11)–N(2)–C(12)	108.4(3)	C(2)–C(7)–H(7C)	109.5
C(11)–N(2)–C(14)	125.1(4)	H(7A)–C(7)–H(7C)	109.5
C(12)–N(2)–C(14)	126.3(4)	H(7B)–C(7)–H(7C)	109.5
C(20)–N(3)–C(22)	107.9(3)	C(4)–C(8)–H(8A)	109.5
C(20)–N(3)–C(19)	125.8(3)	C(4)–C(8)–H(8B)	109.5
C(22)–N(3)–C(19)	126.2(3)	H(8A)–C(8)–H(8B)	109.5
C(20)–N(4)–C(21)	108.1(4)	C(4)–C(8)–H(8C)	109.5
C(20)–N(4)–C(23)	125.3(3)	H(8A)–C(8)–H(8C)	109.5
C(21)–N(4)–C(23)	126.5(4)	H(8B)–C(8)–H(8C)	109.5
C(29)–N(5)–C(31)	108.1(4)	C(6)–C(9)–H(9A)	109.5
C(29)–N(5)–C(28)	125.3(3)	C(6)–C(9)–H(9B)	109.5
H(9A)–C(9)–H(9B)	109.5	C(17)–C(16)–H(16)	108.3
C(6)–C(9)–H(9C)	109.5	C(16)–C(17)–H(17A)	109.5
H(9A)–C(9)–H(9C)	109.5	C(16)–C(17)–H(17B)	109.5
H(9B)–C(9)–H(9C)	109.5	H(17A)–C(17)–H(17B)	109.5

N(1)–C(10)–C(3)	111.5(3)	C(16)–C(17)–H(17C)	109.5
N(1)–C(10)–H(10A)	109.3	H(17A)–C(17)–H(17C)	109.5
C(3)–C(10)–H(10A)	109.3	H(17B)–C(17)–H(17C)	109.5
N(1)–C(10)–H(10B)	109.3	C(16)–C(18)–H(18A)	109.5
C(3)–C(10)–H(10B)	109.3	C(16)–C(18)–H(18B)	109.5
H(10A)–C(10)–H(10B)	108.0	H(18A)–C(18)–H(18B)	109.5
N(1)–C(11)–N(2)	108.7(4)	C(16)–C(18)–H(18C)	109.5
N(1)–C(11)–H(11)	125.7	H(18A)–C(18)–H(18C)	109.5
N(2)–C(11)–H(11)	125.7	H(18B)–C(18)–H(18C)	109.5
C(13)–C(12)–N(2)	106.9(4)	N(3)–C(19)–C(5)	109.2(3)
C(13)–C(12)–H(12)	126.5	N(3)–C(19)–H(19A)	109.8
N(2)–C(12)–H(12)	126.5	C(5)–C(19)–H(19A)	109.8
C(12)–C(13)–N(1)	107.5(4)	N(3)–C(19)–H(19B)	109.8
C(12)–C(13)–H(13)	126.3	C(5)–C(19)–H(19B)	109.8
N(1)–C(13)–H(13)	126.3	H(19A)–C(19)–H(19B)	108.3
N(2)–C(14)–C(16)	110.7(4)	N(3)–C(20)–N(4)	109.5(4)
N(2)–C(14)–C(15)	107.5(4)	N(3)–C(20)–H(20)	125.3
C(16)–C(14)–C(15)	114.6(4)	N(4)–C(20)–H(20)	125.3
N(2)–C(14)–H(14)	107.9	C(22)–C(21)–N(4)	107.3(4)
C(16)–C(14)–H(14)	107.9	C(22)–C(21)–H(21)	126.4
C(15)–C(14)–H(14)	107.9	N(4)–C(21)–H(21)	126.4
C(14)–C(15)–H(15A)	109.5	C(21)–C(22)–N(3)	107.2(4)
C(14)–C(15)–H(15B)	109.5	C(21)–C(22)–H(22)	126.4
H(15A)–C(15)–H(15B)	109.5	N(3)–C(22)–H(22)	126.4
C(14)–C(15)–H(15C)	109.5	N(4)–C(23)–C(24)	108.8(4)
H(15A)–C(15)–H(15C)	109.5	N(4)–C(23)–C(25)	109.7(3)
H(15B)–C(15)–H(15C)	109.5	C(24)–C(23)–C(25)	116.3(4)
C(18)–C(16)–C(14)	112.0(4)	N(4)–C(23)–H(23)	107.2
C(18)–C(16)–C(17)	109.4(4)	C(24)–C(23)–H(23)	107.2
C(14)–C(16)–C(17)	110.4(5)	C(25)–C(23)–H(23)	107.2
C(18)–C(16)–H(16)	108.3	C(23)–C(24)–H(24A)	109.5
C(14)–C(16)–H(16)	108.3	C(23)–C(24)–H(24B)	109.5
H(24A)–C(24)–H(24B)	109.5	N(5)–C(31)–H(31)	126.5
C(23)–C(24)–H(24C)	109.5	N(6)–C(32)–C(33)	109.1(4)
H(24A)–C(24)–H(24C)	109.5	N(6)–C(32)–C(34)	110.0(4)
H(24B)–C(24)–H(24C)	109.5	C(33)–C(32)–C(34)	114.5(4)
C(27)–C(25)–C(23)	112.3(4)	N(6)–C(32)–H(32)	107.7

C(27)–C(25)–C(26)	110.9(5)	C(33)–C(32)–H(32)	107.7
C(23)–C(25)–C(26)	108.6(4)	C(34)–C(32)–H(32)	107.7
C(27)–C(25)–H(25)	108.3	C(32)–C(33)–H(33A)	109.5
C(23)–C(25)–H(25)	108.3	C(32)–C(33)–H(33B)	109.5
C(26)–C(25)–H(25)	108.3	H(33A)–C(33)–H(33B)	109.5
C(25)–C(26)–H(26A)	109.5	C(32)–C(33)–H(33C)	109.5
C(25)–C(26)–H(26B)	109.5	H(33A)–C(33)–H(33C)	109.5
H(26A)–C(26)–H(26B)	109.5	H(33B)–C(33)–H(33C)	109.5
C(25)–C(26)–H(26C)	109.5	C(35)–C(34)–C(36)	110.4(5)
H(26A)–C(26)–H(26C)	109.5	C(35)–C(34)–C(32)	111.8(4)
H(26B)–C(26)–H(26C)	109.5	C(36)–C(34)–C(32)	109.5(4)
C(25)–C(27)–H(27A)	109.5	C(35)–C(34)–H(34)	108.3
C(25)–C(27)–H(27B)	109.5	C(36)–C(34)–H(34)	108.3
H(27A)–C(27)–H(27B)	109.5	C(32)–C(34)–H(34)	108.3
C(25)–C(27)–H(27C)	109.5	C(34)–C(35)–H(35A)	109.5
H(27A)–C(27)–H(27C)	109.5	C(34)–C(35)–H(35B)	109.5
H(27B)–C(27)–H(27C)	109.5	H(35A)–C(35)–H(35B)	109.5
N(5)–C(28)–C(1)	110.8(3)	C(34)–C(35)–H(35C)	109.5
N(5)–C(28)–H(28A)	109.5	H(35A)–C(35)–H(35C)	109.5
C(1)–C(28)–H(28A)	109.5	H(35B)–C(35)–H(35C)	109.5
N(5)–C(28)–H(28B)	109.5	C(34)–C(36)–H(36A)	109.5
C(1)–C(28)–H(28B)	109.5	C(34)–C(36)–H(36B)	109.5
H(28A)–C(28)–H(28B)	108.1	H(36A)–C(36)–H(36B)	109.5
N(6)–C(29)–N(5)	109.3(4)	C(34)–C(36)–H(36C)	109.5
N(6)–C(29)–H(29)	125.4	H(36A)–C(36)–H(36C)	109.5
N(5)–C(29)–H(29)	125.4	H(36B)–C(36)–H(36C)	109.5
C(31)–C(30)–N(6)	107.0(4)		
C(31)–C(30)–H(30)	126.5		
N(6)–C(30)–H(30)	126.5		
C(30)–C(31)–N(5)	107.0(4)		
C(30)–C(31)–H(31)	126.5		

Table 6. Torsion angles (°) for **(156b)**.

C(6)–C(1)–C(2)–C(3)	–0.9(6)	C(10)–N(1)–C(13)–C(12)	176.4(4)
C(28)–C(1)–C(2)–C(3)	179.2(4)	C(11)–N(2)–C(14)–C(16)	114.1(5)
C(6)–C(1)–C(2)–C(7)	179.8(4)	C(12)–N(2)–C(14)–C(16)	–61.7(6)
C(28)–C(1)–C(2)–C(7)	–0.1(6)	C(11)–N(2)–C(14)–C(15)	–120.0(5)
C(1)–C(2)–C(3)–C(4)	–0.5(6)	C(12)–N(2)–C(14)–C(15)	64.2(6)
C(7)–C(2)–C(3)–C(4)	178.8(4)	N(2)–C(14)–C(16)–C(18)	–53.1(5)
C(1)–C(2)–C(3)–C(10)	176.7(3)	C(15)–C(14)–C(16)–C(18)	–174.9(4)
C(7)–C(2)–C(3)–C(10)	–3.9(6)	N(2)–C(14)–C(16)–C(17)	–175.3(4)
C(2)–C(3)–C(4)–C(5)	3.1(6)	C(15)–C(14)–C(16)–C(17)	63.0(6)
C(10)–C(3)–C(4)–C(5)	–174.2(3)	C(20)–N(3)–C(19)–C(5)	140.2(4)
C(2)–C(3)–C(4)–C(8)	–174.6(4)	C(22)–N(3)–C(19)–C(5)	–37.2(5)
C(10)–C(3)–C(4)–C(8)	8.1(6)	C(4)–C(5)–C(19)–N(3)	–58.7(5)
C(3)–C(4)–C(5)–C(6)	–4.2(6)	C(6)–C(5)–C(19)–N(3)	116.8(4)
C(8)–C(4)–C(5)–C(6)	173.4(4)	C(22)–N(3)–C(20)–N(4)	–0.2(5)
C(3)–C(4)–C(5)–C(19)	171.2(3)	C(19)–N(3)–C(20)–N(4)	–178.1(4)
C(8)–C(4)–C(5)–C(19)	–11.1(6)	C(21)–N(4)–C(20)–N(3)	0.6(5)
C(4)–C(5)–C(6)–C(1)	2.9(6)	C(23)–N(4)–C(20)–N(3)	177.4(4)
C(19)–C(5)–C(6)–C(1)	–172.5(3)	C(20)–N(4)–C(21)–C(22)	–0.8(5)
C(4)–C(5)–C(6)–C(9)	–174.6(4)	C(23)–N(4)–C(21)–C(22)	–177.5(4)
C(19)–C(5)–C(6)–C(9)	10.0(6)	N(4)–C(21)–C(22)–N(3)	0.7(5)
C(2)–C(1)–C(6)–C(5)	–0.2(6)	C(20)–N(3)–C(22)–C(21)	–0.3(5)
C(28)–C(1)–C(6)–C(5)	179.6(4)	C(19)–N(3)–C(22)–C(21)	177.6(4)
C(2)–C(1)–C(6)–C(9)	177.3(4)	C(20)–N(4)–C(23)–C(24)	63.6(5)
C(28)–C(1)–C(6)–C(9)	–2.9(6)	C(21)–N(4)–C(23)–C(24)	–120.2(5)
C(11)–N(1)–C(10)–C(3)	–162.3(4)	C(20)–N(4)–C(23)–C(25)	–64.7(5)
C(13)–N(1)–C(10)–C(3)	22.9(6)	C(21)–N(4)–C(23)–C(25)	111.5(5)
C(2)–C(3)–C(10)–N(1)	85.3(4)	N(4)–C(23)–C(25)–C(27)	–57.1(5)
C(4)–C(3)–C(10)–N(1)	–97.4(4)	C(24)–C(23)–C(25)–C(27)	178.8(5)
C(13)–N(1)–C(11)–N(2)	–0.4(5)	N(4)–C(23)–C(25)–C(26)	179.8(4)
C(10)–N(1)–C(11)–N(2)	–176.0(4)	C(24)–C(23)–C(25)–C(26)	55.8(6)
C(12)–N(2)–C(11)–N(1)	–0.3(5)	C(29)–N(5)–C(28)–C(1)	–23.1(6)
C(14)–N(2)–C(11)–N(1)	–176.7(4)	C(31)–N(5)–C(28)–C(1)	156.3(4)
C(11)–N(2)–C(12)–C(13)	0.9(5)	C(2)–C(1)–C(28)–N(5)	–77.6(5)
C(14)–N(2)–C(12)–C(13)	177.2(4)	C(6)–C(1)–C(28)–N(5)	102.6(4)
N(2)–C(12)–C(13)–N(1)	–1.1(5)	C(30)–N(6)–C(29)–N(5)	1.5(5)
C(11)–N(1)–C(13)–C(12)	1.0(5)	C(32)–N(6)–C(29)–N(5)	–176.2(4)

C(31)–N(5)–C(29)–N(6)	–1.6(5)
C(28)–N(5)–C(29)–N(6)	177.9(4)
C(29)–N(6)–C(30)–C(31)	–0.9(5)
C(32)–N(6)–C(30)–C(31)	176.8(4)
N(6)–C(30)–C(31)–N(5)	–0.1(5)
C(29)–N(5)–C(31)–C(30)	1.0(5)
C(28)–N(5)–C(31)–C(30)	–178.5(4)
C(29)–N(6)–C(32)–C(33)	–127.7(5)
C(30)–N(6)–C(32)–C(33)	55.0(6)
C(29)–N(6)–C(32)–C(34)	105.9(5)
C(30)–N(6)–C(32)–C(34)	–71.4(6)
N(6)–C(32)–C(34)–C(35)	–57.6(5)
C(33)–C(32)–C(34)–C(35)	179.1(5)
N(6)–C(32)–C(34)–C(36)	179.7(4)
C(33)–C(32)–C(34)–C(36)	56.4(6)

Table 7. Anisotropic displacement parameters ($Å^2 x\ 10^3$) for **(156b)**. The anisotropic displacement factor exponent takes the form: $-2\pi^2[\ h^2\ a^{*2}U^{11} + \ldots + 2\ h\ k\ a^*\ b^*\ U^{12}\ ]$.

Atom	U^{11}	U^{22}	U^{33}	U^{23}	U^{13}	U^{12}
P(1)	34(1)	50(1)	27(1)	–12(1)	–3(1)	–1(1)
F(1)	128(5)	201(7)	198(7)	–90(6)	–36(5)	99(5)
F(2)	78(3)	309(9)	41(2)	–15(3)	3(2)	–106(4)
F(3)	48(2)	241(7)	84(3)	–83(4)	–14(2)	–8(3)
F(4)	95(3)	232(6)	50(2)	–49(3)	3(2)	–99(4)
F(5)	52(2)	179(5)	70(3)	24(3)	–15(2)	–28(3)
F(6)	151(6)	78(4)	290(10)	–87(5)	–23(6)	34(4)
P(2)	27(1)	33(1)	27(1)	–8(1)	–4(1)	1(1)
F(7)	91(3)	58(2)	83(2)	–38(2)	–39(2)	39(2)
F(8)	42(2)	87(3)	44(2)	9(2)	–5(1)	–14(2)=
F(9)	51(2)	51(2)	40(2)	–19(1)	–17(1)	–2(1)
F(10)	37(1)	64(2)	46(2)	–22(1)	–17(1)	3(1)

F(11)	70(2)	70(2)	81(2)	–50(2)	–42(2)	37(2)
F(12)	51(2)	123(3)	38(2)	18(2)	–9(2)	–42(2)
P(3)	30(1)	26(1)	41(1)	–12(1)	–1(1)	3(1)
F(13)	40(1)	25(1)	43(1)	–9(1)	4(1)	–1(1)
F(14)	84(2)	46(2)	67(2)	17(2)	–33(2)	–20(2)
F(15)	76(2)	73(3)	114(3)	–60(2)	49(2)	–25(2)
F(16)	37(2)	70(2)	82(2)	–53(2)	2(1)	–4(1)
F(17)	58(2)	80(3)	97(3)	17(2)	–37(2)	7(2)
F(18)	33(2)	49(2)	89(2)	–28(2)	–1(2)	–5(1)
P(4)	26(1)	24(1)	46(1)	–13(1)	–10(1)	4(1)
F(19)	38(2)	37(2)	97(3)	–24(2)	–16(2)	–3(1)
F(20)	36(1)	40(2)	53(2)	–22(1)	–5(1)	9(1)
F(21)	57(2)	48(2)	48(2)	3(1)	–19(1)	–1(1)
F(22)	42(2)	21(1)	77(2)	–13(1)	–1(1)	–1(1)
F(23)	31(1)	36(2)	92(2)	–35(2)	–18(1)	11(1)
F(24)	52(2)	89(2)	45(2)	–28(2)	–13(1)	30(2)
P(5)	55(1)	29(1)	45(1)	0(1)	–18(1)	–3(1)
F(25)	202(6)	139(5)	81(3)	–60(3)	–54(4)	18(4)
F(26)	87(3)	46(2)	138(4)	8(2)	–60(3)	10(2)
F(27)	74(2)	48(2)	86(3)	6(2)	–14(2)	–19(2)
F(28)	102(3)	101(3)	46(2)	–9(2)	9(2)	22(2)
F(29)	57(2)	55(2)	96(3)	–23(2)	–24(2)	8(2)
F(30)	94(3)	35(2)	194(5)	19(2)	–76(3)	–15(2)
P(6)	41(1)	129(2)	77(1)	–69(1)	–10(1)	9(1)
F(31)	102(5)	610(20)	292(11)	–363(14)	102(6)	–143(9)
F(32)	62(2)	73(2)	65(2)	–38(2)	–16(2)	9(2)
F(33)	299(11)	136(6)	195(7)	16(5)	–131(8)	–139(7)
F(34)	78(3)	263(8)	130(4)	–147(5)	–18(3)	2(4)
F(35)	330(14)	164(8)	560(20)	–124(11)	–372(17)	138(9)
F(36)	45(2)	321(10)	199(6)	–171(7)	–11(3)	–36(4)
N(1)	27(2)	21(2)	28(2)	–9(1)	–3(1)	1(1)
N(2)	30(2)	26(2)	27(2)	–7(2)	0(1)	0(1)
N(3)	25(2)	25(2)	20(2)	–5(1)	1(1)	0(1)
N(4)	24(2)	26(2)	29(2)	–3(1)	–3(1)	3(1)
N(5)	34(2)	20(2)	30(2)	–4(1)	–8(2)	2(1)
N(6)	35(2)	27(2)	30(2)	–3(2)	–7(2)	–4(2)

C(1)	19(2)	24(2)	36(2)	–11(2)	1(2)	1(2)
C(2)	21(2)	32(2)	30(2)	–10(2)	–3(2)	0(2)
C(3)	22(2)	22(2)	31(2)	–10(2)	–2(2)	–2(2)
C(4)	21(2)	22(2)	31(2)	–10(2)	0(2)	–2(2)
C(5)	24(2)	24(2)	26(2)	–6(2)	–1(2)	0(2)
C(6)	22(2)	24(2)	31(2)	–11(2)	3(2)	1(2)
C(7)	39(2)	28(2)	35(2)	–7(2)	–10(2)	4(2)
C(8)	47(3)	25(2)	31(2)	–10(2)	–6(2)	9(2)
C(9)	48(3)	24(2)	34(2)	–7(2)	0(2)	–1(2)
C(10)	26(2)	31(2)	25(2)	–13(2)	0(2)	–3(2)
C(11)	28(2)	22(2)	29(2)	–7(2)	–1(2)	–1(2)
C(12)	29(2)	26(2)	36(2)	–11(2)	–8(2)	3(2)
C(13)	33(2)	22(2)	27(2)	–6(2)	–7(2)	–4(2)
C(14)	42(3)	35(2)	37(2)	–18(2)	0(2)	2(2)
C(15)	94(5)	54(3)	45(3)	–17(3)	0(3)	37(3)
C(16)	36(2)	56(3)	28(2)	–9(2)	–4(2)	–5(2)
C(17)	59(4)	95(5)	38(3)	–21(3)	4(2)	15(3)
C(18)	59(3)	45(3)	35(3)	–5(2)	–7(2)	3(2)
C(19)	32(2)	24(2)	29(2)	–9(2)	–1(2)	–5(2)
C(20)	28(2)	30(2)	31(2)	–10(2)	–7(2)	3(2)
C(21)	23(2)	42(3)	34(2)	–8(2)	–8(2)	4(2)
C(22)	26(2)	31(2)	29(2)	–4(2)	–2(2)	4(2)
C(23)	29(2)	28(2)	35(2)	0(2)	–3(2)	–4(2)
C(24)	50(3)	47(3)	34(2)	–6(2)	–5(2)	1(2)
C(25)	38(2)	30(2)	47(3)	–9(2)	–6(2)	1(2)
C(26)	75(4)	35(3)	71(4)	1(3)	–13(3)	4(3)
C(27)	71(4)	54(3)	69(4)	–31(3)	–24(3)	13(3)
C(28)	28(2)	24(2)	40(2)	–9(2)	–7(2)	5(2)
C(29)	35(2)	25(2)	33(2)	–6(2)	–11(2)	0(2)
C(30)	41(3)	32(2)	33(2)	–1(2)	–5(2)	–2(2)
C(31)	47(3)	23(2)	38(2)	–3(2)	–13(2)	5(2)
C(32)	34(2)	43(3)	36(2)	–5(2)	–7(2)	–3(2)
C(33)	54(3)	74(4)	59(3)	–29(3)	–1(3)	–23(3)
C(34)	40(2)	38(3)	35(2)	–6(2)	–7(2)	1(2)
C(35)	68(4)	49(3)	74(4)	–25(3)	11(3)	–13(3)
C(36)	47(3)	86(5)	51(3)	–23(3)	–5(3)	10(3)

Table 8. Hydrogen coordinates (x 10^4) and isotropic displacement parameters ($Å^2$x 10^3) for **(156b)**.

Atom	x	y	z	U(eq)
H(7A)	–1217	5792	2598	51
H(7B)	–1866	6883	2688	51
H(7C)	–2947	5851	2856	51
H(8A)	238	3259	5109	51
H(8B)	155	3016	4438	51
H(8C)	–1286	2804	4973	51
H(9A)	–866	7730	4582	54
H(9B)	–365	6833	5186	54
H(9C)	–2100	7060	5147	54
H(10A)	–1565	3195	3809	32
H(10B)	–2198	4075	3231	32
H(11)	–651	3160	2440	32
H(12)	3454	4160	2562	36
H(13)	1697	4552	3424	33
H(14)	1290	2855	1619	44
H(15A)	4148	2615	2073	97
H(15B)	3573	2001	1611	97
H(15C)	2803	1749	2344	97
H(16)	3673	4423	1305	49
H(17A)	2370	3455	475	97
H(17B)	4026	3266	665	97
H(17C)	3600	4406	221	97
H(18A)	2110	5622	695	71
H(18B)	1329	5219	1429	71
H(18C)	774	4746	897	71
H(19A)	234	4436	5600	34
H(19B)	–820	5364	5724	34
H(20)	–906	2862	6537	35
H(21)	–5124	2865	6180	40
H(22)	–3835	4512	5442	36
H(23)	–4431	1260	7071	40
H(24A)	–2016	1656	7692	68

H(24B)	–3501	951	8028	68
H(24C)	–3587	2217	7744	68
H(25)	–1355	834	6759	47
H(26A)	–3781	–654	7396	95
H(26B)	–2426	–393	7739	95
H(26C)	–2125	–991	7195	95
H(27A)	–2144	47	6026	91
H(27B)	–2644	1259	5843	91
H(27C)	–3844	317	6211	91
H(28A)	–2750	7690	3331	36
H(28B)	–2151	8035	3903	36
H(29)	1163	7352	3475	37
H(30)	1174	9904	1929	44
H(31)	–1454	9494	2456	44
H(32)	3670	7927	2889	47
H(33A)	3971	10041	2029	91
H(33B)	5201	9414	2452	91
H(33C)	3726	9800	2799	91
H(34)	3304	8593	1542	46
H(35A)	3082	6512	2432	96
H(35B)	3199	6730	1666	96
H(35C)	1782	7120	2048	96
H(36A)	5815	8667	1574	92
H(36B)	5537	7534	1468	92
H(36C)	5756	7605	2171	92
H(43A)	2307	5329	6218	71
H(43B)	2934	4472	6808	71
H(43C)	4071	5211	6227	71
H(44A)	3548	5463	8732	50
H(44B)	3256	6661	8739	50
H(44C)	4882	6340	8485	50
H(45A)	1530	9190	6930	52
H(45B)	1356	8877	6286	52
H(45C)	2902	9386	6362	52
H(46A)	2562	6782	5681	35
H(46B)	1476	7687	5810	35
H(47)	6696	9426	4969	38
H(48)	2364	9199	4826	34

H(49)	5624	7810	5824	35
H(50)	3585	10764	4043	47
H(51A)	6694	10504	3733	75
H(51B)	5624	11192	3246	75
H(51C)	5407	9924	3506	75
H(52)	5979	11504	4564	48
H(53A)	4088	12230	5165	75
H(53B)	3960	10956	5388	75
H(53C)	2834	11637	4926	75
H(54A)	3943	12709	3735	91
H(54B)	5709	12667	3541	91
H(54C)	5073	13242	4068	91
H(55A)	4143	4220	7499	40
H(55B)	4793	4642	8032	40
H(56)	796	4734	7989	37
H(57)	1286	2410	9602	50

Table 9. Bond length (Å) and angles (°) for **(179)**.

I(1)–Pd	2.6595(4)	C(13)–H(13B)	0.9900
I(2)–Pd	2.6533(5)	C(2)–C(3)	1.338(7)
Pd–C(1)	1.989(5)	C(2)–N(2)	1.378(6)
Pd–C(15)	1.999(5)	C(2)–H(2)	0.9500
C(1)–N(2)	1.352(6)	C(3)–H(3)	0.9500
C(1)–N(1)	1.360(6)	N(2)–C(14)	1.457(6)
N(1)–C(3)	1.388(6)	C(14)–H(14A)	0.9800
N(1)–C(4)	1.463(6)	C(14)–H(14B)	0.9800
C(4)–C(5)	1.539(7)	C(14)–H(14C)	0.9800
C(4)–H(4A)	0.9900	C(15)–N(3)	1.355(6)
C(4)–H(4B)	0.9900	C(15)–N(4)	1.361(6)
C(5)–C(6)	1.526(7)	N(3)–C(16)	1.370(6)
C(5)–C(13)	1.564(7)	N(3)–C(18)	1.472(6)
C(5)–H(5)	1.0000	C(18)–C(19)	1.539(6)
C(6)–C(7)	1.549(7)	C(18)–H(18A)	0.9900
C(6)–C(9)	1.564(8)	C(18)–H(18B)	0.9900
C(6)–H(6)	1.0000	C(19)–C(20)	1.538(7)
C(7)–C(8)	1.543(8)	C(19)–C(27)	1.558(7)
C(7)–H(7A)	0.9900	C(19)–H(19)	1.0000
C(7)–H(7B)	0.9900	C(20)–C(21)	1.536(7)
C(8)–C(12)	1.506(8)	C(20)–C(23)	1.561(7)
C(8)–C(9)	1.556(8)	C(20)–H(20)	1.0000
C(8)–H(8)	1.0000	C(21)–C(22)	1.547(7)
C(9)–C(10)	1.520(8)	C(21)–H(21A)	0.9900
C(9)–C(11)	1.522(9)	C(21)–H(21B)	0.9900
C(10)–H(10A)	0.9800	C(22)–C(26)	1.530(8)
C(10)–H(10B)	0.9800	C(22)–C(23)	1.560(7)
C(10)–H(10C)	0.9800	C(22)–H(22)	1.0000
C(11)–H(11A)	0.9800	C(23)–C(24)	1.523(7)
C(11)–H(11B)	0.9800	C(23)–C(25)	1.528(7)
C(11)–H(11C)	0.9800	C(24)–H(24A)	0.9800
C(12)–C(13)	1.555(8)	C(24)–H(24B)	0.9800
C(12)–H(12A)	0.9900	C(24)–H(24C)	0.9800
C(12)–H(12B)	0.9900	C(25)–H(25A)	0.9800
C(13)–H(13A)	0.9900	C(25)–H(25B)	0.9800

C(25)–H(25C)	0.9800	C(13)–C(5)–H(5)	107.1
C(26)–C(27)	1.543(7)	C(5)–C(6)–C(7)	105.8(4)
C(26)–H(26A)	0.9900	C(5)–C(6)–C(9)	114.7(4)
C(26)–H(26B)	0.9900	C(7)–C(6)–C(9)	88.0(4)
C(27)–H(27A)	0.9900	C(5)–C(6)–H(6)	115.0
C(27)–H(27B)	0.9900	C(7)–C(6)–H(6)	115.0
C(16)–C(17)	1.339(7)	C(9)–C(6)–H(6)	115.0
C(16)–H(16)	0.9500	C(8)–C(7)–C(6)	86.0(4)
C(17)–N(4)	1.382(7)	C(8)–C(7)–H(7A)	114.3
C(17)–H(17)	0.9500	C(6)–C(7)–H(7A)	114.3
N(4)–C(28)	1.467(6)	C(8)–C(7)–H(7B)	114.3
C(28)–H(28A)	0.9800	C(6)–C(7)–H(7B)	114.3
C(28)–H(28B)	0.9800	H(7A)–C(7)–H(7B)	111.5
C(28)–H(28C)	0.9800	C(12)–C(8)–C(7)	108.2(5)
		C(12)–C(8)–C(9)	112.4(5)
C(1)–Pd–C(15)	90.47(18)	C(7)–C(8)–C(9)	88.5(4)
C(1)–Pd–I(2)	170.43(13)	C(12)–C(8)–H(8)	114.9
C(15)–Pd–I(2)	86.38(13)	C(7)–C(8)–H(8)	114.9
C(1)–Pd–I(1)	90.19(12)	C(9)–C(8)–H(8)	114.9
C(15)–Pd–I(1)	170.45(14)	C(10)–C(9)–C(11)	106.9(6)
I(2)–Pd–I(1)	94.415(14)	C(10)–C(9)–C(8)	111.2(5)
N(2)–C(1)–N(1)	104.9(4)	C(11)–C(9)–C(8)	119.3(5)
N(2)–C(1)–Pd	129.3(4)	C(10)–C(9)–C(6)	112.9(5)
N(1)–C(1)–Pd	125.7(3)	C(11)–C(9)–C(6)	120.3(5)
C(1)–N(1)–C(3)	110.4(4)	C(8)–C(9)–C(6)	85.1(4)
C(1)–N(1)–C(4)	124.0(4)	C(9)–C(10)–H(10A)	109.5
C(3)–N(1)–C(4)	125.5(4)	C(9)–C(10)–H(10B)	109.5
N(1)–C(4)–C(5)	113.8(4)	H(10A)–C(10)–H(10B)	109.5
N(1)–C(4)–H(4A)	108.8	C(9)–C(10)–H(10C)	109.5
C(5)–C(4)–H(4A)	108.8	H(10A)–C(10)–H(10C)	109.5
N(1)–C(4)–H(4B)	108.8	H(10B)–C(10)–H(10C)	109.5
C(5)–C(4)–H(4B)	108.8	C(9)–C(11)–H(11A)	109.5
H(4A)–C(4)–H(4B)	107.7	C(9)–C(11)–H(11B)	109.5
C(6)–C(5)–C(4)	114.9(4)	H(11A)–C(11)–H(11B)	109.5
C(6)–C(5)–C(13)	111.0(4)	C(9)–C(11)–H(11C)	109.5
C(4)–C(5)–C(13)	109.4(4)	H(11A)–C(11)–H(11C)	109.5
C(6)–C(5)–H(5)	107.1	H(11B)–C(11)–H(11C)	109.5

C(4)–C(5)–H(5)	107.1	C(8)–C(12)–C(13)	112.3(4)
C(8)–C(12)–H(12A)	109.2	H(18A)–C(18)–H(18B)	107.9
C(13)–C(12)–H(12A)	109.2	C(20)–C(19)–C(18)	111.9(4)
C(8)–C(12)–H(12B)	109.2	C(20)–C(19)–C(27)	111.5(4)
C(13)–C(12)–H(12B)	109.2	C(18)–C(19)–C(27)	112.8(4)
H(12A)–C(12)–H(12B)	107.9	C(20)–C(19)–H(19)	106.7
C(12)–C(13)–C(5)	115.5(5)	C(18)–C(19)–H(19)	106.7
C(12)–C(13)–H(13A)	108.4	C(27)–C(19)–H(19)	106.7
C(5)–C(13)–H(13A)	108.4	C(21)–C(20)–C(19)	107.0(4)
C(12)–C(13)–H(13B)	108.4	C(21)–C(20)–C(23)	87.8(4)
C(5)–C(13)–H(13B)	108.4	C(19)–C(20)–C(23)	114.7(4)
H(13A)–C(13)–H(13B)	107.5	C(21)–C(20)–H(20)	114.7
C(3)–C(2)–N(2)	107.6(4)	C(19)–C(20)–H(20)	114.7
C(3)–C(2)–H(2)	126.2	C(23)–C(20)–H(20)	114.7
N(2)–C(2)–H(2)	126.2	C(20)–C(21)–C(22)	86.3(4)
C(2)–C(3)–N(1)	106.6(4)	C(20)–C(21)–H(21A)	114.3
C(2)–C(3)–H(3)	126.7	C(22)–C(21)–H(21A)	114.3
N(1)–C(3)–H(3)	126.7	C(20)–C(21)–H(21B)	114.3
C(1)–N(2)–C(2)	110.6(4)	C(22)–C(21)–H(21B)	114.3
C(1)–N(2)–C(14)	124.0(4)	H(21A)–C(21)–H(21B)	111.4
C(2)–N(2)–C(14)	125.4(4)	C(26)–C(22)–C(21)	108.7(4)
N(2)–C(14)–H(14A)	109.5	C(26)–C(22)–C(23)	112.2(4)
N(2)–C(14)–H(14B)	109.5	C(21)–C(22)–C(23)	87.4(4)
H(14A)–C(14)–H(14B)	109.5	C(26)–C(22)–H(22)	115.1
N(2)–C(14)–H(14C)	109.5	C(21)–C(22)–H(22)	115.1
H(14A)–C(14)–H(14C)	109.5	C(23)–C(22)–H(22)	115.1
H(14B)–C(14)–H(14C)	109.5	C(24)–C(23)–C(25)	107.2(4)
N(3)–C(15)–N(4)	104.7(4)	C(24)–C(23)–C(22)	112.3(4)
N(3)–C(15)–Pd	131.2(4)	C(25)–C(23)–C(22)	119.6(4)
N(4)–C(15)–Pd	124.1(3)	C(24)–C(23)–C(20)	110.9(4)
C(15)–N(3)–C(16)	110.6(4)	C(25)–C(23)–C(20)	120.5(4)
C(15)–N(3)–C(18)	125.4(4)	C(22)–C(23)–C(20)	85.0(4)
C(16)–N(3)–C(18)	124.0(4)	C(23)–C(24)–H(24A)	109.5
N(3)–C(18)–C(19)	111.7(4)	C(23)–C(24)–H(24B)	109.5
N(3)–C(18)–H(18A)	109.3	H(24A)–C(24)–H(24B)	109.5
C(19)–C(18)–H(18A)	109.3	C(23)–C(24)–H(24C)	109.5
N(3)–C(18)–H(18B)	109.3	H(24A)–C(24)–H(24C)	109.5
C(19)–C(18)–H(18B)	109.3	H(24B)–C(24)–H(24C)	109.5

C(23)–C(25)–H(25A)	109.5	H(27A)–C(27)–H(27B)	107.5
C(23)–C(25)–H(25B)	109.5	C(17)–C(16)–N(3)	107.7(4)
H(25A)–C(25)–H(25B)	109.5	C(17)–C(16)–H(16)	126.2
C(23)–C(25)–H(25C)	109.5	N(3)–C(16)–H(16)	126.2
H(25A)–C(25)–H(25C)	109.5	C(16)–C(17)–N(4)	106.6(4)
H(25B)–C(25)–H(25C)	109.5	C(16)–C(17)–H(17)	126.7
C(22)–C(26)–C(27)	112.9(4)	N(4)–C(17)–H(17)	126.7
C(22)–C(26)–H(26A)	109.0	C(15)–N(4)–C(17)	110.4(4)
C(27)–C(26)–H(26A)	109.0	C(15)–N(4)–C(28)	125.9(4)
C(22)–C(26)–H(26B)	109.0	C(17)–N(4)–C(28)	123.6(4)
C(27)–C(26)–H(26B)	109.0	N(4)–C(28)–H(28A)	109.5
H(26A)–C(26)–H(26B)	107.8	N(4)–C(28)–H(28B)	109.5
C(26)–C(27)–C(19)	115.3(4)	H(28A)–C(28)–H(28B)	109.5
C(26)–C(27)–H(27A)	108.4	N(4)–C(28)–H(28C)	109.5
C(19)–C(27)–H(27A)	108.4	H(28A)–C(28)–H(28C)	109.5
C(26)–C(27)–H(27B)	108.4	H(28B)–C(28)–H(28C)	109.5
C(19)–C(27)–H(27B)	108.4		

Table 10. Torsion angles (°) for **(179)**.

C(15)–Pd–C(1)–N(2)	–70.9(4)	C(4)–C(5)–C(6)–C(9)	86.2(5)
I(2)–Pd–C(1)–N(2)	–141.5(6)	C(13)–C(5)–C(6)–C(9)	–38.5(6)
I(1)–Pd–C(1)–N(2)	99.6(4)	C(5)–C(6)–C(7)–C(8)	–89.0(5)
C(15)–Pd–C(1)–N(1)	104.3(4)	C(9)–C(6)–C(7)–C(8)	26.2(4)
I(2)–Pd–C(1)–N(1)	33.7(10)	C(6)–C(7)–C(8)–C(12)	86.8(5)
I(1)–Pd–C(1)–N(1)	–85.2(4)	C(6)–C(7)–C(8)–C(9)	–26.3(4)
N(2)–C(1)–N(1)–C(3)	0.9(5)	C(12)–C(8)–C(9)–C(10)	164.3(6)
Pd–C(1)–N(1)–C(3)	–175.3(3)	C(7)–C(8)–C(9)–C(10)	–86.6(6)
N(2)–C(1)–N(1)–C(4)	–177.6(4)	C(12)–C(8)–C(9)–C(11)	39.1(7)
Pd–C(1)–N(1)–C(4)	6.3(6)	C(7)–C(8)–C(9)–C(11)	148.2(5)
C(1)–N(1)–C(4)–C(5)	96.9(5)	C(12)–C(8)–C(9)–C(6)	–83.1(5)
C(3)–N(1)–C(4)–C(5)	–81.4(6)	C(7)–C(8)–C(9)–C(6)	26.1(4)
N(1)–C(4)–C(5)–C(6)	91.6(5)	C(5)–C(6)–C(9)–C(10)	–168.5(5)
N(1)–C(4)–C(5)–C(13)	–142.9(4)	C(7)–C(6)–C(9)–C(10)	85.0(6)
C(4)–C(5)–C(6)–C(7)	–178.6(4)	C(5)–C(6)–C(9)–C(11)	–40.7(7)
C(13)–C(5)–C(6)–C(7)	56.7(6)	C(7)–C(6)–C(9)–C(11)	–147.2(5)

C(5)–C(6)–C(9)–C(8)	80.5(5)	C(26)–C(22)–C(23)–C(24)	167.3(4)
C(7)–C(6)–C(9)–C(8)	–26.0(4)	C(21)–C(22)–C(23)–C(24)	–83.6(5)
C(7)–C(8)–C(12)–C(13)	–51.7(6)	C(26)–C(22)–C(23)–C(25)	40.4(6)
C(9)–C(8)–C(12)–C(13)	44.4(7)	C(21)–C(22)–C(23)–C(25)	149.5(4)
C(8)–C(12)–C(13)–C(5)	10.4(7)	C(26)–C(22)–C(23)–C(20)	–82.1(5)
C(6)–C(5)–C(13)–C(12)	–13.1(7)	C(21)–C(22)–C(23)–C(20)	27.0(4)
C(4)–C(5)–C(13)–C(12)	–140.8(5)	C(21)–C(20)–C(23)–C(24)	84.8(5)
N(2)–C(2)–C(3)–N(1)	0.2(5)	C(19)–C(20)–C(23)–C(24)	–167.5(4)
C(1)–N(1)–C(3)–C(2)	–0.7(5)	C(21)–C(20)–C(23)–C(25)	–148.9(5)
C(4)–N(1)–C(3)–C(2)	177.7(4)	C(19)–C(20)–C(23)–C(25)	–41.2(6)
N(1)–C(1)–N(2)–C(2)	–0.7(5)	C(21)–C(20)–C(23)–C(22)	–27.2(4)
Pd–C(1)–N(2)–C(2)	175.2(3)	C(19)–C(20)–C(23)–C(22)	80.5(4)
N(1)–C(1)–N(2)–C(14)	178.6(4)	C(21)–C(22)–C(26)–C(27)	–50.8(6)
Pd–C(1)–N(2)–C(14)	–5.4(6)	C(23)–C(22)–C(26)–C(27)	44.2(6)
C(3)–C(2)–N(2)–C(1)	0.3(5)	C(22)–C(26)–C(27)–C(19)	9.6(6)
C(3)–C(2)–N(2)–C(14)	–179.0(4)	C(20)–C(19)–C(27)–C(26)	–11.9(6)
C(1)–Pd–C(15)–N(3)	–70.4(5)	C(18)–C(19)–C(27)–C(26)	–138.8(5)
I(2)–Pd–C(15)–N(3)	100.6(4)	C(15)–N(3)–C(16)–C(17)	–1.4(6)
I(1)–Pd–C(15)–N(3)	–164.3(5)	C(18)–N(3)–C(16)–C(17)	–177.9(4)
C(1)–Pd–C(15)–N(4)	113.5(4)	N(3)–C(16)–C(17)–N(4)	–0.3(6)
I(2)–Pd–C(15)–N(4)	–75.6(4)	N(3)–C(15)–N(4)–C(17)	–2.5(5)
I(1)–Pd–C(15)–N(4)	19.5(11)	Pd–C(15)–N(4)–C(17)	174.5(3)
N(4)–C(15)–N(3)–C(16)	2.4(5)	N(3)–C(15)–N(4)–C(28)	178.9(4)
Pd–C(15)–N(3)–C(16)	–174.3(4)	Pd–C(15)–N(4)–C(28)	–4.2(7)
N(4)–C(15)–N(3)–C(18)	178.9(4)	C(16)–C(17)–N(4)–C(15)	1.8(6)
Pd–C(15)–N(3)–C(18)	2.2(7)	C(16)–C(17)–N(4)–C(28)	–179.6(5)
C(15)–N(3)–C(18)–C(19)	–70.9(6)	plane(ring1)–plane(ring2)	85.0(1)
C(16)–N(3)–C(18)–C(19)	105.1(5)		
N(3)–C(18)–C(19)–C(20)	176.7(4)		
N(3)–C(18)–C(19)–C(27)	–56.6(5)		
C(18)–C(19)–C(20)–C(21)	–176.6(4)		
C(27)–C(19)–C(20)–C(21)	56.1(5)		
C(18)–C(19)–C(20)–C(23)	87.9(5)		
C(27)–C(19)–C(20)–C(23)	–39.5(6)		
C(19)–C(20)–C(21)–C(22)	–87.7(4)		
C(23)–C(20)–C(21)–C(22)	27.4(4)		
C(20)–C(21)–C(22)–C(26)	85.2(5)		
C(20)–C(21)–C(22)–C(23)	–27.5(4)		

Table 11. Atomic coordinates (x 10^4) and equivalent isotropic displacement parameters ($Å^2$x 10^3) for **(179)**. U(eq) is defined as one third of the trace of the orthogonalized U^{ij} tensor.

Atom	x	y	z	U(eq)
I(1)	3667(1)	3787(1)	1711(1)	16(1)
I(2)	7066(1)	3779(1)	1001(1)	18(1)
Pd	5342(1)	2466(1)	1326(1)	11(1)
C(1)	4262(4)	1404(3)	1676(2)	13(1)
N(1)	4254(3)	1082(3)	2300(2)	13(1)
C(4)	4961(4)	1542(4)	2825(2)	17(1)
C(5)	4180(5)	2259(3)	3235(2)	16(1)
C(6)	3546(5)	1808(4)	3828(2)	24(1)
C(7)	2796(6)	2647(5)	4151(3)	38(2)
C(8)	4012(6)	2861(4)	4534(3)	33(1)
C(9)	4386(6)	1771(4)	4450(3)	28(1)
C(10)	3827(9)	1142(5)	4983(3)	57(2)
C(11)	5772(6)	1499(4)	4399(3)	35(2)
C(12)	4819(5)	3535(4)	4134(3)	27(1)
C(13)	5020(6)	3148(4)	3434(3)	31(1)
C(2)	2967(4)	118(3)	1777(2)	16(1)
C(3)	3461(4)	283(3)	2363(2)	17(1)
N(2)	3456(4)	806(3)	1360(2)	14(1)
C(14)	3148(5)	897(4)	674(2)	21(1)
C(15)	6451(4)	1482(3)	896(2)	15(1)
N(3)	7276(4)	829(3)	1146(2)	15(1)
C(18)	7518(4)	674(3)	1841(2)	15(1)
C(19)	8234(4)	1538(3)	2143(2)	16(1)
C(20)	8422(4)	1407(4)	2877(2)	17(1)
C(21)	9068(5)	2336(4)	3127(3)	27(1)
C(22)	10324(5)	1824(4)	2958(3)	24(1)
C(23)	9634(5)	833(4)	3070(2)	19(1)
C(24)	9599(6)	545(5)	3783(3)	32(1)
C(25)	10040(5)	–69(4)	2688(2)	20(1)
C(26)	10617(5)	2004(4)	2242(3)	25(1)
C(27)	9502(5)	1755(4)	1792(3)	24(1)

C(16)	7917(5)	364(4)	660(2)	22(1)
C(17)	7482(5)	704(4)	94(2)	22(1)
N(4)	6562(4)	1381(3)	242(2)	17(1)
C(28)	5843(5)	1919(4)	–248(2)	22(1)

Table 12. Anisotropic displacement parameters ($Å^2 x\ 10^3$) for **(179)**. The anisotropic displacement factor exponent takes the form: $-2\pi^2[h^2 a^{*2} U^{11} + ... + 2 h k a^* b^* U^{12}]$

Atom	U^{11}	U^{22}	U^{33}	U^{23}	U^{13}	U^{12}
I(1)	18(1)	12(1)	18(1)	1(1)	0(1)	3(1)
I(2)	24(1)	14(1)	17(1)	–1(1)	5(1)	–6(1)
Pd	14(1)	9(1)	10(1)	0(1)	1(1)	–1(1)
C(1)	12(2)	12(2)	16(2)	–2(2)	0(2)	2(2)
N(1)	14(2)	13(2)	12(2)	1(2)	1(1)	–1(2)
C(4)	15(2)	24(3)	11(2)	–1(2)	–1(2)	–3(2)
C(5)	22(2)	11(2)	14(2)	0(2)	–5(2)	–2(2)
C(6)	26(3)	21(3)	23(3)	–5(2)	8(2)	–6(2)
C(7)	27(3)	36(4)	50(4)	–30(3)	11(3)	–2(3)
C(8)	46(4)	26(3)	26(3)	–18(2)	4(3)	–5(3)
C(9)	50(4)	18(3)	16(2)	–2(2)	1(2)	–12(2)
C(10)	116(7)	39(4)	17(3)	–3(3)	15(4)	–28(5)
C(11)	57(4)	20(3)	28(3)	–6(2)	–23(3)	4(3)
C(12)	31(3)	18(3)	33(3)	–5(2)	–11(2)	–2(2)
C(13)	42(3)	19(3)	31(3)	4(2)	–8(3)	–12(2)
C(2)	21(2)	5(2)	23(2)	–2(2)	3(2)	–2(2)
C(3)	18(2)	10(2)	23(2)	5(2)	5(2)	2(2)
N(2)	13(2)	10(2)	21(2)	–3(2)	–4(2)	0(1)
C(14)	25(3)	19(2)	19(2)	0(2)	–2(2)	–1(2)
C(15)	16(2)	10(2)	19(2)	–1(2)	4(2)	–3(2)
N(3)	16(2)	13(2)	16(2)	0(2)	2(2)	2(2)
C(18)	11(2)	16(2)	19(2)	3(2)	0(2)	–1(2)
C(19)	14(2)	14(2)	18(2)	0(2)	2(2)	2(2)
C(20)	17(2)	19(3)	15(2)	–5(2)	2(2)	0(2)
C(21)	22(3)	19(3)	39(3)	–10(2)	–4(2)	1(2)

C(22)	21(3)	20(3)	32(3)	–5(2)	–9(2)	1(2)
C(23)	13(2)	24(3)	20(2)	–1(2)	–3(2)	0(2)
C(24)	34(3)	38(3)	23(3)	4(2)	–7(3)	8(3)
C(25)	19(2)	14(2)	26(2)	1(2)	2(2)	3(2)
C(26)	13(2)	15(3)	47(3)	3(2)	4(2)	–2(2)
C(27)	25(3)	22(3)	24(3)	5(2)	7(2)	–2(2)
C(16)	26(3)	17(2)	22(2)	–4(2)	4(2)	6(2)
C(17)	31(3)	18(3)	18(2)	–8(2)	5(2)	3(2)
N(4)	27(2)	13(2)	12(2)	–2(2)	1(2)	–4(2)
C(28)	35(3)	20(3)	11(2)	–1(2)	–2(2)	2(2)

Table 13. Hydrogen coordinates (x 10^4) and isotropic displacement parameters ($Å^2$x 10^3) for **(179)**.

Atom	x	y	z	U(eq)
H(4A)	5687	1897	2638	20
H(4B)	5298	1025	3113	20
H(5)	3496	2517	2950	19
H(6)	3050	1202	3740	28
H(7A)	2541	3174	3850	45
H(7B)	2081	2427	4422	45
H(8)	3878	3073	4993	39
H(10A)	3955	451	4879	86
H(10B)	2924	1275	5020	86
H(10C)	4240	1293	5396	86
H(11A)	6165	1549	4827	53
H(11B)	6193	1946	4098	53
H(11C)	5849	829	4239	53
H(12A)	5646	3612	4348	33
H(12B)	4416	4186	4114	33
H(13A)	5913	2957	3385	37
H(13B)	4858	3688	3126	37
H(2)	2385	–382	1668	19
H(3)	3301	–77	2748	20
H(14A)	3396	1545	519	31
H(14B)	2240	810	614	31

H(14C)	3600	395	428	31
H(18A)	8016	70	1898	18
H(18B)	6708	587	2070	18
H(19)	7692	2128	2084	19
H(20)	7647	1214	3120	20
H(21A)	8946	2460	3595	32
H(21B)	8893	2927	2866	32
H(22)	11033	1961	3263	29
H(24A)	9069	–35	3837	47
H(24B)	9252	1085	4039	47
H(24C)	10454	400	3932	47
H(25A)	10857	–297	2848	29
H(25B)	10110	97	2227	29
H(25C)	9413	–587	2743	29
H(26A)	11352	1603	2115	30
H(26B)	10846	2698	2181	30
H(27A)	9732	1178	1529	28
H(27B)	9371	2308	1491	28
H(16)	8556	–115	714	26
H(17)	7753	516	–327	26
H(28A)	5112	1532	–381	33
H(28B)	6379	2044	–626	33
H(28C)	5559	2542	–66	33

Appendix II- anion titration data.

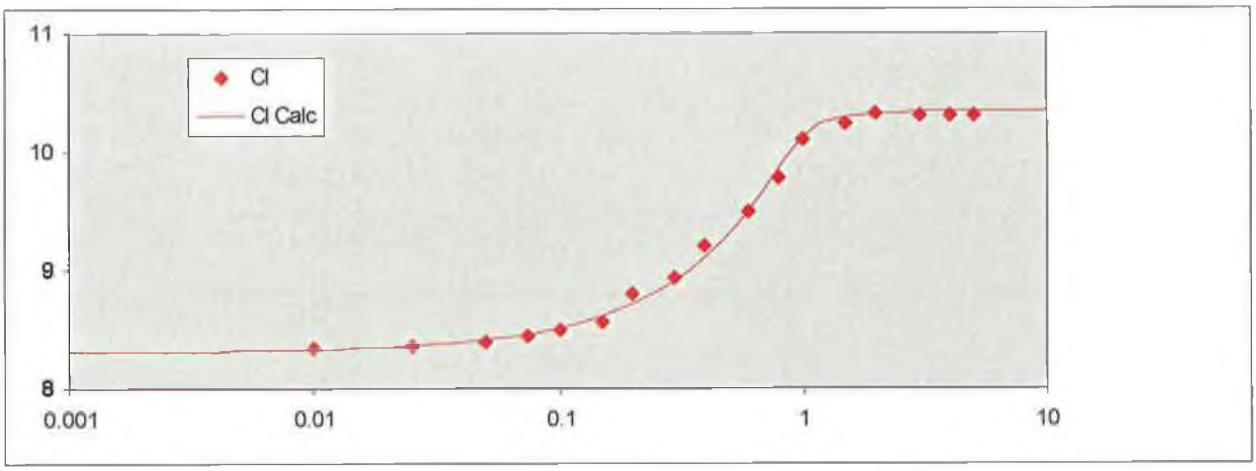
11
10
9
8
0.001
0.01
0.1
1
10
Cl
Cl Calc

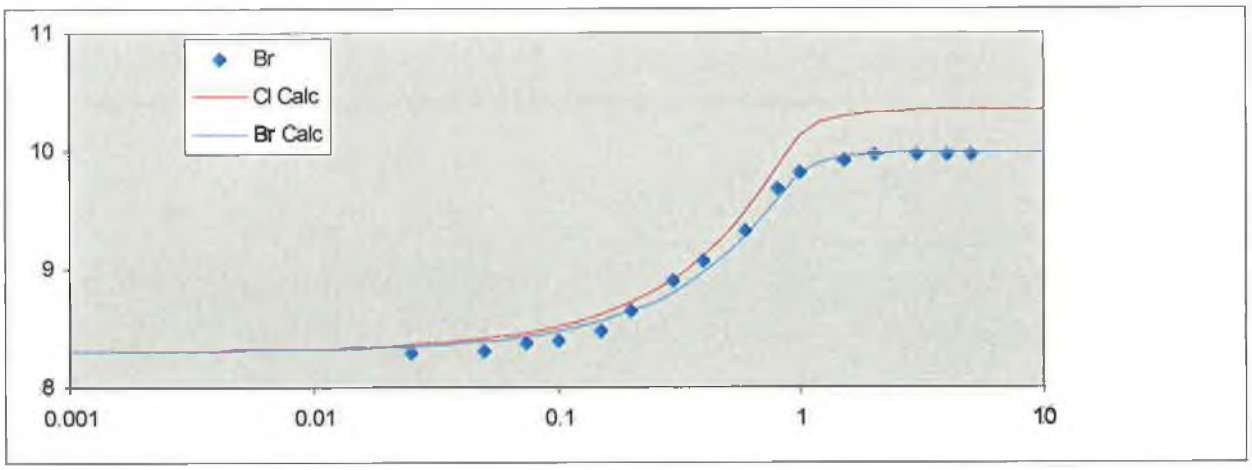
11
10
9
8
0.001
0.01
0.1
1
10
Br
Cl Calc
Br Calc

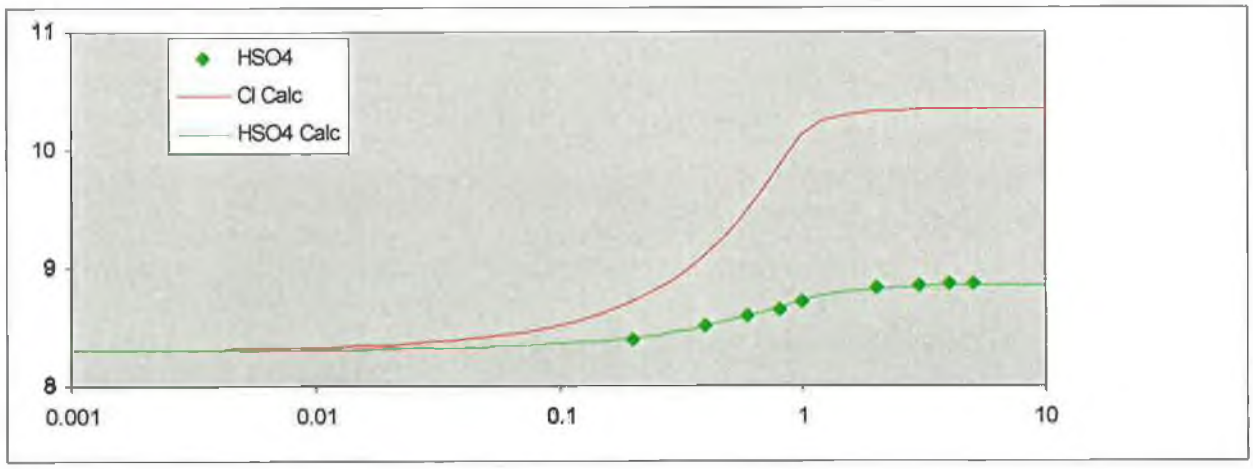
11
10
9
8
0.001
0.01
0.1
1
10
HSO4
Cl Calc
HSO4 Calc

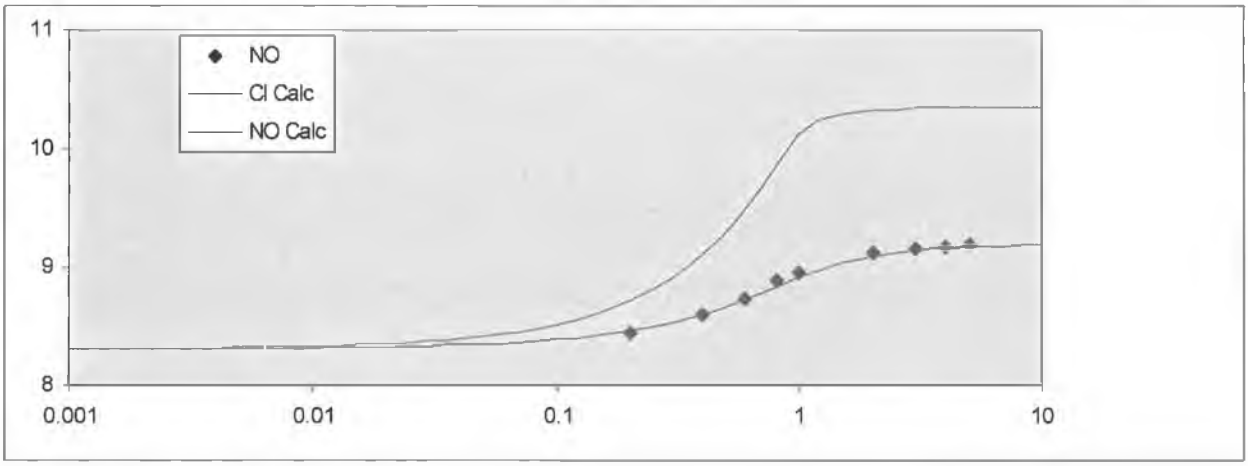

Figure 1. Experimental data and Calculated curves for receptor **(156a)**.

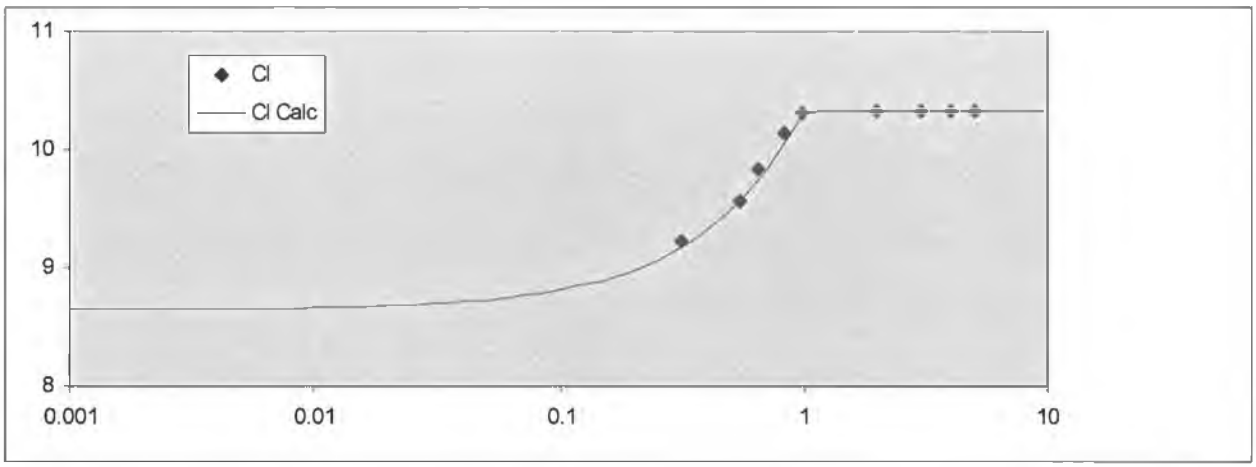

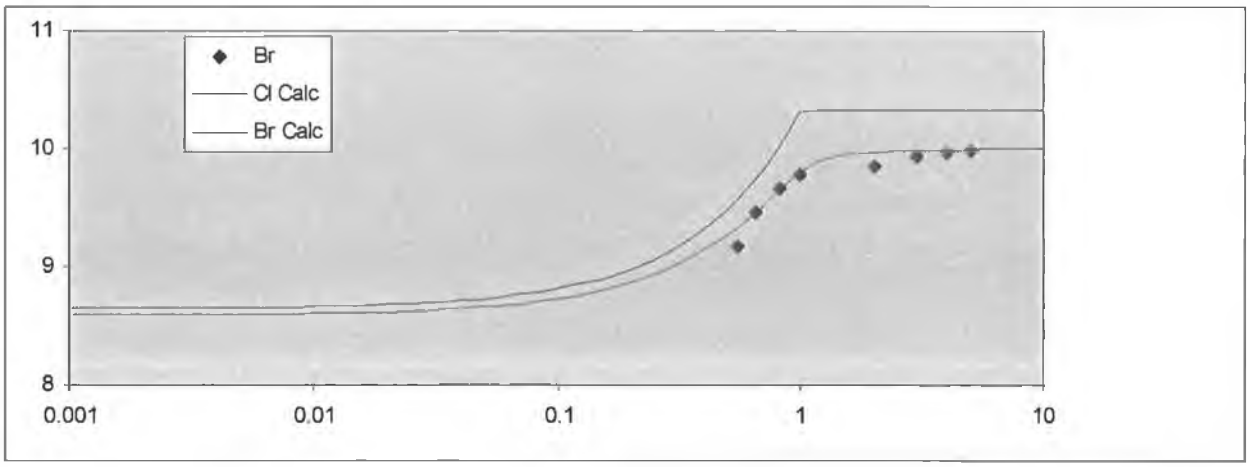

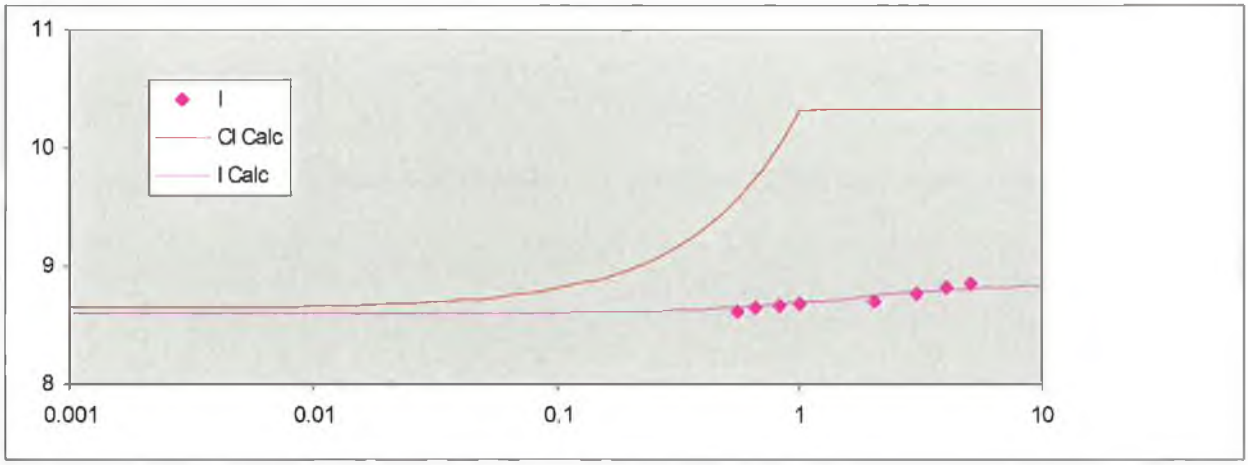

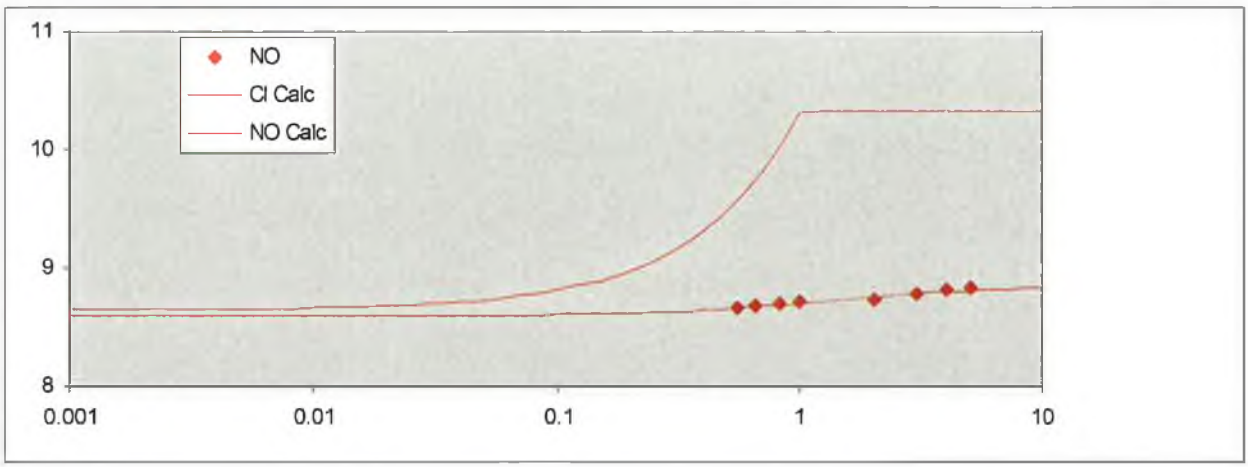

Figure 2. Experimental data and Calculated curves for receptor **(156c)**.

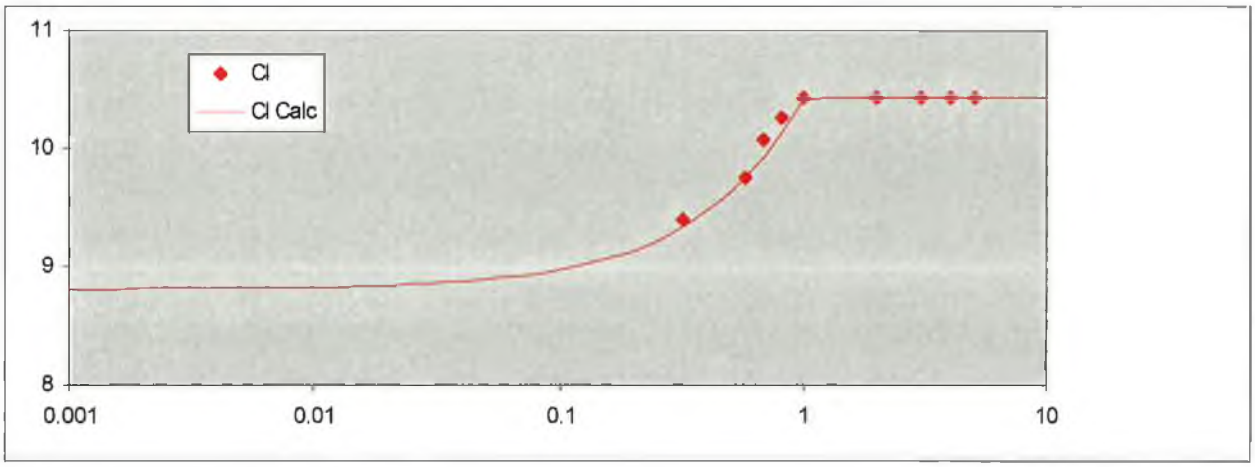

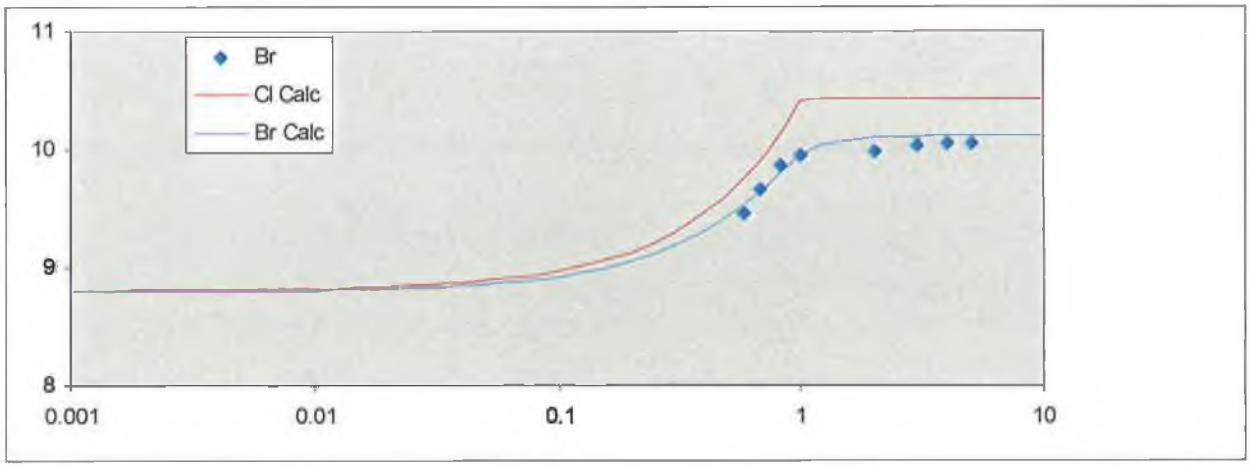

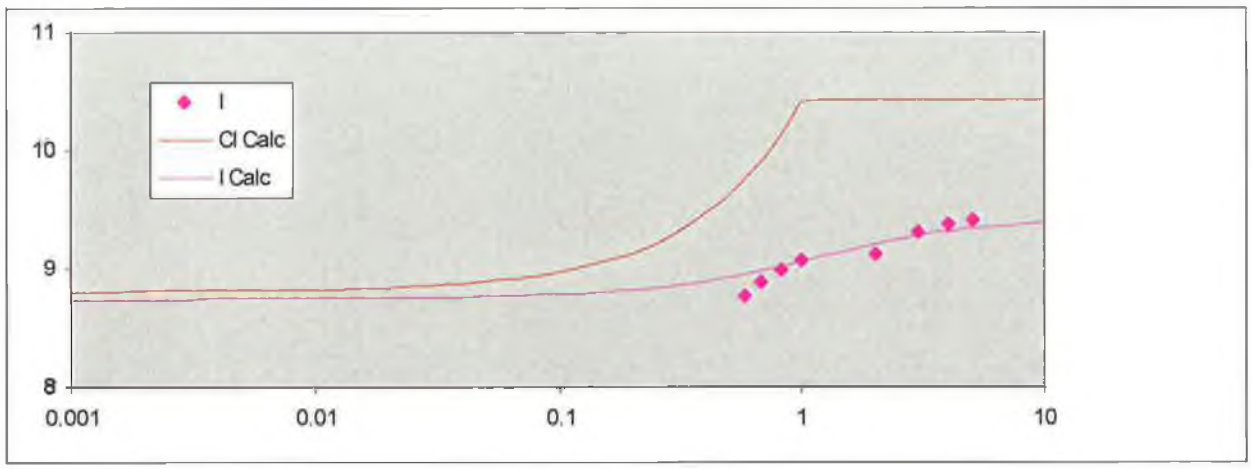

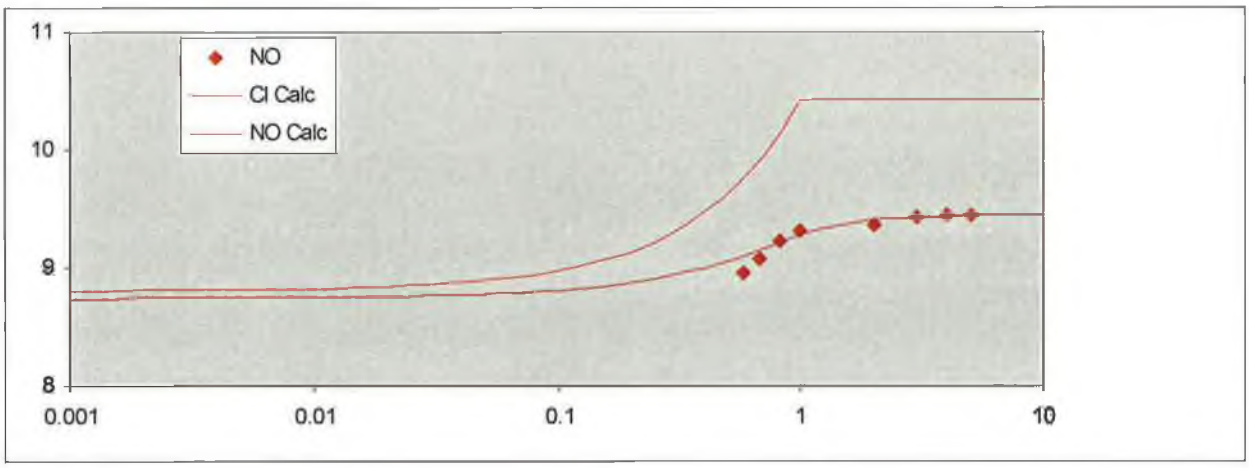

Figure 3. Experimental data and Calculated curves for receptor **(156d)**.

Appendix III- published paper.

Pergamon

Tetrahedron Letters 42 (2001) 5777–5779

TETRAHEDRON LETTERS

A homochiral tripodal receptor with selectivity for sodium (*R*)-2-aminopropionate over sodium (*S*)-2-aminopropionate

Joshua Howarth* and Nameer A. Al-Hashimy

School of Chemical Sciences, Dublin City University, Glasnevin, Dublin 9, Ireland

Received 11 April 2001; revised 12 June 2001; accepted 21 June 2001

Abstract—This paper describes the synthesis and use of a homochiral tripodal imidazolium salt that can distinguish between sodium (*R*)-2-aminopropionate and sodium (*S*)-2-aminopropionate. The imidazolium salt complexes with the (*R*) enantiomer but not with the (*S*) enantiomer.

In spite of their very important roles in chemistry and biology, substrates or cofactors for enzymes,[1] nucleophiles, bases, redox agents and phase transfer catalysts, the synthesis of receptors designed to recognise and coordinate anions has only relatively recently become an area of intense research activity. The combination of a metal unit as a Lewis acid together with an amide N–H group as a hydrogen bond donor have been demonstrated to be the essential components for anion recognition. As such this combination has been widely applied to the design of anion receptors.[2] Recently the ability of 1,3-disubstituted imidazolium cations to enter into hydrogen bonds with halide ions[3–7] has led to the design of new systems based on the azolium entity that have anion recognition properties, such as molecules **1** and **2**.[8–10]

We were intrigued by the tripodal anion receptor **1** used by Sato[8] and the possibility that it could be modified to incorporate chirality. A homochiral tripodal anion receptor may have the potential ability to distinguish between chiral anions and therefore hold promise in biomedical applications.

Therefore, we synthesised four novel homochiral molecules **3**–**6** according to a similar procedure used by Sato and Dias,[11] but incorporating chirality into the compounds. The general synthesis of compounds **3**–**6** is given in Scheme 1. The *N*-((−)-*cis*-myrtanyl) imidazole (**7**), for example, was formed using a modified Arduengo[12] protocol whereby an amine can react with aqueous formaldehyde, glyoxal and aqueous ammonia to effect a ring closure and produce a *N*-substituted imidazole. This was subsequently reacted with 1,3,5-tris(bromomethyl)-2,4,6-trimethyl benzene **8**[13] to form the 1,3,5-tris[*N*-((−)-*cis*-myrtanyl imidazolium)methyl]-

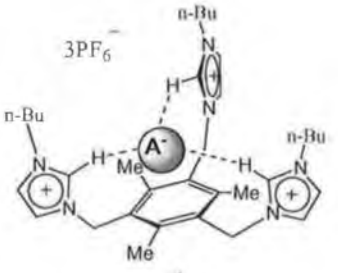

1

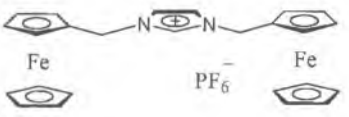

2

Keywords: anion recognition; homochiral; coordination.

* Corresponding author. Tel.: +353 1 7005312; fax: +353 1 7005503; e-mail: joshua.howarth@dcu.ie

0040-4039/01/$ - see front matter
PII: S0040-4039(01)01108-X

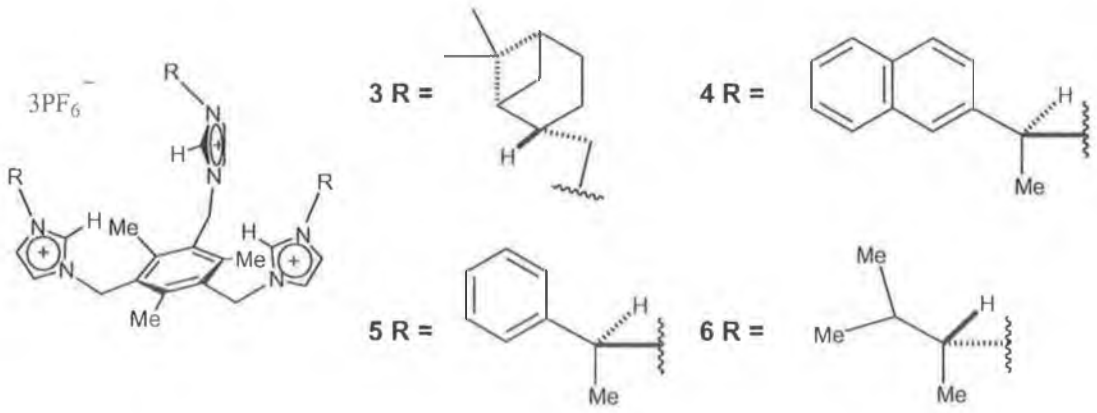

2,4,6-trimethyl benzene trisbromide salt (**9**).[9] Finally this was converted to the corresponding trishexafluorophosphate salt **3**.

In series of ^{1}H HMR experiments[14] sodium (*R*)-2-aminopropionate, sodium (*S*)-2-aminopropionate or a racemic mixture were added separately to each of the four tripodal molecules **3–6** in an 1:1 ratio [1:1:1 for the racemic system (tripodal compound:(*R*)-anion:(*S*)-anion)]. The rational behind these experiments was that if the tripodal molecules act as receptors for the anion enantiomers, a diastereomeric complex would be formed. The formation of a diastereomeric complex would possibly lead to differences in the ^{1}H NMR spectra for either the anion enantiomer or that of the tripodal molecule component of the complex, and those of the uncomplexed components. Should the potential receptor distinguish between anion enantiomers we might see a shift difference in the δ value for a particular proton in the complex, and the magnitude of the shift could depend on which one of the two possible diastereomic complexes is formed. If this were the case, we can establish which complex is formed preferentially.

The results from these experiments were very interesting. For tripodal compounds **4–6**, we observed no difference in the ^{1}H NMR spectra when mixed with either of the anion enantiomers or the racemic mixture. However, when compound **3** was mixed with the anions there was a distinct down-field shift of the δ value of the α proton for the sodium (*R*)-2-aminopropionate anion to 4.42 ppm and broadening of the signal was observed, indicating the formation of a diastereomeric complex. In the absence of **3** this proton has a δ value of 3.62 ppm and is a distinct quartet. In the corresponding experiment with the sodium (*S*)-2-aminopropionate there was no shift in the δ value for the corresponding proton and the signal remained as a quartet. When the experiment was carried out with the 1:1:1 (compound **3**:(*R*)-anion:(*S*)-anion) system both the shifted signal at 4.42 ppm and the unshifted signal at 3.62 ppm were observed in an 1:1 ratio, indicating that all the (*R*)-anion enantiomer has been complexed over the (*S*)-anion enantiomer. Although these are preliminary observations, they suggest that the tripodal homochiral imidazolium salt **3** can distinguish between sodium (*R*)-2-aminopropionate and sodium (*S*)-2-aminopropionate.

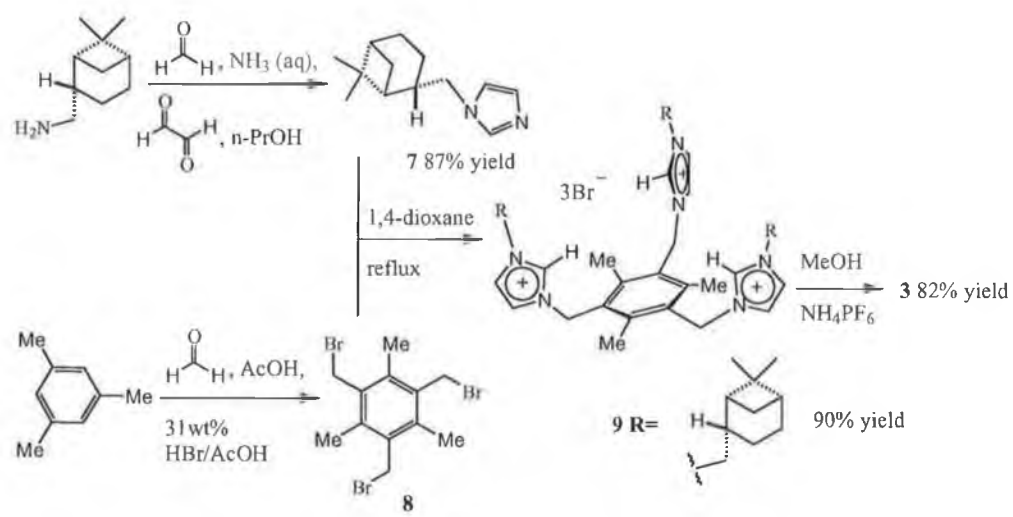

Scheme 1.

Acknowledgements

The authors would like to acknowledge the contribution to this research by Enterprise Ireland.

References

1. Lang, L. G.; Riordon, J. F.; Vallee, B. L. *Biochemistry* **1974**, *13*, 4361.
2. (a) Beer, P. D.; Hadocova, J.; Stokes, S. E. *J. Chem. Soc., Chem. Commun.* **1992**, 270; (b) Beer, P. D.; Hazlewood, C.; Hesek, D.; Hadocova, J.; Stokes, S. E. *J. Chem. Soc., Dalton Trans.* **1993**, 1327; (c) Beer, P. D.; Chen, Z.; Goulden, A. J.; Graydon, A.; Stokes, S. E.; Wear, T. *J. Chem. Soc., Chem. Commun.* **1993**, 1834; (d) Beer, P. D.; Chen, Z.; Goulden, A. J.; Grieve, A.; Hesek, D.; Szemes, F.; Wear, T. *J. Chem. Soc., Chem. Commun.* **1994**, 1269; (e) Beer, P. D.; Drew, M. G. B.; Hesek, D.; Jagessar, R. *J. Chem. Soc., Chem. Commun.* **1995**, 1187; (f) Beer, P. D.; Hesek, D.; Kingston, J. E.; Smith, D. K.; Stokes, S. E.; Drew, M. G. B. *Organometallics* **1995**, *14*, 3288; (g) Beer, P. D; Drew, M. G. B; Grayton, A. R.; Simth, D. K.; Stokes, S. E. *J. Chem. Soc., Dalton Trans.* **1995**, 403; (h) Beer, P. D.; Drew, M. G. B.; Hadocova, J.; Stokes, S. E. *J Chem. Soc., Dalton Trans.* **1995**, 3447; (i) Beer, P. D. *J. Chem. Soc., Chem. Commun.* **1996**, 689.
3. Dieter, K. M.; Dymek, C. J.; Heimer, N. E.; Rovang, J. W.; Wilkes, J. S. *J. Am. Chem. Soc.* **1988**, *110*, 2722.
4. Dymek, C. J.; Stewart, J. J. P. *Inorg. Chem.* **1989**, *28*, 1472.
5. Lapshin, S. A.; Yu. Chervinskii, A.; Litvinento, L. M.; Dadali, V. A.; Kapkan, L. M.; Vdovichenko, A. N. *Zh. Org. Khim.* **1985**, *21*, 357.
6. Avent, A. G.; Chaloner, P. A.; Day, M. P.; Seddon, K. R.; Welton, T. J. *J. Chem. Soc., Dalton Trans.* **1994**, 3405.
7. Elaiwi, A; Hitchcock, P. B.; Seddon, K. R.; Srinivasan, N.; Tan, Y.; Welton, T.; Zora, J. A. *J. Chem. Soc., Dalton Trans.* **1995**, 3467.
8. Sato, K.; Arai, S.; Yamagishi, T. *Tetrahedron Lett.* **1999**, *40*, 5219.
9. Howarth, J.; Thomas, J.-L.; Hanlon, K.; McGuirk, D. *Synth. Commun.* **2000**, *30*, 1865.
10. Howarth, J.; Thomas, J.-L.; Hanlon, K.; McGuirk, D. *Tetrahedron Lett.* **2000**, *41*, 413.
11. Dias, H. V. R.; Jin, W. *Tetrahedron Lett.* **1994**, *35*, 1365.
12. Arduengo, III, A. J. US Patent 5,077,414, 1991: General procedure for the synthesis of compounds **3–6** using 1,3,5-tris[*N*-((−)-*cis*-myrtanyl imidazolium)methyl]-2,4,6-trimethyl benzene trishexafluorophosphate **3** as an example. Formation of (−)-*cis*-myrtanyl imidazole: To a solution of (−)-*cis*-myrtanylamine (2.86 g, 18.6 mmol) and aqueous ammonia (1.00 mL, 18.6 mmol) in propan-1-ol (10 mL), a solution of glyoxal (2.34 mL, 20.00 mmol) and aqueous formaldehyde (37%, 1.45 mL, 20.0 mmol) in propan-1-ol (20 mL) were added dropwise. The solution was then heated to 80°C and left stirring for 2 h. It was then cooled to room temperature and water was added. Subsequently, the mixture was extracted with dichloromethane (3×30 mL) and the combined extracts were washed with water (2×20 mL), dried (anhydrous $MgSO_4$), filtered and the dichloromethane removed in vacuo to leave **7** as a brown oil (3.20 g, 87% yield). This was used without purification in the following step. A small sample of (−)-*cis*-myrtanyl imidazole **7** was purified (flash chromatography, silica gel, 10:1 ethylacetate:methanol) with the following analytical data:
^{1}H NMR (400 MHz, $CDCl_3$) δ (ppm) = 0.83 (1H, d, J = 9.6 Hz), 1.02 (3H, s), 1.3 (3H, s), 1.45 (1H, m), 1.70 (1H, m), 1.84 (4H, m), 2.27 (1H, m), 2.39 (1H, m), 3.84 (1H, d, J = 8.4 Hz) overlapping 3.85 (1H, d, J = 8.0 Hz), 6.81 (1H, s, NCHCH), 6.97 (1H, s, NCHCH), 7.36 (1H, s, NCHN).
^{13}C NMR (100 MHz, $CDCl_3$) δ (ppm) = 19.8 (CH_3), 23.8 (CH_3), 26.1 (CH_2), 28.2 (CH_2), 33.2 (CH_2), 38.9 (CH_2), 41.5 (CH), 43.0 (CH), 43.4 (CH), 52.9 (C), 119.4 (NCHCH), 129.6 (NCHCH), 137.6 (NCHN).
1,3,5-Tris(bromomethyl)-2,4,6-trimethyl benzene (0.50 g, 1.35 mmol) and (−)-*cis*-myrtanyl imidazole (1.00 g, 4.80 mmol) in 1,4-dioxane (15 mL) were heated to 100°C for 24 h. The resulting solid, 1,3,5-tris[*N*-((−)-*cis*-myrtanyl imidazolium)methyl]-2,4,6-trimethyl benzene trisbromide, was collected, rinsed with diethylether (3×100 mL) and dried to leave a light brown solid in 90% yield. The trisbromide salt was converted to the trihexafluorophosphate salt by dissolving the trisbromide salt in methanol (ca. 5% w/v) and adding a saturated aqueous solution of ammonium hexafluorophosphate until no further precipitation occurred. The precipitate was filtered, washed with methanol and dried, to yield **3** (82%) with the following analytical data, mp = 260–262°C.
^{1}H NMR (400 MHz, CD_3COCD_3) δ (ppm) = 0.94 (3H, d, J = 9.6 Hz), 1.10 (9H, s), 1.20 (9H, s), 1.61 (3H, m), 1.93 (21H, m), 2.39 (3H, m), 2.65 (3H, m), 4.31 (6H, d, J = 8.8 Hz), 5.77 (9H, s) 7.63 (3H, s, NCHCH), 7.81 (3H, s, NCHCH), 8.92 (3H, s, NCHN).
^{13}C NMR (100 MHz, CH_3COCH_3) δ (ppm) = 17.1 (CH_3), 19.9 (CH_3), 23.8 (CH_3), 26.6 (CH_2), 28.4 (CH_2), 33.8 (CH_2), 39.6 (CH_2), 42.3 (CH_2), 43.1 (CH), 44.5 (CH), 49.6 (CH), 56.3 (C), 123.8 (CH_3), 124.5 (CH_2), 130.7 (NCH), 136.7 (NCH), 143.1 (NCHN).
13. Van der Made, A. W.; Van der Made, R. H. J. *Org. Chem.* **1993**, *58*, 1262.
14. A 2×10^{-2} molar stock solution for each of the four homochiral imidazolium hexafluorophosphate salts **3–6** in deuterated acetonitrile was prepared. For each salt four ^{1}H NMR experiments were run. To equal aliquots of the stock solution, no chiral anion, (*R*)-2-aminopropionate anion, (*S*)-2-aminopropionate anion, and both (*R*)- and (*S*)-2-aminopropionate anions were added in an 1:1 ratio (1:1:1 for the racemic mixture), the anions being dissolved in deuterated water. The experiments were then run on a Bruker ADVANCE 400 MHz spectrometer. 2-Aminopropionate: ^{1}H NMR (400 MHz, $CDCl_3$) δ (ppm) = 1.36 (3H, d, J = 7.2 Hz), 3.62 (1H, q, J = 7.2 Hz).